Menno Evert Groeneveld was born May 27th 1985 in Singapore. He followed his primary education in Kloof (South Africa), Joppe and Leeuwarden. His secondary education was at the Christelijk Gymnasium in Leeuwarden. In his first university year he studied Law, after which he switched to Medical Studies at the VU University Medical Center in Amsterdam. As a medical student he started his scientific career as a research-student and would later follow a MD-PhD program at the Department of Vascular Surgery in collaboration with the Department of Physiology. Currently, he is general surgical resident in the greater VU University Medical Center region and will commence his vascular surgical residency in 2020. As an entrepreneur he advises several medical clinics and hospitals in correct and optimal medical billing.

Amsterdam UMC
Universitair Medische Centra

Menno E. Groeneveld

Cellular signalling in abdominal aortic aneurysms

Cellular signalling in abdominal aortic aneurysms

Towards better prediction of aneurysm progression and rupture

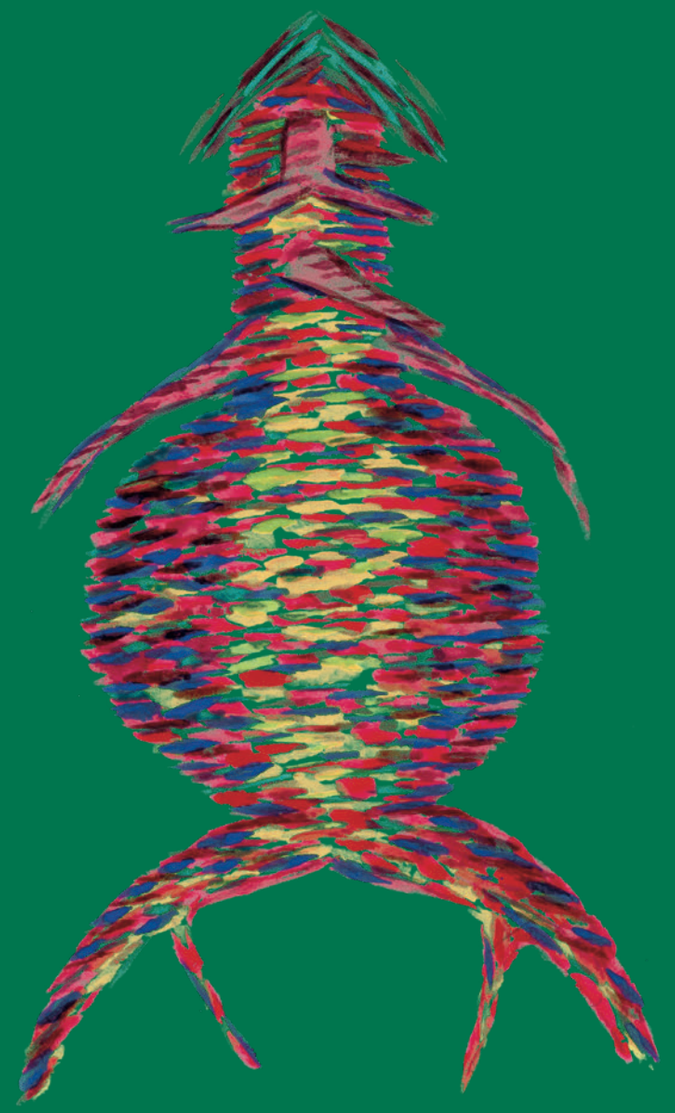

Menno E. Groeneveld

Colofon

Cellular signalling in abdominal aortic aneurysms:
Towards better prediction of aneurysm progression and rupture
ISBN/EAN: 978-94-6375-671-6

For full online version and/ or ThesisApp scan the QR-CODE above or go to thesisapps.com/MGPhD

Financial support by the Dutch Heart Foundation for the publication of this thesis is gratefully acknowledged.

The printing of this thesis was kindly supported by: Terumo Aortic / Vascutek Nederland, Angiocare, Erbe Nederland BV, Chipsoft, Pfizer, SWOAHS,Stichting Chirurg en Wetenschap Kennemerland, Carus Cura BV and Care4DOT BV. The online app was financially supported by Amsterdam Cardiovascular Sciences, Department of Surgery of the AUMC and ThesisApps.

Cover illustration by M.E. Groeneveld
Layout by Selma Hoitink, persoonlijkproefschrift.nl
Printed by Ridderprint BV | www.ridderprint.nl

VRIJE UNIVERSITEIT

Cellular signalling in abdominal aortic aneurysms: Towards better prediction of aneurysm progression and rupture

ACADEMISCH PROEFSCHRIFT

ter verkrijging van de graad Doctor of Philosophy aan
de Vrije Universiteit Amsterdam,
op gezag van de rector magnificus
prof.dr. V. Subramaniam,
in het openbaar te verdedigen
ten overstaan van de promotiecommissie
van de Faculteit der Geneeskunde
op vrijdag 6 maart 2020 om 9.45 uur
in de aula van de universiteit,
De Boelelaan 1105

door

Menno Evert Groeneveld

geboren te Singapore

promotor:	prof.dr. W. Wisselink
copromotoren:	prof.dr. G.W.J.M. Tangelder dr. K.K. Yeung dr. R.J.P. Musters

promotiecommissie:	prof.dr. J.D. Blankensteijn *(voorzitter)*
	prof.dr. R.L. Dalman
	prof.dr. D.A. Legemate
	prof.dr. G.W.H. Schurink
	prof.dr. J.A.M. Zeebregts
	dr. D. Nio
	dr. E.C. Eringa
paranimfen:	dr. C. Zwiers
	dr. H.P. Ebben

This thesis is dedicated to my brother Hessel Lous Groeneveld

CONTENT

CHAPTER 1

GENERAL INTRODUCTION AND THESIS OUTLINE

THESIS INTRODUCTION

Cardiovascular diseases are globally the largest cause of death, according to the World Health Organization, in 2016 accounting for 17.9 million deaths worldwide.[1,2] Major improvements have been made in the treatment of several cardiovascular diseases like myocardial infarction and stroke, which led to a drastic decrease in mortality rates.[3] A somewhat less frequent but equally lethal cardiovascular disease is abdominal aortic aneurysm (AAA).[4] The management of this disorder also has improved considerably in the past decades. Despite the developments, however, identification of patients who require treatment remains challenging. As the treatment of AAA has concomitant morbidity and mortality, accurate selection of patients is of great importance.[5]

Aneurysms are pathological arterial dilations that exceed the original diameter at least 1.5 times.[6] Aneurysms can occur in all major arteries. The most common location of an aneurysm is in the abdominal aorta. Other primary locations include the thoracic aorta, intracranial arteries, iliac arteries and femoropopliteal arteries (see table 1.1 for incidences).[7–10] AAA can be subdivided into supra-renal, juxta-renal or infra-renal aneurysms, depending on their position relative to the renal arteries. Approximately 80% of all AAA are localized in the infra-renal region of the aorta (figure 1.1A).[11,12] The prevalence of AAA is higher in men than in women. More specifically, 1.7 – 4.5% of men older than 65 years have an aneurysm, compared to a prevalence of 0.5 – 1.3% in women older than 70 years of age.[13–15] A suggestion for the higher prevalence in men might be the difference in composition of connective tissue components in the aortic wall, i.e. elastin and collagen, which results in a difference in tensile strength.[16,17]

Table 1.1 Incidences of aneurysm development in arteries of primary locations.

Localisation	Male incidence (per 100.000 per year)
Abdominal aorta[7,8]	
age 55 - 64 (years)	8
age 65 - 74 (years)	55
age 75 - 84 (years)	112
age > 84 (years)	298
Thoracic aorta[7,8]	8.6 – 12
Iliac arteries[9]	6.6
Femoropopliteal arteries[9]	7.4
Intracranial arteries[10]	7.8 – 10

Before addressing potential biomarkers for AAA progression, the main topic of the present thesis, we will first briefly present more detailed information about cells and

structures of a healthy aorta, the pathophysiology of AAA development and rupture as well as treatment options.

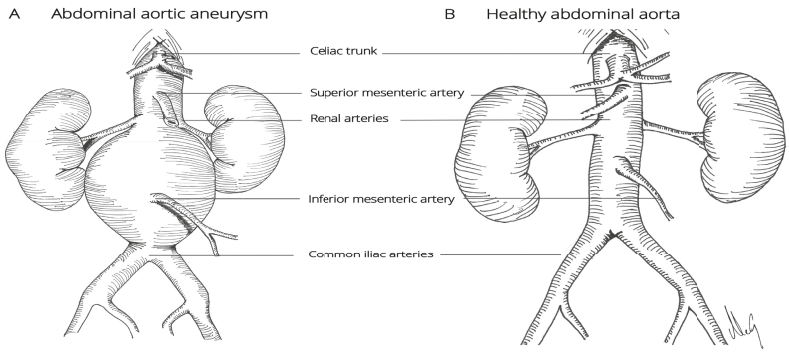

Figure 1.1 Illustration of an abdominal aortic aneurysm (A) and a healthy aorta (B).

Cells and structure of a healthy aorta

A healthy aorta consists of three concentric layers (or tunics) and has a diameter smaller than 3.0 cm. The anatomy of a healthy aorta is depicted in figure 1.1B. Figure 1.2 illustrates the histological characteristics of an AAA (A) and of a healthy aorta (B). Table 1.2 provides an overview of the characteristics of all three layers and their various cell types and functions.

Table 1.2 Cells and structures and their functions in the three adjacent layers of a healthy aorta.

Layer	Cells or structures	Function
Medial layer	Fibroblasts	Production of extracellular matrix components
	Smooth muscle cells	Expression of signalling proteins
		Mediating blood pressure changes
	Extracellular matrix	Stiffening of the vessel wall
		Medium for intercellular signalling
		Regulation of growth factors
Intimal layer	Endothelial cells	Barrier between blood and aortic wall
		Secretion of activators and inhibitors of coagulation
Adventitial layer	Fibroblasts	Production of extracellular matrix components
	Vasa vasorum	Aortic wall blood supply
	Nervi vasorum	Autonomous innervation
	Resident leukocytes	Antigen capture
		Inflammation regulation

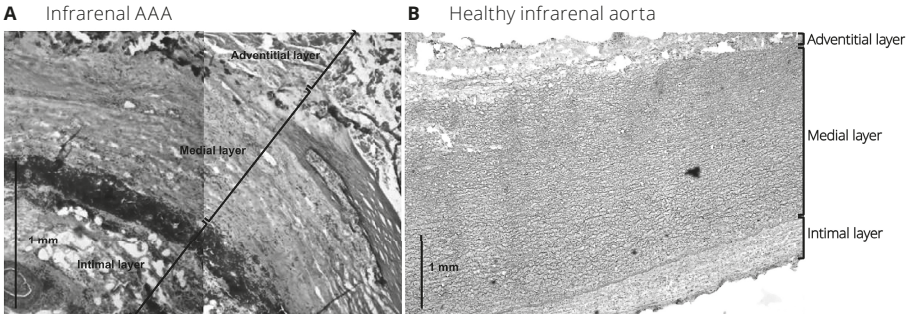

Figure 1.2 A histological overview of the three concentric layers can be seen in these transvers sections of an infrarenal AAA (A) and a healthy aorta (B). In figure A the pathological degeneration of the wall is most pronounced in the decreased medial layer thickness, while the intimal layer in aneurysmal aorta is thicker than in healthy tissue. Furthermore, the laminar arrangement of structures in a healthy aorta has been disturbed. The white spherical openings in the intimal and medial layer are defects in the wall. In figure B the three adjacent layers of the healthy aorta can clearly be recognized. Images were made by light microscopy with a 10X objective after hematoxylin and eosin staining. Please note the difference in scale.

The tunica media is the musculoelastic middle layer, which contains smooth muscle cells and fibroblasts embedded in an extracellular matrix composed mainly of collagen, elastin and proteoglycans. The middle layer provides the wall with tensile strength and is responsible for the viscoelastic properties of the aorta.[18–20] The medial layer is separated from the inner layer by the lamina elastica interna, which can be seen in figure 1.2B as a distinct line.

The tunica intima is the thin inner layer of the aorta, which consists of the basal membrane covered with a single layer of endothelial cells on the luminal side. Endothelial cells, among other functions, form a selective barrier between the lumen and the vessel wall and also play an important role in vascular permeability, vasoconstriction and the regulation of haemostasis by secreting activators and inhibitors of the coagulation cascade.[21]

The tunica adventitia is the fibrous outermost layer, composed mainly of adipose and connective tissue. It contains fibroblasts, resident leukocytes, vasa vasorum and nervi vasorum. Vasa vasorum provide the aortic wall with blood, while the nervi vasorum are responsible for autonomous innervation. The adventitia is separated from the medial layer by a lamina elastica externa (figure 1.2B).

Pathophysiology of AAA development

The pathophysiology of AAA, a multifactorial process that causes progressive degradation of the aortic wall, is still partly unclear. It is known pathophysiological components of this process are: i) chronic inflammation of the vessel wall; ii) an

inflammatory response that activates circulating leukocytes, mainly monocytes, which then infiltrate and accumulate in the vessel wall; and iii) degradation of the extracellular matrix (ECM) and smooth muscle cells (SMC) in the middle layer of the aorta, which should maintain the structure of the aorta.[22] In hereditary AAA, genetic mutations cause connective tissue disorders and lead to abnormalities of the medial layer. They typically cause destructive matrix remodelling, proliferation of vascular smooth muscle cells and a less prominent inflammatory response.[23]

The above-mentioned pathophysiological processes are the result of many cascades, which are activated by a variety of cellular signalling pathways. An example is the activation of matrix metalloproteinases (MMP), leading to ECM degradation but also modulate inflammatory responses.[20,24] All these cellular signalling pathways hold a vast amount of information on the activity and progression of the AAA disease. Therefore, further elucidation of these pathways might result in the identification of biomarkers for AAA progression. Accurate prediction of AAA development and rupture would then be one step closer.

Table 1.3 Diameter dependent annual risk of AAA rupture.

Diameter (cm)	Annual risk of rupture (%)
< 4.0	0
4.0 - 4.9	0.5 - 5
5.0 - 5.9	3 - 15
6.0 - 6.9	10 - 20
7.0 - 7.9	20 - 40
> 7.9	30 - 50

AAA rupture: a life-threatening event

AAA rupture causes a life threatening intra-abdominal bleeding, which results in death in approximately 77% of all cases.[25,26] The annual incidence of an AAA rupture is between 500 and 600 cases per year in the Netherlands.[27] From January 2013 until December 2014, a total of 1319 patients underwent acute AAA surgery in the Netherlands (ruptured AAA: n = 948 and symptomatic AAA: n = 371).[5] The yearly risk of rupture rises with an increase in diameter. AAA with a diameter between 4.0 and 4.9 cm have an annual rupture risk of 0.5 – 5%. AAA larger than 8 cm have an annual rupture risk of up to 30 – 50% (see table 1.3 for rupture risks per diameter range).[28] Until the moment of a rupture, AAA progression depends on several factors. For example, the presence of an intraluminal thrombus, which is associated with a higher growth speed

or the degree of vessel wall deterioration, i.e. the activity of proteases, cytokines and oxidative stress.[29] AAA development is also partly influenced by systemic factors like increased level of blood cholesterol, high blood pressure and smoking.[30] The latter is perceived as the most important general factor.[30] Genetic factors may also lead to aneurysm development. The best known genetic cause is a mutation in Fibrillin-1 gene (*FBN1*), leading to Marfans' disease.[13,31,32] Marfans' disease is characterized by dysregulation of connective tissue, leading to a high risk of aneurysm development throughout the aorta.[32,33] Given the high mortality rates in case of aneurysm rupture, treatment of AAA prior to such an event is essential.

Treatment options for AAA

To date, there is no medical therapy to halt aneurysm growth.[34–36] Therefore, to prevent aneurysm rupture, surgical repair is the only effective treatment.[35,36] The European and American Societies of Vascular Surgery guidelines currently advise to consider surgical repair when: i) the diameter exceeds 5.5 cm in men and 5.0 cm in women; ii) the growth speed exceeds 1.0 cm per year; or iii) an aneurysm becomes symptomatic, e.g. the patient presents with acute pain in the abdomen, back or groins.[35,36]

Traditionally, aortic aneurysms are treated by open repair. For open repair, the abdomen and retroperitoneal spaces are opened, respectively. Exposure of the aorta is then gained, after which it is cross-clamped proximally and distally to the aneurysm. Then, the aneurysmal sac is opened and a prosthetic graft will be inserted into the lumen of the aorta.[34] A less invasive surgical option is endovascular aortic aneurysm repair (EVAR). This technique was first introduced in the 1990s and has now become the standard treatment for most AAA.[37] During EVAR, an endograft is introduced via the femoral arteries and deployed at the site of the aneurysm, excluding the aneurysm sac from the circulation. There are multiple advantages of endovascular repair over open surgery, such as avoiding invasive transabdominal surgery, cross-clamping the aorta and thus avoiding major fluctuations in blood pressure.[34,38] Furthermore, the patients may be treated under local anaesthesia for the two small incisions in the groins where the catheters are inserted.

Although both surgical options have proven to be successful types of treatment, they are not without risks. Post-operative complications after elective surgery include 13% for EVAR, e.g. bleeding in the groins or distal embolization, versus 43% after open repair, i.e. distal embolization, left colon ischaemia or abdominal compartment syndrome.[5,34] Mortality rates are 0.9% after EVAR and 5.0% after open repair.[5] Therefore only AAA with a high risk of rupture should be treated, while low risk aneurysms should be

followed carefully in time. A promising approach for more precise risk estimations could be the use of reliable biomarkers.

Potential biomarkers for AAA progression

The pathophysiology of AAA development was described above in three interconnected processes: a chronic inflammatory process; an infiltrative process; and a degenerative process. Eventually, they lead to medial layer degradation and aortic dilation. Key players of those processes will be the scope of this thesis.

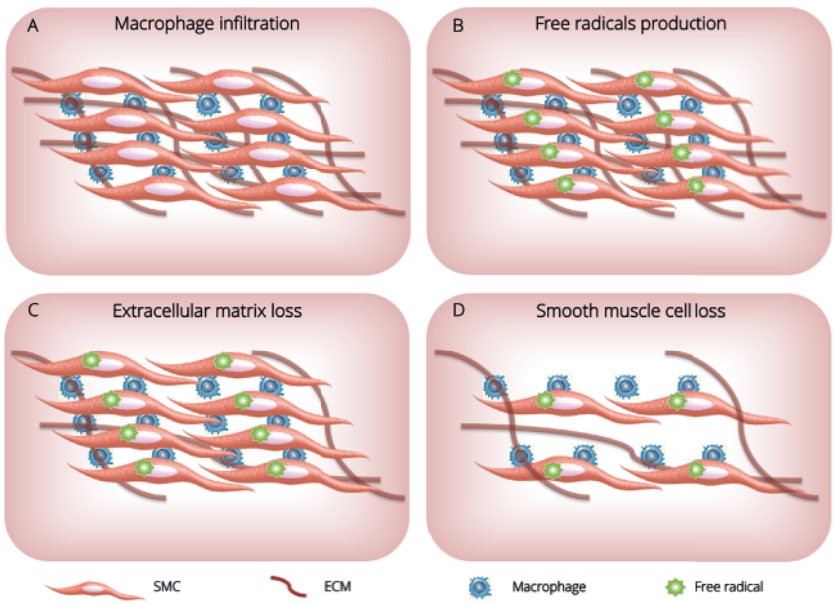

Figure 1.3 The consecutive steps leading to degradation and eventually aortic dilation are represented in this schematic illustration of an abdominal aortic medial layer. In response to chronic inflammation of the aortic wall, activated leukocytes, mainly monocytes, infiltrate into the aortic wall (A). Monocytes differentiate into macrophages when they infiltrate the vessel wall. They are responsible for the production of free radicals (reactive oxygen and nitrogen species; B). Free radicals cause destruction of the extracellular matrix, resulting in the loss the medial layer structure (C). Furthermore, free radicals cause smooth muscle cell apoptosis. These two processes lead to loss of smooth muscle cells and, eventually, reduction of the medial layer thickness (D).

The inflammatory process of the aortic wall results in an excessive production of reactive oxygen and nitrogen species (also called free radicals).[11,39,40] Free radicals are secreted by leukocytes in their attempt to destroy infectious pathogens.[41] Also, a lower dosage of free radicals is required in signalling pathways (i.e. regulating adaptation to hypoxia, autophagy and cell differentiation).[41,42] They are, however, very unstable and

can easily cause damage to surrounding cells and tissues. In a situation of local wall stress, as is the case during an aortic inflammatory process, excessive production of these free radicals results in oxidative and nitrosative stress, damaging the body's own cells and causing extracellular matrix degeneration and loss of smooth muscle cells by apoptosis.[41,43] A schematic illustration of this degenerative process is presented in figure 1.3. In the present thesis we will investigate the potential prognostic value of free radicals as marker for AAA progression and rupture.

The chronic inflammation causes damage to the aortic wall.[44] An intracellular signalling protein with a prominent role in the maintenance of the aortic wall structure is Extracellular signal-regulated kinase (ERK).[45] It is involved in vessel wall repair by cell proliferation but also in vessel wall degradation by smooth muscle cell apoptosis and migration. It remains unclear whether ERK has a protective or a detrimental role in aneurysm development. In rodent models the inhibition of ERK seemed to attenuate AAA progression.[46] In human studies, such results have never been reported. Therefore, in the present thesis we will further elucidate the role of ERK in patients with ruptured and non-ruptured AAA. We hypothesize that ERK has an important role in the maintenance of the aortic wall and thus might have potential as marker for AAA progression.

An acute phase protein called Neutrophil Gelatinase-Associated Lipocalin (NGAL) is involved in leukocyte infiltration of the aortic wall.[47,48] NGAL is stored in the granules of infiltrating neutrophils and has been the topic of interest as a diagnostic and prognostic tool for several cardiovascular diseases.[49–52] In mice, NGAL inhibition even attenuates AAA growth.[49] On the opposite, it is supposed to have a protective role against ROS induced apoptosis.[53,54] NGAL expression has earlier been described in the aortic wall of non-ruptured AAA and its role as a biomarker for AAA presence has even been suggested. In patients with carotid atherosclerosis NGAL demonstrated potential as marker for vulnerable plaques.[51,55–57] Furthermore, NGAL seems to have potential as a marker for acute kidney injury.[58] More specific, NGAL is suggested to predict hemodialysis and poor outcome after major aortic surgery and has already been suggested as a prognostic tool for several other cardiovascular diseases.[50,51,59–61] Therefore, the role of NGAL in AAA development and its potential as marker for aneurysm progression will be investigated in the present thesis.

The inflammatory and infiltrative processes activate factors of the degenerative process in AAA development, i.e. matrix metalloproteinases (MMP). MMP are enzymes that regulate cytokine activation as well as tissue repair.[24] There are more than 200 subtypes

of MMP and every single member of this enzyme superfamily has its own specific function. However, a common role of these proteinases is physiological enzymatic degradation of extracellular matrix to enable cell migration. Excess of these enzymes will result in loss of extracellular matrix. Consequently, the medial layer loses its strength, which results in aortic dilation. Examples of MMP activation consequently to inflammatory and infiltrative processes are: i) MMP-2, which is a downstream target in the ERK signalling pathway, and has a specific role in connective tissue turnover; and ii) MMP-9, which forms a complex with NGAL and thus is prevented from inactivation. It is thus thought that NGAL stimulates aortic wall degeneration.[62,63] The role of MMP-2 and -9 in the development and progression of AAA will be further elucidated.

Hereditary AAA have a different cause and lead to a different pathophysiology than above-described. There are several genetic mutations that cause inadequate aortic connective tissue production. The best known is a fibrillin-1 gene mutation that leads to Marfans' disease.[32] Fibrillin-1 binds free transforming growth factor beta (TGF-ß) in the extracellular matrix. TGF-ß is an important growth factor that activates and inhibits several cellular functions, including the production of connective tissue components for the aortic wall.[64] In a healthy vessel wall TGF-ß is bound to fibrillin-1 until it is released for activation or inhibition of a targeted cell.[65] In the case of a fibrillin-1 gene mutation, there will be an excess of free TGF-ß. This disturbs the delicate balance of connective tissue production, causing loss of aortic wall strength and eventually aortic dilation.[33]

In summary, vessel wall degradation and aortic dilation could be classified in an inflammatory, an infiltrative and a degenerative process. Factors of inflammation are reactive oxygen and nitrogen species and ERK; an infiltrative factor is NGAL and degenerative factors are MMP-2 and MMP-9. In the present thesis we will investigate the role of these factors and their potential role as marker for AAA progression.

AIM OF THE THESIS

AAA rupture is a sudden and potential life-threatening event associated with high mortality rates, which can only be prevented by aneurysm repair surgery. However, surgical repair also has concomitant morbidity and mortality. Therefore, careful patient selection is clinically most relevant. To date, it remains challenging to predict which aneurysm will rupture and which will not.

In this thesis we will focus on several cellular signalling pathways that are involved in aneurysm development and might have prognostic value for AAA rupture. Prognostic biomarkers will contribute to a more accurate prediction of a forthcoming rupture. In this thesis we aim to elucidate several signalling pathways involved in the development and rupture of AAA. Furthermore, we will investigate the potential of possible prognostic biomarkers for AAA growth and rupture.

OUTLINE OF THE THESIS

Part I: Biomarkers for aneurysm growth and rupture

In **chapter 2** we present a systematic review of the current literature regarding biomarkers for AAA growth and rupture. A biomarker could be defined as a measurable factor that provides useful information regarding one or more pathophysiological processes occurring in the body. The search for a prognostic biomarker for AAA growth resulted in a broad collection of circulating biomarkers, biomechanical properties and genetic mutations that hold promise for risk assessment regarding aneurysm growth and eventually rupture.

In **chapter 3** we investigate the production of two potent groups of free radicals in circulating leukocytes of AAA patients: reactive oxygen species and reactive nitrogen species. Excess of free radicals will lead to oxidative and nitrosative stress in the aortic wall, caused by infiltrating leukocytes in the vessel wall. However, it remains unknown which leukocyte type is responsible for the increased production of these free radicals in AAA patients. In addition, we demonstrate the effect of statin therapy on reactive oxygen species production.

In **chapter 4** we measure lipocalin-2 (NGAL) and MMP-9 expression in the aortic wall of ruptured versus non-ruptured AAA. Additionally, we investigate the potential of lipocalin-2 concentration in blood as a biomarker for aneurysm growth. Lipocalin-2 is an acute phase protein that is associated with the presence of asymptomatic AAA. In other cardiovascular diseases it was demonstrated to have potential as a biomarker for acute events. So far, the role of lipocalin-2 in ruptured aortic aneurysms has not been investigated.

Part II: Cellular signalling influences aneurysm growth and rupture

In **chapter 5** we study ERK and MMP-2 in tissue of ruptured versus non-ruptured AAA. We further elucidate the role of ERK in the progression of AAA and in the

pathophysiology leading to rupture. ERK is an intracellular signalling protein expressed, among others, by smooth muscle cells and fibroblasts. Its expression is thought to be influenced by the extracellular available MMP-2. ERK is a key player in the repair of damaged vessel walls, for example by regulating the production of extracellular matrix components. This protein has a potential influence on the aortic strength and the risk of AAA development or rupture. In **chapter 6** we present a short update on the role of ERK in AAA development.

In **chapter 7** we investigate the role of TGF-ß receptor 3 (TGFBR3, also Betaglycan) in the TGF-ß signalling pathway in fibroblasts of Marfan patients. TGF-β is an upstream activator of ERK and the cause of dysfunctional connective tissue in Marfans' disease. Several receptors are involved in the pathological activation of downstream intracellular TGF-ß pathways, but TGFBR3 seems to play an important role.

Part III: Novel technique for investigating cellular signalling pathways

In **chapter 8** we develop a new technique to process and culture explanted aneurysm wall tissue whilst preserving all three layers of the aorta. This procedure provides us with an ex-vivo living aneurysm wall section in which cellular signalling pathways can directly be studied. The recently developed multi-laser microscope, also designated a nanoscope, will enable the study of subcellular and even molecular three-dimensional details in living AAA cells.

In **chapter 9** the conclusions and clinical implications of this thesis are summarized and discussed in a general discussion.

REFERENCES

1. https://www.who.int/en/news-room/fact-sheets/detail/cardiovascular-diseases-(cvds). (2019).
2. Balakumar, M., Maung-U, K. & Jagadeesh, G. Prevalence and prevention of cardiovascular disease and diabetes mellitus. *Pharmacol. Res.* 11, 600–609 (2016).
3. Benjamin, E. J. *et al.* Heart Disease and Stroke Statistics — 2017 Update A Report From the American Heart Association. *Circulation* 3, 146–603 (2017).
4. Golledge, J., Muller, J., Daugherty, A. & Norman, P. Abdominal aortic aneurysm: Pathogenesis and implications for management. *Arterioscler. Thromb. Vasc. Biol.* 26, 2605–2613 (2006).
5. Lijftogt, N. *et al.* Adjusted Hospital Outcomes of Abdominal Aortic Aneurysm Surgery Reported in the Dutch Surgical Aneurysm Audit. *Eur. J. Vasc. Endovasc. Surg.* 53, 520–532 (2017).
6. Johnston, K. *et al.* Suggested standards for reporting on arterial aneurysms . Subcommittee on Reporting Standards for Arterial Aneurysms , Ad Hoc Committee on Reporting Standards , Society for Vascular Surgery and North American Chapter , International Society for Cardiovasc. *J Vasc Surg* 13, 452–8 (1991).
7. Howard, D. P. J. *et al.* Population-Based Study of Incidence of Acute Abdominal Aortic Aneurysms With Projected Impact of Screening Strategy. *J. Am. Heart Assoc.* 4, e001926 (2015).
8. Clouse, W. D. *et al.* Improved Prognosis of Thoracic Aortic Aneurysms. *Jama* 280, 1926 (1998).
9. Lawrence, P. F., Lorenzo-Rivero, S. & Lyon, J. L. The incidence of iliac, femoral, and popliteal artery aneurysms in hospitalized patients. *J. Vasc. Surg.* 22, 409–416 (1995).
10. Menghini, V. V., Brown, R. D., Sicks, J. D., O'Fallon, W. M. & Wiebers, D. O. Incidence and prevalence of intracranial aneurysms and hemorrhage in Olmsted County, Minnesota, 1965 to 1995. *Neurology* 51, 405–411 (1998).
11. Guo, D.-C., Papke, C. L., He, R. & Milewicz, D. M. Pathogenesis of thoracic and abdominal aortic aneurysms. *Ann NY Acad Sci* 1085, 339–352 (2006).
12. Taylor, S. M., Mills, J. L. & Fujitani, R. M. The Juxtarenal Abdominal Aoric Aneurysm. *Arch. Surg.* 129, 734–737 (1994).
13. Wahlgren, C. M., Larsson, E., Magnusson, P. K. E., Hultgren, R. & Swedenborg, J. Genetic and environmental contributions to abdominal aortic aneurysm development in a twin population. *J. Vasc. Surg.* 51, 3–7 (2010).
14. Svensjö, S., Björck, M. & Wanhainen, A. Current prevalence of abdominal aortic aneurysm in 70-year-old women. *Br. J. Surg.* 100, 367–372 (2013).
15. Svensjö, S. *et al.* Low prevalence of abdominal aortic aneurysm among 65-year-old swedish men indicates a change in the epidemiology of the disease. *Circulation* 124, 1118–1123 (2011).
16. Tong, J., Schriefl, A. J., Cohnert, T. & Holzapfel, G. A. Gender differences in biomechanical properties, thrombus age, mass fraction and clinical factors of abdominal aortic aneurysms. *Eur. J. Vasc. Endovasc. Surg.* 45, 364–372 (2013).
17. Vande Geest, J. P. *et al.* Gender-related differences in the tensile strength of abdominal aortic aneurysm. *Ann. N. Y. Acad. Sci.* 1085, 400–402 (2006).

18. Goldstein, S. A. *et al.* Multimodality Imaging of Diseases of the Thoracic Aorta in Adults: From the American Society of Echocardiography and the European Association of Cardiovascular Imaging. *J. Am. Soc. Echocardiogr.* 28, 119–182 (2015).

19. Thompson, R. W., Geraghty, P. J. & Lee, J. K. Abdominal aortic aneurysms: Basic mechanisms and clinical implications. *Curr. Probl. Surg.* 39, 110–230 (2002).

20. Frantz, C., Stewart, K. M. & Weaver, V. M. The extracellular matrix at a glance. *J. Cell Sci.* 123, 4195–4200 (2010).

21. McCarron, J. G., Lee, M. D. & Wilson, C. The Endothelium Solves Problems That Endothelial Cells Do Not Know Exist. *Trends Pharmacol. Sci.* 38, 322–338 (2017).

22. Nordon, I., Hinchliffe, R., Loftus, U. & Thompson, M. Pathophysiology and epidemiology of abdominal aortic aneurysms . *Nat. Rev. Cardiol.* 8, 92–102 (2011).

23. Lindsay, M. E. & Dietz, H. C. Lessons on the pathogenesis of aneurysm from heritable conditions. *Nature* 308–316 (2011). doi:10.1038/jid.2014.371

24. Parks, W. C., Wilson, C. L. & Lopez-Boado, Y. S. Matrix metalloproteinases as modulators of inflammation and innate immunity. *Nat. Rev. Immunol.* 4, 617–629 (2004).

25. Bruce Campbell, W. Mortality statistics for elective aortic aneurysms. *Eur. J. Vasc. Surg.* 5, 111–113 (1991).

26. Heikkinen, M., Salenius, J. P. & Auvinen, O. Ruptured abdominal aortic aneurysm in a well-defined geographic area. *J. Vasc. Surg.* 36, 291–296 (2002).

27. Visser, P., Akkersdijk, G. J. M. & Blankensteijn, J. D. In-hospital operative mortality of ruptured abdominal aortic aneurysm: A population-based analysis of 5593 patients in the Netherlands over a 10-year period. *Eur. J. Vasc. Endovasc. Surg.* 30, 359–364 (2005).

28. Dutch Vascular Surgery Association Guidelines. https://richtlijnendatabase.nl/richtlijn/aneurysma_van_de_abdominale_aorta/operatieve_behandelingen_van_een_aaa.html. (2017).

29. Piechota-Polanczyk, A. *et al.* The abdominal aortic aneurysm and intraluminal thrombus: current concepts of development and treatment. *Front. Cardiovasc. Med.* 2, 19 (2015).

30. Sidloff, D. *et al.* Aneurysm global epidemiology study public health measures can further reduce abdominal aortic aneurysm mortality. *Circulation* 129, 747–753 (2014).

31. De Backer, J. *et al.* Marfan Syndrome and Related Heritable Thoracic Aortic Aneurysms and Dissections. *Curr. Pharm. Des.* 21, 4061–4075 (2015).

32. Dietz, H. C. in *Marfan Syndrome. 2001 Apr 18 [Updated 2017 Feb 2]. In: Pagon RA, Adam MP, Ardinger HH, et al., editors. GeneReviews® [Internet]. Seattle (WA): University of Washington, Seattle; 1993-2017.*

33. Neptune, E. R. *et al.* Dysregulation of TGF-beta activation contributes to pathogenesis in Marfan syndrome. *Nat. Genet.* 33, 407–11 (2003).

34. Bergqvist, D., Björck, M., Ljungman, C., Nyman, R. & Wanhainen, A. in *Rutherford's Vascular Surgery* 325–329 (2018).

35. Moll, F. L. *et al.* Management of abdominal aortic aneurysms clinical practice guidelines of the European society for vascular surgery. *Eur. J. Vasc. Endovasc. Surg.* 41, (2011).

36. Chaikof, E. L. *et al.* SVS practice guidelines for the care of patients with an abdominal aortic aneurysm: Executive summary. *J. Vasc. Surg.* 50, 880–896 (2009).

37. Parodi, J., Palmaz, J. & Barone, H. Transfemoral intraluminal graft implantation for abdominal aortic. *Ann. Vasc. Surg.* 5, 491–9 (1991).

38. Powell, J. T. *et al.* Meta-analysis of individual-patient data from EVAR-1 , DREAM , OVER and ACE trials comparing outcomes of endovascular or open repair for abdominal aortic aneurysm over 5 years. *Br. J. Surg.* 166–178 (2017). doi:10.1002/bjs.10430

39. Ylä-Herttuala, S. *et al.* Expression of monocyte chemoattractant protein 1 in macrophage-rich areas of human and rabbit atherosclerotic lesions. *Proc. Natl. Acad. Sci. U. S. A.* 88, 5252–6 (1991).

40. Sullivan, G. W., Sarembock, I. J. & Linden, J. The role of inflammation in vascular diseases. *J. Leukoc. Biol.* 67, 591–602 (2000).

41. Sena, L. A. & Chandel, N. S. Physiological roles of mitochondrial reactive oxygen species. *Mol. Cell* 48, 158–166 (2012).

42. Martin-Ventura, J. L. *et al.* Erythrocytes, leukocytes and platelets as a source of oxidative stress in chronic vascular diseases: Detoxifying mechanisms and potential therapeutic options. *Thromb. Haemost.* 108, 435–442 (2012).

43. Rowe, V. L. *et al.* Vascular smooth muscle cell apoptosis in aneurysmal, occlusive, and normal human aortas. *J. Vasc. Surg. Off. Publ. Soc. Vasc. Surg. [and] Int. Soc. Cardiovasc. Surgery, North Am. Chapter* 31, 567–576 (2000).

44. Boddy, A. M. *et al.* Basic research studies to understand aneurysm disease. *Drug News Perspect.* 21, 142–148 (2008).

45. Lu, Z. & Xu, S. ERK1/2 MAP kinases in cell survival and apoptosis. *IUBMB Life* 58, 621–631 (2006).

46. Habashi, J. P. *et al.* Angiotensin II Type 2 Receptor Signaling Attenuates Aortic Aneurysm in Mice Through ERK Antagonism. *Science (80-.).* 4, 361–365 (2011).

47. Ramos-Mozo, P. *et al.* Increased plasma levels of NGAL, a marker of neutrophil activation, in patients with abdominal aortic aneurysm. *Atherosclerosis* 220, 552–556 (2012).

48. Houard, X., Ollivier, V., Louedec, L., Michel, J.-B. & Bäck, M. Differential inflammatory activity across human abdominal aortic aneurysms reveals neutrophil- derived leukotriene B 4 as a major chemotactic factor released from the intraluminal thrombus. *FASEB J.* 23, 1376–1383 (2009).

49. Tarín, C. *et al.* Lipocalin-2 deficiency or blockade protects against aortic abdominal aneurysm development in mice. *Cardiovasc. Res.* 111, 262–273 (2016).

50. Serra, R. *et al.* The role of matrix metalloproteinases and neutrophil gelatinase-associated lipocalin in central and peripheral arterial aneurysms. *Surgery* 157, 155–162 (2015).

51. Eilenberg, W. *et al.* Neutrophil Gelatinase-Associated Lipocalin (NGAL) is Associated with Symptomatic Carotid Atherosclerosis and Drives Pro-inflammatory State in Vitro. *Eur. J. Vasc. Endovasc. Surg.* 51, 623–631 (2016).

52. Sivalingam, Z. *et al.* Neutrophil gelatinase-associated lipocalin as a risk marker in cardiovascular disease. *Clin. Chem. Lab. Med.* 56, 5–18 (2018).

53. Roudkenar, M. H. *et al.* Neutrophil Gelatinase-associated Lipocalin Acts as a Protective Factor against H2O2 Toxicity. *Arch. Med. Res.* 39, 560–566 (2008).

54. Roudkenar, M. H. *et al.* Lipocalin 2 regulation by thermal stresses: Protective role of Lcn2/NGAL against cold and heat stresses. *Exp. Cell Res.* 315, 3140–3151 (2009).

55. Eilenberg, W. *et al.* NGAL and MMP-9 / NGAL as biomarkers of plaque vulnerability and targets of statins in patients with carotid atherosclerosis . *Clin. Chem. Lab. Med.* 56, 147–156 (2017).

56. Eilenberg, W. *et al.* Neutrophil gelatinase associated lipocalin (NGAL) is elevated in type 2 diabetics with carotid artery stenosis and reduced under metformin treatment. *Cardiovasc. Diabetol.* 98, 1–11 (2017).

57. Boekhorst, B. C. *et al.* Molecular MRI of murine atherosclerotic plaque targeting NGAL : a protein associated with unstable human plaque characteristics. *Cardiovasc. Res.* 89, 680–688 (2011).

58. Mishra, J. *et al.* Neutrophil gelatinase-associated lipocalin (NGAL) as a biomarker for acute renal injury after cardiac surgery. *Lancet* 365, 1231–38 (2005).

59. Tarin, C. *et al.* Lipocalin-2 deficiency or blockade protects against aortic abdominal aneurysm development in mice. *Cardiovasc. Res.* 111, 262–273 (2016).

60. Gombert, A. *et al.* Urine neutrophil gelatinase-associated lipocalin predicts outcome and renal failure in open and endovascular thoracic abdominal aortic aneurysm surgery. *Sci. Rep.* 8, 12676 (2018).

61. Gombert, A. *et al.* Comparison of urine and serum neutrophil gelatinase-associated lipocalin after open and endovascular thoraco-abdominal aortic surgery and their meaning as indicators of acute kidney injury. *Vasa* 10, 1–9 (2018).

62. Yan, L., Borregaard, N., Kjeldsen, L. & Moses, M. A. The high molecular weight urinary matrix metalloproteinase (MMP) activity is a complex of gelatinase B/MMP-9 and neutrophil gelatinase-associated lipocalin (NGAL): Modulation of MMP-9 activity by NGAL. *J. Biol. Chem.* 276, 37258–37265 (2001).

63. Swedenborg, J. & Eriksson, P. The intraluminal thrombus as a source of proteolytic activity. *Ann. N. Y. Acad. Sci.* 1085, 133–138 (2006).

64. Heldin, C. & Moustakas, A. Signaling Receptors for TGF- b Family Members. *Cold Spring Harb. Perspect. Biol.* 8, (2016).

65. Sakai, L. Y., Keene, D. R., Renard, M. & De Backer, J. FBN1: The disease-causing gene for Marfan syndrome and other genetic disorders. *Gene* 591, 279–291 (2016).

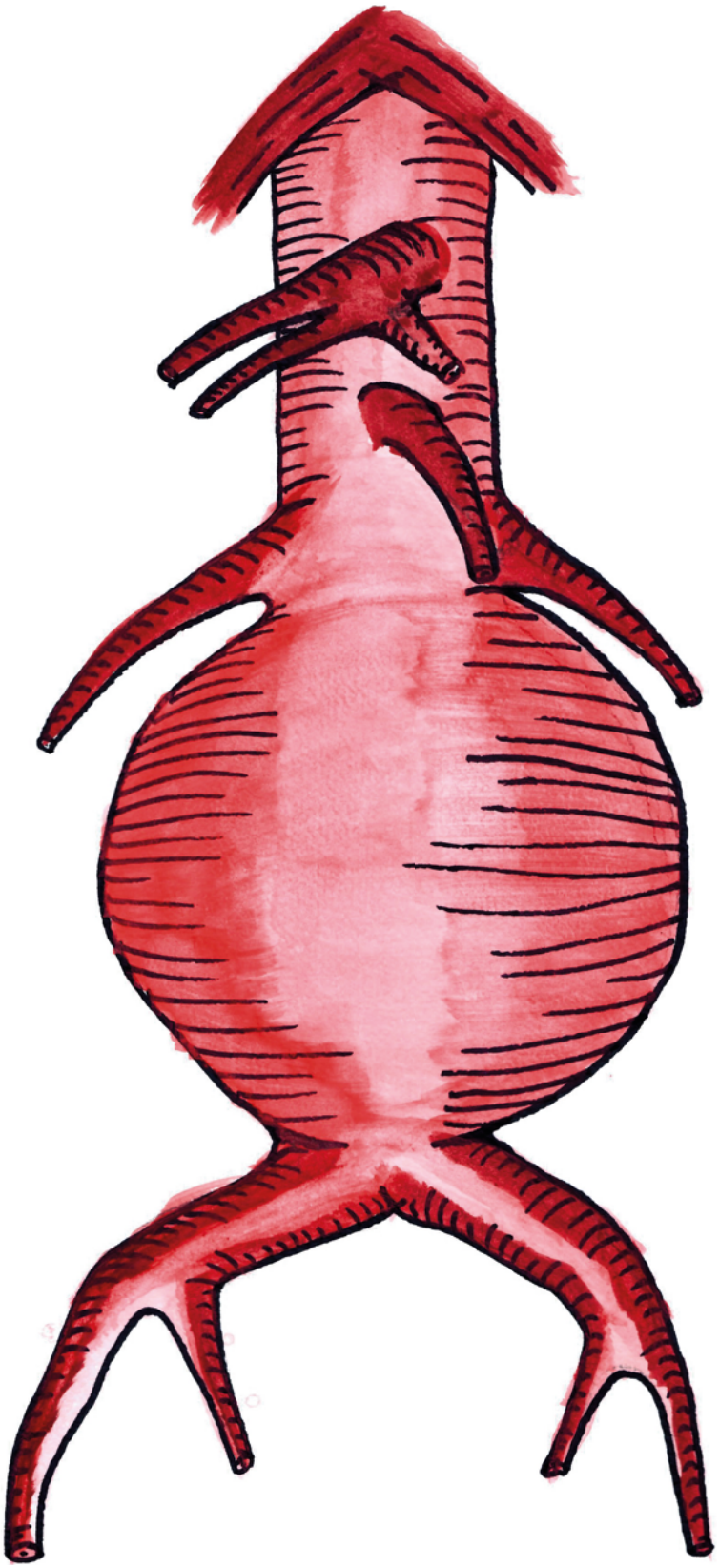

PART I

BIOMARKERS FOR ANEURYSM GROWTH AND RUPTURE

Chapter 2: Systematic review of circulating, biomechanical and genetic markers for the prediction of abdominal aortic aneurysm growth and rupture

Chapter 3: Peroxynitrite footprint in circulating neutrophils of abdominal aortic aneurysm patients is lower in statin than in non-statin users

Chapter 4: The potential role of Neutrophil Gelatinase-Associated Lipocalin (NGAL) in the development of abdominal aortic aneurysms

CHAPTER 2

SYSTEMATIC REVIEW OF CIRCULATING, BIOMECHANICAL AND GENETIC MARKERS FOR THE PREDICTION OF ABDOMINAL AORTIC ANEURYSM GROWTH AND RUPTURE

M.E. Groeneveld[1,2]
J.P. Meekel[1,2]
S. Rubinstein[3]
L. Merkenstein[1]
G.J. Tangelder[2]
W. Wisselink[1]
M. Truijers[1]
K.K. Yeung[1,2]

[1] Department of Vascular Surgery, Amsterdam University Medical Center
[2] Department of Physiology; Amsterdam University Medical Center
[3] Department of Health Sciences, VU University, Amsterdam

Journal of American Heart Association 2018 Jun 30, vol. 7(13), pii: e007791

ABSTRACT

Objectives: The natural course of abdominal aortic aneurysms (AAA) is growth and rupture if left untreated. Numerous markers have been investigated, however, none are broadly acknowledged. Our aim was to identify potential prognostic markers for AAA growth and rupture.

Methods: Potential circulating, biomechanical and genetic markers were studied. A comprehensive search was conducted in PubMed, Embase and Cochrane Library in February 2017, following PRISMA guidelines. Study selection, data extraction and methodological quality assessment were conducted by 2 independent researchers. Plausibility of markers was based on the amount of publications regarding the marker (more than 3), pooled sample size (more than 100), bias risk and statistical significance of the studies.

Results: 82 studies were included, which examined circulating (n=40), biomechanical (n=27), genetic markers (n=7) and combinations of markers (n=8). Factors with an increased expansion risk included: AAA diameter (9 studies;n=1938;low bias risk), chlamydophila pneumonia (4 studies;n=311;medium bias risk), S-elastin peptides (3 studies;n=205;medium bias risk), fluorodeoxyglucose uptake (3 studies;n=104;medium bias risk) and intraluminal thrombus size (5 studies;n=758;medium bias risk). Factors with an increased rupture risk rupture included: peak wall stress (9 studies;n=579;medium bias risk) and AAA diameter (8 studies;n=354;medium bias risk). No meta-analysis was conducted because of clinical and methodological heterogeneity.

Conclusions: We identified 5 potential markers with a prognostic value for AAA growth and 2 for rupture. While interpreting these data one must realize that conclusions are based on small sample sizes and clinical and methodological heterogeneity. Prospective and methodological consonant studies are strongly urged to further study these potential markers.

1. INTRODUCTION

The natural course of an abdominal aortic aneurysm (AAA) is a steady increase of the diameter and eventually, if left untreated, the aneurysm might rupture.[1] In most cases of AAA, this pathophysiological process remains asymptomatic until rupture. Such an event can be prevented by surgical AAA repair. The decision to perform surgery is commonly based on 3 characteristics being: 1) the maximum AAA diameter exceeding 5.0 cm in women and 5.5 cm in men; 2) the experience of symptoms; or 3) the aneurysm growth rate exceeds 1 cm/year.[2,3] The first 2 characteristics are relatively easy to identify by imaging or by questioning the patient. However, the AAA growth rate can only be considered retrospectively, as a prognostic value for expansion has not yet been acknowledged.

In the current AAA management no marker for aneurysm progression or rupture has been implemented as common practice. This might be explained by little existing evidence and lack of experience with prognostic markers. Although numerous potential markers of aneurysm growth and rupture have been examined, a systematic review with a detailed and structured evaluation of markers for AAA expansion and rupture is lacking.

The aim of this systematic review was to identify promising markers of aneurysm expansion and rupture to aid clinicians in AAA management. We searched for retro- and prospective observational studies in which the prognostic value of circulating bloodmarkers, biomechanical properties and genetic variations for AAA expansion or rupture are investigated.

2. METHODS

The data, analytic methods, and study materials will be available to other researchers at the corresponding author for purposes of reproducing the results.

2.1 Search strategy

A comprehensive search was conducted following Preferred Reporting Items for Systematic Reviews and Meta-Analyses (PRISMA) guidelines.[4] Separate searches were performed in PubMed, Embase and Cochrane Library on February 27th 2017 exploring: circulating, biomechanical and genetic markers. The search strategies can be found in the appendix. Study titles and abstracts were screened and full texts were examined when a study appeared to fulfill the inclusion criteria. In addition, reference lists were searched to identify potentially missing studies.

2.2 Study selection and data extraction

Studies were independently selected by 2 reviewers and differences in selected studies were discussed. In case of disagreement during the selection process, a third author would make the final decision.

Studies examining markers for a correlation with AAA expansion or rupture, were included. No limits were placed on year of publication. Inclusion was limited to studies published in English and full publications. No attempt was performed to search for 'grey literature'. Case reports, reviews, animal studies and studies regarding inflammatory AAA were excluded.

Data extraction was performed independently by 2 reviewers and merged by consensus. Using data extraction forms, the following data were extracted: study population (gender, age), sample size, results reported either as Pearson or Spearman correlations, area under curve, odds ratio, differences between groups, means or medians alongside a measure of variance (e.g. range, interquartile range, standard deviations) and statistical significance (P-values).

2.3 Quality appraisal of individual studies

The risk of bias was assessed using guidelines provided by Hayden e.a. for evaluating the quality of prognosis studies in systematic reviews.[5] Accordingly, 6 potential bias items were addressed: i) study participation; ii) study attrition; iii) prognostic factor measurement; iv) outcome measurement; v) measurement and account of confounders; and vi) analysis methods. Every item has 3 to 7 questions; per item an equal amount

of points were attributed, resulting in a total percentile score of bias items excluded. We classified studies as low risk (75% or more bias items excluded), intermediate risk (50-75% bias items excluded) or high risk of bias (less than 50% of bias items excluded). The risk of bias is presented and studies are sorted accordingly.

2.4 Data analysis

Reported outcomes of studies include correlation coefficients, statistical significance, sample size and quality appraisal. The principal measure reported for each study was the correlation between the given biomarkers (i.e. circulating, biomechanical or genetic) and a presented outcome change with growth or rupture of AAA. Factors that to pose an increased risk of growth or rupture were considered plausible if: i) demonstrated to be a marker in 3 or more publications and these publications demonstrated consistent results; ii) pooled sample size of more than 100 patients; iii) at least one-third of the studies demonstrated a low risk of bias; and iv) statistical significance was reached in 2/3 of the studies.

In consensus, the authors concluded that a meta-analysis could not be performed due to clinical and methodological heterogeneity, which is consistent with current thought.[6] Additionally, a meta-analysis of correlation coefficients is only considered to be reliable if more than 30 studies are able to be pooled for the same outcome.[7] In the present review, a maximum of 9 studies were able to be identified per marker.

3. RESULTS

3.1 Search results

The searches resulted in 760 studies (figure 2.1) of which 605 were excluded based on title or abstract (no AAA [n=352]; no biomarker of growth or rupture [n=141]; case report, comment or oral presentation only [n=34]; not English [n=37]; not human [n=9]; other [n=32]). Consequently, 155 articles were retrieved for full text evaluation of which 73 were excluded (no biomarker of growth or rupture [n=54]; review [n=14], no AAA [n=4]; inflammatory AAA [n=1]). A total of 82 articles were included: 40 studies concerned circulating biomarkers; 27 studies concerned biomechanical markers; 7 studies concerned genetic markers; and 8 studies described a circulating biomarker together with a biomechanical or a genetic marker.

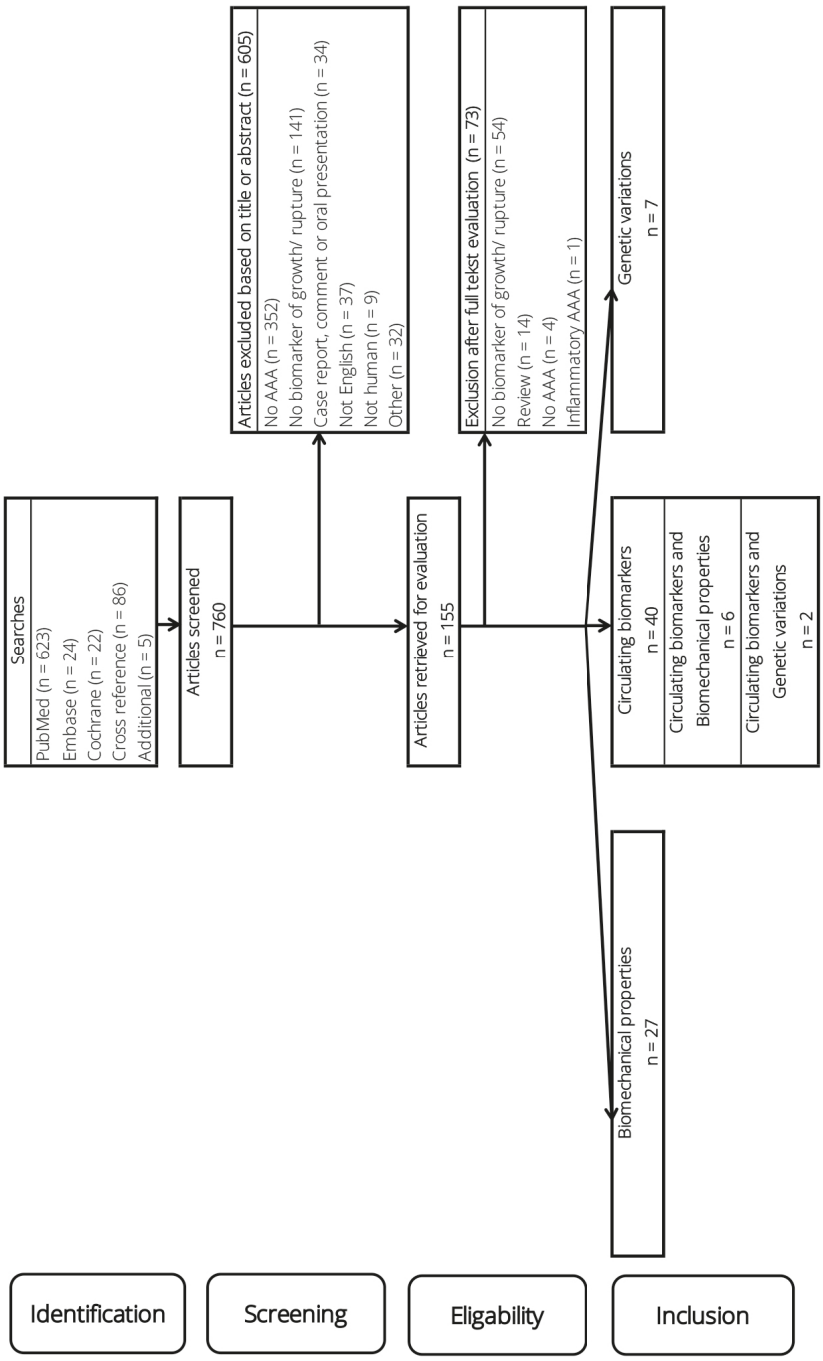

Figure 2.1 Study selection flowchart according to PRISMA guidelines.

3.2 Circulating biomarkers

In 48 studies 63 circulating biomarkers were investigated (table 2.1). Most investigated circulating markers are part of the coagulation cascade (14 markers); then connective tissue turnover (12 markers); lipids (9 markers) and immune response (18 markers). Remaining categories concerned smoking, kidney function, hormones and others. The following focuses on markers described in 3 or more publications.

Table 2.1 Circulating biomarkers that have been investigated for an association with AAA expansion or rupture. Markers are categorized by its (patho)physiological system. Per marker the amount of included studies with significant outcomes are shown, as well as the total number of patients in studies pooled.

Marker	Total studies (n)	Significant outcome	Total patients (n)
Coagulation			
Activated protein C — protein C inhibitor[32]	1	0 of 1 studies	163
Activated prothrombin time (APTT)[27]	1	1 of 1 studies	44
D-dimer (see table 2.4)[26-28]	3	3 of 3 studies	438
Factor XII[40]	1	1 of 1 studies	48
Fibrinogen (see table 2.4)[22,23,27]	3	3 of 3 studies	381
Plasmingon activator inhibitor 1(PAI-1; see table 2.4)[13,27,28,35]	4	4 of 4 studies	304
Plasmin-antiplasmin-complex[36]	1	1 of 1 studies	70
Platelets[27]	1	0 of 1 studies	44
Prothrombin time[27]	1	0 of 1 studies	44
Prothrombin fragment 1 + 2[27]	1	1 of 1 studies	44
Serpine-1[32]	1	0 of 1 studies	163
Tissue plasminogen activator (tPA; see table 2.4)[13,27,28,35]	4	4 of 4 studies	304
tPA serpine-1[32]	1	0 of 1 studies	163
urokinase-like PA[13]	1	0 of 1 studies	70
Connective tissue			
Aminoterminal propeptide of type III procollagen (see table 2.4)[9,10,12]	3	1 of 3 studies	190
Carboxyterminal propeptide of type 1 procollagen[41]	1	0 of 1 studies	86
Elastase[25]	1	1 of 1 studies	79
Matrix metalloproteinase 1 (MMP-1)[34]	1	1 of 1 studies	68
MMP-2[32,34]	2	0 of 2 studies	231
MMP-3[34]	1	0 of 1 studies	68
MMP-9 (see table 2.4)[10,18,32,34]	4	3 of 4 studies	285
S-elastin peptides (see table 2.4)[8,10,36-38]	5	5 of 5 studies	365
Transforming Growth Factor Beta-1[13]	1	0 of 1 studies	70

Table 2.1 Continued

Marker	Total studies (n)	Significant outcome	Total patients (n)
Tissue Inhibtor Metalloproteinase-1 (TIMP-1; see table 2.4)[18,32,34]	3	0 of 3 studies	249
α-1 antitrypsine[10,18,39,40] (see table 2.4)	4	2 of 4 studies	127
α-1 antitrypsine, Factor XII, D-dimer and IgG[40]	1	0 of 1 studies	48
Lipids			
Albumin[23]	1	1 of 1 studies	51
Apolipoprotein A1[42]	1	1 of 1 studies	180
Apolipoprotein B[42]	1	1 of 1 studies	180
Cholesterol[42,59]	2	0 of 2 studies	295
Glycosylphosphatidylinositol phospholipase D[43]	1	1 of 1 studies	133
High density lipoprotein[21,59]	2	0 of 2 studies	295
Low density lipoprotein[59]	1	0 of 1 studies	117
Lipoprotein A[42]	1	0 of 1 studies	180
Triglyceride[42,59]	2	2 of 2 studies	297
Immune respons system			
Chlamydophila pneumoniae (see table 2.4)[11–16]	6	4 of 6 studies	465
CRP (see table 2.4)[17–23]	7	4 of 7 studies	1421
Cytomegalovirus[44]	1	0 of 1 studies	119
Helicobacter pylori[45]	1	0 of 1 studies	119
Herpes simplex 1[16]	1	0 of 1 studies	119
Interleukin-1ß[30]	1	0 of 1 studies	90
Interleukin-2[30]	1	0 of 1 studies	90
Interleukin-6 (see table 2.4)[21,30,31]	3	0 of 3 studies	734
Interleukin-8[30]	1	1 of 1 studies	90
Interferon gamma[95]	1	1 of 1 studies	50
Leukocytes[22]	1	1 of 1 studies	225
Macrophage inhibiting factor[13,47]	2	1 of 2 studies	168
Neutrophil gelastinase-associated lipocalin[48]	1	1 of 1 studies	40
Osteopontin[84]	1	1 of 1 studies	198
Osteoprotegerin[49]	1	1 of 1 studies	146
Peroxiredoxin[50]	1	1 of 1 studies	80
Tumor necrosis factor-α[21,30]	2	1 of 2 studies	268
Tumor Necrosis Factor-Like Weak Inducer of Apoptosis[51]	1	1 of 1 studies	43

Table 2.1 Continued

Marker	Total studies (n)	Significant outcome	Total patients (n)
Smoking			
Cotinine (see table 2.4)[13,24,25]	3	2 of 3 studies	596
Smoking[25]	1	1 of 1 studies	79
Kidney function			
Creatinine[21,52]	2	2 of 2 studies	274
Cystatine C[52,53]	2	2 of 2 studies	238
Hormones			
Endothelin-1,2[54]	1	0 of 1 studies	65
Endothelin-1[21]	1	0 of 1 studies	178
Insulin-like growth factor 1[55]	1	1 of 1 studies	115
Insulin-like growth factor 2[55]	1	0 of 1 studies	115
Others			
Forced expiratory volume in one second[25]	1	0 of 1 studies	79
Homocysteine (see table 2.4)[13,21,29]	3	1 of 3 studies	356

Aminoterminal propeptide of type III procollagen (PIIINP)

A significant correlation with expansion was found in 1 study (r=0.24) in which 99 follow-up patients were included.[8] The quality appraisal attributed this study with medium bias risk. In 2 studies (1 medium and 1 high bias risk) no correlation was found in 91 follow-up patients in total.[9,10] However, Satta e.a. did reach significance after 2 years of follow-up.[9]

Chlamydophila pneumoniae

In 4 studies chlamydophila pneumoniae was investigated as marker for expansion[11–14] and in 2 as marker for rupture.[15,16] In none of the patients an inflammatory AAA was suspected. All studies on expansion had significant outcomes. Lindholt e.a. demonstrated in 2 separate studies (total patients n=194) that AAA expansion rate was faster in patients with a higher immunoglobulin A (IgA) titre. Falkensammer e.a. found the same results for seropositive versus seronegative patients. In a third separate publication, Lindholt e.a. demonstrated a significant correlation (r=0.29) with expansion in 70 follow-up patients. Nyberg e.a. found no difference in seropositivity between ruptured AAA patients and controls.[15] A second study of Nyberg e.a. on the same cohort demonstrated that AAA patients had no increased risk of rupture as compared

to controls when these patients were also seropositive for Helicobacter Pylori, Herpes Simplex or Cytomegalovirus.[16] Overall, the quality of studies was intermediate: 4 had medium risk, 1 had low risk and 1 had high risk of bias.

Complement Reactive Protein (CRP)

CRP was examined as marker for expansion in 5 studies[17–21] and in 2 as marker for rupture.[22,23] De Haro e.a. and Wiernicki e.a. were the only groups to demonstrate significant correlations with expansion. De Haro e.a. included 260 patients, had a low risk of bias and measured a strong correlation ($r=0.71$, $p<0.05$). According to Norman and Flondell-Sité e.a., who included 723 patients in total and were both qualified as low risk of bias, CRP levels did not differ between follow-up patients with high versus low expansion rate. Speelman e.a. also found no correlation, but included only 18 follow-up patients and had a medium risk of bias. Domanovits e.a. measured higher CRP levels in patients presenting with a ruptured AAA than in patients prior to elective repair (low risk of bias and total n=225). Tambyraja e.a., also with a low bias risk, measured 4 times higher CRP levels in symptomatic patients than in asymptomatic patients (total n=112).

Cotinine

Cotinine was examined in 3 studies as marker for AAA expansion. Wilmink e.a.[24], which study was appraised with a medium bias risk, followed 447 AAA patients and found no difference in cotinine levels between follow-up patients with an expanding AAA (growth > 2 mm per year) versus a stable AAA. Lindholt e.a. demonstrated significant correlations ($r=0.23$ and $r=0.24$) in 2 separate studies[13,25] (low and medium bias risks), after including 149 follow-up patients in total from the same screening program.

D-dimer

The association between D-dimer and expansion was demonstrated by Golledge e.a. ($r=0.39$; n=299).[26] In 2 studies an increased D-dimer level was found in patients suffering from AAA rupture (total n=139).[27,28] All studies had a low risk of bias.

Fibrinogen

Levels of fibrinogen were measured in ruptured AAA patients versus symptomatic and asymptomatic patients. All studies had a low risk of bias. In 2 studies fibrinogen was lower in ruptured than in non-ruptured patients (total n=269)[22,27], while Tambyraja e.a. measured higher levels in 12 symptomatic than in 39 asymptomatic AAA patients.[23]

Homocysteine

Homocysteine and AAA expansion were investigated in 3 studies, all with a low risk of bias. Halazun e.a.[29] were the only group to describe a significant correlation (r=0.28; n=108). The other 2 studies observed no association between homocysteine and AAA expansion (total n=248).[13,21]

Interleukin-6 (IL-6)

IL-6 and AAA expansion were examined in 3 studies, but none observed a significant association.[21,30,31] Jones e.a. found no correlation in 466 follow-up patients (low bias risk). Flondell-Sité e.a. (low bias risk) observed no difference in IL-6 between 178 high versus low expansion rate AAA patients. Treska e.a. (high bias risk) included 90 patients and demonstrated no difference between patients that required surgery during follow-up versus asymptomatic patients.

Matrix metalloproteinase 9 (MMP-9)

In 3 studies, circulating MMP-9 was tested as marker for expansion. Flondell-Sité e.a., the largest study with the lowest risk of bias, found no correlation with AAA expansion in 163 follow-up patients.[32] In 2 smaller studies (medium bias risk), with 54 patients in total, significant correlations were described (r=0.32 and r=0.33).[10,33] Wilson e.a. (medium bias risk) demonstrated higher MMP-9 levels in patients with a ruptured AAA than in patients prior to elective repair.[34]

Plasminogen activator inhibitor 1 (PAI-1)

Lindholt e.a. observed a significant but weak correlation between PAI-1 and AAA expansion (r=0.02; n=70; low bias risk).[13] In 3 studies (total n=234; 1 medium risk of bias, 2 low risk), approximately 4 fold higher levels of PAI-1 were found in patients with a ruptured AAA than in non-ruptured AAA patients.[27,28,35]

S-elastin peptides (SEP)

In 3 studies SEP was investigated as marker for expansion[8,10,36] and 2 as marker for rupture.[37,38] Lindholt e.a. performed 3 different studies, including 205 follow-up patients in total, all demonstrating significant correlations with expansion (r=0.51 [medium bias risk], r=0.33 [medium bias risk] and r=0.31 [low bias risk]). In 100 AAA patients with a rupture during follow-up, SEP had a significantly predictive value (area under curve=0.68; medium bias risk).[37] Petersen e.a., appraised with a low risk of bias, found a significant difference between 15 patients with a ruptured AAA versus 45 patients prior to elective repair.[38] Note that 1 research group, using patients from the same AAA

screening cohort, performed 4 of 5 studies. The degree of patient overlap between studies, if any, is not clear.

Tissue inhibitor metalloproteinase 1 (TIMP-1)

Speelman e.a.[18] (n=18) and Flondell-Sité e.a.[32] (n=163) investigated TIMP-1 as marker for expansion. Their studies had, respectively, low and medium bias risk. Wilson e.a.[34] (medium bias risk) examined TIMP-1 as marker for rupture in 68 patients. None found significant outcomes.

Tissue plasminogen activator (tPA)

Lindholt e.a. demonstrated a significant correlation between circulating tPA and AAA expansion (r=0.37; n=70; low bias risk).[13] Remarkably, Adam e.a. and Hobbs e.a. measured lower levels of tPA in patients with a ruptured AAA versus non-ruptured (total n=139; low and medium risk of bias, respectively)[27,35], while Skagius e.a. observed 1.7 fold higher levels in 50 ruptured AAA patients than in 45 electively treated AAA (low bias risk).[28]

α-1 antitrypsine

Significant correlations with expansion were found in 2 studies (1 low and 1 medium bias risk; r=0.55 and r=0.42) with 61 follow-up patients in total[10,39], while 2 studies (1 low and 1 medium bias risk) could not reproduce such significant correlations in 66 follow-up patients.[18,40] Pulinx e.a., however, did reach significance when initial AAA diameter was included in their multivariate model.[40]

Other included biomarkers that have not been mentioned above are markers in the field of connective tissue[41], lipids[42,43], the immune system[44–51], kidney function[52,53] and hormones[54,55] (see table 2.1).

3.3 Biomechanical markers

A total of 33 studies investigated 28 biomechanical AAA properties as marker for expansion or rupture (table 2.2). Markers were categorized as anatomic properties (13 markers), radiographic properties (3 markers) or as vessel wall properties (9 markers). The fourth category contains 3 software calculated predictive indices. The following focuses on markers described in 3 or more publications.

AAA diameter

In 9 studies AAA diameter was described as maker for expansion[8,17,19,21,40,56–59] and in 9 as marker for rupture.[34,37,60–66] Overall, the data is reliable as 2570 patients in total were

included and 8 studies were appraised with low bias risk, 7 with medium risk and only 3 with high risk. In 7 studies significant correlations with expansion were demonstrated in 958 patients in total (r=0.30–0.83)[8,21,40,56–58], and Norman e.a. measured faster growth in patients with a large (≥ 4 cm; n=112) versus small AAA (3 – 4 cm; n=433).[19] In 6 studies, with a total of 552 patients, significant outcomes were demonstrated for AAA diameter as marker for rupture. In 5 studies larger diameters were measured in ruptured (and symptomatic) AAA when compared to asymptomatic patients[34,60,61,64,65], and 1 study demonstrated aneurysm diameter as prognostic marker for rupture (area under curve=0.67).[37] In 3 studies, of which 2 with high bias risk, no difference was found in diameter between ruptured AAA patients versus patients prior to elective repair (total n=80).[62,63,66]

Fluorodeoxyglucose (18F-FDG) uptake

Maximum ^{18}F-FDG uptake after PET-scanning was studied as marker for expansion in 3 studies[67–69] and in 1 study as marker for rupture.[70] All 3 studies demonstrated significant inverse correlations with aneurysm expansion (r=-0.50 (medium bias risk), r=-0.38 (low bias risk) and r=-0.32 (medium bias risk); total n=104). Reeps e.a. however, found higher uptake in symptomatic versus asymptomatic AAA patients (n=15; medium bias risk).

Intraluminal thrombus (ILT) volume

In 3 studies, ILT volume was focused on. In 2 studies as marker for expansion[33,71] and in 1 as marker for rupture[60], all studies had medium risk of bias. Speelman e.a. measured significantly higher expansion rates in patients with a large ILT volume (≥ 32% of the total aneurysm sac) versus a small ILT volume (total n=30). Kontopodis e.a. found a significant correlation (r=0.60) with expansion in 34 follow-up patients. Erhart e.a. measured larger ILT volumes in ruptured AAA than in follow-up patients (total n=75).

Peak wall stress (PWS)

The aortic PWS was investigated as marker for AAA rupture in 9 studies.[60,62–64,66,72–75] In 7 studies, significant higher PWS (ranging 1.29–1.66 fold higher) were found in ruptured (and symptomatic) AAA patients than in asymptomatic AAA patients (2 low risk, 4 medium risk and 1 high risk of bias; total n=536). According to Truijers e.a., PWS was higher in 10 ruptured AAA than in 10 diameter matched asymptomatic patients. In 2 studies no difference was found between ruptured and electively treated AAA. However, the latter 2 included only 43 patients in total and both had high risk of bias.

Other biomechanical markers that have not been mentioned above but are included concern anatomic properties (see table 2.2).[76–79]

Table 2.2 Biomechanical markers that have been investigated for an association with AAA expansion or rupture. Markers are categorized by different properties which can be measured after radiographic scanning. The total amount of studies and significant outcomes are presented as well as the total number of patients in studies pooled.

Marker	Total studies (n)	Significant outcome	Total patients (n)
Anatomic properties			
AAA diameter[8,17,19,21,34,37,40,56–66]	18	15 of 18 studies	2570
AAA expansion[76,77]	2	1 of 2 studies	1125
AAA surface area[76]	1	0 of 1 studies	52
AAA volume[71]	1	1 of 1 studies	34
Aortic diameter asymmetry[78]	1	1 of 1 studies	200
Aortic tortuosity[78]	1	1 of 1 studies	200
Intra luminal thrombus (ILT) area[57,76]	2	2 of 2 studies	469
ILT circumference[78]	1	0 of 1 studies	200
ILT location[79]	1	1 of 1 studies	34
ILT thickness[71,78]	2	1 of 2 studies	234
ILT volume[33,60,71]	3	3 of 3 studies	139
Lumbar 3 vertebral body diameter[78]	1	1 of 1 studies	200
Peak wall stress equivalent diameter[75]	1	0 of 1 studies	243
Predictive indices			
Peak wall rupture index (PWRI)[60,75]	2	2 of 2 studies	303
PWRI equivalent diameter[60,75]	2	1 of 2 studies	303
Rupture potential index[61,62]	2	1 of 2 studies	66
Radiographic properties			
LaPlace[66] *	1	0 of 1 studies	48
Medium filter texture parameter kurtosis[67]	1	1 of 1 studies	40
^{18}F-FDG uptake[67–70] **	4	4 of 4 studies	119
Vessel wall properties			
Stiffnes (ß)[56,65]	2	0 of 2 studies	108
Minimal strenght[61]	1	0 of 1 studies	53
Mean wall stress (MWS)[18,74]	2	1 of 2 studies	99
Peak wall stress (PWS) [60,62–64,66,72–75]	9	7 of 9 studies	579
Pressure strain elastic modules (Ep)[56,65]	2	0 of 2 studies	108
Von Mises strain[61] ***	1	1 of 1 studies	53
Von Mises stress[61] ***	1	1 of 1 studies	53
Wall displacement[61]	1	1 of 1 studies	53
Wall strength[62]	1	1 of 1 studies	13

* LaPlace = law of LaPlace (pressure = surface tension / radius); ** ^{18}F-FDG uptake as measured by positron emission tomography; *** Von Mises strain and stress are calculations of tensile stress according to Maximum Distortion Energy Theory of Failure.

3.4 Genetic variations

In 9 studies 20 genetic markers were elaborated on (table 2.3). None of the following markers were described in more than 1 study. These genetic markers are therefore not evaluated as extensively as circulating and biomechanical markers in this review.

CCR5 gene was the only gene examined as marker for rupture. Ghilardi e.a. demonstrated a higher percentage of *CCR5* gene Δ32 deletion mutation in ruptured AAA patients (n=21) than in electively treated AAA patients (n=49; 48 versus 18%, respectively).[80]

The following markers were all investigated in AAA follow-up patients and were associated with the aneurysm growth rate. Gerdes e.a. identified that *APOE* mutations are associated with higher growth rates in 57 patients.[81] Wiernicki e.a. measured higher growth rates in 41 patients with a Haptoglobin 2-1 phenotype than in 13 patients with a Haptoglobin 1-1 phenotype.[20] Duellman e.a. included 141 patients and demonstrated that mutations in the following genes are associated with a growth speed of 3.25 mm per year or more: *LRP1* (OR 5.0), *MMP9* p-2502 (OR 2.2) and *MTHFR* (OR 3.0)[82]. No such differences were measured with the following genes: *IL-6* (n=466)[31], *Cystatin C* (n=412)[83], *OPN* (n=198)[84] and 9p21 (n=741)[85]. Of 20 investigated genetic markers, 10 were investigated by Wanhainen e.a.[86] in 169 follow-up patients (all concerning microRNA as marker for expansion), of which 8 markers demonstrated significant differences between slow and fast growing AAA.

Table 2.3 Genetic variations that have been investigated for an association with AAA expansion or rupture. The total amount of studies and significant outcomes are presented as well as the total number of patients in studies pooled.

Marker	Total studies (n)	Significant outcome	Total patients (n)
APOE gene[81]	1	1 of 1 studies	57
IL-6 gene[31]	1	0 of 1 studies	466
Cystatin C gene[83]	1	0 of 2 studies	412
CCR5 gene[80]	1	1 of 1 studies	70
OPN gene[84]	1	0 of 1 studies	198
Chromosome 9p21[85]	1	0 of 1 studies	741
Haptoglobin 2-1[20]	1	1 of 1 studies	83
LRP1 gene[82]	1	1 of 1 studies	141
MMP-9 p-2502 gene[82]	1	1 of 1 studies	141
MTHFR gene[82]	1	1 of 1 studies	141
miR-125a-5p[86]	1	1 of 1 studies	169
miR-136-5p[86]	1	0 of 1 studies	169
miR-195-5p[86]	1	1 of 1 studies	169

Table 2.3 Continued

Marker	Total studies (n)	Significant outcome	Total patients (n)
miR-221-3p[86]	1	1 of 1 studies	169
miR-223-3p[86]	1	1 of 1 studies	169
miR-30a-5p[86]	1	0 of 1 studies	169
miR-326[86]	1	1 of 1 studies	169
miR-335-p[86]	1	1 of 1 studies	169
miR-421[86]	1	1 of 1 studies	169
miR-99a-5p[86]	1	1 of 1 studies	169

4. DISCUSSION

Numerous markers have been investigated as predictive factor for AAA expansion and rupture. All markers described in 3 or more studies were described in more detail and summarized in table 2.4. Thus, we focused on 14 markers of which 5 were investigated as marker for expansion, 1 as marker for rupture and 8 as marker for both. Markers were qualified as high potential based on sample size, quality appraisal of the study and significant outcomes. The highest potential as a prognostic marker for AAA expansion are in descending order: AAA diameter, chlamydophila pneumoniae; S-elastin peptides; and ^{18}F-FDG uptake. Factors with high potential as marker for aneurysm rupture are in descending order: PWS, AAA diameter and plasminogen activator inhibitor 1 (PAI-1). The following 2 markers were described in only 2 studies but had remarkable results and are therefore separately mentioned: intraluminal thrombus (ILT) as marker for expansion and S-elastin peptides as marker for rupture. Little research has been done on genetic markers for rupture and growth, as this is a relatively new area of research. We therefore evaluated none of the genetic markers in detail.

AAA diameter is broadly accepted as predictive factor for both aneurysm growth and rupture, and is thus implemented in important AAA follow-up guidelines.[2,3] Our systematic review confirmed the strong prognostic value for expansion as 8 of 9 studies had significant outcomes, with mainly low bias risks and low p-values in a total of 1503 patients. However, correlation coefficients do have a relatively broad range with values varying from r=0.30 to r=0.83. Overall, these studies demonstrate that large aneurysms grow faster than small AAA do.

Chlamydophila pneumoniae was already identified as causative factor for inflammation and atherosclerosis of the aorta.[87] The bacterial infection induces degenerative

processes in the aortic wall, which might explain the strong correlation of antibodies against chlamydophila pneumoniae with AAA expansion. All 4 studies, with mainly medium bias risks, had significant outcomes and consistent results, of which 3 had very low p-values. Therefore it seems to be a reliable marker for AAA expansion in case of seropositivity.

S-elastin peptides are derived from the enzymatic degradation of insoluble elastic polymers in the vessel wall by MMP.[88] In all studies this marker was significantly correlated with AAA expansion and bias risks were medium. However, 1 group performed 4 of 5 studies using patients from the same AAA screening cohort. Therefore other groups should first reproduce these data before S-elastin peptides can be applied as marker for expansion.

Metabolic activity in the aneurysm wall can be measured by positron emission tomography. Locations of high ^{18}F-FDG uptake in the aneurysm wall were demonstrated to accumulate MMP and other factors of aortic deterioration.[89] It therefore seems contradictive that an inverse correlation was found between ^{18}F-FDG uptake and expansion in all 3 studies. The current explanation is that an inflammatory period precedes a phase of rapid growth and is then followed by a period of stasis with low metabolic activity.[67–70] However, this phenomenon is clearly not fully explained yet. Overall, ^{18}F-FDG uptake studies were appraised with medium bias risks and had consistent results with relatively low p-values. Therefore it seems a reliable marker for AAA expansion.

An ILT is the source of many pro-proteolytic processes that stimulate aortic wall degradation.[90] We designated this marker as promising due to a clear association of ILT volume with expansion, even though relatively small patient numbers were included in only 2 studies. However, Kontopodis, Nguyen and Behr-Rahsmussen e.a. also demonstrated the ILT to be correlated with AAA expansion in 694 follow-up patients in total (i.e. ILT thickness, signal intensity and surface area, respectively). [57,71,91] In total, 5 studies have elaborated on the ILT size as marker for expansion in 758 patients, with on average a medium bias risk. These data plead for the ILT size as promising prognostic growth marker. However, there have been several studies demonstrating a correlation between ILT presence and AAA diameter.[58,71] The presented associations between ILT and AAA expansion might be the result of multi-co-linearity due to the strong correlation between AAA diameter and its growth speed. Therefore, before clinical implementation more homogenous studies must be produced. In those studies AAA

diameter should be corrected for as confounding factor before ILT can be considered a reliable growth marker.

A potential marker for rupture is PWS. To determine the stress on the aneurysm wall, a technique called finite element analysis is used. This is a numerical method to approximate the forces that are applied on the aortic wall. As aneurysms are not symmetrical dilations, the pressure in the aneurysm sac is heterogeneously divided. Finite element analysis enables software programs to calculate the peak wall stress (PWS) on the aneurysm wall.[63] In 7 of 9 studies PWS retrospectively differentiated between ruptured and non-ruptured AAA, but none investigated it as a prognostic value. In 2 studies no significant differences were found, but both had high bias risks and a total patient number of only 43. As significant differences were found in 536 patients, we suggest that PWS has high potential to contribute in AAA management.

AAA diameter has since long also been acknowledged as risk factor for aneurysm rupture and is used as indicator for elective repair surgery.[2,3] Our results are in line with this common use, although 3 of 9 studies found no differences between ruptured AAA versus patients prior to elective repair. It must be noted that in those 3 studies aneurysm diameters of the elective repair groups were all larger than current guidelines apply (6.8±1.5, 6.1±0.5 and 6.1±0.2 cm).

Another marker for rupture with promising results is PAI-1, a known marker for coronary heart disease that plays an essential role in fibrinolysis.[92] Its levels were approximately 4 times higher in 102 patients with a ruptured AAA than in asymptomatic patients. However, as the massive retroperitoneal hematoma and blood clotting could be the cause of PAI-1 activation, its use a prospective marker for rupture must be reconsidered. The activation of this pathway should first be fully elucidated before it is investigated as a marker for AAA rupture in a prospective trial.

S-elastin peptides have been investigated as marker for rupture by 2 separate groups. Promising results were demonstrated as both groups found highly significant associations. However, only 2 groups have reported on this marker yet in a total of 160 patients. Before it is implemented in a clinical setting, it should be studied more extensively.

Genetic variations and microRNA are relatively new markers for AAA expansion and rupture. Therefore little is known about its potential as prognostic tools, when compared to circulating and biomechanical markers. Gene mutations in the *FBN1*[93]

and *COL3A1*[94] genes, responsible for Marfans disease and Ehlers Danlos vascular type disease, respectively, are perhaps the best known genetic disorders leading to aortic aneurysms. However, despite the broad amount of studies describing these 2 important genetic mutations, no studies about *FBN1 or COL3A1* met our inclusion criteria. This might be explained by the fact that these disorders commonly cause thoracic and thoracoabdominal aortic aneurysms and also that growth rate and rupture are often totally unpredictable in these cases.

One major limitation of this review is the inability to pool data due to high clinical and methodological heterogeneity. Also, we considered biomarkers in the evidence which demonstrated a statistically significant association with an outcome (AAA rupture or growth); however, we recognize that this may have severe limitations as this choice is subject to type II errors, particularly in the case of studies with small sample sizes. Furthermore, the potential markers provided such heterogenic threshold values that direct clinical implementation is not possible based on the current data. More specific, prospective and methodological consonant research is necessary for the promising markers that we have identified, in which threshold values for follow-up and surgical intervention must be determined.

This review has identified several circulating and biomechanical markers with potential value for the prognosis of AAA expansion and rupture. As possible markers for expansion we suggest the use of AAA diameter, chlamydophila pneumonia in case of seropositivity, S-elastin peptides, inverse fluorodeoxyglucose uptake and ILT size. Markers with the best prognostic value for rupture are PWS and AAA diameter. Prospective trials are now required to determine threshold values for the clinical implementation of these markers. In conclusion, there are several potential markers for AAA expansion and rupture, which could contribute to better decision making in the management of AAA.

Table 2.4 All markers for AAA expansion or rupture that have been described in 3 or more studies have been evaluated in more detail. Presented are: the subject of the marker (on which aspect the marker was investigated: AAA expansion or rupture); first author and date of publication of the reference; the risk of bias; statistical method of measurement; the moment of data retrieval (during conservative follow-up of maximum aortic diameter, at time of presentation with symptomatic AAA or AAA rupture) and if applicable main clinical characteristic of the study and control groups (varying per study); the total sample size (cases and controls pooled); the correlation coefficient (negative correlation: -1 to 0; and positive correlation: 0 to 1) or the fold change (decrease: 0 to 1; and increase: above 1) of study group versus control group; and p-values. Note that significant ($p < 0.05$) outcomes are presented in bold font.

Marker subject	Reference	Risk of bias	Measurement	Study group
Cicrculating markers				
Aminoterminal propeptide of type III procollagen (PIIINP)				
Expansion	Lindholt e.a. (2001)[8]	Medium	Pearson	Follow-up
Expansion	Lindholt e.a. (2000)[10]	Medium	Spearman	Follow-up
Expansion	Satta e.a. (1997)[9]	High	Pearson	Follow-up
Chlamydophila pneumonia				
Expansion	Lindholt e.a. (2003)[13]	Low	Spearman	Follow-up
Expansion	Lindholt e.a. (1999)[11]	Medium	Fold change	Follow-up: IgA titre ≥ 20
Expansion	Lindholt e.a. (2001)[12]	Medium	Fold change	Follow-up: IgA titre ≥ 64
Expansion	Falkensammer e.a. (2007)[14]	High	Fold change	Follow-up: seropositive
Rupture	Nyberg e.a. (2007)[15]	Medium	Fold change	Rupture
Rupture	Nyberg e.a. (2008)[16]	Medium	Fold change	Rupture
CRP				
Expansion	De Haro e.a. (2012)[17]	Low	Spearman	Follow-up
Expansion	Norman e.a. (2004)[19]	Low	Fold change	Follow-up: expansion ≥ 3 mm/year
Expansion	Flondell-Sité e.a. (2009)[21]	Low	Fold change	Follow-up: expansion ≥ 2.5 mm/year
Expansion	Wiernicki e.a. (2010)[20]	Medium	Spearman	Follow-up
Expansion	Speelman e.a. (2010)[18]	Medium	Partial correlation	Follow-up
Rupture	Domanovits e.a. (2002)[22]	Low	Fold change	Rupture
Rupture	Tambyraja e.a. (2007)[23]	Low	Fold change	Symptomatic
Cotinine				
Expansion	Lindholt e.a. (2003)[13]	Low	Spearman	Follow-up
Expansion	Lindholt e.a. (2003)[25]	Medium	Spearman	Follow-up
Expansion	Wilmink e.a. (1999)[24]	Medium	Fold change	Follow-up: expansion ≥ 2 mm/year
D-dimer				
Expansion	Golledge e.a. (2011)[26]	Low	Spearman	Follow-up
Rupture	Adam e.a. (2002)[27]	Low	Fold change	Rupture

	Control group	N (total)	Correlation	Fold change	p-value
	–	99	0,24	–	**significant**
	–	36	no correlation	–	0,180
	–	55	0,15	–	0,260
	–	70	0,29	–	**0,006**
	Follow-up: IgA titre < 20	139	–	1,48	**0,003**
	Follow-up: IgA titre <64	55	–	1,69	**<0,050**
	Follow-up: seronegative	47	–	1,67	**0,046**
	Controls	77	–	1,01	0,397
	Controls	77	–	NA	ns
	–	260	0,71	–	**<0,050**
	Follow-up: expansion < 3 mm/year	545	–	NA	ns
	Follow-up: expansion < 2.5 mm/year	178	–	1,07	0,721
		83	–	0,32	**0,003**
	–	18	0,06	–	0,720
	Elective	225	–	4,80	**<0,050**
	Asymptomatic	112	–	4,40	**<0,001**
	–	70	0,23	–	**0,038**
	–	79	0,24	–	**0,040**
	Follow-up: expansion < 2 mm/year	447	–	1,00	ns
	–	299	0,39	–	**<0,001**
	Symptomatic	44	–	2,52	**0,005**

Table 2.4 Continued

Marker subject	Reference	Risk of bias	Measurement	Study group
Rupture	Skagius e.a. (2008)[28]	Low	Fold change	Rupture
Fibrinogen				
Rupture	Adam e.a. (2002)[27]	Low	Fold change	Rupture
Rupture	Domanovits e.a. (2002)[22]	Low	Fold change	Rupture
Rupture	Tambyraja e.a. (2007)[23]	Low	Fold change	Symptomatic
Homocysteine				
Expansion	Lindholt e.a. (2003)[13]	Low	Spearman	Follow-up
Expansion	Halazun e.a. (2007)[29]	Low	Spearman	Follow-up
Expansion	Flondell-Sité e.a. (2009)[21]	Low	Fold change	Follow-up: expansion ≥ 2.5 mm/year
IL-6				
Expansion	Jones e.a. (2001)[31]	Low	Spearman	Follow-up
Expansion	Flondell-Sité e.a. (2009)[21]	Low	Fold change	Follow-up: expansion ≥ 2.5mm/year
Expansion	Treska e.a. (2000)[30]	High	Fold change	Surgery during follow-up
MMP-9				
Expansion	Flondell-Sité e.a. (2010)[32]	Low	Spearman	Follow-up
Expansion	Lindholt e.a. (2000)[10]	Medium	Spearman	Follow-up
Expansion	Speelman e.a. (2010)[18]	Medium	Partial correlation	Follow-up
Rupture	Wilson e.a. (2008)[34]	Medium	Fold change	Rupture
Plasminogen activator inhibitor 1				
Expansion	Lindholt e.a. (2003)[13]	Low	Spearman	Follow-up
Rupture	Adam e.a. (2002)[27]	Low	Fold change	Rupture
Rupture	Skagius e.a. (2008)[28]	Low	Fold change	Rupture
Rupture	Hobbs e.a. (2007)[35]	Medium	Fold change	Rupture
S-elastin peptides				
Expansion	Lindholt e.a. (2001)[36]	Low	Pearson	Follow-up
Expansion	Lindholt e.a. (2001)[8]	Medium	Pearson	Follow-up
Expansion	Lindholt e.a. (2000)[10]	Medium	Spearman	Follow-up
Rupture	Petersen e.a. (2001)[38]	Low	Fold change	Rupture
Rupture	Lindholt e.a. (2001)[37]	Medium	AUC met 95% CI	Rupture

	Control group	N (total)	Correlation	Fold change	p-value
	Elective	95	–	4,53	**<0,001**
	Symptomatic	44	–	0,53	**0,033**
	Asymptomatic	225	–	0,94	**0,049**
	Asymptomatic	112	–	1,28	**<0,001**
	–	70	0,06	–	0,535
	–	108	0,28	–	**0,003**
	Follow-up: expansion < 2.5mm/year	178	–	1,00	0,940
	–	466	no correlation	–	ns
	Follow-up: expansion < 2.5mm/year	178	–	2,29	0,820
	Asymptomatic	90	–	2,19	ns
	–	163	no correlation	–	ns
	–	36	0,33	–	**0,010**
	–	18	0,32	–	**<0,050**
	Elective	68	–	3,37	**0,006**
	–	70	0,02	–	**0,015**
	Symptomatic	44	–	4,92	**0,023**
	Elective	95	–	4,33	**0,002**
	Elective	95	–	3,73	**0,001**
	–	70	0,31	–	**0,050**
	–	99	0,33	–	**Significant**
	–	36	0,51	–	**0,010**
	Elective	60	–	0,80	**0,001**
	–	100	0,68	–	**significant**

Table 2.4 Continued

Marker subject	Reference	Risk of bias	Measurement	Study group
TIMP-1				
Expansion	Flondell-Sité e.a. (2010)[32]	Low	Spearman	Follow-up
Expansion	Speelman e.a. (2010)[18]	Medium	Partial correlation	Follow-up
Rupture	Wilson e.a. (2008)[34]	Medium	Fold change	Rupture
Tissue plasminogen activator (tPA)				
Expansion	Lindholt e.a. (2003)[13]	Low	Spearman	Follow-up
Rupture	Adam e.a. (2002)[27]	Low	Fold change	Rupture
Rupture	Skagius e.a. (2008)[28]	Low	Fold change	Rupture
Rupture	Hobbs e.a. (2007)[35]	Medium	Fold change	Rupture
α-1 antitrypsine				
Expansion	Vega de Céniga e.a. (2009)[39]	Low	Spearman	Follow-up
Expansion	Pulinx e.a. (2011)[40]	Low	AUC met 95% CI	Follow-up
Expansion	Lindholt e.a. (2000)[10]	Medium	Spearman	Follow-up
Expansion	Speelman e.a. (2010)[18]	Medium	Partial correlation	Follow-up
Biomechanical markers				
AAA diameter				
Expansion	De Haro e.a. (2012)[17]	Low	Spearman	Follow-up
Expansion	Norman e.a. (2004)[19]	Low	OR	Follow-up ≥ 4 cm
Expansion	Tong e.a. (2015)[58]	Low	Pearson	Elective and Rupture
Expansion	Flondell-Sité e.a. (2010)[21]	Low	Pearson	Follow-up
Expansion	Pulinx e.a. (2011)[40]	Low	AUC met 95% CI	Follow-up
Expansion	Behr-Rasmussen e.a. (2014)[57]	Low	Pearson	Follow-up
Expansion	Lindholt e.a. (2001)[8]	Medium	Spearman	Follow-up
Expansion	Lindholt e.a. (2001)[8]	Medium	Pearson	Follow-up
Expansion	Wilson e.a. (1999)[56]	High	Spearman	Follow-up
Rupture	Fillinger e.a. (2003)[64]	Low	Fold change	Rupture and Symptomatic
Rupture	Fillinger e.a. (2002)[66]	Low	Fold change	Rupture
Rupture	Lindholt e.a. (2001)[37]	Medium	ROC curve	Rupture
Rupture	Wilson e.a. (2003)[65]	Medium	Fold change	Rupture
Rupture	Maier e.a. (2010)[61]	Medium	Fold change	Rupture and Symptomatic
Rupture	Erhart e.a. (2015)[60]	Medium	Fold change	Rupture
Rupture	Wilson e.a. (2008)[34]	Medium	Fold change	Rupture

	Control group	N (total)	Correlation	Fold change	p-value
	–	163	no correlation	–	ns
	–	18	0,12	–	0,510
	Elective	68	–	0,50	0,456
	–	70	0,37	–	**0,002**
	Symptomatic	44	–	0,16	**0,023**
	Elective	95	–	1,71	**<0,001**
	Elective	95	–	0,22	**0,036**
	–	25	0,55	–	**0,004**
	–	48	no correlation	–	ns
	–	36	0,42	–	**0,050**
	–	18	0,00	–	0,990
	–	435	0,31	–	>0,050
	Follow-up < 4 cm	545	–	7,20	**0,050**
	–	33	0,70	–	**0,010**
	–	178	0,39	–	**0,001**
	–	48	0,83	–	**0,001**
	–	416	0,30	–	**0,001**
	–	124	0,30	–	**0,010**
	–	99	0,48	–	**0,000**
	–	60	0,60	–	**<0,050**
	Elective	61	–	1,03	**0,000**
	Elective	40	–	1,13	0,100
	–	100	0,67	–	**0,011**
	Follow-up	210	–	1,12	**0,001**
	Elective	53	–	1,33	**0,006**
	Follow-up	60	–	1,42	**<0,001**
	Elective	68	–	1,67	**<0,001**

Table 2.4 Continued

Marker subject	Reference	Risk of bias	Measurement	Study group
Rupture	Venkatasubramaniam ea (2004)[63]	High	Fold change	Rupture
Rupture	Vande Geest e.a. (2006)[62]	High	Fold change	Rupture
Fluorodeoxyglucose (18F-FDG)				
Expansion	Kotze e.a. (2014)[67]	Low	Spearman	Follow-up
Expansion	Morel e.a. (2015)[69]	Medium	Spearman	Follow-up
Expansion	Kotze e.a. (2011)[68]	Medium	Spearman	Follow-up
Rupture	Reeps e.a. (2008)[70]	Medium	Fold change	Symptomatic
ILT volume				
Expansion	Speelman e.a. (2010)[33]	Medium	Fold change	Follow-up: ILT volume ≥ 32%
Expansion	Kontopodis e.a. (2014)[71]	Medium	Spearman	Follow-up
Rupture	Erhart e.a. (2015)[60]	Medium	Fold change	Rupture
Peak wall stress (PWS)				
Rupture	Fillinger e.a. (2003)[64]	Low	Fold change	Rupture and Symptomatic
Rupture	Fillinger e.a. (2002)[66]	Low	Fold change	Rupture
Rupture	Gasser e.a. (2014)[75]	Medium	Fold change	Rupture
Rupture	Erhart e.a. (2015)[60]	Medium	Fold change	Rupture
Rupture	Truijers e.a. (2007)[72]	Medium	Fold change	Rupture
Rupture	Heng e.a. (2008)[73]	Medium	Fold change	Rupture
Rupture	Venkatasubramaniam ea (2004)[63]	High	Fold change	Rupture
Rupture	Vande Geest e.a. (2006)[62]	High	Fold change	Rupture
Rupture	Vande Geest e.a. (2008)[74]	High	Fold change	Rupture

	Control group	N (total)	Correlation	Fold change	p-value
	Elective	27	–	1,11	0,197
	Elective	13	–	1,11	0,260
	–	40	-0,38	–	**0,015**
	–	39	-0,32	–	**0,049**
	–	25	-0,50	–	**0,011**
	Elective	15	–	2,14	**<0,001**
	Follow-up: ILT volume < 32%	30	–	NA*	**<0,010**
	–	34	0,60	–	**0,001**
	Follow-up	75	–	2,00	**0,015**
	Elective	61	–	1,38	**<0,001**
	Elective	40	–	1,29	**0,030**
	Follow-up	243	–	1,62	**<0,001**
	Follow-up	75	–	1,57	**<0,001**
	Follow-up	20	–	1,30	**0,040**
	Elective	70	–	1,66	**0,008**
	Elective	27	–	1,65	**0,004**
	Elective	13	–	1,08	0,620
	Elective	30	–	1,09	0,550

REFERENCES

1. Kuivaniemi H, Ryer EJ, Elmore JR, Tromp G. Understanding the pathogenesis of abdominal aortic aneurysms. *Expert Rev Cardiovasc Ther*. 2015;13:975-987. doi:10.1586/14779072.2015.1074861.
2. Chaikof EL, Brewster DC, Dalman RL, Makaroun MS, Illig KA, Sicard GA, Timaran CH, Upchurch GR, Veith FJ. SVS practice guidelines for the care of patients with an abdominal aortic aneurysm: Executive summary. *J Vasc Surg*. 2009;50:880-896. doi:10.1016/j.jvs.2009.07.001.
3. Moll FL, Powell JT, Fraedrich G, Verzini F, Haulon S, Waltham M, Van Herwaarden JA, Holt PJE, Van Keulen JW, Rantner B, Schlosser FJV, Setacci F, Ricco JB. Management of abdominal aortic aneurysms clinical practice guidelines of the European society for vascular surgery. *Eur J Vasc Endovasc Surg*. 2011;41(SUPPL. 1). doi:10.1016/j.ejvs.2010.09.011.
4. Moher, D; Liberati, A; Tetzlaff J, Altman D. Preferred reporting items for systematic reviews and meta-analyses: the PRISMA statement... Preferred Reporting Items for Systematic reviews and Meta-Analyses. *Int J Surg*. 2010;8:336-341. doi:10.1016/j.ijsu.2010.02.007.
5. Hayden J a, Cote P, Bombardier C. Annals of Internal Medicine Academia and Clinic Evaluation of the Quality of Prognosis Studies in Systematic Reviews. *Ann Intern Med*. 2006;144:427-438. http://www.annals.org/content/144/6/427.short.
6. Higgins JPT, Thompson SG, Deeks JJ, Altman DG. Measuring inconsistency in meta-analyses. *BMJ Br Med J*. 2003;327(7414):557-560. doi:10.1136/bmj.327.7414.557.
7. Field AP. Meta-analysis of correlation coefficients: A Monte Carlo comparison of fixed- and random-effects methods. *Psychol Methods*. 2001;6:161-180. doi:10.1037//1082-989X.6.2.161.
8. Lindholt JS, Heickendorff L, Vammen S, Fasting H, Henneberg EW. Five-year results of elastin and collagen markers as predictive tools in the management of small abdominal aortic aneurysms. *Eur J Vasc Endovasc Surg*. 2001;21:235-240. doi:10.1053/ejvs.2001.1329.
9. Satta J, Haukipuro K, Kairaluoma MI, Juvonen T. Aminoterminal propeptide of type III procollagen in the follow-up of patients with abdominal aortic aneurysms. *J Vasc Surg*. 1997;25:909-915. doi:10.1016/S0741-5214(97)70222-2.
10. Lindholt J, Vammen S, Fasting H, Henneberg E, Heickendorff L. The plasma level of matrix metalloproteinase 9 may predict the natural history of small abdominal aortic aneurysms. A preliminary study. *Eur J Vasc Endovasc Surg*. 2000;20:281-285. doi:10.1053/ejvs.2000.1151.
11. Lindholt JS, Juul S, Vammen S, Lind I, Fasting H, Henneberg EW. Immunoglobulin A antibodies against Chlamydia pneumoniae are associated with expansion of abdominal aortic aneurysm. *Br J Surg*. 1999;86:634-638. doi:10.1046/j.1365-2168.1999.01126.x.
12. Lindholt JS, Ashton HA, Scott RAP. Indicators of infection with Chlamydia pneumoniae are associated with expansion of abdominal aortic aneurysms. *J Vasc Surg*. 2001;34:212-215. doi:10.1067/mva.2001.115816.
13. Lindholt JS, Jørgensen B, Shi GP, Henneberg EW. Relationships between activators and inhibitors of plasminogen, and the progression of small abdominal aortic aneurysms. *Eur J Vasc Endovasc Surg*. 2003;25:546-551. doi:10.1053/ejvs.2002.1872.

14. Falkensammer B, Duftner C, Seiler R, Pavlic M, Walder G, Wilflingseder D, Stoiber H, Klein-Weigel P, Dierich M, Fraedrich G, Würzner R, Schirmer M. Lack of microbial DNA in tissue specimens of patients with abdominal aortic aneurysms and positive Chlamydiales serology. *Eur J Clin Microbiol Infect Dis*. 2007;26:141-145. doi:10.1007/s10096-006-0245-5.

15. Nyberg A, Skagius E, Nilsson I, Ljungh A, Henriksson AE. Lack of Association Between Chlamydophila Pneumoniae Seropositivity and Abdominal Aortic Aneurysm. *Vasc Endovascular Surg*. 2007;41:246-248. doi:10.1161/01.CIR.0000054210.62588.ED.

16. Nyberg A, Skagius E, Englund E, Nilsson I, Ljungh Å, Henriksson AE. Abdominal Aortic Aneurysm and the Impact of Infectious Burden. *Eur J Vasc Endovasc Surg*. 2008;36:292-296. doi:10.1016/j.ejvs.2008.04.017.

17. De Haro J, Acin F, Bleda S, Varela C, Medina FJ, Esparza L. Prediction of asymptomatic abdominal aortic aneurysm expansion by means of rate of variation of C-reactive protein plasma levels. *J Vasc Surg*. 2012;56:45-52. doi:10.1016/j.jvs.2012.01.003.

18. Speelman L, Hellenthal FA, Pulinx B, Bosboom EMH, Breeuwer M, Van Sambeek MR, Van de Vosse FN, Jacobs MJ, Wodzig WKWH, Schurink GWH. The Influence of Wall Stress on AAA Growth and Biomarkers. *Eur J Vasc Endovasc Surg*. 2010;39:410-416. doi:10.1016/j.ejvs.2009.12.021.

19. Norman P, Spencer CA, Lawrence-Brown MM, Jamrozik K. C-reactive protein levels and the expansion of screen-detected abdominal aortic aneurysms in men. *Circulation*. 2004;110:862-866. doi:10.1161/01.CIR.0000138746.14425.00.

20. Wiernicki I, Safranow K, Baranowska-Bosiacka I, Piatek J, Gutowski P. Haptoglobin 2-1 phenotype predicts rapid growth of abdominal aortic aneurysms. *J Vasc Surg*. 2010;52:691-696. doi:10.1016/j.jvs.2010.03.016.

21. Flondell-Sité D, Lindblad B, Gottsäter A. High levels of endothelin (ET)-1 and aneurysm diameter independently predict growth of stable abdominal aortic aneurysms. *Angiology*. 2010;61:324-328. doi:10.1177/0003319709344190.

22. Domanovits H, Schillinger M, Müllner M, Hölzenbein T, Janata K, Bayegan K, Laggner AN. Acute phase reactants in patients with abdominal aortic aneurysm. *Atherosclerosis*. 2002;163:297-302. http://www.ncbi.nlm.nih.gov/pubmed/12052476.

23. Tambyraja AL, Dawson R, Valenti D, Murie JA, Chalmers RT. Systemic inflammation and repair of abdominal aortic aneurysm. *World J Surg*. 2007;31:1210-1214. doi:10.1007/s00268-007-9014-6.

24. Wilmink TBM, Quick CRG, Day NE. The association between cigarette smoking and abdominal aortic aneurysms. *J Vasc Surg*. 1999;30:1099-1105. doi:10.1016/S0741-5214(99)70049-2.

25. Lindholt JS, Jørgensen B, Klitgaard NA, Henneberg EW. Systemic levels of cotinine and elastase, but not pulmonary function, are associated with the progression of small abdominal aortic aneurysms. *Eur J Vasc Endovasc Surg*. 2003;26:418-422. doi:10.1016/S1078-5884(03)00177-1.

26. Golledge J, Muller R, Clancy P, McCann M, Norman PE. Evaluation of the diagnostic and prognostic value of plasma D-dimer for abdominal aortic aneurysm. *Eur Heart J*. 2011;32:354-364. doi:10.1093/eurheartj/ehq171.

27. Adam DJ, Haggart PC, Ludlam CA, Bradbury AW. Hemostatic markers before operation in patients with acutely symptomatic nonruptured and ruptured infrarenal abdominal aortic aneurysm. *J Vasc Surg*. 2002;35:661-665. doi:10.1067/mva.2002.121755.

28. Skagius E, Siegbahn A, Bergqvist D, Henriksson AE. Fibrinolysis in patients with an abdominal aortic aneurysm with special emphasis on rupture and shock. *J Thromb Haemost*. 2008;6:147-150. doi:10.1111/j.1538-7836.2007.02791.x.

29. Halazun KJ, Bofkin KA, Asthana S, Evans C, Henderson M, Spark JI. Hyperhomocysteinaemia is Associated with the Rate of Abdominal Aortic Aneurysm Expansion. *Eur J Vasc Endovasc Surg*. 2007;33:391-394. doi:10.1016/j.ejvs.2006.10.022.

30. Třeška V, Topolčan O, Pecen L. Cytokines as plasma markers of abdominal aortic aneurysm. *Clin Chem Lab Med*. 2000;38:1161-1164. doi:10.1515/CCLM.2000.178.

31. Jones KG, Brull DJ, Brown LC, Sian M, Greenhalgh RM, Humphries SE, Powell JT. Interleukin-6 (IL-6) and the Prognosis of Abdominal Aortic Aneurysms. *Circulation*. 2001;103:2260-2265. doi:10.1007/978-1-60327-204-9.

32. Flondell-Sité D, Lindblad B, Kölbel T, Gottsäter A. Markers of proteolysis, fibrinolysis, and coagulation in relation to size and growth rate of abdominal aortic aneurysms. *Vasc Endovasc Surg*. 2010;44:262-268. doi:10.1177/1538574410361971.

33. Speelman L, Schurink GWH, Bosboom EMH, Buth J, Breeuwer M, Van de Vosse FN, Jacobs MH. The mechanical role of thrombus on the growth rate of an abdominal aortic aneurysm. *J Vasc Surg*. 2010;51:19-26. doi:10.1016/j.jvs.2009.08.075.

34. Wilson WRW, Anderton M, Choke EC, Dawson J, Loftus IM, Thompson MM. Elevated Plasma MMP1 and MMP9 are Associated with Abdominal Aortic Aneurysm Rupture. *Eur J Vasc Endovasc Surg*. 2008;35:580-584. doi:10.1016/j.ejvs.2007.12.004.

35. Hobbs SD, Haggart P, Fegan C, Bradbury AW, Adam DJ. The role of tissue factor in patients undergoing open repair of ruptured and nonruptured abdominal aortic aneurysms. *J Vasc Surg*. 2007;46:682-686. doi:10.1016/j.jvs.2007.05.057.

36. Lindholt JS, Jørgensen B, Fasting H, Henneberg EW. Plasma levels of plasmin-antiplasmin-complexes are predictive for small abdominal aortic aneurysms expanding to operation-recommendable sizes. *J Vasc Surg*. 2001;34:611-615. doi:10.1067/mva.2001.119040.

37. Lindholt JS, Ashton HA, Heickendorff L, Scott RAP. Serum elastin peptides in the preoperative evaluation of abdominal aortic aneurysms. *Eur J Vasc Endovasc Surg*. 2001;22:546-550. doi:10.1053/ejvs.2001.1516.

38. Petersen E, Gineitis A, Wågberg F, Ängquist KA. Serum levels of elastin-derived peptides in patients with ruptured and asymptomatic abdominal aortic aneurysms. *Eur J Vasc Endovasc Surg*. 2001;22:48-52. doi:10.1053/ejvs.2001.1404.

39. Vega de Céniga M, Esteban M, Quintana JM, Barba A, Estallo L, De la Fuente N, Viviens B, Martin-Ventura JL. Search for Serum Biomarkers Associated with Abdominal Aortic Aneurysm Growth – A Pilot Study. *Eur J Vasc Endovasc Surg*. 2009;37:297-299. doi:10.1016/j.ejvs.2008.11.014.

40. Pulinx B, Hellenthal FAMVI, Hamulyák K, Van Dieijen-Visser MP, Schurink GWH, Wodzig WKWH. Differential Protein Expression in Serum of Abdominal Aortic Aneurysm Patients e A Proteomic Approach. *Eur J Vasc Endovasc Surg*. 2011;42:563-570. doi:10.1016/j.ejvs.2011.07.019.

41. Treska V, Topolcan O. Plasma and tissue levels of collagen types I and III markers in patients with abdominal aortic aneurysms. *Int Angiol*. 2000;19:64-68.

42. Watt HC, Law MR, Wald NJ, Craig WY, Ledue TB, Haddow JE. Serum triglyceride: a possible risk factor for ruptured abdominal aortic aneurysm. *Int J Epidemiol*. 1998;27:949-952. doi:10.1093/ije/27.6.949.

43. Lindqvist M, Wallinder J, Bergström J, Henriksson AE. Plasma glycosylphosphatidylinositol phospholipase D (GPI-PLD) and abdominal aortic aneurysm. *Int J Clin Exp Med*. 2012;5:306-309.

44. Nyberg A, Skagius E, Nilsson I, Ljungh A, Henriksson AE. Abdominal aortic aneurysm and cytomegalovirus infection. *J Med Virol*. 2008;80:667-669. doi:10.1002/jmv.21022.

45. Nyberg A, Skagius E, Nilsson I, Ljungh A, Henriksson AE. Abdominal aortic aneurysm and infection with CagA positive strains of Helicobacter pylori. *Scand J Infect Dis*. 2008;40:204-207. doi:10.1080/00365540701642153.

46. Martelli-Junior H, Cotrim P, Graner E, Sauk JJ, Coletta RD. Effect of Transforming Growth Factor-ß1, Interleukin-6, and Interferon-γ on the Expression of Type I Collagen, Heat Shock Protein 47, Matrix Metalloproteinase (MMP)-1 and MMP-2 by Fibroblasts from Normal Gingiva and Hereditary Gingival Fibromatosis. *J Periodontol*. 2003;74:296-306.

47. Pan J-H, Lindholt JS, Sukhova GK, Baugh JA, Henneberg EW, Bucala R, Donnelly SC, Libby P, Metz C, Shi G-P. Macrophage migration inhibitory factor is associated with aneurysmal expansion. *J Vasc Surg*. 2003;37:628-635. doi:10.1067/mva.2003.74.

48. Ramos-Mozo P, Madrigal-Matute J, Vega de Ceniga M, Blanco-Colio LM, Meilhac O, Feldman L, Michel JB, Clancy P, Golledge J, Norman PE, Egido J, Martin-Ventura JL. Increased plasma levels of NGAL, a marker of neutrophil activation, in patients with abdominal aortic aneurysm. *Atherosclerosis*. 2012;220:552-556. doi:10.1016/j.atherosclerosis.2011.11.023.

49. Moran CS, McCann M, Karan M, Norman P, Ketheesan N, Golledge J. Association of osteoprotegerin with human abdominal aortic aneurysm progression. *Circulation*. 2005;111:3119-3125. doi:10.1161/CIRCULATIONAHA.104.464727.

50. Martinez-Pinna R, Ramos-Mozo P, Madrigal-Matute J, Blanco-Colio LM, Lopez JA, Calvo E, Camafeita E, Lindholt JS, Meilhac O, Delbosc S, Michel JB, De Ceniga MV, Egido J, Martin-Ventura JL. Identification of peroxiredoxin-1 as a novel biomarker of abdominal aortic aneurysm. *Arterioscler Thromb Vasc Biol*. 2011;31:935-943. doi:10.1161/ATVBAHA.110.214429.

51. Martín-Ventura JL, Lindholt JS, Moreno JA, Vega de Céniga M, Meilhac O, Michel JB, Egido J, Blanco-Colio LM. Soluble TWEAK plasma levels predict expansion of human abdominal aortic aneurysms. *Atherosclerosis*. 2011;214:486-489. doi:10.1016/j.atherosclerosis.2010.11.009.

52. Vega de Ceniga M, Esteban M, Barba A, Estallo L, Blanco-Colio LM, Martin-Ventura JL. Assessment of biomarkers and predictive model for short-term prospective abdominal aortic aneurysm growth-A pilot study. *Ann Vasc Surg*. 2014;28:1642-1648. doi:10.1016/j.avsg.2014.02.025.

53. Lindholt JS, Erlandsen EJ, Henneberg EW. Cystatin C deficiency is associated with the progression of small abdominal aortic aneurysms. *Br J Surg*. 2001;88:1472-1475. doi:10.1046/j.0007-1323.2001.01911.x.

54. Třeška V, Wenham PW, Valenta J, Topolčan O, Pecen L. Plasma Endothelin Levels in Patients with Abdominal Aortic Aneurysms. *Eur J Vasc Endovasc Surg*. 1999;17:424-428.

55. Lindholt JS, Martin-Ventura JL, Urbonavicius S, Ramos-Mozo P, Flyvbjerg A, Egido J, Henneberg EW, Frystyk J. Insulin-like growth factor i - A novel biomarker of abdominal aortic aneurysms. *Eur J Vasc Endovasc Surg*. 2011;42:560-562. doi:10.1016/j.ejvs.2011.07.013.

56. Wilson K, Whyman M, Hoskins P, Lee, AJ, Bradbury AW, Fowkes FGR, Ruckley CV. The relationship between abdominal aortic aneurysm wall compliance, maximum diameter and growth rate. *Cardiovasc Surg*. 1999;7:208-213. doi:10.1016/S0967-2109(98)00041-6.

57. Behr-Rasmussen C, Grøndal N, Bramsen MB, Thomsen MD, Lindholt JS. Mural thrombus and the progression of abdominal aortic aneurysms: A large population-based prospective cohort study. *Eur J Vasc Endovasc Surg*. 2014;48:301-307. doi:10.1016/j.ejvs.2014.05.014.

58. Tong J, Cohnert T, Holzapfel GA. Diameter-related variations of geometrical, mechanical, and mass fraction data in the anterior portion of abdominal aortic aneurysms. *Eur J Vasc Endovasc Surg*. 2015;49:262-270. doi:10.1016/j.ejvs.2014.12.009.

59. Lindholt JS, Heegaard NHH, Vammen S, Fasting H, Henneberg EW, Heickendorff L. Smoking, but not lipids, lipoprotein (a) and antibodies against oxidised LDL, is correlated to the expansion of abdominal aortic aneurysms. *Eur J Vasc Endovasc Surg*. 2001;21:51-56. doi:10.1053/ejvs.2000.1262.

60. Erhart P, Hyhlik-Dürr A, Geisbüsch P, Kotelis D, Müller-Eschner M, Gasser TC, Von Tengg-Kobligk H, Böckler D. Finite element analysis in asymptomatic, symptomatic, and ruptured abdominal aortic aneurysms: In search of new rupture risk predictors. *Eur J Vasc Endovasc Surg*. 2015;49:239-245. doi:10.1016/j.ejvs.2014.11.010.

61. Maier A, Gee MW, Reeps C, Pongratz J, Eckstein HH, Wall WA. A comparison of diameter, wall stress, and rupture potential index for abdominal aortic aneurysm rupture risk prediction. *Ann Biomed Eng*. 2010;38:3124-3134. doi:10.1007/s10439-010-0067-6.

62. Vande Geest JP, Di Martino ES, Bohra A, Makaroun MS, Vorp DA. A biomechanics-based rupture potential index for abdominal aortic aneurysm risk assessment: Demonstrative application. *Ann N Y Acad Sci*. 2006;1085:11-21. doi:10.1196/annals.1383.046.

63. Venkatasubramaniam AK, Fagan MJ, Mehta T, Mylankal KJ, Ray B, Kuhan G, Chetter IC, McCollum PT. A comparative study of aortic wall stress using finite element analysis for ruptured and non-ruptured abdominal aortic aneurysms. *Eur J Vasc Endovasc Surg*. 2004;28:168-176. doi:10.1016/j.ejvs.2004.03.029.

64. Fillinger MF, Marra SP, Raghavan ML, Kennedy FE. Prediction of rupture risk in abdominal aortic aneurysm during observation: Wall stress versus diameter. *J Vasc Surg*. 2003;37:724-732. doi:10.1067/mva.2003.213.

65. Wilson KA, Lee AJ, Hoskins PR, Fowkes FGR, Ruckley CV, Bradbury AW. The relationship between aortic wall distensibility and rupture of infrarenal abdominal aortic aneurysm. *J Vasc Surg*. 2003;37:112-117. doi:10.1067/mva.2003.40.

66. Fillinger MF, Raghavan ML, Marra SP, Cronenwett JL, Kennedy FE. In vivo analysis of mechanical wall stress and abdominal aortic aneurysm rupture risk. *J Vasc Surg*. 2002;36:589-597. doi:10.1067/mva.2002.125478.

67. Kotze CW, Rudd JHF, Ganeshan B, Menezes LJ, Brookes J, Agu O, Yusuf SW, Groves AM. CT signal heterogeneity of abdominal aortic aneurysm as a possible predictive biomarker for expansion. *Atherosclerosis*. 2014;233:510-517. doi:10.1016/j.atherosclerosis.2014.01.001.

68. Kotze CW, Groves AM, Menezes LJ, Harvey R, Endozo R, Kayani IA, Ell PJ, Yusuf SW. What is the relationship between 18F-FDG aortic aneurysm uptake on PET/CT and future growth rate? *Eur J Nucl Med Mol Imaging*. 2011;38:1493-1499. doi:10.1007/s00259-011-1799-8.

69. Morel O, Mandry D, Micard E, Kauffmann C, Lamiral Z, Verger A, Chevalier-Mathias E, Mathias J, Karcher G, Meneroux B, Rossignol P, Marie P-Y. Evidence of Cyclic Changes in the Metabolism of Abdominal Aortic Aneurysms During Growth Phases: 18F-FDG PET Sequential Observational Study. *J Nucl Med*. 2015;56:1030-1035. doi:10.2967/jnumed.114.146415.

70. Reeps C, Essler M, Pelisek J, Seidl S, Eckstein HH, Krause BJ. Increased 18F-fluorodeoxyglucose uptake in abdominal aortic aneurysms in positron emission/computed tomography is associated with inflammation, aortic wall instability, and acute symptoms. *J Vasc Surg*. 2008;48:417-423. doi:10.1016/j.jvs.2008.03.059.

71. Kontopodis N, Metaxa E, Papaharilaou Y, Georgakarakos E, Tsetis D, Ioannou CV. Value of volume measurements in evaluating abdominal aortic aneurysms growth rate and need for surgical treatment. *Eur J Radiol*. 2014;83:1051-1056. doi:10.1016/j.ejrad.2014.03.018.

72. Truijers M, Pol JA, SchultzeKool LJ, van Sterkenburg SM, Fillinger MF, Blankensteijn JD. Wall Stress Analysis in Small Asymptomatic, Symptomatic and Ruptured Abdominal Aortic Aneurysms. *Eur J Vasc Endovasc Surg*. 2007;33:401-407. doi:10.1016/j.ejvs.2006.10.009.

73. Heng MS, Fagan MJ, Collier JW, Desai G, McCollum PT, Chetter IC. Peak wall stress measurement in elective and acute abdominal aortic aneurysms. *J Vasc Surg*. 2008;47:17-22. doi:10.1016/j.jvs.2007.09.002.

74. Vande Geest JP, Schmidt DE, Sacks MS, David A. The effects of anisotropy on the stress analyses of patient- specific abdominal aortic aneurysms. *Ann Biomed Eng*. 2008;36:921-932. doi:10.1007/s10439-008-9490-3.

75. Gasser TC, Nchimi A, Swedenborg J, Roy J, Sakalihasan N, Böckler D, Hyhlik-Dürr A. A novel strategy to translate the biomechanical rupture risk of abdominal aortic aneurysms to their equivalent diameter risk: Method and retrospective validation. *Eur J Vasc Endovasc Surg*. 2014;47:288-295. doi:10.1016/j.ejvs.2013.12.018.

76. Stenbaek J, Kalin B, Swedenborg J. Growth of thrombus may be a better predictor of rupture than diameter in patients with abdominal aortic aneurysms. *Eur J Vasc Endovasc Surg*. 2000;20:466-469. doi:10.1053/ejvs.2000.1217.

77. Thompson AR, Cooper JA, Ashton HA, Hafez H. Growth rates of small abdominal aortic aneurysms correlate with clinical events. *Br J Surg*. 2010;97:37-44. doi:10.1002/bjs.6779.

78. Fillinger MF, Racusin J, Baker RK, Cronenwett Jack L, Teutelink A, Schermerhorn ML, Zwolak RM, Powell RJ, Walsh DB, Rzucidlo EM. Anatomic characteristics of ruptured abdominal aortic aneurysm on conventional CT scans: Implications for rupture risk. *J Vasc Surg*. 2004;39:1243-1252. doi:10.1016/j.jvs.2004.02.025.

79. Metaxa E, Kontopodis N, Tzirakis K, Ioannou C V., Papaharilaou Y. Effect of Intraluminal Thrombus Asymmetrical Deposition on Abdominal Aortic Aneurysm Growth Rate. *J Endovasc Ther*. 2015;22:406-412. doi:10.1177/1526602815584018.

80. Ghilardi G, Biondi ML, Battaglioli L, Zambon A, Guagnellini E, Scorza R. Genetic risk factor characterizes abdominal aortic aneurysm from arterial occlusive disease in human beings: CCR5 Delta 32 deletion. *J Vasc Surg*. 2004;40:995-1000. doi:10.1016/j.jvs.2004.08.014.

81. Gerdes LU, Lindholt JS, Vammen S, Henneberg EW, Fasting H. Apolipoprotein E genotype is associated with differential expansion rates of small abdominal aortic aneurysms. *Br J Surg*. 2000;87:760-765. doi:10.1046/j.1365-2168.2000.01486.x.

82. Duellman T, Warren CL, Matsumura J, Yang J. Analysis of multiple genetic polymorphisms in aggressive-growing and slow-growing abdominal aortic aneurysms. *J Vasc Surg*. 2014;60:613-621.e3. doi:10.1016/j.jvs.2014.03.274.

83. Eriksson P, Jones KG, Brown LC, Greenhalgh RM, Hamsten A, Powell JT. Genetic approach to the role of cysteine proteases in the expansion of abdominal aortic aneurysms. *Br J Surg*. 2004;91:86-89. doi:10.1002/bjs.4364.

84. Golledge J, Muller J, Shephard N, Clancy P, Smallwood L, Moran C, Dear AE, Palmer LJ, Norman PE. Association between osteopontin and human abdominal aortic aneurysm. *Arterioscler Thromb Vasc Biol*. 2007;27:655-660. doi:10.1161/01.ATV.0000255560.49503.4e.

85. Thompson AR, Golledge J, Cooper JA, Hafez H, Norman PE, Humphries SE. Sequence variant on 9p21 is associated with the presence of abdominal aortic aneurysm disease but does not have an impact on aneurysmal expansion. *Eur J Hum Genet*. 2009;17:391-394. doi:10.1038/ejhg.2008.196.

86. Wanhainen A, Mani K, Vorkapic E, De Basso R, Björck M, Lanne T, Wagsater D. Screening of circulating microRNA biomarkers for prevalence of abdominal aortic aneurysm and aneurysm growth. *Atherosclerosis*. 2017;256:82-88. doi:10.1016/j.atherosclerosis.2016.11.007.

87. Lindholt JS, Fasting H, Henneberg EW, Østergaard L. A review of Chlamydia pneumoniae and atherosclerosis. *Eur J Vasc Endovasc Surg*. 1999;17:283-289. doi:10.1053/ejvs.1998.0757.

88. Heinz A, Taddese S, Sippl W, Neubert RHH, Schmelzer CEH. Insights into the degradation of human elastin by matrilysin-1. *Biochimie*. 2011;93:187-194. doi:10.1016/j.biochi.2010.09.011.

89. Courtois A, Nusgens B V, Hustinx R, Namur G, Gomez P, Somja J, Defraigne J-O, Delvenne P, Michel J-B, Colige AC, Sakalihasan N. 18F-FDG uptake assessed by PET/CT in abdominal aortic aneurysms is associated with cellular and molecular alterations prefacing wall deterioration and rupture. *J Nucl Med*. 2013;54:1740-1747. doi:10.2967/jnumed.112.115873.

90. Swedenborg J, Eriksson P. The intraluminal thrombus as a source of proteolytic activity. *Ann N Y Acad Sci*. 2006;1085:133-138. doi:10.1196/annals.1383.044.

91. Nguyen VL, Leiner T, Hellenthal FAMVI, Backes WH, Wishaupt MCJ, Van der Geest RJ, Heeneman S, Kooi ME, Schurink GWH. Abdominal Aortic Aneurysms with High Thrombus Signal Intensity on Magnetic Resonance Imaging are Associated with High Growth Rate. *J Vasc Surg*. 2014;60:1713. doi:10.1016/j.jvs.2014.10.092.

92. Song C, Burgess S, Eicher JD, CHARGE Consortium Hemostatic Factor Working Group, ICBP Consortium, CHARGE Consortium Subclinical Working Group, O'Donnell CJ, Johnson AD. Causal effect of plasminogen activator inhibitor type 1 on coronary heart disease. *J Am Heart Assoc*. 2017;6. doi:10.1161/JAHA.116.004918.

93. Dietz HC. Marfan syndrome. In: *Marfan Syndrome. 2001 Apr 18 [Updated 2017 Feb 2]. In: Pagon RA, Adam MP, Ardinger HH, et al., Editors. GeneReviews® [Internet]. Seattle (WA): University of Washington, Seattle; 1993-2017.* https://www.ncbi.nlm.nih.gov/books/NBK1335/.

94. Beridze N, Frishman H. Vascular Ehlers-Danlos Syndrome: Pathophysiology, Diagnosis, and Prevention and Treatment of Its Complications. *Cardiol Rev*. 2012;20:4-7. doi:10.1097/CRD.0b013e3182342316.

95. Juvonen J, Surcel H-M, Satta J, Teppo A-M, Bloigu A, Syrjälä H, Airaksinen J, Leinonen M, Saikku P, Juvonen T. Elevated Circulating Levels of Inflammatory Cytokines in Patients With Abdominal Aortic Aneurysm. *Arterioscler Thromb Vasc Biol*. 1997;17:2843-2847.

CHAPTER 3

PEROXYNITRITE FOOTPRINT IN CIRCULATING NEUTROPHILS OF ABDOMINAL AORTIC ANEURYSM PATIENTS IS LOWER IN STATIN THAN IN NON-STATIN USERS

M.E. Groeneveld[1,2]
J.J. van der Reijden[3]
G.J. Tangelder[2]
L.C. Westin[4]
L. Renwarin[5]
R.J.P Musters[2]
W. Wisselink[1]
K.K. Yeung[1,2]

[1] Department of Vascular Surgery, Amsterdam University Medical Center
[2] Department of Physiology; Amsterdam University Medical Center
[3] Department of Radiology, Deventer Ziekenhuis, Deventer
[4] Center for Digestive Diseases, Karolinska University Hospital, Stockholm
[5] Medical Department Royal Netherlands Navy

European Journal of Vascular and Endovascular Surgery 2017 Sep, vol. 54(3), pag. 331-339

ABSTRACT

Objective: Extensive reactive oxygen and nitrogen species (also reactive species) production is a mechanism involved in abdominal aortic aneurysm (AAA) development. White blood cells (WBC) are a known source of reactive species. Its production is possibly decreased by statins, thereby reducing AAA growth rate. We investigated reactive oxygen and nitrogen species production in circulating WBC of AAA patients and the effect of statins on its production.

Methods: Venous blood from patients prior to elective AAA repair (n=34;1 8 statin users) and from healthy volunteers (n=10). Reactive species production was quantified in circulating WBC by immunofluorescence microscopy: nitrotyrosine (footprint of peroxynitrite, a potent reactive nitrogen species) in snap-frozen blood smears; mitochondrial superoxide and cytoplasmic hydrogen peroxide (both reactive oxygen species) by live cell imaging. We individually examined neutrophils, lymphocytes, and monocytes.

Results: In AAA patients using statins, the median neutrophil nitrotyrosine level was 646 (range: 422–2059), in lymphocytes 125 (range: 74–343) and in monocytes 586 (range: 291–663). Median levels in AAA patients not using statins were in neutrophils 928 (range: 552–2095, p=0.03), in lymphocytes 156 (range: 101–273; not significant [ns]) and in monocytes 536 (range: 535–1635; ns). Statin dose tended to correlate negatively with nitrotyrosine in neutrophils (Rs -0.32, p=0.06). The median levels in controls were lower in neutrophils 466 (range: 340–820, p<0.01) and in monocytes 191 (range: 102–386, p=0.03), while similar in lymphocytes 99 (range: 82–246) as compared to AAA patients pooled. There were no differences in mitochondrial superoxide and cytoplasmic hydrogen peroxide between statin and non-statin users within AAA patients.

Conclusions: We found that peroxynitrite footprint in circulating neutrophils and monocytes of AAA patients are higher than in controls. AAA patients treated by statins had lower levels of peroxynitrite footprint in neutrophils than non-statin users.

1. INTRODUCTION

Extensive production of reactive nitrogen and oxygen species (RNS and ROS), also referred to as reactive species, results in oxidative stress. Circulating white blood cells (WBC), mainly neutrophils, are capable of RNS and ROS production.[1] In the aortic wall oxidative stress can cause extracellular matrix (ECM) degeneration and smooth muscle cell apoptosis, which are recognized as hallmarks of abdominal aortic aneurysm (AAA) pathogenesis.[1–3]

Production of ROS, of which superoxide (O_2^-) and hydrogen peroxide (H_2O_2) are typical examples, and production of RNS, mainly peroxynitrite which is formed by a reaction of superoxide and nitric oxide, are among others facilitated by endothelial cells, smooth muscle cells and locally infiltrating WBC.[4–7] Nitrotyrosine is a footprint left after peroxynitrite and other RNS production.[8,9] Nitrotyrosine levels in cells therefore indicate the amount of RNS the cell has encountered. Several factors tend to influence levels of reactive species in the aneurysm wall.[10] Smoking is suggested to increase locally-produced oxidative stress in the aortic wall.[10] Statin therapy is thought to decrease local oxidative stress levels in the aneurysm wall.[11,12] An improved antioxidant capacity is likely involved, but a decrease in the formation of free radicals, if any, has so far not been shown and remains to be investigated.[13] Statins have even been proposed to decrease the aneurysm growth rate of small AAA.[14] However, not much is known about reactive species production in AAA patients and how statins can affect their production systemically. We sought to determine if systemically circulating WBC are also a source of reactive species in AAA patients and whether the production is influenced by statin therapy.

We hypothesized that in patients treated by statins the production of reactive species in circulating WBC will be lower than in untreated patients. In this study, we analyzed individual production of reactive species by circulating neutrophils, lymphocytes, and monocytes in AAA patients. We measured RNS via nitrotyrosine levels in the WBC and quantified ROS by direct measurement of mitochondrial superoxide and cytoplasmic hydrogen peroxide production via live cell imaging. We differentiated between AAA patients with and without statin therapy.

2. MATERIAL AND METHODS

The study was approved by the Medical Ethical Committee of the Amsterdam University Medical Center (AUMC) (reference number: 2010/193). Written informed consent was obtained from all patients and volunteers.

2.1 Patient selection and blood sample gathering

We consecutively included 34 AAA patients, of which 30 were males (in accordance with current epidemiology).[3] Venous blood from AAA patients was collected in EDTA-containing tubes prior to elective aneurysm repair in our medical center. Excluded subjects were those with acutely-treated AAA, ruptured or thoraco-abdominal aortic aneurysms, as the latter have a pathogenesis distinct from AAA.[15] As controls, we consecutively included the first 10 healthy persons (9 males) that voluntarily applied for the study. Exclusion criteria for the control group were any comorbidities, use of medications and age younger than 40 years.

Blood smears were made immediately and then snap frozen and stored in -80˚C until use. Blood samples were cooled at 4˚C and directly centrifuged, finally, the buffy coat was extracted. The buffy coat extract was then immediately resuspended for immunofluorescence labeling and live cell imaging (see below). Live cell imaging was performed within 2 hours after sample procurement (see study design in figure 3.1). Preoperative creatinine and total leukocyte measurements were performed by the department of Clinical Chemistry in the AUMC Manual leukocyte differential counts were performed on all blood smears. Aneurysm diameters were measured by computed tomography angiography. If multiple angiographies had been performed (n=12), aneurysmal growth is presented in cm per month.

2.2 Immunofluorescence staining

2.2.1 Measurement of peroxynitrite levels via nitrotyrosine

Blood smears were air-dried, fixed with 4% formalin, and washed in 0.05% Tween (cell washing solution). Smears were stained at room temperature with anti-nitrotyrosine rabbit IgG primary antibody for one hour (1:50; Molecular Probes) and Alexa 488 anti-rabbit secondary antibody for 30 minutes (1:100; Molecular Probes). The cell membrane glycocalyx was labeled with Alexa 555 fluorescent wheat-germ-agglutinin probe (1:50; Molecular Probes) and then mounted with Vectashield™ mounting medium-containing DAPI nuclear stain (Vector Laboratories Inc.). Negative control smears were treated in the same fashion, but without primary antibodies.

Table 3.1 AAA patient characteristics.
Patient characteristics of total AAA patients, subdivided in non-statin users and statin users. Data are presented as number (n), medians with ranges (outliers indicated separately) or as percentages. P-values are presented for comparison between the non-statin users and statin users (=p^1) and for comparison between control and total AAA patients (=p^2). Statistically significant differences are indicated by an asterisk.

	Total AAA patients	Non-statin users	Statin users	p^1	Controls	p^2
n	34	16	18	–	10	–
Male / Female *(n)*	30 / 4	14 / 2	16 / 2	1.00	9 / 1	1.00
Age *(years)*	74 (54 – 91)	74 (57 – 85)	74 (54 – 91)	0.51	53 (40 – 62)	0.03
Aneurysm diameter *(cm)*	6.3 (3.5 – 10.0)	6.3 (3.5 – 10.0)	6.4 (5.5 – 9.0)	0.86	–	–
Aneurysm growth *(cm/month)*	0.07 (0.05 – 0.13)	0.07 (0.06 – 0.10)	0.08 (0.05 – 0.13)	0.76	–	–
Aneurysm length *(cm)*	9.7 (5.1 – 18.0)	9.8 (5.5 – 18.0)	9.2 (5.1 – 17.7)	0.42	–	–
Aneurysm supra- vs infrarenal *(n)*	12 / 22	6 / 10	6 / 12	1.00	–	–
Symptoms *(n(%))*	12 (35)	6 (38)	6 (33)	0.80	–	–
Claudication[a] (n(%))	*9 (26)*	*3 (19)*	*6 (33)*	0.45	–	–
Restpain[a] (n(%))	*5 (15)*	*2 (13)*	*3 (17)*	1.00	–	–
Backpain (n(%))	*8 (24)*	*5 (31)*	*3 (17)*	0.43	–	–
Positive smoking history *(n(%))*	26 (76)	12 (75)	14 (78)	1.00	3 (33)	0.02
Coronary heart disease *(n(%))*	24 (71)	8 (50)	16 (89)	0.02*	0 (0)	<0.01
Hypertension *(n(%))*	26 (76)	13 (81)	13 (72)	0.69	0 (0)	<0.01
Hypercholesterolemia[b] *(n(%))*	14 (41)	1 (6)	13 (72)	<0.01*	0 (0)	<0.01
Diabetes *(n(%))*	4 (12)	1 (6)	3 (17)	0.60	0 (0)	0.56
Statin *(n(%))*	18 (53)	0 (0)	18 (100)	–	0 (0)	–
Antihypertensives *(n(%))*	28 (82)	12 (75)	16 (89)	0.39	0 (0)	–
Antiplatelets[c] *(n(%))*	17 (50)	3 (19)	14 (78)	0.02*	0 (0)	–
Creatinine[d] *(µmol/l)*	111 (64 – 447)	103 (85 – 259)	91 (64 – 447)	0.05*	not available	–
eGFR[e] *(ml/min/1.73m^2)*	63 (11 – 105)	58 (22 – 78)	70 (11 – 105)	0.08	not available	–
Leukocytes[f] *(10^9/l)*	8.0 (2.4 – 12.6)	8.2 (4.7 – 12.6)	8.0 (2.4 – 12.1)	0.68	8.4 (3.5 – 10.2)	0.48
Neutrophils (%)	81 (53 – 100)	80 (53 – 100)	81 (59 – 93)	0.69	80 (69 – 100)	0.74
Lymphocytes (%)	12 (0 – 39)	14 (0 – 39)	12 (0 – 24)	0.30	17 (0 – 26)	0.44
Monocytes (%)	2 (0 – 25)	0 (0 – 25)	10 (0 – 25)	0.22	3 (0 – 10)	0.35

[a] Fontaine 2a or 2b for claudication; 3 or 4 for leg rest pain; [b] Total cholesterol (TC) > 6.5 mmol/l or TC/ High Density Lipoprotein (HDL) ratio > 8; [c] Mainly aspirin, occasionally combined with dipyridamole; [d] Reference value between 40 and 100 µmol/l; [e] Estimated glomerular filtration rate (calculated by modification of diet in renal disease). Reference value is > 65 ml/min/1.73m^2; [f] Reference value is < 10 * 10^9/l.

2.2.2 Measurement of superoxide and hydrogen peroxide production via live cell imaging

Buffy coat extract was resuspended in ADS buffer at 37˚C (116mM NaCl/ 5.3mM KCL/ 1.2mM $MgSO_4$.$7H_2O$/ 1.13mM NaH_2PO_4.H_2O/ 20mM Hepes/5mM Glucose/ 1mM $CaCl_2$) and labeled with MitoSOX Red superoxide indicator (mitochondrial ROS) and 5-6-chloromethyl-2',7'-dichlorodihydrofluorescein diacetate (CM-DCF) acetyl ester C6827, sensitive for hydrogen peroxide (cytoplasmic ROS) according to the manufacturer

instructions (Molecular Probes). After 30 minutes of incubation at 37˚C with the latter probes, samples were then immediately analyzed by live cell imaging.

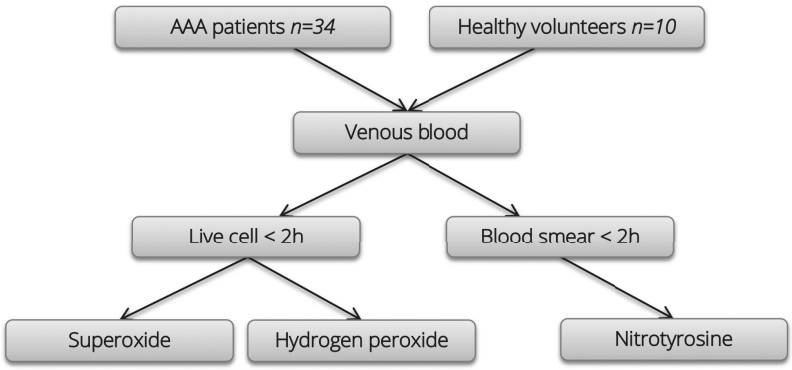

Figure 3.1 Study design
Diagram of the study design. Venous blood from AAA patients and healthy volunteers was analyzed. Superoxide and hydrogen peroxide were measured by live cell imaging and nitrotyrosine was measured by immunofluorescence microscopy.

2.3 Quantitative immunofluorescence microscopy: image acquisition, masking, and analysis

2.3.1 Image acquisition

A Zeiss Axiovert 200M Marianas™ inverted microscope was used, equipped with a motorized stage (stepper-motor) with z-axis increments of 0.1µm, and a turret with a DIC brightfield cube and three epifluorescence cubes. DAPI was visualised in blue, FITC in green (nitrotyrosine and hydrogen peroxide), and Cy3 in red (cell membrane and superoxide). A cooled Sensicam SVGA CCD camera (1280x1024 pixels; Cooke Co., USA), linear over its full dynamic range, recorded images with true 16-bit capability. The microscope, camera, and data processing were controlled by SlideBook™ software (version 4.2.0.1, Intelligent Imaging Innovations). Images were taken with a custom 40X oil objective (CARL ZEISS). Figures 3.2A–D, 3.4A–B and 3.5A–B show representative images of blood smear and live cell imaging, respectively.

To avoid artifactual induction of ROS generation, prior identification of WBC with CD45 antibodies was not performed. Manual differential count was performed based on morphological criteria (nucleus, cytoplasm and diameter) as described earlier.[16] Cells were identified as neutrophil (lobed nucleus; granule-filled cytoplasm), monocyte (round or kidney shaped nucleus; little cytoplasm; diameter ≥8μm) or lymphocyte (round nucleus; little cytoplasm; diameter <8μm; see 2A for example). Of each blood smear and buffy coat sample, approximately 100 WBC per patient were imaged on the whole glass slide.

2.3.2 Masking and quantification of the images

An operator-dependant binary overlay outlining the segment of interest was used for quantification of fluorescence, examples are given in figure 3.2B, 3.4B and 3.5B. Levels of nitrotyrosine, superoxide and hydrogen peroxide were measured in mean fluorescence intensity (representing the mean pixel intensity given in Analog-to-digital Units [A.U.], being an equipment dependant unit defined by SlideBook™ software). Fluorescence intensity was corrected for differences in total area size of the masks as well for the varying non-specific background that was quantified by analysis of negative control smears of the same sample, which were included in every staining. Mean levels per cell per patient were used and for each group of patients the median with ranges.

2.4 Statistical analysis

Data were analyzed with SPSS (IBM Statistics v20, U.S.A.). For multiple non-parametric distributed groups the Kruskal–Wallis test was used first and subsequently the Mann–Whitney U test for comparing two groups. Fisher's exact test was used for categorical variables in two groups. Correlations were tested with Spearman's Rank Correlation (Rs). Raw data are given as medians with ranges and presented graphically as scatter, or boxplots (showing medians and quartiles) with outliers (according to Tukey's criteria) indicated separately. For univariate analysis, a general linear model was made, by adding log-transformed parameters to the model, or for dichotomous parameters, dummy variables (0=absence and 1=presence of covariate). Parameters with p-value <0.15 were accepted. Tests were considered statistically significant at $p \leq 0.05$.

3. RESULTS

3.1 Protein nitrosylation in circulating white blood cells

Patient characteristics of 34 AAA patients are shown in table 3.1. In AAA patients, median nitrotyrosine fluorescent intensity levels (in A.U., Analog-to-digital Units) were in neutrophils 865 (313–2144), in lymphocytes 144 (68–555) and in monocytes 490 (112–2238; figure 3.2E-G). The median levels of the healthy volunteers (controls, n=10) were in neutrophils 466 (340–820), in lymphocytes 99 (82–246) and in monocytes 191 (102–386; figure 3.2E-G). Control levels in neutrophils and monocytes were lower than in AAA patients ($p \leq 0.03$). Age was not correlated with nitrotyrosine in neither control and patient groups nor when groups were pooled (Rs -0.54; Rs -0.15; Rs 0.15, $p \geq 0.27$ respectively).

Different types of statin products were used (simvastatin: n=12; atorvastatin: n=4; pravastatin: n=1; fluvastatin; n=1). To compare the dose effect of statins we converted other types to an equivalent simvastatin dose according to a statin conversion chart.[17] Equivalent simvastatin doses varied from 5 to 80mg per day. The following comorbidities and drug use were more frequent in the statin group than in the non-statin group: coronary heart disease, hypercholesterolemia, use of antiplatelets and creatinine levels (table 3.1; $p \leq 0.05$). Univariate analysis after log-transformation showed that these characteristics were no confounding factors for nitrotyrosine production (coefficients=0.00–0.08, ns). All patients using statins were treated for at least 6 months. Patients in the non-statin group had either ceased the therapy (all since at least 5 months) due to complaints of mainly myopathy, or did not start the therapy yet as the aneurysm was recently diagnosed. The median nitrotyrosine levels in the neutrophils were higher in AAA patients not using statins (non-statin group; n=16; 929 [553–2144]) than in the statin group (646 [313–1706]; n=18; p=0.03; figure 3.2E). In neutrophils and monocytes, statin users in the AAA group had higher nitrotyrosine levels than controls (p=0.03 and p=0.04, respectively). The difference in nitrotyrosine production in neutrophils between statin users and non-statin users was confirmed by univariate analysis (coefficient=-0.12, R^2=0.11, p=0.05). Intercept of the model was 3.01 and model R^2 was 0.29. The equivalent simvastatin dose tended to correlate negatively with nitrotyrosine levels (Rs -0.32, p=0.06; figure 3.3). Univariate analysis showed that age, other drug use, symptoms and other comorbidities from table 3.1 were no confounding factors. We found no association between equivalent simvastatin dose and aneurysm diameter, growth, length or localization.

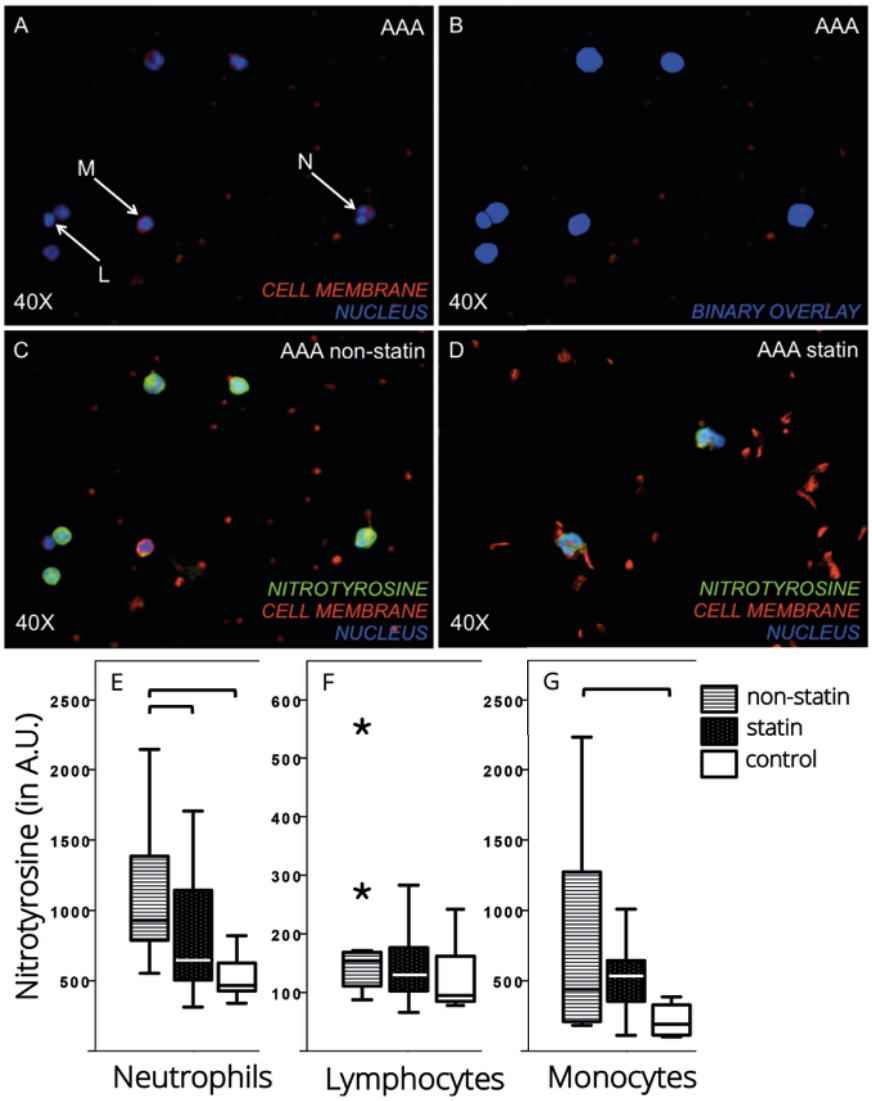

Figure 3.2 In vivo peroxynitrite production
An example of characteristic cell morphology is given in figure A and the binary overlay for masking in figure B. In figure C and D, representative images of nitrotyrosine in AAA patients with no statin therapy (C) and with statin therapy (D) are presented. The quantification of nitrotyrosine in neutrophils (E), lymphocytes (F) and monocytes (G) in AAA patients (subdivided in non-statin and statin users) and controls is given. Data are presented as boxplots with interquartile ranges. Note the differences in scale for the lymphocytes. A.U. = Analog-to-digital Units; an accolade indicates significant difference between groups ($p<0.05$); outliers are indicated by an asterisk.

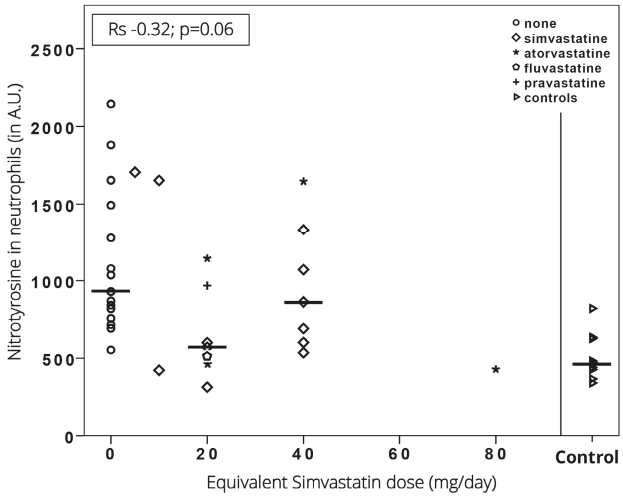

Figure 3.3 Nitrotyrosine production in neutrophils for varying statin doses
In this scatterplot the nitrotyrosine production in neutrophils of AAA patients and controls is given (y-axis) for the different statin doses and types. Dose is given in mg per day as equivalent simvastatin doses (corrected according to the statin conversion chart as described in the text). The correlation (Spearmans Rank [Rs]) is given with p-value for AAA patients. Different statin types are recognizable by there own marker (see legend). Controls are given in the right end of the figure. Median values are indicated by a horizontal bar in case of 3 or more values per dose.

Since smoking is a known factor of increased ROS production, we analyzed patients with positive smoking history (smokers group, n=26) separately.[10] No significant difference was found in nitrotyrosine production between active smokers and patients with negative smoking history. Subgroup analysis in the smokers group showed similar levels between statin users and non-statin users (p>0.18). In the statin group, smokers (n=14) had significantly higher median nitrotyrosine levels in lymphocytes than non-smokers (n=12; 159 (100–285) and 94 (68–122), respectively; p=0.03)). In the other WBC types, no differences were found.

3.2 Live mitochondrial and cytoplasmic oxidative stress production

Mitochondrial superoxide median fluorescent intensity levels (in A.U.) in AAA patients were in neutrophils 352 (101–947), in lymphocytes 997 (118–2745) and in monocytes 754 (224–2099; figure 3.4C-E). Median control levels were in neutrophils 268 (201–459), in lymphocytes 877 (762–951) and in monocytes 361 (199–492; figure 3.4C-E). No differences were found in all three cell types between AAA patients using statins and not using statins (p>0.20). Control levels in monocytes of healthy volunteers were lower than in AAA patients (p=0.05; figure 3.4E).

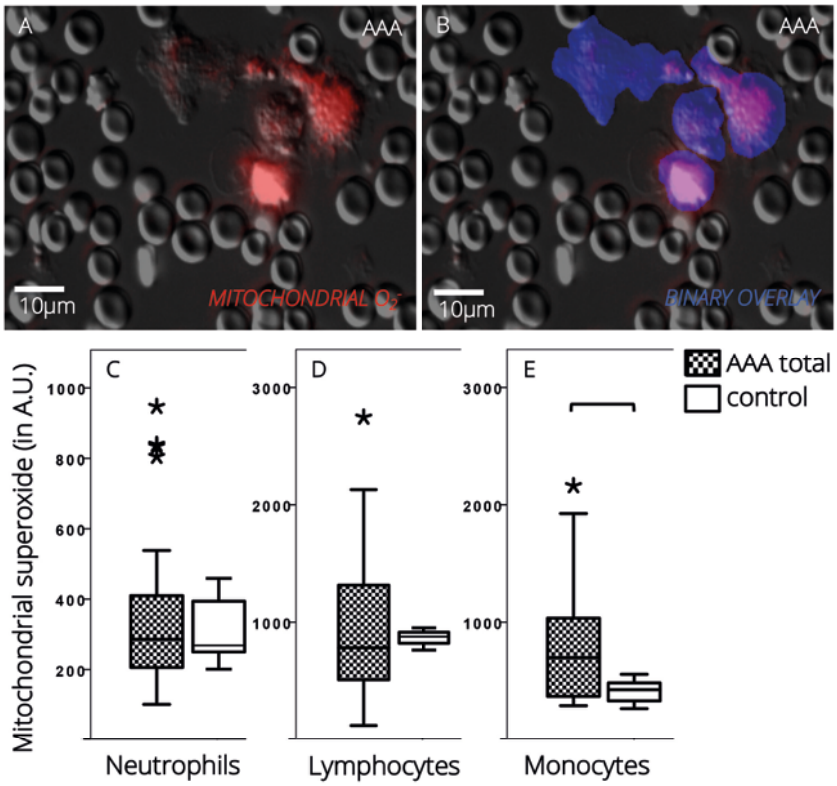

Figure 3.4 Mitochondrial superoxide production.
Examples of live cell imaging of mitochondrial superoxide (O_2^-) production (A), and the binary overlay for masking (B). The quantification of superoxide production in neutrophils (C), lymphocytes (D) and monocytes (E) in AAA and controls is given. Data are presented as boxplots with median and interquartile ranges. Note the differences in scale for neutrophils. A.U. = Analog-to-digital Units; an accolade indicates significant difference between groups ($p<0.05$); outliers are indicated by an asterisk.

Median cytoplasmic hydrogen peroxide levels (in A.U.) in AAA patients were in neutrophils 90 (62–209), in lymphocytes 60 (31-1193) and in monocytes 80 (61–880; figure 3.5C-E). Median levels in AAA patients were similar to controls, being in neutrophils 105 (85–134), in lymphocytes 47 (31–71) and in monocytes 105 (83–146). There were no differences between AAA patients using statins and not using statins. The patient characteristics and comorbidities presented in table 3.1 were not correlated to mitochondrial superoxide and cytoplasmic hydrogen peroxide levels in circulating WBC.

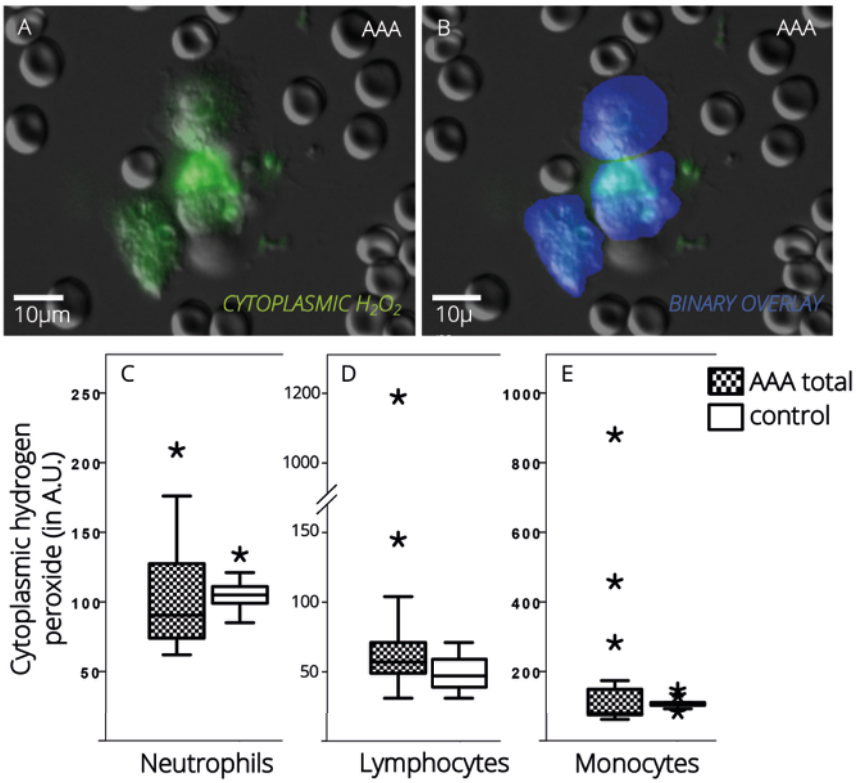

Figure 3.5 Cytoplasmic hydrogen peroxide production.
Examples of live cell imaging of cytoplasmic hydrogen peroxide (H_2O_2) production (A), and the binary overlay for masking (B). The quantification of hydrogen peroxide production in neutrophils (C), lymphocytes (D) and monocytes (E) in AAA and controls is given. Data are presented as boxplots with median and interquartile ranges. Note the differences in scale for monocytes. A.U. = Analog-to-digital Units; outliers are indicated by an asterisk.

4. DISCUSSION

In this study, RNS production was increased in circulating neutrophils and monocytes of AAA patients as compared to healthy volunteers. In neutrophils its production was lower in patients using statins than in patients who were not treated so. The statin dose tended to correlate negatively with RNS production. Mitochondrial superoxide production was elevated in circulating monocytes of AAA patients, but not in their neutrophils or lymphocytes. Hydrogen peroxide production was not elevated in AAA patients in any cell-type. Statins had no influence on these ROS-levels.

Of all ROS and RNS investigated in WBC of AAA patients, peroxynitrite seems to be the most important source of reactive species produced in circulating WBC. WBC are known to be activated by endothelial-WBC interactions in order to produce reactive species.[18] Chronic inflammation in AAA can increase expression of adhesion molecules over the inner surface of the aneurysm. We suggest that as WBC pass the aneurysm, they are activated by adhesion molecules to produce peroxynitrite. Such a mechanism could be responsible for increased RNS production in circulating WBC.

Our data show that RNS produced by circulating neutrophils is lower in AAA patients treated by statins than in patients not treated so. This is possibly the result of decreased peroxynitrite production in the WBC themselves. In order to produce RNS, a WBC must first be primed.[19] Hyperlipidemic patients have more circulating primed neutrophils than patients with normal ranged lipid levels.[20] As statins are lipid lowering drugs, less potent peroxynitrite-producing neutrophils circulate. Statins also reduce vessel wall inflammation, resulting in fewer endothelial-leukocyte interactions and therefore fewer primed neutrophils.[18,19] The influence on total RNS production by circulating WBC would be the greatest when its production in neutrophils is inhibited, as they are the most numerous and have the highest peroxynitrite production. Lymphocytes are the only WBC type with similar RNS production in AAA and controls. In this WBC type no differences in peroxynitrite footprint was observed between statin and non-statin users. This could indicate that statins might only reduce enhanced levels of RNS production in AAA patients, and have no influence on WBC with normal levels of RNS production. Future research investigating the effect of statins on RNS production in healthy subjects could possibly explain the lack of effect on lymphocytes. Effective reduction of vessel wall inflammation in AAA by statins is earlier described to be dose-dependent.[21] In circulating neutrophils the observed peroxynitrite lowering effect of statins might also be dose-dependent. However, the patient numbers from which this suggestion is derived are small. The majority of patients in our study used simvastatin. We recalculated the doses of other statin types using with the conversion table for the lipid lowering effect, since no such conversion data exists for pleiotropic actions of statins (i.e. independent of lipid lowering). We did so as a first approximation, although we realize that it is possible that statins may vary in relative strength for different actions.

Statins have earlier been demonstrated to improve antioxidant capacity, and thus reduce destructive effects of oxidative stress in the aneurysm wall.[11,12] Of note, a decrease in hydrogen-peroxide (H_2O_2) production by statins was not observed in AAA tissue.[11,13] This complies with our finding that statins had no effect on H_2O_2 production in

WBC of AAA patients. Moreover, we saw a similar H_2O_2 production in AAA patients and controls, the latter group being absent in the study of Piechota et al.[12] In addition, we provide for the first time direct measurements of mitochondrial superoxide production in AAA patients, using a thoroughly checked, specific marker that not signals reactive sulfide species.[22–24] Interestingly, again no effect of statins on the formation of this oxygen-radical was observed, while AAA patients had an increased formation only in monocytes, but not neutrophils or lymphocytes. Hence, in contrast to RNS formation, ROS production is not influenced by statins, and also seems less prominently increased, if any, in AAA patients. Future research might focus on nitric oxide metabolism to find an explanation for these differences between oxygen and nitrogen radical production in AAA patients.

Multiple clinical trials have investigated the influence of statin therapy on aneurysm development and growth rate.[14,25–29] However, to date it remains a matter of debate. A meta-analysis of observational comparative studies showed that the effect of statin therapy on AAA development, if any, is likely to be on the growth prevention of small AAA.[30] We found no correlation between the statin therapy and AAA diameter or growth. The absence of this correlation might be explained by the fact that all patients included in our study, with the exception of one, had a large diameter AAA. This might indicate that statin therapy has less effect on progression of larger aneurysms. However, the present study was not designed to demonstrate this correlation, and therefore no definitive conclusions can be drawn based on these data.

Cigarette smoke contains several substances, like cathechol and hydroquinone, which increase RNS and ROS production.[31] Our data showed that only lymphocyte peroxynitrite footprint was higher in smokers. Also, contrary to the total AAA group and non-smokers, we found that within the smoking group, no lower levels of peroxynitrite footprint were seen in AAA patients using statins. We speculate that smoking might have a selective effect on reactive species production in circulating WBC and disrupts a possible RNS-decreasing effect of statins on circulating WBC.

A limiting factor of our study is the younger age of the control group. It has been demonstrated that with ageing the adequate anti-oxidative response declines.[32] However, we have demonstrated by univariate analysis in our cohort that age had no significant influence on peroxynitrite footprint in circulating neutrophils. Also, a limitation is the observational design of our study, which hinders to draw causative correlations between the investigated factors. This explains partly that we found none of the individual patient characteristics to be associated with aneurysm growth,

while some are proven independent risk factors for aneurysm diameter and growth. However, one must also acknowledge the complexity and multifactorial nature of AAA development, making it difficult to point out a single factor as causative.

The current study contributes to a better understanding of oxidative stress production in AAA patients, and additionally the RNS lowering effect of statins in circulating neutrophils. For the surgeons that treat AAA patients with statins during their follow-up, these results emphasize the pleiotropic effects of its use. Additionally, these results seem to indicate that smoking might possibly disrupt the oxidative stress lowering effects of statins. This suggestion should help persuade the patient to persist in not smoking at all, even when considering that the evidence for this finding is not very strong. Furthermore, our results show no differences in hydrogen peroxide and superoxide production between AAA patients and controls, except for superoxide production in monocytes, suggesting that ROS are a less important source of oxidative stress than RNS are. Therefore, future research could more specifically focus on the possibilities of RNS reduction, in particular its production by circulating neutrophils.

In conclusion, we found that peroxynitrite footprint in circulating neutrophils and monocytes of AAA patients are higher than in controls. Patients treated by statins had lower levels of peroxynitrite footprint in neutrophils than non-statin users.

REFERENCES

1. Ramos-Mozo P, Madrigal-Matute J, Martinez-Pinna R, Blanco-Colio LM, Lopez JA, Camafeita E, et al. Proteomic analysis of polymorphonuclear neutrophils identifies catalase as a novel biomarker of abdominal aortic aneurysm: Potential implication of oxidative stress in abdominal aortic aneurysm progression. *Arterioscler Thromb Vasc Biol*. 2011;31(12):3011-3019. doi:10.1161/ATVBAHA.111.237537.

2. Boddy AM, Lenk GM, Lillvis JH, Nischan J, Kyo Y, Kuivaniemi H. Basic research studies to understand aneurysm disease. *Drug News Perspect*. 2008;21(3):142-148. doi:10.1358/dnp.2008.21.3.1203410.

3. Kuivaniemi H, Ryer EJ, Elmore JR, Hinterseher I, Smelser DT, Tromp G. Update on abdominal aortic aneurysm research: from clinical to genetic studies. *Scientifica (Cairo)*. 2014;14:564734. doi:10.1155/2014/564734.

4. Martin-Ventura JL, Madrigal-Matute J, Martinez-Pinna R, Ramos-Mozo P, Blanco-Colio LM, Moreno JA et al. Erythrocytes, leukocytes and platelets as a source of oxidative stress in chronic vascular diseases: Detoxifying mechanisms and potential therapeutic options. *Thromb Haemost*. 2012;108(3):435-442. doi:10.1160/TH12-04-0248.

5. Miller FJ, Sharp WJ, Fang X, Oberley LW, Oberley TD, Weintraub NL. Oxidative stress in human abdominal aortic aneurysms: A potential mediator of aneurysmal remodeling. *Arterioscler Thromb Vasc Biol*. 2002;22(4):560-565. doi:10.1161/01.ATV.0000013778.72404.30.

6. Cafueri G, Parodi F, Pistorio A, Bertolotto M, Ventura F, Gambini C, et al. Endothelial and smooth muscle cells from abdominal aortic aneurysm have increased oxidative stress and telomere attrition. *PLoS One*. 2012;7(4). doi:10.1371/journal.pone.0035312.

7. McCormick ML, Gavrila D, Weintraub NL. Role of oxidative stress in the pathogenesis of abdominal aortic aneurysms. *Arterioscler Thromb Vasc Biol*. 2007;27(3):461-469. doi:10.1161/01.ATV.0000257552.94483.14.

8. Ischiropoulos H, Al-Mehdi AB. Peroxynitrite-mediated oxidative protein modifications. *FEBS Lett*. 1995;364(3):279-282. doi:10.1016/0014-5793(95)00307-U.

9. Viappiani S, Schulz R. Detection of specific nitrotyrosine-modified proteins as a marker of oxidative stress in cardiovascular disease. *Am J Physiol Heart Circ Physiol*. 2006;290:H2167-H2168. doi:10.1152/ajpheart.00128.2006.

10. Guzik B, Sagan A, Ludew D, Mrowiecki W, Chwała M, Bujak-Gizycka B, et al. Mechanisms of oxidative stress in human aortic aneurysms--association with clinical risk factors for atherosclerosis and disease severity. *Int J Cardiol*. 2013;168:2389-2396. doi:10.1016/j.ijcard.2013.01.278.

11. Yoshimura K, Nagasawa A, Kudo J, Onoda M, Morikage N, Furutani A, et al. Inhibitory Effect of Statins on Inflammation-Related Pathways in Human Abdominal Aortic Aneurysm Tissue. *Int J Mol Sci*. 2015;16(5):11213-11228. doi:10.3390/ijms160511213.

12. Piechota-Polanczyk A, Goraca A, Demyanets S, Mittlboeck M, Domenig C, Neumayer C, et al. Simvastatin decreases free radicals formation in the human abdominal aortic aneurysm wall via NF-κB. *Eur J Vasc Endovasc Surg*. 2012;44(2):133-137. doi:10.1016/j.ejvs.2012.04.020.

13. Vega de CM. Commentary on "Simvastatin Decreases Free Radicals Formation in the Human Abdominal Aortic Aneurysm Wall via NF-kappaB." *EurJ Vasc Endovasc Surg*. 2012;44. doi:10.1016/j.ejvs.2012.04.030.

14. Mosorin M, Niemelä E, Heikkinen J, Lahtinen J, Tiozzo V, Satta J, et al. The use of statins and fate of small abdominal aortic aneurysms. *Interact Cardiovasc Thorac Surg*. 2008;7(4):578-581. doi:10.1510/icvts.2008.178103.

15. Matsumoto KI, Satoh K, Maniwa T, Tanaka T, Okunishi H, Oda T. Proteomic comparison between abdominal and thoracic aortic aneurysms. *Int J Mol Med*. 2014;33(4):1035-1047. doi:10.3892/ijmm.2014.1627.

16. Shirazi SH, Umar AI, Naz S, Razzak MI. Efficient leukocyte segmentation and recognition in peripheral blood image. *Technol Heal Care*. 2016:Epub ahead of print. doi:10.3233/WOR-141961.

17. Food and Drug Administration statin conversion chart.pdf. 17-01-2017. http://www.fda.gov/Drugs/DrugSafety/ucm256581.htm.

18. Kar S, Kavdia M. Local oxidative and nitrosative stress increases in the microcirculation during leukocytes-endothelial cell interactions. *PLoS One*. 2012;7(6). doi:10.1371/journal.pone.0038912.

19. Farah R, Jubran F, Khamisy-Farah R. Effects of statins on oxidative stress and primed polymorphonuclear leukocytes in hyperlipidemic patients. *Biotech Histochem*. 2012;87(8):519-525. doi:10.3109/10520295.2012.719243.

20. Farah R, Shurtz-Swirski R, Dorlechter F. Primed polymorphonuclear leukocytes constitute a possible link between inflammation and oxidative stress in hyperlipidemic patients: Effect of statins. *Minerva Cardioangiol*. 2010;58(2):175-181. doi:10.1016/j.atherosclerosis.2007.08.014.

21. Van der Meij E, Koning GG, Vriens PW, Peeters MF, Meijer CA, Kortekaas KE, et al. A Clinical Evaluation of Statin Pleiotropy: Statins Selectively and Dose-Dependently Reduce Vascular Inflammation. *PLoS One*. 2013;8(1). doi:10.1371/journal.pone.0053882.

22. DeLeon ER, Gao Y, Huang E, Arif M, Arora N, Divietro A, et al. A case of mistaken identity: are reactive oxygen species actually reactive sulfide species? *Am J Physiol Regul Integr Comp Physiol*. 2016;310(7):R549-60. doi:10.1152/ajpregu.00455.2015.

23. Mukhopadhyay, P., Rajesh, M., Yoshihiro, K., Hasko, G., Pacher, P. Simple quantitative detection of mitochondrial superoxide production in live cells. Biochem. Biophys. Res. Commun. 358, 203–208 (2007). doi:10.1016/j.bbrc.2007.04.106.

24. Robinson KM, Janes MS, Pehar M, Monette JS, Ross MF, Hagen TM, et al. Selective fluorescent imaging of superoxide in vivo using ethidium-based probes. *Proc Natl Acad Sci U S A*. 2006;103(41):15038-15043. doi:10.1073/pnas.0601945103.

25. Ferguson CD, Clancy P, Bourke B, Walker PJ, Dear A, Buckenham T, et al. Association of statin prescription with small abdominal aortic aneurysm progression. *Am Heart J*. 2010;159(2):307-313. doi:10.1016/j.ahj.2009.11.016.

26. Schouten O, van Laanen JHH, Boersma E, Vidakovic R, Feringa HH, Dunkelgrün M, et al. Statins are associated with a reduced infrarenal abdominal aortic aneurysm growth. *Eur J Vasc Endovasc Surg*. 2006;32(1):21-26. doi:10.1016/j.ejvs.2005.12.024.

27. Sukhija R, Aronow WS, Sandhu R, Kakar P, Babu S. Mortality and size of abdominal aortic aneurysm at long-term follow-up of patients not treated surgically and treated with and without statins. *Am J Cardiol*. 2006;97(2):279-280. doi:10.1016/j.amjcard.2005.08.033.

28. Karrowni W, Dughman S, Hajj GP, Miller FJ. Statin therapy reduces growth of abdominal aortic aneurysms. *J Investig Med*. 2011;59(8):1239-1243. doi:10.231/JIM.0b013e31823548e8.

29. Periard D, Guessous I, Mazzolai L, Haesler E, Monney P, Hayoz D. Reduction of small infrarenal abdominal aortic aneurysm expansion rate by statins. *Vasa*. 2012;41(1):35-42.

30. Takagi H, Yamamoto H, Iwata K, Goto S, Umemoto T. Effects of statin therapy on abdominal aortic aneurysm growth: A meta-analysis and meta-regression of observational comparative studies. *Eur J Vasc Endovasc Surg*. 2012;44(3):287-292. doi:10.1016/j.ejvs.2012.06.021.

31. Moldoveanu SC, Kiser M. Gas chromatography/mass spectrometry versus liquid chromatography/fluorescence detection in the analysis of phenols in mainstream cigarette smoke. *J Chromatogr A*. 2007;1141(1):90-97. doi:10.1016/j.chroma.2006.11.100.

32. Finkel T, Holbrook NJ. Oxidants, oxidative stress and the biology of ageing. *Nature*. 2000;408(6809):239-247. doi:10.1038/35041687.

CHAPTER 4

THE POTENTIAL ROLE OF NEUTROPHIL GELATINASE-ASSOCIATED LIPOCALIN (NGAL) IN THE DEVELOPMENT OF ABDOMINAL AORTIC ANEURYSMS

M.E. Groeneveld[1,2]
J.A. Struik[1,2]
R.J.P. Musters[2]
G.J. Tangelder[2]
P. Koolwijk[2]
H.W. Niessen[3]
A.W.J. Hoksbergen[1]
W. Wisselink[1]
K.K. Yeung[1,2]

[1] Department of Vascular Surgery, Amsterdam University Medical Center
[2] Department of Physiology; Amsterdam University Medical Center
[3] Department of Pathology and Cardiac Surgery, Amsterdam University Medical Center

Annals of Vascular Surgery, 2019 May;57:210-219.

ABSTRACT

Objective: In abdominal aortic aneurysm (AAA) pathophysiology deterioration of the medial aortic layer plays a critical role. Key players in vessel wall degeneration are reactive oxygen species (ROS), smooth muscle cell apoptosis and extracellular matrix degeneration by matrix metalloproteinase-9 (MMP-9). Lipocalin-2, also Neutrophil Gelatinase-Associated Lipocalin (NGAL), is suggested to be involved in these degenerative processes in other cardiovascular diseases. We aimed to further investigate the role of NGAL in AAA development and rupture.

Methods: In this observational study aneurysm tissue and blood of ruptured (n=13) AAA patients were investigated versus non-ruptured (n=26). Non-dilated aortas (n=5) from deceased patients and venous blood from healthy volunteers (n=10) served as controls. NGAL concentrations in tissue and blood were measured by Enzyme-Linked Immuno Sorbent Assay and immunofluorescence microscopy. Nitrotyrosine (marker of ROS), MMP-9 and caspase-3 (marker of apoptosis) in aneurysm tissue were measured by immunofluorescence microscopy. AAA expansion rates were calculated retrospectively.

Results: NGAL (in µg/mL) blood concentration in ruptured AAA was 46 (range: 22–122) versus 26 (range: 6–55) in non-ruptured AAA ($p<0.01$) and 14 (range: 12–22) in controls ($p<0.01$). In the aneurysm wall of ruptured AAA NGAL concentration was 4.7 (range: 1.4–25) versus 4.4 (range: 0.2–14) in non-ruptured AAA (not significant) and 1.8 (range: 1.2–2.7) in non-dilated aortas ($p=0.04$). In the medial layer, NGAL correlated positively with nitrotyrosine ($Rs=0.80;p<0.01$), MMP-9 ($Rs=0.56;p=0.02$) and caspase-3 ($Rs=0.75;p=0.01$). NGAL did not correlate to AAA expansion rate in blood or tissue ($p=0.34$ and $p=0.95$, respectively).

Conclusions: This study demonstrates that NGAL blood concentration is higher in ruptured AAA patients than in non-ruptured AAA. NGAL expression in the AAA wall is also higher than in non-dilated aorta. Furthermore, it's expression is associated with factors of vessel wall deterioration. Based on our study results, we could not determine NGAL as biomarker for AAA growth or rupture. However, our findings do support a potential role of NGAL in the development of AAA.

1. INTRODUCTION

Abdominal aortic aneurysm (AAA) development is associated with aortic medial layer deterioration. This is a multifactorial process in which smooth muscle cell (SMC) apoptosis and migration are important features, which are facilitated by loss of the vessel wall structure due to enzymatic degradation of the extracellular matrix (ECM).[1–5] Matrix metalloproteinases (MMP), mainly MMP-2 and MMP-9, are responsible for ECM degeneration.[1,2] Reactive oxygen species (ROS), among others, have been reported to play a prominent role in SMC apoptosis in AAA.[3] These processes result in medial layer decline, AAA development and eventually may lead to a life threatening intra-abdominal bleeding in case of a rupture.[6]

Neutrophil Gelatinase-Associated Lipocalin (NGAL) is an acute phase protein stored in the granules of neutrophils and has been the topic of interest as a diagnostic and prognostic tool for several cardiovascular diseases.[7–10] NGAL may prevent MMP-9 from inactivation, and doing so, is thought to stimulate aortic wall degeneration.[11,12] In mice NGAL inhibition even attenuates AAA growth.[7] On the opposite, it is supposed to have a protective role against ROS induced apoptosis.[13,14] NGAL expression has earlier been described in the aortic wall of non-ruptured AAA and its role as a biomarker for AAA presence has even been suggested. In patients with carotid atherosclerosis NGAL demonstrated potential as marker for vulnerable plaques.[9,15–17] Furthermore, NGAL seems to have potential as a marker for acute kidney injury.[18] More specific, NGAL is suggested to predict hemodialysis and poor outcome after major aortic surgery.[19,20] However, to date expression of NGAL in ruptured AAA patients was never assessed.[21–23]

In the present study, we aimed to investigate the role of NGAL in the pathophysiology of AAA rupture. We hypothesized that NGAL is increased in the aneurysm wall and in blood of ruptured AAA as compared to non-ruptured AAA. NGAL concentrations in blood and aneurysm tissue of ruptured AAA, non-ruptured AAA and non-dilated aorta's were measured. To investigate its role in the pathophysiology, we investigated correlations between NGAL and factors of aneurysm development, i.e. MMP-9, ROS and SMC apoptosis.

2. MATERIALS AND METHODS

The study was approved by the Medical Ethics Committee of the Amsterdam University Medical Center (reference number: 2010/193). Written informed consent was obtained from all patients or from the patient's family in case of decease.

2.1 Patients, tissue and blood samples

We measured NGAL concentration in full thickness aortic biopsies of the aneurysm wall of ruptured and non-ruptured AAA, which were obtained during surgery. Additionally, we measured NGAL blood concentration (all samples were taken immediately after patient was anesthetized before incision). The expression and localisation of NGAL were determined separately in the medial layer and atherosclerotic plaque, the two adjacent vessel wall layers where we expected the highest activity of NGAL. We also examined the expression of indicators for aneurysm development, i.e. MMP-9, ROS and SMC apoptosis, in ruptured and non-ruptured AAA. Ruptured and non-ruptured AAA measurements were compared to tissue and blood control groups. As leukocytes and impaired kidney function are associated with increased NGAL expression we analyzed total circulating leukocytes and kidney function (via MDRD) to exclude these factors as potential confounders.[22,23] NGAL blood concentration was also correlated with the retrospectively determined AAA expansion rate.

All consecutive patients with a ruptured and non-ruptured AAA in the period March 2010 until May 2014 of which blood samples and aortic tissue was available, were included. The ruptured AAA group consisted of 13 patients (8 males), the non-ruptured AAA group of 26 patients (17 males). AAA diameter (in cm) was measured by computed tomography or ultrasound and in case of multiple measurements the expansion rate was calculated (all non-ruptured AAA; n=7). In the ruptured group the preoperative aneurysm diameter was significantly larger than in the non-ruptured (7.0 versus 6.1 cm, respectively; p=0.04; table 4.1). The tissue control group consisted of 5 people (3 males) and the blood control group of 10 healthy volunteers (9 males) with no comorbidities and no medication (table 4.1).

NGAL concentration in both blood and in full thickness biopsies of the aneurysm wall was measured by Enzyme-Linked Immuno Sorbent Assay (ELISA). Expression in the medial layer and atherosclerotic plaque was measured by immunofluorescence microscopy. In contrast to ELISA, the expression of NGAL in these specific layers could selectively be measured by microscopy. As indicators of aneurysm development

Table 4.1 Baseline patient characteristics and blood values of both abdominal aortic aneurysm (AAA) groups. P-values are given to compare both AAA groups. Significant differences are indicated by an asterisk. Also characteristics of both tissue and blood controls are given. Data are presented as absolute values, as medians with range or as percentages.

	Non-ruptured	Ruptured	P	Tissue controls	Blood controls
N	26	13	-	5	10
Male / female *(N)*	17 / 9	8 / 5	0.71	3 / 2	9 / 1
Age *(years)*	71 (53 – 77)	70 (64 – 89)	0.24	69 (64 – 87)	53 (40 – 62)
Aneurysm diameter *(cm)*	6.1 (3.6 – 10.4)	7.0 (4.0 – 10.0)	0.04*	-	-
Aneurysm growth *(cm/year)*	0.9 (0.1 – 4.4)	NA	-	-	-
Aneurysm location[a]					
Suprarenal (%)	*4*	*8*	1.00	-	-
Juxtarenal (%)	*35*	*54*	0.31	-	-
Infrarenal (%)	*54*	*31*	0.31	-	-
Symptoms *(%)*	36	100	<0.01*	0	0
Claudication (%)	*27*	*8*	0.38	0	0
Backpain (%)	*0*	*46*	0.03*	0	0
Abdominal pain (%)	*5*	*17*	0.28	0	0
Other (%)	*5*	*25*	0.12	0	0
Procedure and outcome					
Suprarenal clamping *(%)*	35	46	0.49	-	-
Posoperative ICU[b] *(days)*	1 (0 - 7)	2 (1 - 15)	<0.01*	-	-
Total hospital admission (*days)*	8 (1 - 46)	14 (4 - 58)	0.12	-	-
Postoperative AKI[c] *(%)*	8	23	0.15	-	-
Mortality *(%)*	8	15	0.59	-	-
Co morbidity					
Positive smoking history *(%)*	74	56	0.10	20	33
Coronary heart disease *(%)*	41	46	0.76	0	0
COPD[d] *(%)*	36	23	0.48	0	0
Hypertension *(%)*	68	62	0.73	20	0
Medication					
Antihypertensives *(%)*	82	75	0.68	0	0
Statins *(%)*	91	58	0.07	0	0
Anticoagulants *(%)*	82	67	0.38	0	0
Blood values					
MDRD[e] *(mL/min/1.73 m^2)*	75 (12 – 90)	52 (21 – 90)	0.57	101 (47 – 120)	NA
CRP[f] *(mg/L)*	3 (3-62)	14 (3 - 124)	0.56	23 (18 – 33)	NA
Leukocytes[g] *(10^9/L)*	9 (3-11)	12 (7 - 30)	0.96	9 (9 – 10)	9 (4 – 10)

[a] Aneurysm location was not available in 2 non-ruptured and 1 ruptured patient; [b] ICU = intensive care unit; [c] AKI = acute kidney injury; [d] COPD = chronic obstructive pulmonary disease; [e] MDRD = modification of diet in renal disease; reference value > 90 mL/min/1.73m^2; [f] CRP = complement reactive protein; reference value < 10 mg/L; in one non-ruptured AAA patient it was not measured;
[g] reference value < 10 *10^9/L.

expression of MMP-9, nitrotyrosine (a footprint marker of ROS production) and caspase-3 (an essential protein in the apoptosis cascade) were examined.[24]

The ventral aneurysm wall was harvested during open repair of ruptured and non-ruptured AAA. Blood samples were preoperatively drawn, immediately after patients were anesthetized before incision and then centrifuged (20 minutes at 4˚C) to subtract blood plasma. For baseline values, the ventral aortic wall of deceased patients without an AAA, was harvested immediately after death. Blood was drawn from healthy volunteers with no aneurysm and no comorbidity. All tissues and blood samples were snap frozen and stored at -80˚C.

2.2 ELISA for NGAL concentration in tissue and blood plasma

The human NGAL ELISA was developed in our laboratory using the matched antibody pair HYB 211-01 and the biotinylated HYB 211-02B (Thermo Fisher Scientific, USA). Briefly, the primary antibody HYB 211-01 (0.5 µg/mL in PBS) was coated to high-binding ELISA plates (Corning, USA, catalog number 2592) overnight at 4°C. After washing with phosphate-buffered saline (PBS) supplemented with 0.5% Tween 20 (PBST), the plates were blocked using PBST + 0.1% casein for 2 hours at room temperature and subsequently, after washing, incubated with a series of dilutions of a recombinant human NGAL calibrator (12.5 ng/mL – 200 ng/mL; Thermo Fisher Scientifi, USA) or 100 x diluted tissue samples in PBST + 0.1% casein, overnight at 4°C. After washing, biotinylated HYB 211-02B was added as detecting antibody (0.5 µg/mL in PBST + 0.1% casein) for 3 hours at room temperature, washed with PBST and incubated with streptavidin-HRP. Bound streptavidin was detected with TMB substrate and the optical density was measured after 15 minutes of incubation using an ELISA reader.

2.3 Immunofluorescence staining

Cryosections were cut (5 and 20µm thick), air-dried and fixed in 4% formaldehyde containing PBS, then washed in PBST. All were double stained with the following primary antibodies (separately incubated for 1 hour; dilution in PBS [1:50]): NGAL and nitrotyrosine; NGAL and MMP-9; NGAL and caspase-3. Primary antibodies were: anti-NGAL mouse monoclonal (NGAL HYB 211-01, sc-59622, Santa Cruz Biotechnology Inc., USA); anti-nitrotyrosine rabbit polyclonal (A-21285, Molecular Probes Inc., USA); anti-MMP-9 goat polyclonal (MMP-9 M-17, sc-6841, Santa Cruz Biotechnology Inc., USA) and anti-caspase-3 rabbit polyclonal (anti-ACTIVE® Caspase-3 pAb, G748, Promega Corporation, USA). After washing, secondary antibodies (Molecular Probes, USA) were incubated (30 minutes; dilution in PBS [1:100]) and washed before staining the cell membrane glycocalyx with wheat germ agglutinin ([WGA]; Alexa 555, Molecular

Probes, USA) for 20 minutes in PBS [1:50]). Sections were washed and mounted using Vectashield™ mounting medium containing DAPI nuclear stain (Vector Laboratories Inc., USA). All steps were performed at room temperature. Negative control sections were treated the same, but without primary antibodies.

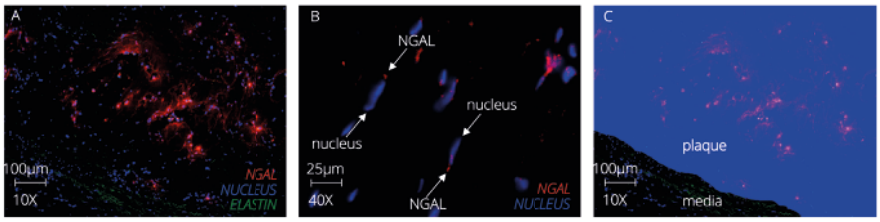

Figure 4.1 Example of the medial layer and atherosclerotic plaque of a ruptured AAA with a 10X objective (A): NGAL is red, the cell nuclei are blue and the auto-immunofluorescent extracellular matrix in the media is green. NGAL expression in the medial layer was measured using a 40X. In figure B an example is given of the medial layer of a ruptured AAA: NGAL is red and cell nuclei are blue, arrows point in the longitudinal direction of smooth muscle cells. For quantification of fluorescence a mask (blue overlay) is produced. When placed over the initial figure A the mask differentiates the atherosclerotic plaque from the medial layer in order to selectively measure the NGAL expression in the atheroscelerotic plaque (C).

2.4 Quantitative immunofluorescence microscopy: image acquisition, masking and analysis

2.4.1 Image acquisition

Sections were examined with a Zeiss Axiovert 200M Marianas™ inverted microscope, equipped with a motorized stage (stepper-motor, z-axis increments 0.1µm), and a turret with four epifluorescence cubes, having emission in blue (DAPI; cell nuclei), green (FITC; secondary antibodies), red (Cy3; Rhodamine-WGA-stained-glycocalyx of cell membranes) or infrared (Cy5; secondary antibodies). A cooled CCD camera (Cooke Sensicam SVGA (Cooke Co., Tonawanda, U.S.), 1280 x 1024 pixels), linear over its full dynamic range, recorded images with true 16-bit capability. The microscope, camera, and data processing were controlled by SlideBook™ software (version 5.0.1.8, Intelligent Imaging Innovations, Denver, U.S.). Images were taken with custom 10X air, 40X air and 63X oil-immersion objectives (CARL ZEISS, The Netherlands).

Based on morphological criteria (nuclei, membranes and extracellular matrix) vessel segments were identified as medial layer (10 images per patient with 40X objective), atherosclerotic plaque (15 images per patient with 10X objective) or intimal layer in non-dilated aortas for comparison with atherosclerotic plaques (5 images per patient with 10X objective). Also 3D image stacks were made (20µm sections, 20 focal planes per stack, 63X objective). We used the 10X objective in the atherosclerotic plaque for a representative view of the uneven distribution of, mainly, lipocalin-2 and nitrotyrosine

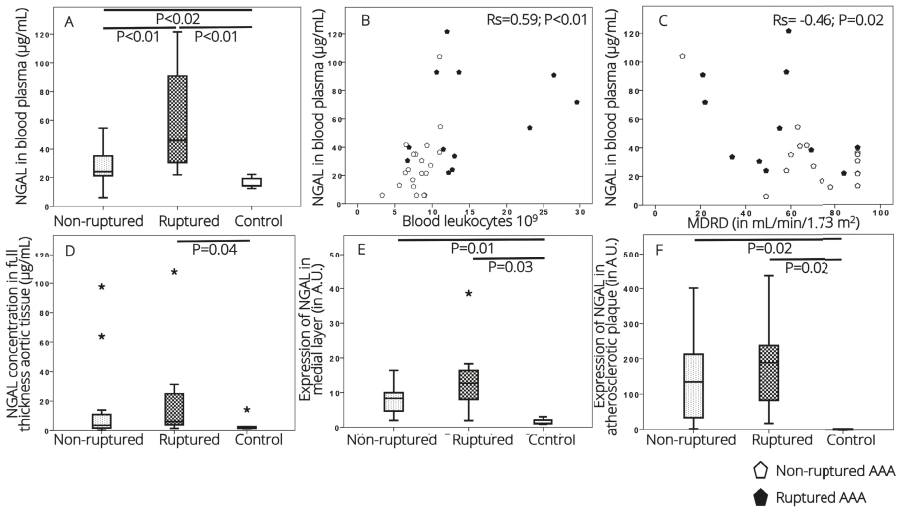

Figure 4.2 NGAL concentration in blood (µg/mL) are presented for the three groups (A) and its correlations with blood leukocytes *10^9 (B) and MDRD (C). In the latter two, ruptured and non-ruptured AAA groups are pooled. NGAL concentration in full thickness aortic biopsies in µg/mL (D) and its expression in the medial layer (E) and the atherosclerotic plaque (F) are given per group. Outliers are indicated by an asterisk. Brackets indicate P<0.05 in comparing groups. Expressions in the medial layer and atherosclerotic plaque are given in arbitrary fluorescence units (ADU*10^6); note differences in the scales of NGAL tissue expression.

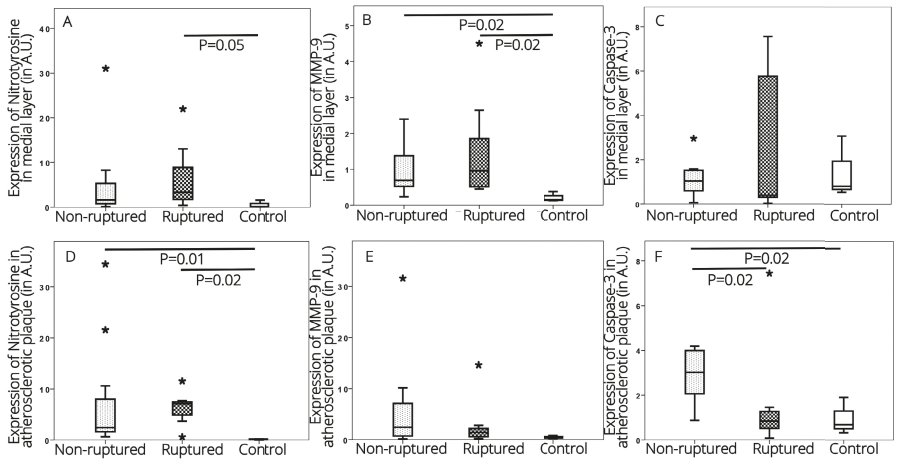

Figure 4.3 Expression of nitrotyrosine, MMP-9 and caspase-3 in the medial layer (A–C) and atherosclerotic plaque (D–F) of ruptured and non-ruptured aneurysms and in non-dilated aortas. Outliers are indicated by an asterisk. Brackets indicate P<0.05 in comparing groups. Expression is given in arbitrary fluorescence units (ADU*10^6); note differences in scale.

(figure 4.1A). The 40X objective was used in the medial layer to define the measured proteins as intra- or extracellular (figure 4.1B).

2.4.2 Masking and quantification of the medial layer and atherosclerotic plaque

A mask is an operator-dependant binary overlay outlining the segment of interest to measure a certain expression (example in figure 4.1C). In the medial layer fluorescent objects were selected manually based on the following criteria: being not part of or embedded in the auto-immunofluorescent ECM; XY-axes ratio is circular and not ellipsoid and with sharply defined borders. This was repeated by a second independent observer with similar results (p=0.73). The sum intensity of fluorescence, representing the cumulative pixel intensity in analog-to-digital units (ADU; an arbitrary unit defined by SlideBook™ software), was measured and corrected for differences in area size and non-specific background. Per patient the mean of all images was used and for each group of patients the median with ranges.

2.5 Statistical analysis

We employed SPSS v24 (IBM, USA). Because of sample size and skewed distribution, the Kruskal–Wallis and Mann–Whitney U tests were used to compare continuous variables in multiple or two groups, respectively, and Fisher's exact test for two groups with categorical variables. A logistic regression model was used to describe the relationship between dependant and multiple independent variables. Boxplots and bar charts were used to graphically present medians with 25^{th}-75^{th} percentiles (box) and ranges (figures 4.2 and 4.3). Outliers, according to Tukey's criteria, are indicated separately. Correlations were tested with Spearman's Rank Correlation (Rs). Tests were considered statistically significant at $p<0.05$.

3. RESULTS

3.1 NGAL concentration in blood

NGAL concentration in blood of ruptured AAA (46 µg/mL [range: 22-122]) was significantly higher than in non-ruptured AAA (26 µg/mL [range: 6-55]); $p<0.01$; figure 4.2A). Both ruptured and non-ruptured AAA had higher NGAL blood levels than controls (14 µg/mL [12-22]; $p<0.01$ and $p<0.02$, respectively). In both aneurysm groups pooled NGAL blood plasma levels correlated positively with the amount of circulating leukocytes (Rs 0.59; $p<0.01$; figure 4.2B) and correlated negatively with MDRD (Rs -0.46; p=0.02; figure 4.2C). There was no correlation between blood levels of NGAL and CRP (Rs 0.19; p=0.36).

A logistic regression analysis was performed to analyze the relationship between AAA rupture (dependant variable) with the following independent variables: AAA diameter, AAA location, age in years (three groups: <65; 65-75; >75), smoking history, circulating leukocytes, MDRD and NGAL blood plasma concentration in µg/mL (three groups: <30; 30-80; >80). Independent variables accepted in the model were: i) positive smoking history (OR 4.1; 95% CI 0.7–26; p=0.11); ii) blood plasma NGAL group 30-80 µg/mL (OR 5.1; 95% CI 0.4–69; P=0.22); and iii) blood plasma NGAL group > 80 µg/mL (OR 16; CI 1.4–209; P=0.03).

3.2 Concentration of NGAL in the full thickness aortic biopsies

The median concentration of NGAL in aortic wall tissue of ruptured AAA (4.7 µg/mL [range: 1.4 – 31]; figure 4.2D) was similar to non-ruptured AAA (4.4 µg/mL [range: 0.2 – 14]). The walls of ruptured AAA had significantly higher NGAL concentrations than the walls of non-dilated aortas (1.8 µg/mL [range: 1.2 – 2.7]; p=0.04). NGAL concentrations in full thickness aortic biopsies were not correlated to its concentrations in blood (Rs 0.23; p=0.43).

3.3 Expression of NGAL, nitrotyrosine, MMP-9 and caspase-3 in the medial layer

Ruptured and non-ruptured AAA had similar expressions of NGAL (respectively, 12 [range: 2.0-18] and 8 [range: 2.0-16]; figure 4.2E), nitrotyrosine (respectively, 3.3 [range: 0.4-22] and 1.6 [range: 0.1-31]; figure 4.3A), MMP-9 (respectively, 1.0 [range: 0.5-4.5] and 0.7 [range: 0.2-2.4]; figure 4.3B) and caspase-3 (respectively, 0.4 [range: 0.04-7.6] and 1.0 [range: 0.1-30]; figure 4.3C). NGAL, nitrotyrosine and MMP-9 had significantly higher expressions in ruptured AAA than in non-dilated aortas (for all P≤0.05; figure 4.2E and 4.3A-B).

The expression of NGAL was mostly seen in round particles (figure 4.1B), as opposed to the smears of NGAL seen in the atherosclerotic plaque (figure 4.1A). 3D stacks with a 63X objective demonstrate that NGAL and nitrotyrosine were present both within the stained cell membranes and around, suggesting that it was present intracellular and extracellular.

In the medial layer NGAL expression had a significant positive correlation with nitrotyrosine (Rs 0.80; p<0.01), MMP-9 (Rs 0.56; p=0.02) and caspase-3 (Rs 0.75; p<0.01; table 4.2). There was no correlation between NGAL expression in the medial layer and its blood concentration (Rs 0.39; p=0.12; table 4.2).

3.4 Expression of NGAL, nitrotyrosine, MMP-9 and caspase-3 in the atherosclerotic plaque

Expression in ruptured and in non-ruptured AAA was similar for NGAL 189 (range: 16-436) versus 135 (range: 1-400), respectively (figure 4.2F), nitrotyrosine (respectively, 7.1 [range: 0.6-12] and 2.4 [range: 0.6-34]; figure 4.3D) and MMP-9 (respectively, 1.4 [range: 0.2-15] and 2.4 [range: 0.2-32]; figure 4.3E). NGAL and nitrotyrosine expression in both ruptured and non-ruptured AAA were significantly higher than in non-dilated aortas (P≤0.02; figure 4.2F and 4.3D). Caspase-3 expression in ruptured AAA (0.8 [range: 0.1-7.4]) was significantly lower than in non-ruptured AAA (3.4 [range: 0.9-4.2], P=0.02). Non-ruptured AAA had a significantly higher caspase-3 expression than in non-dilated aortas (0.7 [range: 0.3-1.9]; P=0.02; figure 4.3F).

Localisation of nitrotyrosine and NGAL showed a typical pattern (figure 4.4A-C): nitrotyrosine was expressed throughout the entire atherosclerotic plaque, but accumulated in circumscriptive spots, surrounded by a diffuse smear of NGAL. However, no overlap between the nitrotyrosine and NGAL staining was seen, so nitrotyrosine fitted exactly in the opening of the NGAL smear.

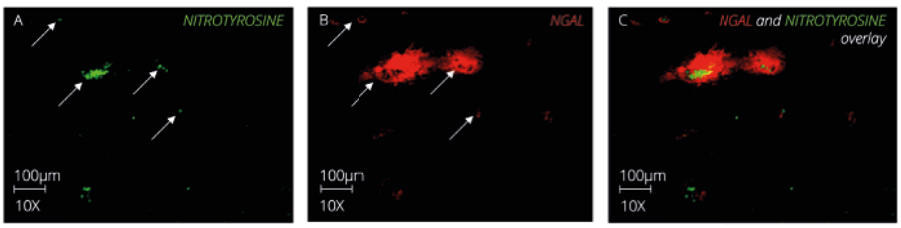

Figure 4.4 Typical coinciding expression of nitrotyrosine (A) and NGAL (B) in the atherosclerotic plaque of AAA, i.e. non-ruptured. The left and right picture represent two layers from the same image. Arrows show nitrotyrosine (green in A) and NGAL (red in B). In the overlay of both images it is clear that nitrotyrosine fits exactly in the areas free of NGAL (C).

NGAL expression in the atherosclerotic plaque had a significant positive correlation with its blood concentration (Rs 0.51; P=0.04; table 4.2). Despite the typical coinciding expression pattern of NGAL and nitrotyrosine we found no quantitative correlation (table 4.2). Neither was NGAL in the atherosclerotic plaque correlated with MMP-9 or caspase-3 (table 4.2).

Table 4.2 Correlations in tissue are given in the upper table between NGAL expression with factors of aneurysm development in the medial layer and atherosclerotic plaque and also with plasma NGAL concentrations. In the lower table correlations in blood are given between plasma NGAL concentrations with kidney function (given in MDRD) and inflammatory markers (leukocytes and CRP). Spearmans Rho correlations are given in the right upper part of the table and its corresponding p-values between brackets in the lower left part. Significant correlations are indicated by an asterisk.

Correlations in tissue	*NGAL medial layer*	*NGAL atherosclerotic plaque*
Nitrotyrosine	0.80 (<0.01)*	-0.25 (0.47)
MMP-9	0.56 (0.02)*	0.12 (0.65)
Caspase-3	0.75 (<0.01)*	0.08 (0.75)
NGAL (plasma)	0.39 (0.12)	0.51 (0.04)*

Correlations in blood	*NGAL (plasma)*	*MDRD*	*Leukocytes*	*CRP*
NGAL (plasma)	–	-0.46	0.59*	0.19
MDRD[a]	(0.09)	–	-0.43*	-0.25
Leukocytes	(<0.01)	(0.01)	–	0.35
CRP[b]	(0.36)	(0.21)	(0.07)	–

[a]MDRD=Modification of Diet in Renal Disease; [b]CRP=complement reactive protein

3.5 AAA expansion rate and NGAL blood concentrations

All AAA of which the growth rate could be calculated were expanding aneurysms (median 0.9 cm/year [range: 0.1 – 4.4]; table 4.1). The AAA expansion rate was not correlated to NGAL blood plasma (p=0.34) or full thickness aortic wall (p=0.95) concentrations, nor was it correlated to its expression in the medial layer (p=0.30) or atherosclerotic plaque (p=0.69).

4. DISCUSSION

The major findings of the present study are: i) NGAL concentration in blood plasma is significantly higher in ruptured than in non-ruptured AAA patients; ii) NGAL expression in the AAA wall did not differentiate between ruptured and non-ruptured aneurysm patients; iii) NGAL expression in the atherosclerotic plaque had a significant positive correlation with its blood concentration; iv) NGAL expression in the medial layer is associated with indicators of aneurysm development, i.e. MMP-9, nitrotyrosine and caspase-3; and v) NGAL levels in blood and tissue are not correlated to AAA expansion rate.

In earlier studies NGAL was associated with the presence of AAA.[22,23,25] It remains a matter of debate whether NGAL can be correlated to AAA growth. In a review of Karaolanis et al. the authors conclude that NGAL appears to be a hopeful prognostic biomarker for AAA progression.[23] However, that conclusion is based on the result of one study that demonstrated a retrospective correlation between plasma NGAL and expansion, but the authors could not reproduce that correlation in a prospective follow up.[22] Our data show that NGAL is increased in blood plasma of ruptured AAA as compared to non-ruptured AAA. However, we found no correlations between AAA expansion rate and NGAL concentrations in blood plasma or in the AAA wall. These results might indicate that NGAL is associated with AAA rupture. However, our data do not clarify whether NGAL was increased before the rupture occurred, or as a consequence of the rupture. Furthermore, NGAL is more and more being acknowledged as a very early marker for acute kidney injury, and so its increase could also indicate acute kidney injury in patients with AAA rupture and concomitant hemodynamic shock.[19,20] The latter theory is supported by the inverse correlation we found between NGAL concentration in blood with kidney function (in MDRD). Additionally, the absence of retrospective correlations between AAA expansion rate and NGAL levels in our cohort seem to comply with the point of view that NGAL also has no potential as a prognostic biomarker for aneurysm growth.

By use of immunofluorescence microscopy on transverse sections of the aneurysm wall we found that NGAL concentrations did not differentiate between ruptured and non-ruptured aneurysm patients. Again, a finding that makes it less probable that NGAL could be valuable as a marker for aneurysm rupture. NGAL expression in the atherosclerotic plaque had a significant positive correlation with NGAL blood concentration, but no such correlations were found between NGAL in the medial layer or NGAL in full thickness biopsies. In the medial layer NGAL was present both intracellular and extracellular of SMC, indicating expression by SMC. In an earlier study SMC in carotid arteries have been demonstrated to produce NGAL in response to vessel wall damage.[26] Our data suggest that SMC in AAA are also involved in NGAL expression and thus that the presence of NGAL in the aneurysmal wall might have multiple sources, namely SMC expression alongside the earlier described increased leukocyte secretion.[22]

To determine a possible role of NGAL in the pathological process of aneurysm development, we investigated several known indicators of aneurysm development. First, we investigated a possible association of NGAL with ROS.[3] The latter not only stimulates vessel wall inflammation, but also induces MMP-9 expression and SMC apoptosis, leading to aortic wall degeneration and dilation.[2–5] Sources of ROS in AAA

are leukocytes and local production by SMC and endothelial cells. [27,28] We demonstrated that a footprint of ROS production was increased in AAA and also that it was positively correlated to NGAL expression in the medial layer. These findings suggest a possible role of NGAL in ROS management. Second, we investigated NGAL and MMP-9, the latter known for ECM degradation.[11,21] We found a quantitative association between NGAL and MMP-9 in the medial layer of both ruptured and non-ruptured aneurysms. This finding indicates that NGAL might be involved in medial layer degeneration of AAA. Furthermore, NGAL expression in the medial layer was associated with expression of caspase-3, a marker of apoptosis. In a recent study NGAL was shown to play a role in cardiomyocyte apoptosis.[29] Based on earlier results and our present findings we suggest that NGAL might also be involved in apoptosis of cells in the aortic medial layer. However, due to the observational design of the study we cannot draw conclusions on causality of NGAL and the investigated indicators of aneurysm development.

The relevance of the present study is that, to the best of our knowledge, for the first time NGAL expression is measured in ruptured AAA. NGAL expression indeed seems associated with AAA development, but no difference was found between its expression in ruptured and non-ruptured aneurysm tissue. Further, this study demonstrated that NGAL is increased in blood of ruptured AAA patients as compared to non-ruptured AAA, but blood levels were not correlated with AAA expansion rate. However, a possible prognostic role is still not fully elucidated and therefore future research should prospectively investigate NGAL plasma levels in an AAA follow up cohort to determine its potential as a biomarker for AAA progression and rupture.

It might be seen as a limitation that non-dilated aortas were taken from deceased patients and might be less representable as control tissue. However, the fact that levels of caspase-3 in the non-dilated aortas were higher than in the non-ruptured AAA indicates that proteins were not per se lost. Further, no histological evidence for cell degeneration was seen in the non-dilated aortas. A limitation of the study is that the total number of patients included might not be adequate to determine the value of NGAL as a circulating biomarker. Also, only one blood sample per patient was taken and not consecutive samples peri-operative. These limitations withhold us from drawing firm conclusions on the potential of NGAL as marker for AAA rupture.

In conclusion, we have demonstrated that NGAL concentration is higher in blood of ruptured than in non-ruptured AAA patients. Also, that NGAL expression in the AAA wall is higher than in non-dilated aorta and is associated with factors of vessel wall deterioration in the medial layer, i.e. ROS production, ECM degeneration and apoptosis.

Based on our study results we could not determine NGAL as biomarker for AAA growth or rupture. However, our findings do support a potential role of NGAL in the development of AAA.

REFERENCES

1. Palombo D, Maione M, Cifiello BI, Udini M, Maggio D, Lupo M. Matrix metalloproteinases. Their role in degenerative chronic diseases of abdominal aorta. J Cardiovasc Surg (Torino). 1999;40(2):257–60.
2. Matthew Longo G, Xiong W, Greiner TC, Zhao Y, Fiotti N, Timothy Baxter B. Matrix metalloproteinases 2 and 9 work in concert to produce aortic aneurysms. J Clin Invest. 2002;110(5):625–32.
3. McCormick ML, Gavrila D, Weintraub NL. Role of oxidative stress in the pathogenesis of abdominal aortic aneurysms. Arteriosclerosis, Thrombosis, and Vascular Biology. 2007. p. 461–9.
4. Choke E, Cockerill G, Wilson WRW, Sayed S, Dawson J, Loftus I, et al. A review of biological factors implicated in abdominal aortic aneurysm rupture. European Journal of Vascular and Endovascular Surgery. 2005. p. 227–44.
5. Thompson RW, Liao S, Curci JA. Vascular smooth muscle cell apoptosis in abdominal aortic aneurysms. [Internet]. Coronary artery disease. 1997. p. 623–31. Available from: http://www.ncbi.nlm.nih.gov/pubmed/9457444
6. Visser P, Akkersdijk GJM, Blankensteijn JD. In-hospital operative mortality of ruptured abdominal aortic aneurysm: A population-based analysis of 5593 patients in the Netherlands over a 10-year period. Eur J Vasc Endovasc Surg. 2005;30(4):359–64.
7. Tarín C, Fernandez-Garcia CE, Burillo E, Pastor-Vargas C, Llamas-Granda P, Castejón B, et al. Lipocalin-2 deficiency or blockade protects against aortic abdominal aneurysm development in mice. Cardiovasc Res [Internet]. 2016;111(3):262–73. Available from: http://cardiovascres.oxfordjournals.org/lookup/doi/10.1093/cvr/cvw112
8. Serra R, Grande R, Montemurro R, Butrico L, Calio FG, Mastrangelo D, et al. The role of matrix metalloproteinases and neutrophil gelatinase-associated lipocalin in central and peripheral arterial aneurysms. Surgery. 2015;157(1):155–62.
9. Eilenberg W, Stojkovic S, Piechota-Polanczyk A, Kaun C, Rauscher S, Gröger M, et al. Neutrophil Gelatinase-Associated Lipocalin (NGAL) is Associated with Symptomatic Carotid Atherosclerosis and Drives Pro-inflammatory State in Vitro. Eur J Vasc Endovasc Surg. 2016;51(5):623–31.
10. Sivalingam Z, Larsen SB, Grove EL, Hvas A-M, Steen DK, Magnusson NE. Neutrophil gelatinase-associated lipocalin as a risk marker in cardiovascular disease. Clin Chem Lab Med [Internet]. 2018;56(1):5–18. Available from: https://doi.org/10.1515/cclm-2017-0120
11. Yan L, Borregaard N, Kjeldsen L, Moses MA. The high molecular weight urinary matrix metalloproteinase (MMP) activity is a complex of gelatinase B/MMP-9 and neutrophil gelatinase-associated lipocalin (NGAL): Modulation of MMP-9 activity by NGAL. J Biol Chem. 2001;276(40):37258–65.
12. Swedenborg J, Eriksson P. The intraluminal thrombus as a source of proteolytic activity. Ann N Y Acad Sci. 2006;1085:133–8.
13. Roudkenar MH, Halabian R, Ghasemipour Z, Roushandeh AM, Rouhbakhsh M, Nekogoftar M, et al. Neutrophil Gelatinase-associated Lipocalin Acts as a Protective Factor against H2O2 Toxicity. Arch Med Res. 2008;39(6):560–6.

14. Roudkenar MH, Halabian R, Roushandeh AM, Nourani MR, Masroori N, Ebrahimi M, et al. Lipocalin 2 regulation by thermal stresses: Protective role of Lcn2/NGAL against cold and heat stresses. Exp Cell Res [Internet]. Elsevier B.V.; 2009;315(18):3140–51. Available from: http://dx.doi.org/10.1016/j.yexcr.2009.08.019

15. Eilenberg W, Stojkovic S, Kaider A, Kozakowski N, Domenig C, Burghuber C, et al. NGAL and MMP-9 / NGAL as biomarkers of plaque vulnerability and targets of statins in patients with carotid atherosclerosis . Clin Chem Lab Med. 2017;56(1):147–56.

16. Eilenberg W, Stojkovic S, Polanczyk AP, Kaider A, Kozakowski N, Weninger WJ, et al. Neutrophil gelatinase associated lipocalin (NGAL) is elevated in type 2 diabetics with carotid artery stenosis and reduced under metformin treatment. Cardiovasc Diabetol. BioMed Central; 2017;98(16):1–11.

17. Boekhorst BC, Bovens SM, Hellings WE, Kraak PH Van Der, Kolk KW Van De, Vink A, et al. Molecular MRI of murine atherosclerotic plaque targeting NGAL : a protein associated with unstable human plaque characteristics. Cardiovasc Res. 2011;89:680–8.

18. Mishra J, Dent C, Tarabishi R, Mitsnefes M, Ma Q, Kelly C, et al. Neutrophil gelatinase-associated lipocalin (NGAL) as a biomarker for acute renal injury after cardiac surgery. Lancet. 2005;365(9466):1231–8.

19. Gombert A, Prior I, Martin L, Grommes J, Barbati M, Foldenauer A, et al. Urine neutrophil gelatinase-associated lipocalin predicts outcome and renal failure in open and endovascular thoracic abdominal aortic aneurysm surgery. Sci Rep. 2018;8(1):12676.

20. Gombert A, Martin L, Foldenauer A, Krajewski C, Greiner A, Kotelis D, et al. Comparison of urine and serum neutrophil gelatinase-associated lipocalin after open and endovascular thoraco-abdominal aortic surgery and their meaning as indicators of acute kidney injury. Vasa. 2018;10:1–9.

21. Folkesson M, Kazi M, Zhu C, Silveira A, Hemdahl AL, Hamsten A, et al. Presence of NGAL/MMP-9 complexes in human abdominal aortic aneurysms. Thromb Haemost [Internet]. 2007;98(2):427–33. Available from: http://www.ncbi.nlm.nih.gov/pubmed/17721627

22. Ramos-Mozo P, Madrigal-Matute J, Vega de Ceniga M, Blanco-Colio LM, Meilhac O, Feldman L, et al. Increased plasma levels of NGAL, a marker of neutrophil activation, in patients with abdominal aortic aneurysm. Atherosclerosis [Internet]. 2012;220(2):552–6. Available from: http://www.ncbi.nlm.nih.gov/pubmed/22169111

23. Karaolanis G.; Moris D.; Pala VV.; Karanikola E.; Bakoyiannis C.; Georgopoulos S. Neutrophil Gelatinase Associated Lipocalin (NGAL) as a Biomarker. Does It Apply in Abdominal Aortic Aneurysms? A Review of Literature. Indian J Surg [Internet]. 2015;77(12):1313–7. Available from: http://www.ncbi.nlm.nih.gov/pubmed/27011557

24. Duncan MW. A review of approaches to the analysis of 3-nitrotyrosine. Amino Acids. 2003. p. 351–61.

25. Roudkenar MH, Kuwahara Y, Baba T, Roushandeh AM, Ebishima S, Abe S, et al. Oxidative stress induced lipocalin 2 gene expression: addressing its expression under the harmful conditions. J Radiat Res [Internet]. 2007;48(1):39–44. Available from: papers://1fa4e632-4d39-4b47-95a2-5a607126d96f/Paper/p360%5Cnhttp://joi.jlc.jst.go.jp/JST.JSTAGE/jrr/06057?from=CrossRef

26. Bu D, Hemdahl A-L, Gabrielsen A, Fuxe J, Zhu C, Eriksson P, et al. Induction of neutrophil gelatinase-associated lipocalin in vascular injury via activation of nuclear factor-kappaB. Am J Pathol [Internet]. 2006;169(6):2245–53. Available from: http://dx.doi.org/10.2353/ajpath.2006.050706

27. Ramos-Mozo P, Madrigal-Matute J, Martinez-Pinna R, Blanco-Colio LM, Lopez JA, Camafeita E, et al. Proteomic analysis of polymorphonuclear neutrophils identifies catalase as a novel biomarker of abdominal aortic aneurysm: Potential implication of oxidative stress in abdominal aortic aneurysm progression. Arterioscler Thromb Vasc Biol. 2011;31(12):3011–9.

28. Pandey D, Patel A, Patel V, Chen F, Qian J, Wang Y, et al. Expression and functional significance of NADPH oxidase 5 (Nox5) and its splice variants in human blood vessels. Am J Physiol Heart Circ Physiol [Internet]. 2012;302(10):H1919-28. Available from: http://www.pubmedcentral.nih.gov/articlerender.fcgi?artid=3362115&tool=pmcentrez&rendertype=abstract

29. Xu G, Ahn J, Chang S, Eguchi M, Ogier A, Han S, et al. Lipocalin-2 induces cardiomyocyte apoptosis by increasing intracellular iron accumulation. J Biol Chem. 2012;287(7):4808–17.

PART II

CELLULAR SIGNALLING INFLUENCES ANEURYSM GROWTH AND RUPTURE

Chapter 5: Activation of Extracellular signal-Regulated Kinase in abdominal aortic aneurysm

Chapter 6: Update on Activation of Extracellular signal-Regulated Kinase in abdominal aortic aneurysm

Chapter 7: Betaglycan (TGFBR3) upregulation correlates with increased TGF-ß signalling in Marfan patient fibroblasts in vitro

CHAPTER 5

ACTIVATION OF EXTRACELLULAR SIGNAL-REGULATED KINASE IN ABDOMINAL AORTIC ANEURYSM

M.E. Groeneveld[1,2]
M.V. van Burink[1]
M.P.V. Begieneman[3,4]
H.W.M. Niessen[3]
W. Wisselink[1]
E.C. Eringa[2]
K.K. Yeung[1,2]

[1] Department of Vascular Surgery, Amsterdam University Medical Center
[2] Department of Physiology; Amsterdam University Medical Center
[3] Department of Pathology and Cardiac Surgery, Amsterdam University Medical Center
[4] Netherlands Forensic Institute, The Hague

European Journal of Clinical Investigation 2016, vol. 46, pag. 440–447

ABSTRACT

Objective: Extracellular matrix degeneration, caused by matrix metalloproteinase-2, facilitates smooth muscle cell migration leading to medial layer decline and, ultimately, abdominal aortic aneurysm. It remains unclear what exactly causes aneurysms to rupture, which leads to death in most patients. The extracellular signal-regulated kinase may be linked to the latter process. We aimed to clarify the role of extracellular signal-regulated kinase in aortic aneurysm development and rupture in patients.

Methods: Aortic fragments were harvested during open repair of non-ruptured (n=20) and ruptured (n=8) aneurysms. As control, non-dilated aortas (n=6) were obtained during autopsy. We determined levels of phosphorylated and total extracellular signal-regulated kinase by Western blot, matrix metalloproteinase-2 by immunohistochemistry, and medial layer thickness by conventional microscopy.

Results: Non-ruptured aneurysms had 1.8-times higher activation of extracellular signal-regulated kinase (ratio: phosphorylated/total) than controls ($p=0.011$). However, the ruptured aneurysms had only 0.9-times the activation of controls (ns). Both non-ruptured and ruptured aneurysms showed significantly higher matrix metalloproteinase-2 than controls (3.8 and 4.0-times, respectively; $p<0.005$). Of the medial layer thickness in controls the median was 1.5 mm, in non-ruptured 1.0 mm and in ruptured aneurysms 0.7 mm. Activation of extracellular signal-regulated kinase correlated positively to medial layer thickness ($Rs=0.48$; $p=0.014$), but not to matrix metalloproteinase-2 ($Rs=-0.36$; $p=0.10$).

Conclusions: In this study, non-ruptured aneurysms are associated with increased extracellular signal-regulated kinase activation while ruptured aneurysms are not. Extracellular signal-regulated kinase was not related to total matrix metalloproteinase-2 expression. We therefore speculate that increased extracellular signal-regulated kinase, in response to medial layer decline, could be protective against aneurysm rupture.

1. INTRODUCTION

Abdominal aortic aneurysm (AAA) development is caused by aortic medial layer degeneration. This is a multifactorial process featuring apoptosis of non-proliferating smooth muscle cells (SMC) and SMC migration from the medial to the intimal layer, facilitated via extracellular matrix (ECM) degradation by matrix metalloproteinases (MMP). These processes cause medial layer thinning, leading to AAA development and life threatening intra-abdominal bleeding in case of rupture.

A signalling pathway that may be involved in all aforementioned processes is extracellular signal-regulated kinase1/2 (ERK1/2).[1-2] ERK1/2 is one of four major mitogen-activated protein kinase signalling pathways that regulates aortic wall structure by stimulating proliferation and cell survival on one hand, and by activating SMC migration and apoptosis on the other.[3] It is stimulated by growth factors, cytokines and SMC damage.[4-5] In case of aortic wall inflammation or SMC damage, ERK1/2 stimulates SMC proliferation.[4,6] In contrast, ERK1/2 also stimulates ECM degradation, leading to SMC migration and medial layer decline.[1,7-8] ECM degradation is mainly performed by MMP-2 and -9.[7-8] MMPs are produced, among others, by SMC and infiltrating leukocytes.[9-10] In a rodent AAA model ERK1/2 was shown to be a critical regulator of MMP expression and Habashi e.a. concluded ERK1/2 to be a stimulating factor of rodent AAA development, as they demonstrated ERK1/2 inhibition to delay AAA growth. [11-12] In humans, ERK1/2 levels were demonstrated to be higher in patients who underwent elective surgical treatment of non-ruptured AAA as compared to healthy controls, and in human aortic SMC MMP-2 expression was regulated by ERK 1/2 activation.[11,13] However, ERK1/2 levels were never investigated in tissue of ruptured AAA.

We hypothesized that ERK1/2 and MMP-2 are higher in non-ruptured and ruptured AAA than in controls, with the highest levels in ruptured. Furthermore, we assessed whether ERK1/2 could be linked to factors of medial layer decline.

To test these hypotheses, we studied ERK1/2 in three groups: healthy aortas, non-ruptured AAA and ruptured AAA. Secondly, to examine if ERK1/2 is associated with key factors of AAA development, we investigated potential relationships with medial MMP-2 expression and medial layer thickness.

2. MATERIAL AND METHODS

The study was approved by the VU University Medical Center Medical Ethical Committee. Informed consent was obtained from all patients or family.

2.1 Patients and tissue collection

Aneurysm tissue was harvested from the ventral wall during open surgical repair of consecutively treated non-ruptured and ruptured AAA. The non-ruptured group consisted of 20 patients (15 men, median age 67 years) and the ruptured group of 8 patients (4 men, median age 74 years (table 5.1)). We also obtained ventral abdominal aortic tissue of 6 deceased patients (4 men, ages ranging from 51 – 71 years) at the start of autopsy, who had no AAA and no macroscopic atherosclerosis.

All tissues were snap frozen, cut in 5μm thick cryosections, air-dried and stored at -80˚C until use. Total leukocyte count, C-reactive protein and estimated glomerular filtration rate were measured by the department of clinical chemistry.

2.2 Western blot analysis

Western blotting of aortic samples was performed as described before.[14] Full thickness samples (i.e. intimal, medial and adventitial layer) of frozen tissue were used. Total and phosphorylated ERK1/2 (tERK1/2 and pERK1/2), the latter being the activated form, were quantified using AIDA software (Raytest, version 4.1.5). ERK1/2 activation was given as the ratio of pERK1/2 and tERK1/2.

2.3 Hematoxylin-Eosin staining

Cryosections were air-dried, fixed in 10% formalin and stained by hematoxylin-eosin staining. The medial layer was identified (representative image in figure 5.3A) and its thickness was measured using ImageJ software (National Institutes of Health, ImageJ, version 1.47).

2.4 Immunohistochemistry

Cryosections were stained for MMP-2 (Genetex; GTX27033; 1:100), visualized using 3,3'-diaminobenzidine (DAB) and counterstained with hematoxylin. PBS controls were included as negative control (all negative results, data not shown). Images were made as described above. MMP-2 levels in the medial layer were measured using ImageJ software by two independent observers in blinded fashion.

2.5 Statistical analysis

For continuous variables Kruskal–Wallis (multiple groups) and Mann–Whitney U (two groups) tests were used, Spearman's Rank (Rs) for correlations and Fisher's exact test for two groups with categorical variables (SPSS 20.0, USA). Boxplots with medians, interquartile ranges and outliers (Tukey's criteria) are given. Tests were considered statistically significant at p≤0.05.

Table 5.1 Baseline patient characteristics
Data are given for non-ruptured and ruptured AAA groups. P-values are given to compare both groups. Significant differences are indicated with an asterisk. Of four patients in the non-ruptured group C-reactive protein was not measured pre-operatively and the medication of one patient in the ruptured group was not known.

	Non-ruptured	**Ruptured**	***p***
N	20	8	
Male / female	15 / 5	4 / 4	0.371
Age *(years)*	67 (53 - 78)	74 (64 - 89)	0.067
Aneurysm diameter *(cm)*	5.6 (3.6 – 7.1)	8.0 (6.8 – 10.0)	0.045*
Smoking history *(%)*	65%	50%	0.671
Symptoms *(%)*	35%	100%	0.002*
Claudication (%)	*35%*	*0%*	0.008*
Backpain (%)	*0%*	*50%*	0.003*
Other (%)	*5%*	*50%*	0.015*
Coronary heart disease *(%)*	40%	63%	0.410
Hypertension *(%)*	75%	75%	1.000
Hypercholesterol *(%)*	35%	25%	1.000
COPD† *(%)*	30%	38%	1.000
Diabetes Mellitus *(%)*	15%	25%	0.606
Antihypertensives *(%)*	80%	75%	1.000
Statins*(%)*	40%	38%	1.000
Anticoagulants *(%)*	85%	63%	0.311
Leukocytes *(10^9/l)*	7.7 (3.3 – 11.1)	23 (13 - 30)	0.013*
C-reactive protein *(mg/l)*	2.5 (2.5 – 3.6; 37.7)	31 (8 - 124)	0.008*
eGFR‡ *(ml/min/1.73m^2)*	67 (49-90)	46 (21 - 55)	0.003*

*p ≤ 0.05; †COPD = chronic obstructive pulmonary disease; ‡ eGFR = estimated glomerular filtration.

3. RESULTS

3.1 Larger aneurysm diameter and systemic inflammation in ruptured AAA

In non-ruptured AAA median aneurysm diameter was 5.6 cm, while in ruptured AAA it was 8.0 cm (p=0.045; table 5.1). The non-ruptured group consisted of 1 supra-, 8 juxta- and 11 infra-renal AAA. In the ruptured group were 4 juxta- and 4 infra-renal AAA. For all below measured parameters no differences were found between these subgroups. One third of non-ruptured AAA patients suffered from symptoms, mainly claudication. In contrast all ruptured AAA patients suffered from symptoms, being back pain or other (p=0.002).

Median total leukocyte count and C-reactive protein (normal range values used by our clinical chemistry department are $<10*10^9$/l and <5 mg/l, respectively) were markedly and significantly increased in ruptured AAA ($23*10^9$ and 31 mg/ml, respectively; table 5.1) as compared to non-ruptured AAA ($7.7*10^9$ and 2.5 mg/ml, p=0.013 and p=0.008, respectively). Estimated glomerular filtration rate was 67 ml/min/1.73m^2 in non-ruptured AAA and was declined significantly in ruptured AAA to 46 ml/min/1.73m^2 (p=0.003).

3.2 ERK1/2 levels were highest in non-ruptured AAA

Median pERK1/2 and median ERK1/2 activation (ratio of pERK1/2 and tERK1/2) were highest in non-ruptured AAA. Levels were increased 5.0 and 1.8-times, respectively, as compared to controls and 11.1 and 2.0-times, respectively, as compared to ruptured AAA (pERK1/2: p≤0.011, figure 5.1B; ERK1/2 activation: p≤0.022, figure 5.1C). The highest levels of tERK1/2 were found in non-ruptured AAA, however, no statistically significant differences in tERK1/2 were found when compared to controls and ruptured AAA (p=0.191 and p=0.075, respectively; see figure 5.1A).

3.3 MMP-2 levels increased in both ruptured and non-ruptured AAA

In controls MMP-2 showed weak staining in the medial layer (figure 5.2A). In non-ruptured AAA MMP-2 was markedly increased compared to controls and was localized mainly in the medial layer centre in well-defined circular areas (figure 5.2B). In ruptured AAA a global MMP-2 staining was seen throughout the medial layer, collected in well-defined circular areas as well (figure 5.2C). Quantification of MMP-2 expression showed that in both non-ruptured and ruptured AAA MMP-2 expression was higher than in controls. The highest levels of MMP-2 were found in ruptured AAA followed by non-ruptured (4.0 and 3.8 times higher than controls, p=0.004 and p=0.001, respectively, figure 5.2D), albeit not significantly.

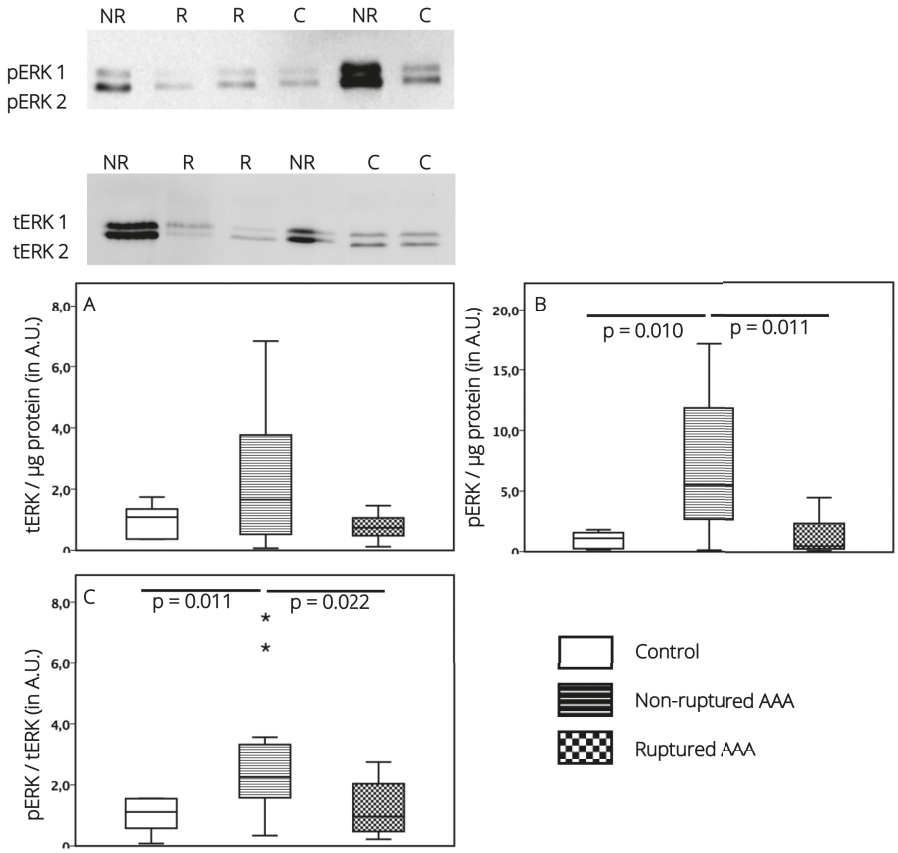

Figure 5.1 ERK1/2 signalling in healthy aorta, non-ruptured and ruptured AAA
Examples of western blot analysis of tERK1/2 and pERK1/2 are seen above. Concentrations of tERK1/2 (A), pERK1/2 (B) and ratio of pERK1/2 and tERK1/2 (C) as an indication of ERK1/2 activation are given in the graphs underneath. Data are presented as boxplots with interquartile ranges. Outliers are indicated by an asterisk. ERK1/2 per µg tissue is given in arbitrary units (A.U.). Statistically significant differences are given with p-values below the horizontal bar.

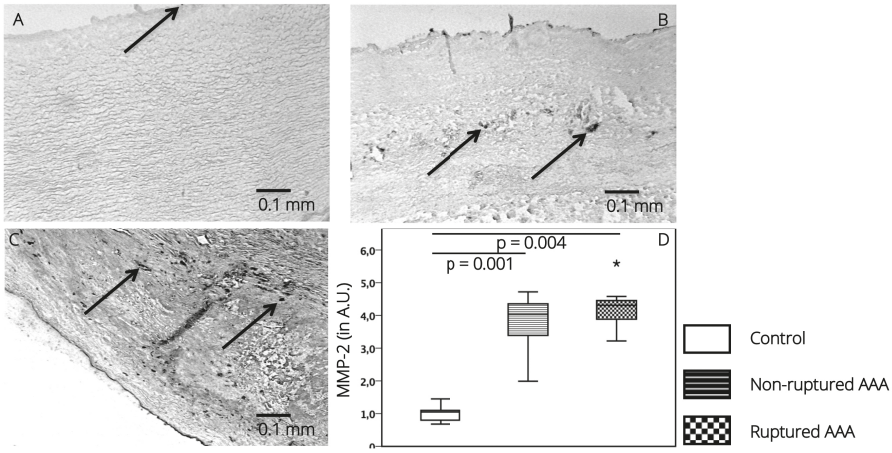

Figure 5.2 MMP-2 expression in healthy aorta, non-ruptured and ruptured AAA
In figures A, B and C representative images of MMP-2 expression in the medial layer are given of healthy aorta, non-ruptured AAA and ruptured AAA, respectively. Black staining in the images indicates MMP-2 expression (see arrows). Pictures were made using a 20X objective. In figure D the amounts of MMP-2, measured in the medial layer by immunohistochemistry staining, are given in arbitrary units (A.U.). Data are presented as boxplots with interquartile ranges. Outliers are indicated by an asterisk. Statistically significant differences are given with p-values below the horizontal bar.

3.4 Medial layer thickness declined in ruptured AAA

In healthy control aorta the medial layer comprises the greater part of the vessel wall and the collagen fibres, as can be seen in figure 5.2A, are organised in regular patterns; the median medial layer thickness was 1.5 mm (figure 5.3B). In non-ruptured AAA the median medial layer thickness was declined and the regular pattern of collagen fibres was disturbed (figure 5.2B). Median medial layer was 1.0 mm thick (figure 5.3B) and covered a smaller part of the total vessel wall than in controls, due to decreased medial layer thickness and an increased intimal layer thickness. In ruptured AAA the medial layer thickness further declined and the regular pattern of collagen fibres was disrupted (figure 5.2C and 5.3A). Median medial layer thickness in ruptured AAA was 0.7 mm (figure 5.3B). Controls had a 2.0-times thicker medial layer than ruptured AAA (p=0.019, figure 5.3B). No significant differences existed between non-ruptured and ruptured AAA, or between non-ruptured AAA and controls.

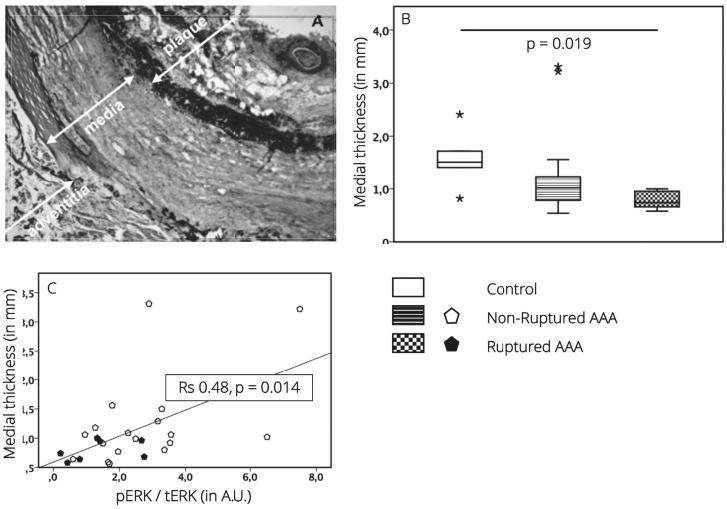

Figure 5.3 Medial layer thickness and association with ERK1/2 signalling
A representative image of a ruptured AAA stained by hematoxylin-eosin is given in figure A (20X objective). The three separate layers are indicated, from lumen outwards: atherosclerotic plaque, medial layer and adventitial layer. Thickness of the medial layer in millimetres (mm) are presented as boxplots with interquartile ranges in figure B. Outliers are indicated by an asterisk. Statistically significant differences are given with p-values below the horizontal bar. In the graphs below, the correlations between ERK1/2 activation, given as ratio of pERK1/2 and tERK1/2 in arbitrary units (A.U.), and the aortic medial thickness (in mm) are presented for non-ruptured and ruptured AAA pooled (figure C). A line of best fit is drawn. The correlation is given as a Spearmans Rank (Rs) with p-value.

3.5 ERK1/2 is associated with medial layer thickness and circulating leukocytes but not with MMP-2 expression.

Sub-group analysis showed a positive association between the medial layer thickness and ERK1/2 activation in non-ruptured and ruptured AAA groups pooled (Rs 0.48; p=0.014 figure 5.3C). AAA patients with the highest ERK1/2 signalling retained the thickest medial layer. There was no such correlation found for MMP-2 expression and medial thickness (Rs -0.02; p=0.929).

As ERK1/2 is supposed to stimulate MMP-2 expression, we investigated a possible correlation between MMP-2 expression in the medial layer and levels of pERK1/2, tERK1/2 or ERK1/2 activation in the total vessel wall.[9] We found a trend towards association between ERK1/2 activation and MMP-2 (Rs -0.36; p=0.099). Total circulating leukocyte counts were negatively correlated with pERK1/2 and ERK1/2 activation in the vessel wall (Rs-0.63; p≤0.017), and as well with medial thickness (Rs -0.61; p=0.02). No correlation existed between circulating leukocytes and MMP-2 expression (Rs

0.38; p=0.23). Estimated glomerular filtration rate was positively correlated to ERK1/2 activation in the vessel wall (Rs 0.70; p=0.005).

4. DISCUSSION

The major findings of our study are: I) pERK1/2 and ERK1/2 activation are higher in non-ruptured AAA than in ruptured AAA and control tissue; II) ERK1/2 activation is positively associated with medial layer thickness in dilated aortas; III) in contrary to what was earlier described in rodent models, no association exists between ERK1/2 and MMP-2 expression in human AAA medial layer.

In our study, we demonstrated that levels of pERK1/2 and ERK1/2 activation are significantly higher in non-ruptured AAA than in ruptured. Interestingly, ERK1/2 activation in ruptured AAA is similar to that in controls. This observation could be explained by the fact that aortic SMC are responsible for ERK1/2 production and activation. In the developing aneurysm SMC are known to migrate from the medial to the intimal layer where they go into apoptosis.[15-17] Increased migration and apoptosis cause decreased SMC numbers and consequently medial layer thinning. We found that medial thickness declines as the healthy aorta develops from a non-ruptured to a ruptured AAA. In AAA patients, we found that pERK1/2 and ERK1/2 activation were positively correlated with medial thickness. This association means that when ERK1/2 levels decrease, the medial thickness declines and vice versa. It could be explained, as suggested above, that ERK1/2 is produced and activated by SMC in the aortic aneurysm wall. Consequently, when the aneurysm develops the medial thickness declines and less SMC remain to keep up the production of ERK1/2 levels. Or, on the other hand, medial thickness is preserved as long as ERK1/2 levels are high, due to SMC proliferation by ERK1/2 signalling.[18] When ERK1/2 levels decrease, as is the case in ruptured AAA, the medial layer is no longer capable to reactively proliferate SMC and eventually becomes thinner.

AAA formation is characterised by ECM degradation and medial layer destruction. The medial layer becomes thinner and the aortic diameter increases. MMP are enzymes that traditionally are known for ECM degradation in the vessel wall. However, recently MMP-2 was demonstrated to be not only responsible for ECM degradation but for ECM proliferation as well, by stimulating collagen and elastin production.[19] In earlier studies mainly MMP-2 and -9 have increased activity in the vessel wall of aortic aneurysms and could be related to aneurysm size and rupture.[20] As mentioned above, MMP-2

and -9 expression are thought to be regulated by ERK1/2 and delay AAA growth by ERK 1/2 inhibition.[12,21] To verify these hypotheses for human AAA we measured MMP-2 expression in the medial layer of patients and controls. Our data show an increased MMP-2 expression in the non-ruptured and ruptured AAA as compared to healthy aorta. ERK1/2 levels are high in non-ruptured AAA but not in ruptured, and MMP-2 expression is not associated with ERK1/2. This lack of association can be explained by the recently discovered divergent role of MMP-2, providing evidence that MMP-2 expression in the aneurysm wall is not only associated with aortic degeneration but with ECM repair and synthesis as well.[19] However, we hypothesize that in human aortic SMC MMP-2 expression can be regulated by ERK1/2 signalling, but as an association lacks it is probably not responsible for total MMP-2 expression. Therefore we suggest that MMP-2 expression, as opposed to earlier findings in rodent studies, is not fully dependant on ERK1/2 stimulation and there should be another source of MMP-2.

Based on previous studies and our recent findings we suggest that aneurysm development initiates with inflammation of the aortic wall where factors of inflammation stimulate ERK1/2 signalling to induce SMC proliferation.[22-24] Consequently MMP-2 expression rises and the medial ECM will be enzymatically degraded (figure 5.4). This degradation facilitates SMC to migrate.[22,25] SMC migration and apoptosis might decrease the total amount of SMC and so total ERK1/2 signalling declines. This might explain the lower ERK1/2 levels in ruptured AAA . However, this does still not clarify the increased MMP-2 levels we found in both non-ruptured and ruptured AAA. Locally infiltrating leukocytes could be a possible alternative source of MMP-2. In ruptured AAA the total amount of circulating leukocytes was higher than in non-ruptured, and were negatively correlated to ERK1/2 activity. However, with our available data we could not investigate a possible association between total locally infiltrated leukocytes and ERK1/2 signalling. Therefore we can only speculate that, due to increased ERK1/2 signalling in the inflammatory aorta, vascular cell adhesion molecule-1 is overexpressed and augments leukocyte infiltration in the vessel wall.[26-27] As leukocytes, particularly neutrophils, are a known source of MMP-2 expression we suggest that leukocytes in the AAA wall could be responsible for the increasing MMP-2 levels, rather than SMC via ERK1/2 signalling.[28] This hypothesis is in part supported by our finding that in ruptured AAA patients we found higher circulating leukocyte counts in the blood than in non-ruptured AAA.

Two limitations of the present study should be considered. First, we could only include the ventral wall of the aneurysm, while rupture of the wall often occurs in the dorsal part of the aorta. However, as all the included aneurysms were fusiform one may

assume that the pathogenic process affects the aorta circularly, even if one takes the heterogeneity of the aneurysmal disease into account. Therefore we consider the specimens representative of the aneurysmatic aortic wall. Second, our conclusions are based on observational ex-vivo research. Further research in the role of ERK1/2 in inflammation of the aorta leading to SMC dysfunction and ECM degradation in aneurysm development is warranted. This might be performed by in-vitro experiments using SMC cultures to determine whether ERK1/2 provides protection against apoptosis.

In summary, the findings of the present study demonstrate for the first time that ERK1/2 activation in the medial layer of human aortas is higher in non-ruptured AAA than in ruptured AAA. Furthermore, ERK1/2 activation might be involved in preserving medial layer thickness, however, this is not regulated by MMP-2 expression. We suggest that in response to damage of the medial layer, ERK1/2 signalling performs a protective role against ECM degradation and, contrary to conclusions from earlier rodent studies, reduces medial layer decline and AAA rupture.

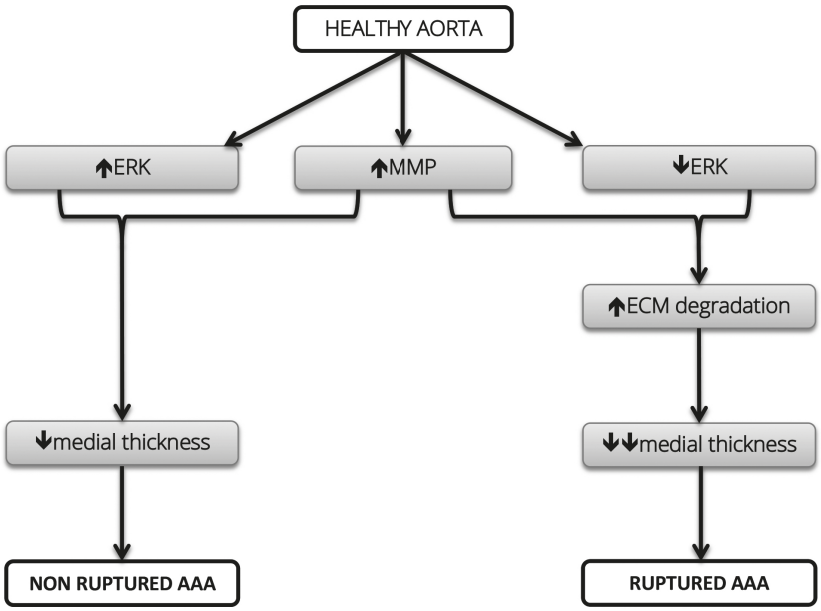

Figure 5.4 Model of aorta wall degeneration in AAA
The multifactorial process of AAA development initiates with inflammation of the aortic wall. ERK1/2 signalling potentially has both an active as a reactive role in an inflammatory environment. In this model we simplified the process of aortic wall degeneration leading to aneurysm development and rupture. One should keep into account that individual steps can be influenced by more factors than those implemented in this model. In non-ruptured AAA we measured increased MMP-2 expression as well as increased ERK1/2 activity, when compared to healthy controls. In ruptured AAA MMP-2 expression was increased, but ERK1/2 activity was not when compared to controls. ERK1/2 activity was positively associated with medial layer thickness in non-ruptured and ruptured AAA. We suggest that the increased ERK1/2 activity in non-ruptured AAA might be protective against AAA rupture.

REFERENCES

1. Nelson PR, Yamamura S, Mureebe L, Itoh H, Kent KC. Smooth muscle cell migration and proliferation are mediated by distinct phases of activation of the intracellular messenger mitogen-activated protein kinase. J Vasc Surg 1998; 27:117-25.
2. Chen Z, Cai Y, Zhang W, Liu X, Liu S. Astragaloside IV inhibits platelet-derived growth factor-BB-stimulated proliferation and migration of vascular smooth muscle cells via the inhibition of p38 MAPK signalling. Exp Ther Med. 2014 Oct;8(4):1253-1258.
3. Le Gall M, Chambard JC, Breittmayer JP, Grall D, Pouysségur J, Van Obberghen-Schilling E. The p42/p44 MAP Kinase Pathway Prevents Apoptosis Induced by Anchorage and Serum Removal. Mol Biol Cell. 2000 Mar;11(3):1103-12.
4. Koyama H, Olson NE, Dast van FF, Reidy MA. Cell Replication in the Arterial Wall Activation of Signaling Pathway Following In Vivo Injury. Circ Res. 1998;82:713-721.
5. Katz M, Amit I, Yarden Y. Regulation of MAPKs by growth factors and receptor tyrosine kinases. Biochim Biophys Acta. 2007 Aug;1773(8):1161-76.
6. Lu Z, Xu S., ERK1/2 MAP Kinases in Cell Survival and Apoptosis. IUBMB Life. 2006 Nov;58(11):621-31.
7. Palombo D, Maione M, Cifiello BI, Udini M, Maggio D, Lupo M. Matrix metalloproteinases. Their role in degenerative chronic diseases of abdominal aorta. J Cardiovasc Surg (Torino). 1999 Apr;40(2):257-60.
8. Longo GM, Xiong W, Greiner TC, Zhao Y, Fiotti N, Baxter BT. Matrix metalloproteinases 2 and 9 work in concert to produce aortic aneurysms. J Clin Invest. 2002 Sep;110(5):625-32.
9. Ferrans VJ.New insights into the world of matrix metalloproteinases. Circulation. 2002 Jan 29;105(4):405-7.
10. Reeps C, Pelisek J, Seidl S, Schuster T, Zimmermann A, Kuehnl A, Eckstein HH. Inflammatory infiltrates and neovessels are relevant sources of MMPs in abdominal aortic aneurysm wall. Pathobiology. 2009;76(5):243-52.
11. Ghosh A, DiMusto PD, Ehrlichman LK, Sadiq O, McEnvoy B, Futchko FS, Henke PK, Eliason JL, Upchurch GR. The role of Extracellular Signal Related Kinase during abdominal aortic aneurysm formation. J Am Coll Surg. 2012 Nov;215(5):668-680.
12. Habashi JP, Doyle JJ, Holm TM, Aziz H, Schoenhoff F, Bedja D, Chen Y, Modiri AN, Judge DP, Dietz HC. Angiotensin II Type 2 Receptor Signaling Attenuates Aortic Aneurysm in Mice Through ERK Antagonism. Science. 2011 Apr 15;332(6027):361-5.
13. Wang C, Qian X, Sun X, Chang Q. Angiotensin II increases matrix metallaproteinase 2 expression in human aortic smooth muscle cells via AT1R and ERK 1/2. Exp Biol Med (Maywood). 2015 Mar 11.
14. Eringa EC, Stehouwer CDA, Nieuw Amerongen GP, Ouwehand L, Westerhof N, Sipkema P. Vasoconstrictor effects of insulin in skeletal muscle arterioles are mediated by ERK1/2 activation in endothelium. Am J Physiol Heart Circ Physiol. 2004;287:H2043–H2048.
15. Goodall S, Porter KE, Bell PR, Thompson MM. Enhanced invasive properties exhibited by smooth muscle cells are associated with elevated production of MMP-2 in patients with aortic aneurysms. Eur J Vasc Endovasc Surg. 2002 Jul;24(1):72-80.

16. López-Candales A, Holmes DR, Liao S, Scott MJ, Wickline SA, Thompson RW. Decreased vascular smooth muscle cell density in medial degeneration of human abdominal aortic aneurysms. Am J Pathol. 1997 Mar;150(3):993-1007.

17. Thompson RW, Liao S, Curci JA. Vascular smooth muscle cell apoptosis in abdominal aortic aneurysms. Coron Artery Dis. 1997 Oct;8(10):623-31.

18. Isenovic ER, Trpkovic A, Zakula Z, Koricanac G, Marche P Role of ERK1/2 Activation In Thrombin-Induced Vascular Smooth Muscle Cell Hypertrophy. Current Hypertension Reviews, 2016; 4(3): 190-196.

19. Shen M, Lee J, Basu R, Sakamuri SS, Wang X, Fan D, Kassiri Z. Divergent roles of matrix metalloproteinase 2 in pathogenesis of thoracic aortic aneurysm. Arterioscler Thromb Vasc Biol. 2015;35:888-898.

20. Petersen E, Gineitis A, Wågberg F, Angquist KA. Activity of Matrix Metalloproteinase-2 and -9 in Abdominal Aortic Aneurysms. Relation to Size and Rupture. Eur J Vasc Endovasc Surg 20, 457–461 (2000).

21. Chakraborti S, Mandal M, Das S, Mandal A, Chakraborti T. Regulation of matrix metalloproteinases: an overview. Mol Cell Biochem. 2003 Nov;253(1-2):269-85.

22. Watanabe A, Ichiki T, Sankoda C, Takahara Y, Ikeda J, Inoue E, Tokunou T, Kitamoto S, Sunagawa K. Suppression of abdominal aortic aneurysm formation by inhibition of prolyl hydroxylase domain protein through attenuation of inflammation and extracellular matrix disruption. Clin Sci (Lond). 2014 May;126(9):671-8.

23. Ghoshal S, Loftin CD. Cyclooxygenase-2 inhibition attenuates abdominal aortic aneurysm progression in hyperlipidemic mice. PloS One. 2012;7(11).

24. Wang X, Liu JZ, Hu JX, Wu H, Li YL, Chen HL, Bai H, Hai CX. ROS-activated p38 MAPK/ERK-Akt cascade plays a central role in palmitic acid-stimulated hepatocyte proliferation. Free Radic Biol Med. 2011 Jul 15;51(2):539-51.

25. Thompson RW, Parks WC. Role of matrix metalloproteinases in abdominal aortic aneurysms. Ann N Y Acad Sci. 1996 Nov 18;800:157-74.

26. Rui W, Guan L, Zhang F, Zhang W, Ding W. PM2.5 -induced oxidative stress increases adhesion molecules expression in human endothelial cells through the ERK/AKT/NF-κB-dependent pathway. J Appl Toxicol. 2015 Apr 15.

27. Liu J, Wang Y, Ouyang X. Beyond toll-like receptors: Porphyromonas gingivalis induces IL-6, IL-8, and VCAM-1 expression through NOD-mediated NF-κB and ERK signaling pathways in periodontal fibroblasts. Inflammation. 2014 Apr;37(2):522-33.

28. Fontaine V, Jacob MP, Houard X, Rossignol P, Plissonnier D, Angles-Cano E, Michel JB. Involvement of the mural thrombus as a site of protease release and activation in human aortic aneurysms. Am J Pathol. 2002; 161: 1701–1710.

CHAPTER 6

UPDATE ON ACTIVATION OF EXTRACELLULAR SIGNAL-REGULATED KINASE IN ABDOMINAL AORTIC ANEURYSM

M.E. Groeneveld[1,2]
K.K. Yeung[1,2]

[1] Department of Vascular Surgery, Amsterdam University Medical Center
[2] Amsterdam Cardiovascular Sciences, Amsterdam University Medical Center

European Journal of Clinical Investigation 2018 Aug 12:e13016

Update on literature

Extracellular signal-regulated kinase (ERK) activation is associated with aortic aneurysm (AA) development and is enhanced in nonruptured AA.[1] ERK is a signalling protein responsible for aortic wall maintenance by vascular smooth muscle cell (VSMC) proliferation and migration.

When ERK activation is inhibited, it can reduce the inflammatory response in VSMC and eventually reduces AAA development.[2,3] When ERK activation was blocked in TGBR1 deficient mice, aneurysmal degeneration was prevented.[4]

Increased ERK activation in rats leads to enhanced aortic VSMC contractility resulting in hypertension and eventually cardiovascular disease like AAA.[5] However, in our unpublished pilot-studies, we measured impaired VSMC contractility in sporadic AAA and demonstrated a correlation between AAA growth rate in vivo versus contractility in vitro. The correlation of VSMC contraction with ERK-pathway is now still under investigation.

The above mentioned findings suggest that ERK has a deteriorating effect, rather than a protective role in AAA development.

Update on statements from: Activation of extracellular signal-related kinase in abdominal aortic aneurysm[1]

Statement 1: "Nonruptured aneurysms are associated with increased extracellular signal-regulated kinase activation while ruptured aneurysms are not"

The evidence that has accumulated in the meanwhile enforces this statement as stated above in the update.

Statement 2: "Extracellular signal-regulated kinase was not related to total matrix metalloproteinase-2 expression"

The evidence that has accumulated in the meanwhile weakens this statement. There are increasing signs that ERK activation and MMP expression are related.

REFERENCES

1. Groeneveld ME, van Burink MV, Begieneman MPV, et al. Activation of extracellular signal-related kinase in abdominal aortic aneurysm. *Eur J Clin Invest*. 2016;46(5). doi:10.1111/eci.12618.
2. Hao Q, Dong X, Chen X, et al. ACE2 Inhibits Angiotensin II-Induced Abdominal Aortic Aneurysm in Mice. *Hum Gene Ther*. 2017:hum.2016.144. doi:10.1089/hum.2016.144.
3. Yu M, Chen C, Cao Y, Qi R. Inhibitory effects of doxycycline on the onset and progression of abdominal aortic aneurysm and its related mechanisms. *Eur J Pharmacol*. 2017;811:101-109. doi:10.1016/j.ejphar.2017.05.041.
4. Yang P, Schmit BM, Fu C, et al. Smooth muscle cell-specific Tgfbr1 deficiency promotes aortic aneurysm formation by stimulating multiple signaling events. *Sci Rep*. 2016;6(September):1-15. doi:10.1038/srep35444.
5. Zhao Z, Wang J, Huo Z, Wang Z, Mei Q. FTY720 elevates smooth muscle contraction of aorta and blood pressure in rats via ERK activation. *Pharmacol Res Perspect*. 2017;5(3):e00308. doi:10.1002/prp2.308.

CHAPTER 7

BETAGLYCAN (TGFBR3) UPREGULATION CORRELATES WITH INCREASED TGF-ß SIGNALLING IN MARFAN PATIENT FIBROBLASTS IN VITRO

M.E. Groeneveld[1,2]
N. Bogunovic[1,2]
R.J.P. Musters[2]
G.J. Tangelder[2]
D. Micha[3]
W. Wisselink[1]
G. Pals[3]
K.K. Yeung[1,2]

[1] Department of Vascular Surgery, Amsterdam University Medical Center
[2] Department of Physiology, Amsterdam University Medical Center
[3] Department of Clinical Genetics, Amsterdam University Medical Center

Cardiovascular Pathology 2018 Jan – Feb, vol. 32, pag. 44-49

ABSTRACT

Background: Marfan syndrome (MFS), a congenital connective tissue disorder leading to aortic aneurysm development, is caused by fibrillin-1 (FBN1) gene mutations. Transforming growth factor beta (TGF-ß) might play a role in the pathogenesis. It is still a matter of discussion if and how TGF-ß upregulates the intracellular downstream pathway, although TGF-ß receptor 3 (TGFBR3 or Betaglycan) is thought to be involved. We aimed to elucidate the role of TGFBR3 protein in TGF-ß signaling in Marfan patients.

Methods: Dermal fibroblasts of MFS patients with haploinsufficient (HI; n=9) or dominant negative (DN; n=4) *FBN1* gene mutations, leading to insufficient or malfunctioning fibrillin-1, respectively, were used. Control cells (n=10) were from healthy volunteers. We quantified TGFBR3 protein expression by immunofluorescence microscopy and gene expression of *FBN1*, *TGFB1*, its receptors and downstream transcriptional target genes by quantitative PCR.

Results: Betaglycan protein expression in *FBN1* mutants pooled was higher than in controls (p=0.004) and in DN higher than in HI (p=0.015). In DN significant higher mRNA expression of *FBN1* (p=0.014), *SMAD7* (p=0.019), *HSP47* (p=0.023) and *SERPINE1* (p=0.008) was observed than in HI, but lower *HSPA5* expression (p=0.029). A pattern of higher expression was noted for *TGFB1* (p=0.059), *FN1* (p=0.089) and *COL1A1* (p=0.089) in DN as compared to HI. TGFBR3 protein expression in cells, both presence in the endoplasmic reticulum and amount of vesicles per cell, correlated positively with *TGFB1* mRNA expression (Rs=0.60, p=0.017; Rs=0.55, p=0.029; respectively). *TGFBR3* gene expression did not differ between groups.

Conclusion: We demonstrated that activation of TGF-ß signaling is higher in patients with a DN than a HI *FBN1* gene mutation. Also, TGFBR3 protein expression is increased in the DN group and correlates positively with *TGFB1* expression in groups pooled. We suggest that TGFBR3 protein expression is involved in upregulated TGF-ß signaling in MFS patients with a DN *FBN1* gene mutation.

1. INTRODUCTION

Marfan syndrome (MFS) is a connective tissue disorder that is characterized by abnormalities in the skeletal, ocular, pulmonary, nervous and cardiovascular system.[1–3] The most severe cardiovascular manifestation of MFS is the development of aortic aneurysms (AA), predominantly thoracic AA, which can lead to rupture associated with high mortality.[4,5] The syndrome is caused by mutations in the fibrillin-1 gene (*FBN1*). Fibrillin-1 constitutes the core of microfibrils, which provide structural stability to extracellular matrix (ECM) and are also responsible for the elastic properties of the vessel wall.[6,7] Mutations can be classified as dominant negative (DN) or as haploinsufficient (HI), depending on the effect that the mutation has on the fibrillin-1 protein.[8] DN mutations lead to a malfolded or malfunctioning fibrillin-1 protein and thus a disturbed ECM.[9,10] HI mutations are caused by the deletion of one copy of the whole gene, degradation of the mutant protein, or nonsense-mediated decay by degradation of fibrillin-1 mRNA.[10–12] The latter mutation will lead to reduced level of wild type fibrillin-1 protein, and thus compromised functionality.[9,10] In the ECM, fibrillin-1, together with fibrillin-2, also regulates the bioavailability of transforming growth factor ß (TGF-ß) by binding this growth factor in a latent complex.[13] TGF-ß signaling is responsible for the expression of connective tissue components in the ECM.[4,13] In MFS, excessive TGF-ß signaling is observed as a result of mutated fibrillin-1 in the ECM, which is thought to be responsible for AA development.[14] Malfolded fibrillin-1 proteins, may be subjected to degradation in the endoplasmic reticulum (ER) mediated by heat shock proteins A5 (HSPA5) and 47 (HSP47).[15,16]

TGF-ß isoforms regulate transcription of ECM components such as collagen and fibrin.[4,13,17–19] By binding to cell surface TGF-ß receptors (TGFBR1, -2 and –3; TGFBR3 is also known as Betaglycan), their downstream intracellular pathway is activated by SMADS, the intracellular effectors of TGF-ß signaling.[13,19–23] SMADS are recruited to the activated receptor complex and after phosphorylation they form a complex, which is transported into the nucleus.[23] This results in the transcription of their target genes collagen type 1 alpha 1 (*COL1A1*), fibronectin (*FN1)*, *SERPINE1* and connective tissue growth factor (*CTGF*).[24–27] A negative feedback loop on the expression of TGF-ß itself is provided by the transcriptional TGF-ß target SMAD7.[19,28] TGF-ß has long been acknowledged as a major factor of MFS development, however, in the past years more studies question whether such a role can be attributed to TGF-ß.[29]

TGFBR3 is a co-receptor of the TGF-ß superfamily that increases the binding of TGF-ß to TGFBR1 and TGFBR2. In recent years however, more functions of TGFBR3 have been

identified, expanding its role from a simple co-receptor to a broader and more complex receptor. It has been suggested to influence cellular processes such as TGF-ß receptor trafficking and regulation of signaling output.[30] We hypothesized that the expression TGFBR3 may modulate TGF-ß signaling. In the current work we aimed to elucidate the role of TGFBR3 in the TGF-ß signaling pathway of MFS patients. This was investigated by the quantification of mRNA expression of *TGFBR3* and *TGFB*, as well as a panel of TGF-ß signaling-associated target genes in primary dermal fibroblasts of MFS patients. TGFBR3 expression was studied at the protein level by immunofluorescence staining in MFS fibroblasts. As the type of mutation modulates the effect on a protein level, a differentiation was made for patients with a DN and a HI *FBN1* gene mutation.[8]

2. MATERIAL AND METHODS

2.1 Patients and healthy volunteers

The study was approved by the Medical Ethical Committee of the Amsterdam University Medical Center. Primary dermal fibroblasts were cultured from skin biopsies taken from the upper arm of thirteen patients (7 men) with a median age (with range) of 37 years (9 – 64), all with a known mutation in the *FBN1* gene (4 DN and 9 HI mutations). As control fibroblasts of 10 healthy volunteers were used (7 men) with median age 34 (0 – 56). Controls were gender-matched healthy volunteers without a medical history of cardiovascular disease. Table 7.1 shows the characteristics and *FBN1* mutations of the patients and controls.

2.2 Cell culture preparation

Primary human dermal fibroblasts were cultured in Ham's F10 Nutrient Mix Medium (Thermo Fischer Scientific; catalog number 31550031) supplemented with 10% fetal bovine serum (Thermo Fischer Scientific; catalog number 10270106), 100 units/mL penicillin and 100 µg/mL streptomycin (Thermo Fischer Scientific; catalog number 15070063). The cells were maintained in a humidified incubator at 37˚C and 5% CO_2. Cells were seeded in chamber slides (Thermo Fischer Scientific; catalog number 154534) and were left to attach and establish a monolayer during five days prior to immunofluorescence.

Table 7.1. Genotypic characteristics of all 13 included patients are presented. The *FBN1* mutation type is given as haploinsufficient (HI) or dominant negative (DN).

Mutants	Age	Gender	Type	Domain	Mutation	Effect
1	37	M	HI	8Cys-4	4605T>A	Y1535X
2	17	F	HI	INTRON	1468+2T>C	retention intron 11
3	20	M	HI	NA	0-allele	NA
4	39	F	HI	INTRON	3464-6C>A	splice error insACAG and NMD
5	9	M	HI	cb-EGF45	7732C>T	Q2578X and 0-allele
6	27	M	HI	cb-EGF25	4428C>A	Y1476X
7	43	F	HI	Proline-rich	1285C>T	R429X
8	64	M	HI	cb-EGF29	5368C>T	R1790X
9	24	M	HI	cb-EGF6	1387G>T	G463X
10	50	M	DN	cb-EGF24	4291T>C	C1431R
11	56	F	DN	8Cys-4	4588C>T	R1530C
12	40	F	DN	8Cys-3	2946 C>G	C982W
13	33	F	DN	cb-EGF8	1701G>T leads to 1700_1714del	G567_Q571del

2.3 Quantification of protein expression by immunofluorescence microscopy

Cells were rinsed with phosphate buffered saline (PBS) (3 times 3 minutes at 37˚C), then fixed in 4% formaldehyde containing PBS and rinsed again in 0.05% Tween (PBST) for 3 minutes. After cell membrane permeabilization by 0.2% Triton for 10 minutes, the cells were rinsed, and incubated overnight at 4˚C with the primary antibody for TGFBR3 (dilution 1:100; sc-75411, Santa Cruz, USA). After washing, cells were incubated with the secondary antibody (dilution 1:100; Molecular Probes, USA) for 30 minutes at room temperature. Additionally, samples were incubated for 20 minutes in wheat-germ-agglutinin (WGA) Alexa 555 fluorescent probes, targeting the cell membrane glycocalyx (dilution 1:50 in PBS; Molecular Probes, USA). After staining, samples were rinsed and mounted on a glass slide using VectashieldTM mounting medium containing DAPI nuclear stain (Vector Laboratories Inc., USA) and sealed using a cover glass.

Sections were examined with a Zeiss Axiovert 200M MarianasTM inverted microscope, equipped with a motorized stage (stepper-motor) z-axis increments 0.1µm, and a turret with a DIC brightfield cube and four epifluorescence cubes, having emission in blue (DAPI for cell nuclei), green (FITC for TGFBR3), red (Cy3 for cell membrane). A cooled CCD camera (Cooke Sensicam SVGA (Cooke Co., USA), 1280 x 1024 pixels), linear over

its full dynamic range, recorded images with true 16-bit capability. The microscope, camera, and data processing were controlled by SlideBookTM software (version 5.0.1.8, Intelligent Imaging Innovations, Denver, U.S.). Fifteen images covering the whole slide per patient were taken with a 63X oil-immersion objectives (CARL ZEISS, The Netherlands).

Analysis of images was conducted by a manual operator-dependent count of TGFBR3 positive vesicles and cells, which was performed by two independent researchers (representative images are seen in figure 7.1A-D). Vesicles were defined as spherical structures that demonstrate staining for both TGFBR3 and glycocalyx from the cell membrane. Vesicles were characterized as large (>6μm) or small. Furthermore, cells were counted and distinguished into positive and negative for the presence of intracellular TGFBR3. Vesicles per cell and the ratio between TGFBR3 positive cells and total cell counts were calculated after automatic nuclei counts (performed by SlideBook TM software). No interobserver variability was found in the measurements (vesicles: p=0.69; TGFBR3 positive cells: p=1.0).

2.4 Quantification of gene expression by quantitative polymerase chain reaction

Total RNA was isolated using the NucleoSpin Triprep Kit (Macherey-Nagel, Düren, Germany). Complementary DNA synthesis was performed using the VILO kit (Macherey-Nagel, Düren, Germany), in a 20μL reverse transcription reaction, according to manufacturer's instructions. Quantitative PCR (qPCR) was performed to show the effect of the mutations on mRNA level in *FBN1* (NM_000138), and to analyze the potential effect of the mutation on the expression of related and target genes: *FBN*2 (NM_001999), *FBN*3 (NM_032447), *FN*1 (NM_002026), *SERPINE*1 (NM_000602), SMAD7 (NM_005904), *TGFB1* (NM_000660), *TGFBR1* (NM_004612), *TGFBR2* (NM_003242), *TGFBR3* (NM_003243), *COL1A1* (NM_000088), *CTGF* (NM_001901) *HSP47* (NM_001207014) and *HSPA5* (NM_005347). As housekeeping genes for the normalization of the acquired data *YWHAZ* (NM_003406), *HPRT* (NM_000194) and *UBC* (NM_021009) were used. The analysis was performed using the using the Light Cycler SYBR Green I Master (Roche Applied Science, Penzberg, Germany) in the LightCycler 480 Instrument II (Roche Applied Science, Penzberg, Germany), as described before in more detail.[31]

Each qPCR reaction was prepared in a total volume of 10μL, consisting of 2μl PCR grade water, 1μL forward primer (10pM), 1μL reverse primer (10pM) and 5μL Light Cycler Mastermix (Light Cycler 480 SYBR Green I Master; Roche Applied Science), to which 2μL of the synthesized cDNA was added. Using absolute quantification, all values were determined based on standard curve of four serial dilutions ranging from 10ng

until 0.08ng of human reference cDNA (Agilent Technologies, Santa Clara, CA). qPCR efficiency was assessed using the fit points method, and gene expression data was analyzed with the efficiency ranging between1.7-2.0. Moreover, mRNA expression of the investigated genes was normalized by a normalization factor derived from the expression of three housekeeping genes (*YWHAZ*, *HPRT* and *UBC*).

2.5 Statistical analysis

Data were analyzed with SPSS (IBM Statistics v24, Chicago, IL). For multiple groups, the Kruskal–Wallis was used first to compare continuous variables with nonparametric distribution; subsequently, the Mann–Whitney U test was used for comparing two groups. Fisher's exact test was used for categorical variables in two groups. Raw data are given in the text as median with ranges in between brackets and data are presented graphically as boxplots (showing median and quartiles) with outliers (according to Tukey's criteria) indicated separately. Correlations between two continuous variables were calculated by Spearman rank. Tests were considered statistically significant at $P<0.05$. In case of multiple testing, corrected p-values are used according to Bonferroni.

3. RESULTS

3.1 Protein expression in cell lines

By immunofluorescence microscopy, a significantly higher ratio of TGFBR3 positive cells was observed in the cell cultures of both DN and HI groups pooled (median 0.35 [0.11 - 0.80]) as compared to controls (median 0.00 [0.00 - 0.37]; p=0.004). DN patients had higher ratios of TGFBR3 positive cells (median 0.47 [0.14 – 0.80]) than HI patients (median 0.33 [0.11 – 0.80]; p=0.015). No differences were found in the expression of TGFBR3 vesicles between *FBN1* mutant cells and controls or between DN and HI patients (table 7.2 and figure 7.1).

Table 7.2. TGF-ß receptor 3 protein expression was demonstrated by immunofluorescence microscopy in membrane-encapsulated vesicles or in the endoplasmic reticulum. Vesicles were classified as small (≤ 6µm) or large. The ratio of vesicles per nucleus is given, as well as the ratio of cells positive for TGF-ß receptor 3 in the endoplasmic reticulum per total cell count. Median ratios are given with ranges in between brackets. Genetic expressions were measured by quantitative polymerase chain reaction and presented in arbitrary units. Statistical differences between *FBN1* mutants pooled and controls are given by p-values, as well as between DN and HI *FBN1* mutations. P-values <0.05 were considered significant and are indicated by an asterisk.

Immunofluorescence microscopy	**Mutants (total)**	**Control**	**p-value**	**DN**	**HI**	**p-value**
	n = 13	*n = 10*		*n = 4*	*n = 9*	
Small vesicles (per nucleus)	0.14 (0.03 - 0.60)	0.14 (0.03 - 0.30)	0.419	0.26 (0.07 - 0.41)	0.12 (0.03 - 0.60)	0.643
Large vesicles (per nucleus)	0.02 (0.00 - 0.07)	0.01 (0.00 - 0.04)	0.651	0.01 (0.00 - 0.07)	0.02 (0.00 - 0.04)	1.000
Total vesicles (per nucleus)	0.16 (0.04 - 0.61)	0.16 (0.03 - 0.30)	0.420	0.30 (0.07 - 0.41)	0.14 (0.04 - 0.61)	0.643
ß-glycan positive cells (of total)	0.35 (0.11 - 0.80)	0.00 (0.00 - 0.37)	0.004*	0.47 (0.14 - 0.80)	0.33 (0.11 - 0.80)	0.015*
Quantitative PCR	*n = 10*	*n = 6*		*n = 4*	*n = 6*	
TGFB1	7.23 (4.55 - 11.1)	4.64 (2.76 - 6.97)	0.027*	7.59 (7.19 - 11.06)	6.17 (4.55 - 7.83)	0.059
TGFBR1	1.09 (0.71 - 2.01)	1.39 (0.79 - 1.96)	0.615	1.04 (0.84 - 1.70)	1.21 (0.71 - 2.01)	0.705
TGFBR2	2.25 (1.14 - 7.95)	1.59 (0.62 - 3.75)	0.191	2.45 (1.85 - 7.95)	2.25 (1.14 - 3.11)	0.345
TGFBR3	3.65 (1.78 - 7.69)	4.33 (0.41 - 7.03)	0.688	3.21 (2.5 - 4.01)	4.74 (1.78 - 7.69)	0.257
SMAD7	7.29 (4.77 - 15.5)	5.61 (3.03 - 6.73)	0.044*	9.24 (7.09 - 15.47)	6.43 (4.77 - 11.7)	0.019*
FBN1 P1	2.08 (0.74 - 6.20)	1.83 (0.88 - 5.04)	0.546	3.48 (2.10 - 6.20)	1.93 (0.74 - 2.59)	0.014*
FBN1 P2	0.66 (0.34 - 1.25)	0.79 (0.34 - 2.12)	0.315	0.79 (0.63 - 1.25)	0.51 (0.34 - 1.21)	0.089
FBN2	8.13 (0.49 - 52.4)	11.28 (7.81 - 101.3)	0.228	8.13 (4.68 - 34.4)	8.72 (0.49 - 52.4)	0.450
HSP47	41.2 (27.9 - 75.5)	29.8 (4.56 - 50.3)	0.070	53.6 (37.5 - 75.5)	34.1 (27.9 - 51.2)	0.023*
HSPA5	2.77 (1.99 - 4.20)	2.48 (1.62 - 3.28)	0.131	2.49 (1.99 - 2.89)	3.18 (2.58 - 4.20)	0.029*
SERPINE1	42.7 (24.8 - 71.5)	35.2 (13.24 - 87.5)	0.688	51.8 (46.6 - 71.5)	39.5 (24.8 - 45.0)	0.008*
FN1	21.1 (10.4 - 64.6)	22.7 (7.61 - 33.9)	0.688	37.2 (17.5 - 64.6)	19.1 (10.4 - 27.0)	0.089
CTGF	39.5 (4.40 - 163.9)	23.6 (16.5 - 44.0)	0.615	48.5 (11.1 - 163.9)	30.2 (4.40 - 78.6)	0.571
COL1A1	1898.0 (939.0 - 2689.4)	1137.8 (406.1 - 1589.5)	0.088	2314.2 (1894.1 - 2360.0)	1269.3 (939.0 - 2689.4)	0.089

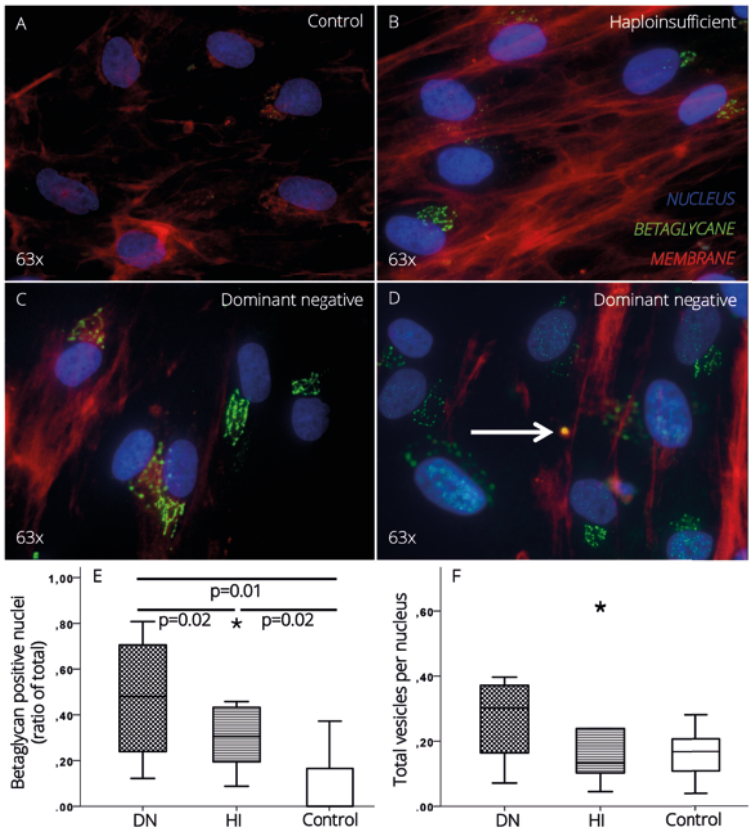

Figure 7.1 Representative immunofluorescence microscopy images of Betaglycan expression in fibroblast cell cultures of a control (A), a haploinsufficient (B) and dominant negative (C) *FBN1* gene mutation. Betaglycan was seen in the endoplasmic reticulum or in membrane encapsulated vesicles as indicated by the arrow in image D. Ratios of Betaglycan positive cells per total cell count (E) and vesicles per nucleus (F) are given as median with interquartile ranges in the boxplots. Significant differences (p≤0.05) are highlighted by a horizontal line and outliers are indicated separately by an asterisk.

3.2 Gene expression in cell cultures

By qPCR, a significantly higher gene expression was measured in *FBN1* mutant cells than in controls for both *TGFB1* (median 7.23 [4.55 - 11.1] versus 4.64 [2.76 - 6.97]; p=0.027; respectively) and *SMAD7* (median 7.29 [4.77 - 15.5] versus 5.61 [3.03 - 6.73]; p=0.044; respectively). *COL1A1* had a tendency to be higher (median 1898.0 [939.0 - 2689.4]) than in controls (median 1137.8 [406.1 - 1589.5]; p=0.088), as well *HSP47* (median 41.2 [27.9 - 75.5] versus 29.8 [4.56 - 50.3]; p=0.070, respectively). No differences were found in *TGFR1*, *-2* and *–3* expression between groups, or in downstream proteins *FBN1* and *FBN2*, HSPA5, *FN1*, *SERPIN1* and *CTGF*. See figure 7.2 for boxplots of a selection of gene expressions.

Subgroup analysis showed higher gene expressions in DN as compared to HI of *SMAD7* (median 9.24 [7.09 - 15.47] versus 6.43 [4.77 - 11.7]; p=0.019; respectively), *FBN1* P1 (median 3.48 [2.10 - 6.20] versus 1.93 [0.74 - 2.59]; p=0.014; respectively), *HSP47* (median 53.6 [37.5 - 75.5] versus 34.1 [27.9 - 51.2]; p=0.023; respectively) and *SERPIN1* (median 51.8 [46.6 - 71.5] versus 39.5 [24.8 - 45.0]; p=0.008; respectively). DN had lower gene expression of *HSPA5* than HI (median 2.49 [1.99 - 2.89] versus 3.18 [2.58 - 4.20]; p=0.029; respectively). DN tended to have higher gene expressions than HI of *TGFB1* (median 7.59 [7.19 - 11.06] versus 6.17 [4.55 - 7.83]; p=0.059; respectively), *FBN1* P2 (median 0.79 [0.63 - 1.25] versus 0.51 [0.34 - 1.21]; p=0.089; respectively) *FN1* (median 37.2 [17.5 - 64.6] versus 19.1 [10.4 - 27.0]; p=0.089; respectively) and *COL1A1* (median 2314.2 [1894.1 - 2360.0] versus 1269.3 [939.0 - 2689.4]; p=0.089; respectively).

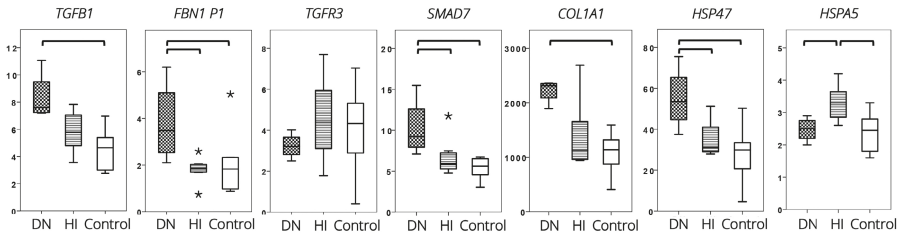

Figure 7.2 A selection of the results of quantitative polymerase chain reaction in arbitrary units in dominant negative and haploinsufficient *FBN1* mutations and controls are graphically represented as boxplots with interquartile ranges. Significant differences between groups (p≤0.05) are highlighted by an accolade. Outliers are separately indicated by an asterisk.

3.3 Correlations between protein and mRNA expression

The correlation between *TGFB1* mRNA expression with *TGFBR3* mRNA and TGFBR3 positive cells (both ratio and total positive cells) was tested (significance level after Bonferroni correction for multiple testing is p≤0.017). *TGFB1* mRNA expression was positively correlated with the ratio of TGFBR3 positive cells (Rs=0.60; p=0.017; figure 7.3). No correlation was found between TGFBR3 protein expression and *TGFBR3* mRNA expression.

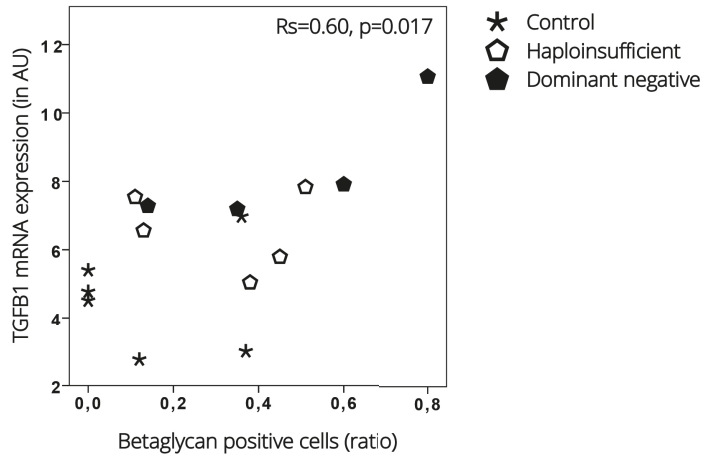

Figure 7.3 Correlations between TGFBR3 protein expression and *TGFB1* mRNA expression. The ratio of TGFBR3 positive cells to the total cell count is given on the x-axis, *TGFB1* mRNA expression on the Y-axis (in AU). Correlations are given in Spearman rank (Rs) correlation with p-value.

4. DISCUSSION

The major findings of the present study are: i) in patients with a DN *FBN1* gene mutation, fibroblasts have upregulated *TGFB1* and associated downstream signaling activation as compared to controls. Also, DN *FBN1* gene mutants have a tendency of upregulated *TGFB1* and associated signaling activation as compared to HI *FBN1* gene mutants; ii) TGFBR3 protein expression in patients with a DN *FBN1* gene mutation is higher than in the HI group; iii) *TGFB1* expression is positively correlated with TGFBR3 protein expression.

The intracellular downstream pathway of TGF-ß involves, among others, SMAD7 activation as well as transcription of COL1A1 and FN1.[20–27] In figure 7.4 we graphically represented the investigated part of the pathway in DN mutants. We demonstrated upregulated TGF-ß activation and downstream signaling. On a protein level we observed more TGFBR3 expression in DN *FBN1* gene mutants than in HI patients. It has been suggested that TGFBR3 is able to inhibit as well as enhance downstream TGF-ß signaling.[30] However, it remains a matter of debate how TGFBR3 provides the downstream TGF-ß signaling in MFS.[30] It has been acknowledged that TGFBR3 stimulates downstream signaling by presenting TGF-ß to TGFBR2.[18] Recently, however, two studies suggested that TGFBR3 regulates the signaling turnover by adjusting the ratio of soluble

to membrane bound receptors.[32,33] In the current study we demonstrated a positive correlation between TGFBR3 protein expression and TGF-ß signaling. We acknowledge that no knock-out or over-expression experiments have been performed, which hinders providing causative correlations. However, our data suggest that increased expression of TGFBR3 in MFS patients with DN mutation enhances activation of the TGF-ß signaling pathway. Our study warrants further investigation of the role of TGFBR3.

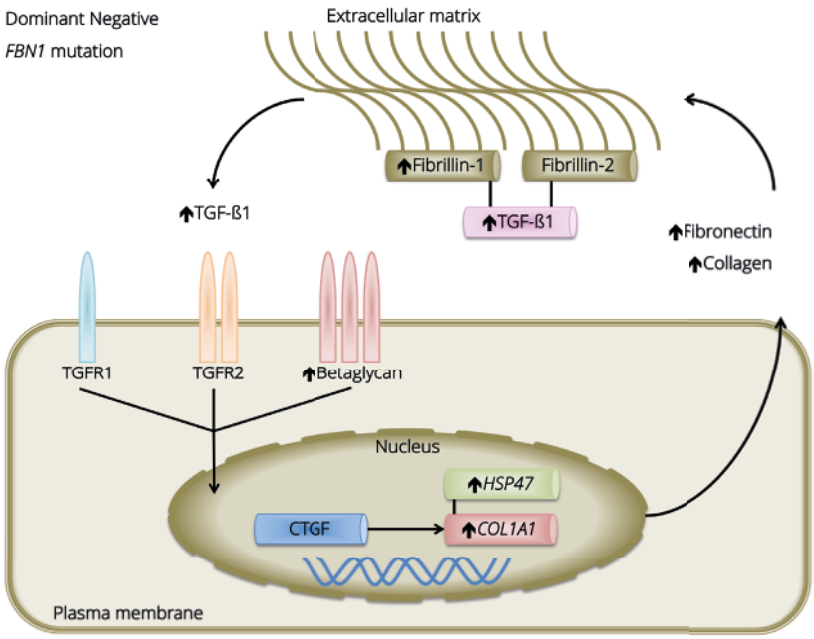

Figure 7.4 TGF-ß signaling and its partially downstream pathways in dominant negative *FBN1* mutations. Upward pointing arrows indicate increased expression as compared to healthy controls. In the extracellular matrix fibrillin-1 expression is upregulated, though it partly concerns wild type but also malfolded proteins. Therefore its binding capacity to TGF-ß1 is affected, resulting in high levels of free TGF-ß1 in the extracellular matrix. The intracellular downstream pathway of TGF-ß1 is consequently activated in higher amounts. Interestingly, increased downstream activation occurs while the amount of TGF-ß receptors are similar to controls. Eventually, intranuclear transcription of COL1A1 and its chaperone protein HSP47 are upregulated resulting in increased collagen expression and the tendency of higher fibronectin expression.

TGFBR3 protein expression was observed in two distinct locations in the cell, either in the ER or in intracellular membrane encapsulated vesicles. We observed higher expressions of TGFBR3 in MFS patients with a DN than a HI mutation. However, no differences were found in gene expression of *TGFBR3* between mutants and controls or between DN and HI. We hypothesize that the encapsulated TGFBR3 is stored in vesicles in order to regulate the total amount of receptors that are expressed on the

cell membrane. By doing so, as described above, TGFBR3 might adjust the ratio of soluble to membrane bound receptors and influence TGF-ß signaling.[33] This hypothesis could explain the discrepancy between *TGFBR3* mRNA and TGFBR3 protein expression in fibroblasts. However, one must realize that we investigated cell cultures of skin fibroblasts that lack an ECM like in the aortic wall. The lack of ECM might alter the stimulation and direction of the TGFBR3 filled vesicles.

As discussed earlier, fibrillin-1 protein is involved in the regulation of TGF-ß bioavailability in the ECM by binding to complexes of latent TGF-ß.[13] In patients with a DN *FBN1* mutation we observed upregulated *FBN1* gene expressions as compared to controls and a tendency of higher expressions in the DN than in the HI group. In MFS patients with a DN mutation this will lead to malfunctioning fibrillin-1 protein, with less capacity to bind latent TGF-ß in the ECM.[9] We suggest that in DN *FBN1* gene mutants this might be the cause of increased free TGF-ß in the ECM of diseased vessel walls, as was earlier demonstrated.[34] Fibrillin-2 protein has also been acknowledged to have a role in the regulation of free TGF-ß in the ECM.[13] However, we found that TGF-ß and its downstream signaling was increased in DN mutants, despite similar *FBN2* gene expression. Therefore, we suggest that fibrillin-2 has only a limited role in the level of TGF-ß expression.

A remarkable contradiction was the finding of upregulated expression of *HSP47* in the DN group as compared to HI patients, versus downregulated expression of *HSPA5* in the DN group as compared to HI patients. Both genes are acknowledged as ER stress markers, more specifically as markers of activated unfolded protein response.[35,36] Furthermore, TGF-ß has been demonstrated to upregulate the expression of *HSP47*.[37] Therefore, increased *HSP47* expression was expected in the DN group, as DN *FBN1* mutations lead to malfolded fibrillin-1 proteins and consequently to activation of the unfolded protein response. We did not expect *HSPA5* expression to be increased in the HI group as compared to the DN group and controls. This could be explained by the fact that HSPA5 also functions as a chaperone protein, transporting newly synthesized polypeptides and facilitates their assembly into proteins. This process may be disturbed in DN mutants.[15,16]

The use of fibroblasts may be regarded as a limitation of this study, as it possibly does not fully reflect aortic cell pathology. These cells have the genotype but not the phenotype. However, it has been demonstrated that patients with enhanced TGF-ß signaling in dermal fibroblasts also are associated with multiple syndromic presentations of aortic aneurysms.[38] We therefore consider these cells to be representative for this part of the investigated pathway. Furthermore, in the current work we have mainly focused

on the genetically stimulation. Therefore, at this time our data lack clinical information. Therefore, our model does not take into account the potential impact of aspects such as phenotypic variation between patients and pharmacological treatments.

The implication of the present work is that it emphasizes important differences in patients between the effects of DN versus HI mutations of the *FBN1* gene. A recent study showed that MFS patients with HI *FBN1* mutations had higher therapeutic benefit from Losartan treatment compared to patients with DN *FBN1* mutations which indicates a distinct pathological mechanism.[8] Thus, the different types of *FBN1* mutations must be approached in a different manner in the search for therapeutic options.

In conclusion, we demonstrated an increased activation of TGF-ß and its downstream signaling pathway in patients with a DN *FBN1* gene mutation as compared to patients with a HI *FBN1* mutation and to control groups. Also, TGFBR3 protein expressions are increased in the DN group and correlate positively with *TGFB1* expressions in groups pooled. We suggest that TGFBR3 expression is involved in upregulated TGF-ß signaling in MFS patients with a DN *FBN1* gene mutation.

REFERENCES

1. Dietz HC. Marfan syndrome. In: *Marfan Syndrome. 2001 Apr 18 [Updated 2017 Feb 2]. In: Pagon RA, Adam MP, Ardinger HH, et Al., Editors. GeneReviews® [Internet]. Seattle (WA): University of Washington, Seattle; 1993-2017.* https://www.ncbi.nlm.nih.gov/books/NBK1335/.
2. Takeda N, Yagi H, Hara H, et al. Pathophysiology and Management of Cardiovascular Manifestations in Marfan and Loeys-Dietz Syndromes. *Int Heart J*. 2016:271-277. doi:10.1536/ihj.16-094.
3. Sakai LY, Keene DR, Renard M, De Backer J. FBN1: The disease-causing gene for Marfan syndrome and other genetic disorders. *Gene*. 2016;591(1):279-291. doi:10.1016/j.gene.2016.07.033.
4. Gillis E, Van Laer L, Loeys BL. Genetics of thoracic aortic aneurysm: At the crossroad of transforming growth factor-β signaling and vascular smooth muscle cell contractility. *Circ Res*. 2013;113(3):327-340. doi:10.1161/CIRCRESAHA.113.300675.
5. Attenhofer Jost CH, Greutmann M, Connolly HM, et al. Medical treatment of aortic aneurysms in Marfan syndrome and other heritable conditions. *Curr Cardiol Rev*. 2014;10(2):161-171. doi:10.2174/1573403X1002140506124902.
6. Zeyer KA, Reinhardt DP. Engineered mutations in fibrillin-1 leading to Marfan syndrome act at the protein, cellular and organismal levels. *Mutat Res - Rev Mutat Res*. 2015;765:7-18. doi:10.1016/j.mrrev.2015.04.002.
7. Jensen S, Handford P. New insights into the structure, assembly and biological roles of 10-12 nm connective tissue microfibrils from fibrillin-1 studies. *Biochem Jounal*. 2016;473(7):827-838. doi:10.1042/BJ20151108.
8. Franken R, Den Hartog AW, Radonic T, et al. Beneficial Outcome of Losartan Therapy Depends on Type of FBN1 Mutation in Marfan Syndrome. *Circ Cardiovasc Genet*. 2015;8(2):383-388. doi:10.1161/CIRCGENETICS.114.000950.
9. Faivre L, Collod-Beroud G, Loeys BL, et al. Effect of Mutation Type and Location on Clinical Outcome in 1,013 Probands with Marfan Syndrome or Related Phenotypes and FBN1 Mutations: An International Study. *Am J Hum Genet*. 2007;81(3):454-466. doi:10.1086/520125.
10. Hilhorst-Hofstee Y, Hamel BCJ, Verheij JBGM, et al. The clinical spectrum of complete FBN1 allele deletions. *Eur J Hum Genet*. 2011;19(3):247-252. doi:10.1038/ejhg.2010.174.
11. Schrijver I, Liu W, Odom R, et al. Premature Termination Mutations in FBN1: Distinct Effects on Differential Allelic Expression and on Protein and Clinical Phenotypes. *Am J Hum Genet*. 2002;71(2):223-237. doi:10.1086/341581.
12. Schrijver I, Liu W, Brenn T, Furthmayr H, Francke U. Cysteine substitutions in epidermal growth factor-like domains of fibrillin-1: distinct effects on biochemical and clinical phenotypes. *Am J Hum Genet*. 1999;65(4):1007-1020. doi:10.1086/302582.
13. Ten Dijke P, Arthur HM. Extracellular control of TGFβ signalling in vascular development and disease. *Nat Rev Mol Cell Biol*. 2007;8(11):857-869. doi:10.1038/nrm2262.
14. Habashi JP, Judge DP, Holm TM, et al. Losartan, an AT1 antagonist, prevents aortic aneurysm in a mouse model of Marfan syndrome. *Science (80-)*. 2006;312(5770):117-121. doi:10.1126/science.1124287.
15. Zhu G, Lee AS. Role of the unfolded protein response, GRP78 and GRP94 in organ homeostasis. *J Cell Physiol*. 2015;230(7):1413-1420. doi:10.1002/jcp.24923.

16. Morry J, Ngamcherdtrakul W, Gu S, et al. Dermal delivery of HSP47 siRNA with NOX4-modulating mesoporous silica-based nanoparticles for treating fibrosis. *Biomaterials*. 2015;66:41-52. doi:10.1016/j.biomaterials.2015.07.005.

17. López-Casillas F, Payne HM, Andres JL, Massagué J. Betaglycan can act as a dual modulator of TGF-β access to signaling receptors: Mapping of ligand binding and GAG attachment sites. *J Cell Biol*. 1994;124(4):557-568. doi:10.1083/jcb.124.4.557.

18. López-Casillas F, Wrana JL, Massagué J. Betaglycan presents ligand to the TGFß signaling receptor. *Cell*. 1993;73(7):1435-1444. doi:10.1016/0092-8674(93)90368-Z.

19. Massagué J, Gomis RR. The logic of TGFβ signaling. *FEBS Lett*. 2006;580(12):2811-2820. doi:10.1016/j.febslet.2006.04.033.

20. Hill CS. Nucleocytoplasmic shuttling of Smad proteins. *Cell Res*. 2009;19(1):36-46. doi:10.1038/cr.2008.325.

21. Heldin C, Moustakas A. Signaling Receptors for TGF- b Family Members. *Cold Spring Harb Perspect Biol*. 2016;8(8). doi:10.1101/cshperspect.a022053.

22. Xie S, Sukkar MB, Issa R, Oltmanns U, Nicholson AG, Chung KF. Regulation of TGF-ß1-induced connective tissue growth factor expression in airway smooth muscle cells. *Am J Physiol Lung Cell Mol Physiol*. 2005;288:68-76. doi:10.1152/ajplung.00156.2004.

23. Feng X-H, Derynck R. Specificity and Versatility in Tgf-B Signaling Through Smads. *Annu Rev Cell Dev Biol*. 2005;21(1):659-693. doi:10.1146/annurev.cellbio.21.022404.142018.

24. Lindahl GE, Chambers RC, Papakrivopoulou J, et al. Activation of fibroblast procollagen α1(I) transcription by mechanical strain is transforming growth factor-ß-dependent and involves increased binding of CCAAT-binding factor (CBF/NF-Y) at the proximal promoter. *J Biol Chem*. 2002;277(8):6153-6161. doi:10.1074/jbc.M108966200.

25. Pan X, Chen Z, Huang R, Yao Y, Ma G. Transforming Growth Factor β1 Induces the Expression of Collagen Type I by DNA Methylation in Cardiac Fibroblasts. *PLoS One*. 2013;8(4). doi:10.1371/journal.pone.0060335.

26. Ignotz RA, Massagué J. Transforming growth factor-beta stimulates the expression of fibronectin and collagen and their incorporation into the extracellular matrix. *J Biol Chem*. 1986;261(9):4337-4345. http://www.ncbi.nlm.nih.gov/pubmed/3456347.

27. Dallas SL, Sivakumar P, Jones CJP, et al. Fibronectin regulates latent transforming growth factor-β (TGFβ) by controlling matrix assembly of latent TGFβ-binding protein-1. *J Biol Chem*. 2005;280(19):18871-18880. doi:10.1074/jbc.M410762200.

28. Yan X, Liu Z, Chen Y. Regulation of TGF-beta signaling by Smad7. *Acta Biochim Biophys Sin (Shanghai)*. 2009;41(4):263-272. doi:10.1093/abbs/gmp018.Review.

29. Akhurst RJ. The paradoxical TGF-β vasculopathies. *Nat Genet*. 2013;44(8):838-839. doi:10.1002/ana.22528.Toll-like.

30. Bilandzic M, Stenvers KL. Betaglycan: A multifunctional accessory. *Mol Cell Endocrinol*. 2012;359(1-2):13-22. doi:10.1016/j.mce.2012.03.020.

31. Yeung KK, Bogunovic N, Keekstra N, et al. Transdifferentiation of Human Dermal Fibroblasts to Smooth Muscle-Like Cells to Study the Effect of *MYH11* and *ACTA2* Mutations in Aortic Aneurysms. *Hum Mutat*. 2017. doi:10.1002/humu.23174.

32. Derynck R, Zhang YE. Smad-dependent and Smad-independent pathways in TGF-β family signalling. *Nature*. 2003;425(6958):577-584. doi:10.1038/nature02006.

33. Elderbroom JL, Huang JJ, Gatza CE, et al. Ectodomain shedding of TßRIII is required for TßRIII-mediated suppression of TGF-ß signaling and breast cancer migration and invasion. *Mol Biol Cell*. 2014;25(16):2320-2332. doi:10.1091/mbc.E13-09-0524.

34. Chaudhry SS, Cain SA, Morgan A, Dallas SL, Shuttleworth CA, Kielty CM. Fibrillin-1 regulates the bioavailability of TGFβ1. *J Cell Biol*. 2007;176(3):355-367. doi:10.1083/jcb.200608167.

35. Wang J, Lee J, Liem D, Ping P. HSPA5 Gene encoding Hsp70 chaperone BiP in the endoplasmic reticulum. *Gene*. 2017;618:14-23. doi:10.1016/j.gene.2017.03.005.

36. Kawasaki K, Ushioda R, Ito S, Ikeda K, Masago Y, Nagata K. Deletion of the collagen-specific molecular chaperone Hsp47 causes endoplasmic reticulum stress-mediated apoptosis of hepatic stellate cells. *J Biol Chem*. 2015;290(6):3639-3646. doi:10.1074/jbc.M114.592139.

37. Martelli-Junior H, Cotrim P, Graner E, Sauk JJ, Coletta RD. Effect of Transforming Growth Factor-ß1, Interleukin-6, and Interferon-γ on the Expression of Type I Collagen, Heat Shock Protein 47, Matrix Metalloproteinase (MMP)-1 and MMP-2 by Fibroblasts from Normal Gingiva and Hereditary Gingival Fibromatosis. *J Periodontol*. 2003;74(3):296-306.

38. Doyle AJ, Doyle JJ, Bessling SL, et al. Mutations in the TGF-β Repressor SKI Cause Shprintzen-Goldberg Syndrome with Aortic Aneurysm. *Nat Genet*. 2013;44(11):1249-1254. doi:10.1038/ng.2421. Mutations.

PART III

NOVEL TECHNIQUE FOR INVESTIGATING CELLULAR SIGNALLING PATHWAYS

Chapter 8: An in-vitro method to keep human aortic tissue sections functionally and structurally intact for over 60 days

CHAPTER 8

AN IN-VITRO METHOD TO KEEP HUMAN AORTIC TISSUE SECTIONS FUNCTIONALLY AND STRUCTURALLY INTACT FOR OVER 60 DAYS

J.P. Meekel[1,2]
M.E. Groeneveld[1,2]
N. Keekstra[1,2]
R.J.P. Musters[2]
B.Z. Doulabi[3]
D. Micha[3]
G Pals[3]
H.W.M. Niessen[4]
A.M. Wiersema[5]
J. Kievit[5]
A.W.J. Hoksbergen[1]
W. Wisselink[1]
J.D. Blankensteijn[1]
K.K. Yeung[1,2]

[1] Department of Vascular Surgery, Amsterdam University Medical Center
[2] Department of Physiology, Amsterdam University Medical Center
[3] Department of Clinical Genetics, Amsterdam University Medical Center
[4] Department of Pathology and Cardiac Surgery, University Medical Center
[5] Department of Vascular Surgery, West Fries Gasthuis, Hoorn

Scientific Reports 2018, vol. 8, pag. 8094

ABSTRACT

Objective: The pathophysiology of aortic aneurysms (AA) remains unclear. AA is an unpredictable disease, which often results in rupture, causing bleeding and death. Currently, research on aortic aneurysm pathophysiology is limited to fixated cells or isolated cell cultures. However, due to these techniques, cell receptor functions, cell-cell interactions and communication with extracellular matrix are lost. These interactions are likely to play a role in AA pathogenesis. We hereby present an innovative method to cut live aneurysmal aortic tissue sections for preservation of viability and cellular organization.

Methods: Peroperatively harvested live tissue was transported in transplant medium Custodiol® and cut into sections (150 µm), using a vibratome. Hereafter sections were cultured in media supplemented with antibiotics. Viability analysis was performed by immunofluorescence quantification using LIVE/DEAD® Kit until 92 days. Cell type characterization was achieved by immunostaining for CD45, CD68, α-SMA and smoothelin. Additionally, at day 14 of culturing, live tissue sections were broken down into individual cells by use of collagenase. Separate cells were examined for further viability analysis using Muse®, an absolute cell count and viability analyzer for cell suspensions.

Results: Analysis of abdominal AA tissue (N=8) showed a viability of 40% until 7 days. Protocol optimization (pre-sectioning removing of calcium depositions, direct tissue culturing during sectioning, heated transport of tissue sections, staining performed in culture medium and shorter tissue-out-of-incubator times, N=4) improved viability of initial tissue until 62 days. Live cells were mainly seen at the interior of tissue and dead cells at the cutting edges. At day 92, outgrowth of many new cells from the original tissue was observed. Analysis of cell-specific marker expression showed SMC, leukocytes and macrophages. Enzymatically digested cells showed different cell type characteristics and a viability of 75% was observed using Muse®.

Conclusions: Viability and cellular organization of aortic tissue sections can be preserved until at least 62 days after harvesting. During culturing, tissues can be broken down to into separate cells with a high viability for additional techniques like FACS, MACS and traction force microscopy. This model provides an appropriate ex vivo setting to discover, study and stimulate pathways and mechanisms in human aneurysmal tissue.

1. INTRODUCTION

Aortic aneurysm (AA) is a common health problem, which is associated with high mortality rates in the event of a rupture. This unpredictable life-threatening rupture leads to rapid aortic exsanguination into thorax, abdominal cavity or retroperitoneum.[1-3] To date, studies investigating the pathophysiology of AA have produced inconclusive results concerning the underlying mechanisms. Although different meaningful disease models exist, the lack of a functionally and structurally intact live aortic human tissue model which can bioactively be stimulated *ex vivo*, has posed severe limitations to the study of AA in understanding the pathophysiological mechanism which has restricted the identification of therapeutic targets and the development of efficient therapy.[4]

It has been observed previously that an increase of AA diameter occurs in relation to the transformation of the aortic vessel wall composition. Part of this transformation is a combination of vascular smooth muscle cell (SMC) loss and inflammation and degeneration of extracellular matrix (ECM). These changes are suggested to play a role in the pathogenesis of AA, but mechanisms contributing to these processes, are still poorly understood.[5, 6]

Although numerous *in vivo* animal models to study AA exist, investigation of human material is limited to the use of fixated tissue or isolated cell cultures.[7-12] Such approaches, however, have failed to retain the complex organ function of the aorta, which is based on cell-cell interactions, communication with ECM, immune cell infiltration and constant tissue remodelling.[13-16]

Unfortunately, fixated aortic tissue only provides a snapshot into the microstructural characteristics of the diseased tissue, and isolated cultured aortic cells cannot reproduce the complexity of cell-ECM interactions and live pathways. Additionally, usage of animal models is costly, ethically and technically challenging and animal models do not completely resemble the human conditions, as the aortic aneurysms need to be created in the animal model.

Hence, there is a need to provide a new *in vitro* model to study the pathophysiological processes, which are involved human AA. Live sectioning and preservation of human (aneurysmal) aortic tissue can lead to improvement of the understanding of AA pathogenesis. In this study, we present an innovative method for the investigation of human AA pathophysiology by preserving tissue viability and cellular organization of human aneurysmal tissue *ex vivo* for several weeks.

2. METHODS

2.1 Human tissues

The present study was approved by the Medical Ethical Committee of the Amsterdam University Medical Center. Informed consent files were signed prior to surgery. In case of acute surgery for ruptured aneurysm repair, delayed informed consent was received in the postoperative period as soon as permitted by the health situation of the patients. All experiments were performed in accordance with relevant guidelines and regulations.

Human aortic tissue was collected from the operating theatre in two hospitals (AUMC, location VUmc, the Netherlands and Westfriesgasthuis, Hoorn, the Netherlands) during open abdominal AA (AAA) surgery (N=9). Additional vascular tissues were harvested from human non-aortic anatomical sites (N=4): external iliac artery punch and renal artery. Using nine consecutively harvested human vascular tissues (N[AAA]=5 and N[additional vascular tissues]=4), a pilot study with primary viability analysis until 14 days was performed. These results were evaluated to further develop the protocol with minor improvements. Subsequently, new AAA tissue (N=4) was harvested and subjected to the new protocol to evaluate the maximum life span of human AAA tissue sections *ex vivo* (figure 8.1A).

2.2 Transport and vascular section preparation

Directly after harvesting tissue at the operating theatre, the vascular tissue was submerged in Custodiol (Dr. Franz Köhler Chemie GmbH, Bensheim, Germany) at 4°Celsius. The tubes containing tissue were transported on ice to the vibratome (Leica VT1200 S, Leica Biosystems, Nussloch, Germany). Vascular cubes of 5x5x5 mm were cut using a scalpel. These cubes contained intima, media and adventitia. Cubes were then glued on a specimen anvil using Roti Coll superglue (Carl Roth GmbH + Co. KG, Karlsruhe, Germany). The intimal layer of the cubes was facing the knife of the vibratome, to ensure that after cutting, aortic sections were containing all layers. Fixed cubes were embedded in agarose gel solution (1 g agarose in 50 mL 0.5x TAE buffer, UltraPure™ Agarose, Thermo Fisher Scientific Inc., Waltham, MA, USA) using a self-designed 3D-printed mould (figure 8.1B).

After cooling down and thereby stiffening of agarose gel, the mould was removed. The entirety of anvil, tissue and agarose was immersed in a small reservoir filled with Custodiol at 4°C. The reservoir was placed under the razor blade (Croma Stabil, Feintechnik GmbH, Eisfeld, Germany) of the vibratome (figure 8.1C). Cutting of sections containing intima, media and adventitia was performed. The first three consecutive

sliced sections were discarded, since these often macroscopically did not contain all layers of the vascular wall and lower viability in these sections was to be expected. From earlier (unpublished) pilot experiments, we determined that the best viability results were acquired by cutting 150-µm-thick sections with the vibratome at a speed of 0.08 mm/s with a horizontal amplitude of the razor blade fixed at 2.65 mm. For the development of the present protocol, live bovine tissues were firstly used to set up the optimum settings for the vibratome. Abdominal bovine aorta was obtained from an abattoir (Abattoir Amsterdam B.V, Amsterdam, the Netherlands) directly after euthanization.

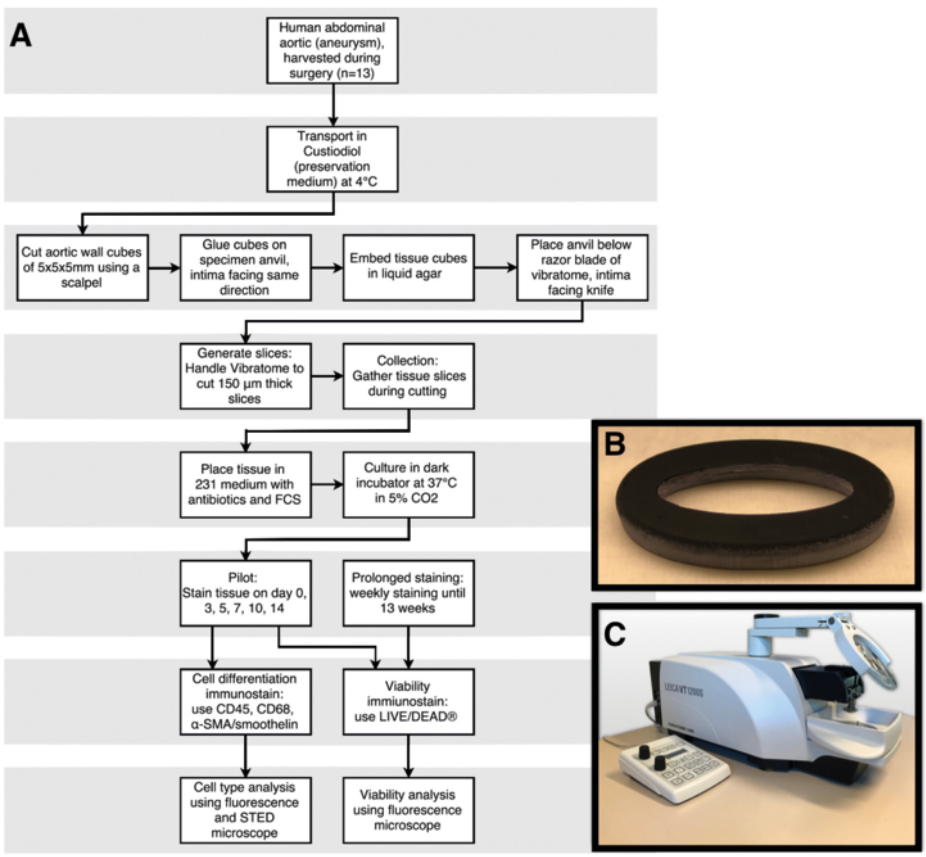

Figure 8.1 Overview of experimental setup. A: Flow chart of protocol: vascular tissue cubes were cut into sections using a vibrating blade microtome (Leica VT1200 S). Tissue sections were cultured in supplemented culture medium in 24-well plates in a dark humidified atmosphere at 37°C in 5% CO2. B: Photograph of self-designed 3D-printed mould in which tissue cubes are fixed in agarose. C: Photograph of vibratome Leica VT1200S, used for tissue sectioning. α-SMA indicaties alpha smooth muscle actin; FCS, fetal calf serum and STED, stimulated emission depletion.

2.3 Tissue preservation

Immediately after sectioning with the vibratome, tissue sections were transferred in culture medium. Tissue sections were conserved in 24 wells plates, each well filled with 500µl of one of two different media; either Ham's F10 (Ham's F10 Nutrient Mix , Gibco, Life Technologies, Carlsbad, CA, USA) supplemented with Penicillin-Streptomycin (PS, 25,000 U, Gibco, Life Technologies, Carlsbad, CA, USA) and 10% Fetal Bovine Serum (FBS, Gibco, Life Technologies, Carlsbad, CA, USA) or M231 (Medium 231, Smooth Muscle Cell medium, Gibco, Life Technologies, Carlsbad, CA, USA) supplemented with PS (25,000 U) and 5% Smooth Muscle Growth Supplement (SMGS, Gibco, Life Technologies, Carlsbad, CA, USA). Both supplemented culture media (Ham's F10 and M231) of the first 4 consecutively harvested tissues were compared to determine best outcome on tissue viability. Sections were cultured in wells plates in a dark humidified atmosphere at 37°C in 5% CO_2 and culture media were replaced daily.

2.4 Immunofluorescence staining: viability and characterization of cell types

Viability was examined by immunofluorescence staining at day 0, 3, 5, 7, 10 and 14 for primary analysis (N=9). After protocol optimization, the newly harvested tissues (N=4) were kept viable as long as possible and were examined monthly by the immunostaining for viability. For analysis, tissues were removed from the culture medium and washed in PBS solution for two minutes. Subsequently, the tissue was incubated in chamber slides for 30 minutes in 300µl of 0.04% calcein acetoxymethyl (calcein AM) and 0.16% ethidium homodimer-1 (EthD-1) solution (LIVE/DEAD® Viability/Cytotoxicity Kit and PBS solution, Life Technologies, Carlsbad, CA, USA). LIVE/DEAD® Kit stains live and dead cells by accordingly indicating intracellular esterase activity or loss of plasma membrane integrity. Cell-permeant nonfluorescent calcein AM is enzymatically converted to intensely fluorescent calcein (green) by live cell intracellular esterases, which hydrolyse acetoxymethyl ester. EthD-1 becomes fluorescent (red) in cell nuclei upon binding to nucleic acids after entering through the damaged cell membrane of dead cells. Given that live cells have intact cell membranes, transmembrane passage of EthD-1 in live cells does not take place.

Earlier, in feasibility tissues, staining with anthracycline derivative 1% DRAQ7 dye (DRAQ7™, Cell Signaling Technology, Inc., Danvers, MA, USA) in combination with 1% Hoechst (Hoechst 33342™, Cell Signaling Technology, Inc., Danvers, MA, USA) and DNA dye 1% DRAQ5™ (DRAQ5™, Cell Signaling Technology, Inc., Danvers, MA, USA) were used to monitor cell death. However, the latter stained only the upper layer of the tissue, while LIVE/DEAD® Kit stained through the whole thickness of the

aortic tissue; making quantification of the live and dead cells possible. In order to characterise cell type composition of the tissue, SMC, leukocytes and macrophages were subjected to immunofluorescence staining against α-SMA/smoothelin, CD45, CD68 respectively. First, tissue was washed twice with 300µl of PBS and fixated in 300µl of 4% formaldehyde solution (Sigma-Aldrich, St. Louis, MO, USA) for 20 minutes. Fixated tissue was subsequently washed three times for five minutes in 300µl of 0.05% PBST (Tween and PBS solution, Sigma-Aldrich, St. Louis, MO, USA) and submerged in a 0.2% solution of Triton (Triton x-100 and PBS solution, Sigma-Aldrich, St. Louis, MO, USA) for twenty minutes and rinsed with a 1.0% BSA solution (Bovine Serum Albumine and PBS solution, Vector Laboratories, Inc, Burlingame, CA, USA). After three PBST washing steps of five minutes, the tissue was incubated overnight in 2% Monoclonal Mouse Anti-Human Smooth Muscle Actin solution at dilution; (DAKO, Glostrup, Denmark). Hereafter, five washing steps of five minutes using PBST, were followed by one hour incubation of 1% Anti-Mouse Alexa Fluor 647 secondary antibody (Thermo Fisher Scientific Inc.). After five PBST washing steps, overnight incubation using 2% Polyclonal Rabbit Anti-Human Primary Smoothelin Antibody (H-300, Santa Cruz Biotechnology, Dallas, TX, USA) was performed. Five PBST washing steps were then followed by incubation of one hour using 1% Anti-Rabbit Alexa Fluor 488 secondary antibody (Thermo Fisher Scientific Inc.).

In additional slides, leukocytes were stained with 2% Monoclonal Mouse Anti-human CD45 (N=1, DAKO, Glostrup, Denmark) and macrophages were stained with 2% Monoclonal Mouse Anti-human CD68 (N=1, DAKO, Glostrup, Denmark) in fixated coupes and after washing with PBST (five steps) followed by incubation of one hour using 1% Anti-Mouse Alexa Fluor 647 secondary antibody (Thermo Fisher Scientific Inc.). Where overnight staining was done at 4°C, the remainder steps were performed at room temperature. Aforementioned α-SMA/smoothelin, CD45 and CD68 stainings were followed by 15 minutes staining for 2% DAPI (4',6-Diamidino-2-Phenylindole, Dihydrochloride, Thermo Fisher Scientific Inc.) to show cell nuclei and tissue was washed with PBST twice and once with PBS solution at room temperature. Slides with tissue were mounted with VECTASHIELD® Antifade Mounting Medium (Vector Laboratories, Inc, Burlingame, CA, USA) and closed using coverslips. As negative controls for α-SMA/Smoothelin, CD45 and CD68, tissue sections were used in which the primary antibody was omitted from the staining procedure.

In order to assess wall composition over time, aortic tissue sections of one AAA patient were cultured until 14 days in daily replaced supplemented M231 culture medium. After 0, 7 and 14 days, different tissue sections were removed from the culture medium and snap-frozen for analysis. Therefore, the sections were immunostained for smoothelin, as

a marker of mature SMC, and DAPI according to above described protocol. Additionally, phalloidin (Rhodamine-phalloidin, Thermo Fisher Scientific Inc.) immunostaining was performed simultaneously with DAPI immunostaining, to present all aortic wall cells and their relation within the tissue sections. Again, after immunostaining, tissues were washed, mounted with VECTASHIELD® and slides were closed using coverslips.

2.5 Vascular enzymatic tissue digestion for analysis with individual cells

Multiple tissue sections of two AAA patients were separately submerged in 1 mg/ml collagenase type II (Worthington, Lakewood, NJ, USA) and M231 in tubes. These were placed in a rotator in a dark atmosphere at 37°C for 3 hours. The mixture was then filtrated through a 100μM gauze and centrifuged at 300g for 10 minutes. Supernatant was removed and cell pallet was resuspended in 500μL of M231. These cells were used for further qualitative immunofluorescence analysis and count and viability assay.

2.6 Immunofluorescence staining in digested cells

After primary analysis at day 0, tissues were digested at day 7 and 14 as described above, to quantitatively analyze cell viability and qualitatively analyze characteristics in individual cells. Cells were stained with LIVE/DEAD® Kit, using the same staining protocol as for tissues.

2.7 Analysis of immunofluorescence staining

Viability examination of sections was performed using Zeiss Axiovert 200M Marianas™ digital imaging inverted microscope system. The set-up was provided with a non-stepper-motor (z-axis increments: 0.1 μm) and a filter turret with individual filter blocks for fluorescein isothiocyanate (FITC), a pair of cyanine dyes (CY5 and CY3), aminomethylcoumarin acetate (AMCA) and a differential interference contrast (DIC) brightfield cube. FITC and CY3 were handled to respectively demonstrate live (calcein) and dead (EthD-1) cells. Imaging was performed using a 16-bit, cooled charge-coupled device camera (Cooke Sensicam SVGA, Cooke Co., Tonawanda, NY, USA). Aforementioned set-up was connected to Slidebook™ (Slidebook v. 5.5 software, Intelligent Imaging Innovations, Inc., Denver, CO, USA) to control hardware and to view and process images. Zeiss air objective lenses at magnifications of 2.5X (for quantitative overview images), 10X and 40X (for detailed higher resolution images and 3D stacks) and 63X (oil objective lens to study individual cells) were used to obtain images. Unspecific background and disproportional intensity staining was corrected for by Slidebook software. The viability proportion of tissue sections was calculated by dividing calcein intensity in square micron by the sum of calcein and EthD-1 in square micron.

Analysis of different cell types was again performed using Zeiss Axiovert 200M Marianas™. Depending on choice of different secondary antibodies CY5, CY3, FITC and DAPI were utilized. Magnifications of 2.5X, 10X and 40X were used for analysis. For characterization of cell type, shutter speeds were based on primary antibody positive stained tissues, while use of Renormalize Button in Slidebook™ was based on negative controls (without primary antibody). To obtain super resolution images a Confocal Laser Scanning Microscope Leica TCS SP8 (Leica Microsystems, Mannheim, Germany) was used. Regions of interest in images previously captured with fluorescence microscope were reviewed using 40X and 63X Leica oil-immersion lenses. Unfortunately, photo bleaching of calcein interfered with visualization of live cells. Therefore, for live and dead quantification solely fluorescence microscopy was used. LAS-X software was used to analyse images of cell type differentiation. Excitation/emission spectra used for secondary antibodies (Alexa Fluor 488, Alexa Fluor 555, Alexa Fluor 647) were chosen out of identically named pre-set excitation/emission spectra in Leica LAS-X.

Aortic wall composition analysis was performed using Nikon A1R (Nikon Instruments, Tokyo, Japan) confocal microscope with 40 X oil objective. Using NIS-Elements C Software (Nikon Instruments), super high-resolution (5120x5120 pixels) intima-to-adventitia stitched images of 5x5 fields of view. Excitation/emission spectra used to capture fluorescent signal of phalloidin (Alexa Fluor 546), and secondary antibody of smoothelin (Alexa Fluor 647) were chosen out of pre-set excitation/emission spectra in NIS-Elements C. Fluorescence levels of smoothelin and phalloidin were quantified using FIJI/ImageJ (v1.0. National Institutes of Health, Bethesda, MD, USA). Following background subtraction, masks of selected tissue areas were created and quantified. Outcomes were corrected for number of cells using DAPI count.

2.8 Count and viability assay following tissue digestion

On day 14, individual cell viability assay was performed by the Muse Count & Viability reagent (Millipore, Billerica, MA, USA) following the manufacturer's protocols. Harvested cells in M231 (50µL) were added to 450µL Count & Viability reagent (Millipore). The system was gated for viability and exclusion of both cellular debris and cell clusters, which was based on cultured commercially available smooth muscle cells of a 31-year old healthy male (Thermo Fisher Scientific Inc., Waltham, MA, USA). The results were analyzed with Muse Count & Viability software module.

2.9 Proof of concept: ex vivo tissue stimulation and quantification of gene expression by qPCR

Live aortic tissues of AAA patients (N=8) were sectioned according to above described protocol. Complete M231 culture medium (including PS and SMGS) was supplemented with TGF-β (5 ng/ml, BioVision, Milpitas, CA) to stimulate the tissue sections, since dysregulation of TGF-β is often described in literature, as a key player an in the development and progression of AAA. Culturing of sections was performed in complete M231 medium with (stimulated) and without TGF-β (non-stimulated) supplement in a dark humidified atmosphere at 37°C in 5% CO_2. Culture medium was replaced daily to ensure constant TGF-β stimulation. After 7 days, both stimulated and non-stimulated tissues were rinsed in PBS and directly snap-frozen. Tissue pieces were stored at -80°Celsius until analysis.

AAA patient pooled (N=8) stimulated and non-stimulated, tissue sections were homogenized apart from each other in two 2.0 mL eppendorfs in 300 µL lysis buffer (Zymo Research, Irvine, CA, U.S.A.). Total RNA of both eppendorfs was isolated using Quick-RNA™ MiniPrep kit (Zymo Research). Synthesis of complementary DNA was performed in a reverse transcription reaction using VILO kit (Thermo Fisher Scientific Inc.). Quantitative PCR (qPCR) was performed to analyze gene expression. *YWHAZ* was used as housekeeping gene. By use of LightCycler® SYBR Green I Master (Roche Applied Science, Penzberg, Germany) gene expression was analyzed by the LightCycler® 480 Instrument II (Roche Applied Science). Potential differences in expression of interleukin 6 *(IL6),* calponin 1 *(CNN1),* transforming growth factor beta 1 *(TGFB1),* monocyte chemotactic protein 1 *(MCP1),* transforming growth factor beta receptor 1 *(TGFBR1),* smoothelin *(SMTN),* intercellular adhesion molecule 3 *(ICAM3),* matrix metalloproteinase-2 *(MMP2),* alpha smooth muscle actin 2 *(ACTA2),* tumor necrosis factor *(TNF),* protein tyrosine phosphatase, receptor type, C *(PTPRC),* antigen KI-67 *(Ki67),* intercellular adhesion molecule 1 *(ICAM1),* interleukin 8 *(IL8 or CXCL8)* and matrix metalloproteinase-9 *(MMP9)* in stimulated and non-stimulated AAA tissue sections were evaluated (the entire list of corresponding NCBI Reference Sequence Database codes and forward and reverse primer sequences can be found as Supplementary Table S1 online). RNA expression was shown as a ratio; relative expressions based on non-stimulated tissue sections was calculated after seven days culturing *ex vivo*.

2.10 Statistical analysis

The data was analyzed with SPSS Statistics 22.0 (IBM Corporation, Armonk, NY, USA). Measurements of viability are shown in box-plots. Wilcoxon signed-rank test was performed to compare viability of corresponding tissue cultured in different media

(Ham's F10 and M231). Comparisons of viability in the first nine consecutive patient sample on multiple time points were made by repeated measures of analysis of variance (one-way Anova) using the Bonferroni correction for multiple-comparison testing. P-value of < 0.05 is considered statistically significant. Muse Count & Viability software module showed percentage of viable single cells of enzymatically digested tissues.

2.11 Data Availability

The datasets generated during and analysed during the current study are available from the corresponding author on reasonable request.

3. RESULTS

Primary viability analysis was performed in 9 vascular specimens. After a few adjustments of the protocol (i.e. life-span optimization during sectioning and culturing of the tissues), maximum life endurance of live aortic *ex vivo* tissues was examined in 4 additional aortic tissues. Viability staining showed no difference in viability between cultured tissues (N=4) in Ham's F10 or M231 culture media (α=0.465). Since no significant difference was observed between tissue viability cultured in different media, the mean outcomes of tissues in either Ham's F10 or M231 per day per corresponding donor were used for further analysis.

Qualitative evaluation of all images of the first 9 vascular tissues showed that dead cells were located mostly on the surface of the tissue, while live cells were mainly localized in the center of vascular tissue sections (figure 8.2A-F). Figure 8.2G shows tissue viability during the experiments; human tissues at day 0 showed a mean viability proportion of 0.42 (N=9, SD: 0.16). Consecutively, mean viability proportion was 0,38 (SD: 0.15) for day 3; 0,43 (SD: 0.12) for day 5; 0,38 (SD: 0.13) for day 7; 0,27 (SD: 0.17) for day 10; and 0,18 (SD: 0.15) for day 14. There was a significant difference in viability proportion between day 0 and day 14 (P=0.026) and between day 5 and day 14 (P=0.015). AAA tissue viability at day 0 was 0.42(N=5, SD: 0.2), which was almost similar to the non-aortic-tissue viability at day 0, being 0.41 (N=4, SD: 0.14). Small protocol adjustments were implemented, including pre-sectioning removal of calcium depositions, warmed (37°Celsius) tissue section transport, immunostaining within culture medium and shorter tissue-out-of-incubator times. After implementing the new protocol, an improved tissue viability proportion of 0.58 after 62 days was observed (figure 8.3A) in AAA tissue. After 92 culturing days (viability proportion: 0.85), outgrowth of many new cells around the initial tissue was observed, but no viability in the original tissue was seen (figure 8.3B-C).

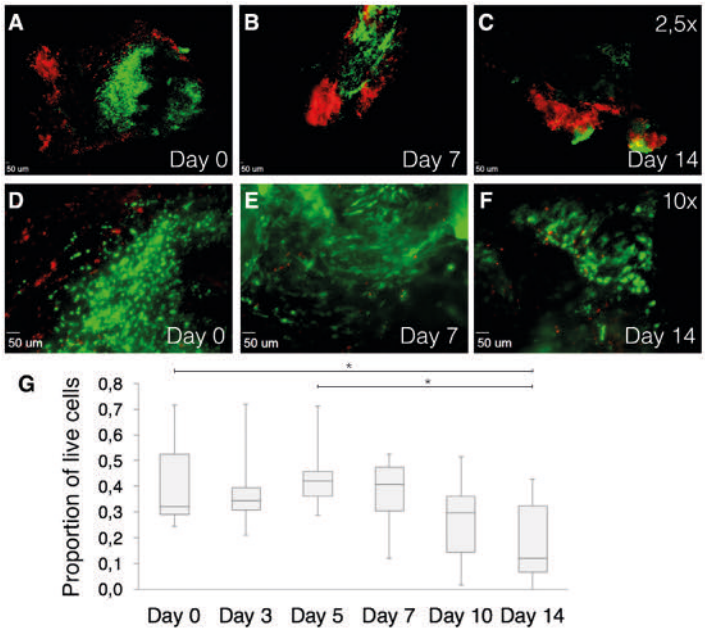

Figure 8.2 Immunofluorescence images using Zeiss Axiovert 200M Marianas™ Microscope. Cells stained with LIVE/DEAD® Viability/Cytotoxicity Kit. A, B and C: 2.5x magnification of cultured tissues at day 0, 7 and 14, respectively. D, E and F: 10x magnification of cultured tissues at day 0, 7 and 14, respectively. Green fluorescence shows live cells, while red fluorescence indicates dead nuclei. Live cells are mainly located central to tissue. G: Quantification of live human cells in harvested vascular tissues of distinct patients (n=9). Box plots show proportions of square micron of green fluorescence divided by the sum of green and red fluorescence. *p<0.05 compared with other time points using ANOVA with Bonferroni test.

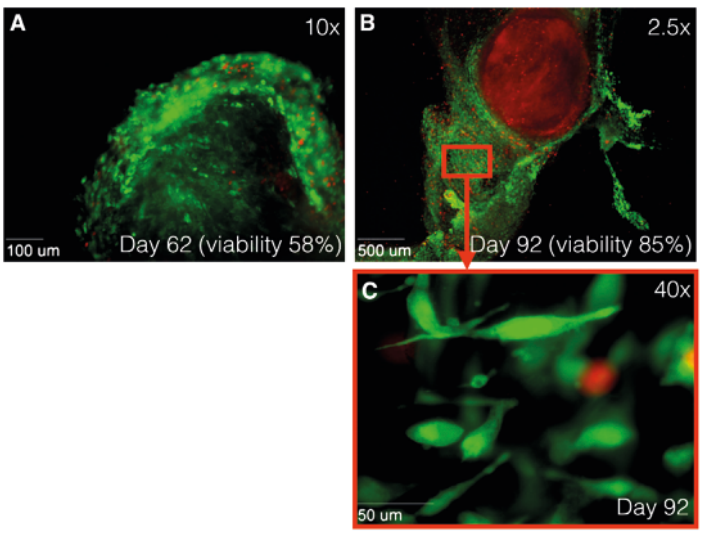

Figure 8.3 Immunofluorescence images at 10x magnification using Zeiss Axiovert 200M Marianas™ Microscope. Human tissue stained with LIVE/DEAD® Viability/Cytotoxicity Kit. Green fluorescence shows live cells, while red fluorescence indicates dead nuclei. A: Alive tissue at day 62 after harvesting. Tissue viability of 58%. B: Alive tissue at day 62 after harvesting at 2.5x magnification and C: at 40x magnification. Outgrowth of new cells is observed after 92 days, while original tissue shows only staining of EthD-1 (dead cells). Tissue viability of 85%. EthD-1 indicaties ethdium homodimer-1.

3.1 Immunofluorescence: smooth muscle cells, leucocytes and macrophages, and aortic wall composition

Given that primary analysis showed best viability outcomes on day 5 and 7, these days were designated to perform further experiments. Cells with a similar shape to SMC were observed during analysis of viability images using LIVE/DEAD® Kit (figure 8.3C). Digital imaging microscope analysis of immunofluorescence staining showed cells with colocalized α-SMA and smoothelin, early and late SMC marker, respectively (figure 8.4A-C), again with aforementioned characteristic SMC shape. Additionally, confocal scanning laser microscopy was utilized to gain high quality images, which confirmed the presence smooth muscle cells (figure 8.4D-F). Moreover, fixated immunostaining for CD45 and CD68 showed leukocytes and macrophages, respectively (figure 8.5A-D). By retrospectively analyzing the images of tissues immunostained with LIVE/DEAD® Kit, the morphological form of live leukocytes could be recognized.

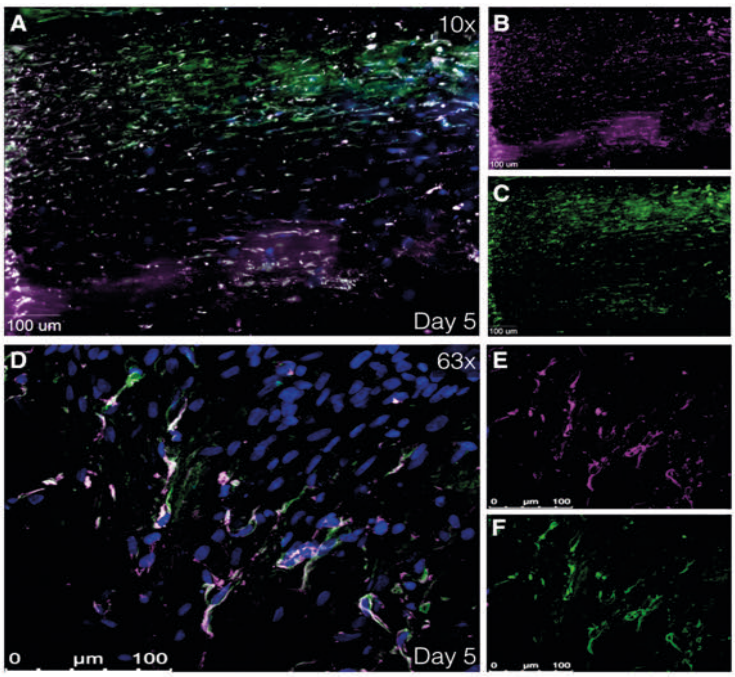

Figure 8.4 Immunofluorescence images showing smooth muscle cells. A-C: Immunofluorescence images at 40x magnification using using Zeiss Axiovert 200M Marianas™ Microscope at day 5 after harvesting. D-F: Immunofluorescence image at 63x magnification using super resolution Confocal Laser Scanning Microscope Leica TCS SP8.
Human tissue stained with α-SMA and smoothelin (smooth muscle cell markers) at day 5 after harvesting. A,D: Merged image of α-SMA (purple), smoothelin (green) and DAPI (blue). B,E: Isolated α-SMA staining. C,F: Isolated smoothelin staining. α-SMA indicaties alpha smooth muscle actin and DAPI, 4',6-diamidino-2-phenylindole.

Stitched overview images of the aneurysmal aortic wall show smooth muscle cells (immunostained by smoothelin) in the upper part of the tissues at day 0, 7 and 14 after culturing (figure 8.6). Phalloidin immunostaining shows all cells of the aortic wall. Thereby, co-staining of both smoothelin and phalloidin indicates the tunica media (mainly consisting of smooth muscle cells), while in underlying tissue only expression of phalloidin is observed, indicating the tunica adventitia (mainly consisting of fibroblasts). This distinction between tunica media and tunica adventitia is observed at day 0, 7 and 14. Fluorescence quantification of smoothelin per nucleus shows a fold increase of 1.6 and 2.3 for day 7 and day 14, respectively. Fluorescence quantification of phalloidin per nucleus shows a fold increase of 4.8 and 5.5 for day 7 and day 14, respectively.

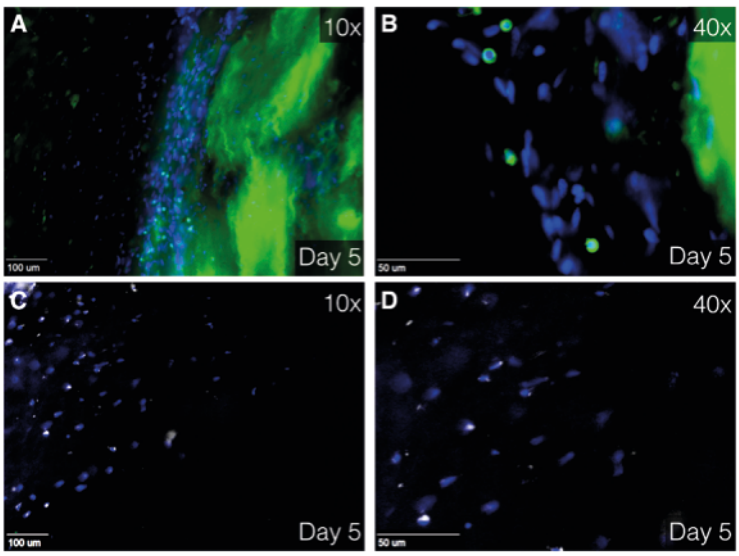

Figure 8.5 Immunofluorescence image at 10x (A,C) and 40x (B,D) magnification using Zeiss Axiovert 200M Marianas™ Microscope. Human tissue stained with DAPI (blue), CD45 (green, A,B) and CD68 (white, C,D) Green staining at the right side (A,B) is due to unintentional fluorescence of elastin. CD indicates cluster of differentiation and DAPI, 4',6-diamidino-2-phenylindole.

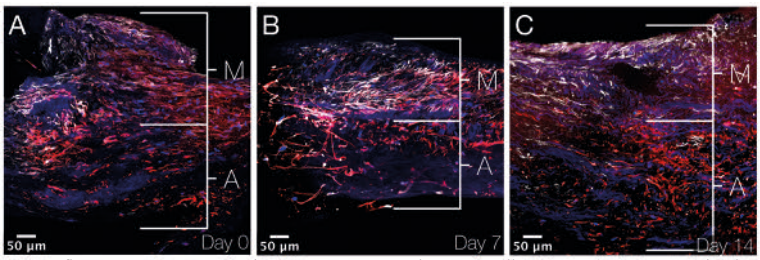

Figure 8.6 Immunofluorescence images showing aneurysmal aortic wall sections. A-C: XY stitched images at 40x magnification using Nikon A1R confocal microscope on day 0, 7 and 14 after culturing. Smooth muscle cells are immunostained by smoothelin (white), actin (found in practically all eukaryotic cells) by phalloidin (red) and cell nuclei by DAPI (blue). Smooth muscle cells are found in the media and other cells (mainly fibroblasts) in the adventitia. M indicates media; A, adventitia and DAPI, 4',6-diamidino-2-phenylindole.

3.2 Outcome of enzymatic digestion of the aortic tissue: individual cell analysis

Tissues of AAA patients (N=2) at day 14 in culture were enzymatically digested. Fluorescent calcein was observed in cytoplasm of enzymatically-digested cells, surrounding the nucleus. Separate cells attached to the slide after enzymatic digestion with collagenase. Different cell shapes and nuclei were observed in the individual cells (figure 8.7). Digested tissue sections showed viability of 0.75 (in 950.000 cells) in one patient and viability of 0.83 (in 800.000 cells) in the other patient.

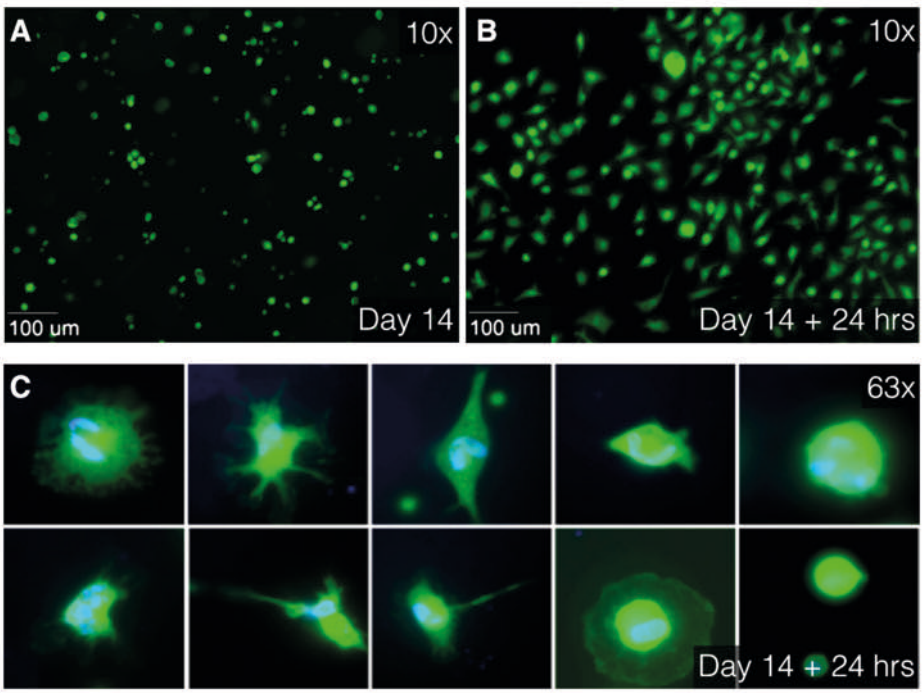

Figure 8.7 Immunofluorescence images at 10x (A,B) and 63x oil (C) magnification using Zeiss Axiovert 200M Marianas™ Microscope. A: After 14 days of culturing, tissues were enzymatically digested using collagenase. Live separate cells, stained with Calcein AM (green), float as round cells in culture medium. B: After 24 hours of additional culturing, the cells were attached to the slide. C: Different cell type characteristics and differences in cell nuclei are observed in attached cells. Live cytoplasm is stained with Calcein AM (green) and cell nuclei are stained with DAPI (blue). AM indicaties acetoxymethyl and DAPI, 4',6-diamidino-2-phenylindole.

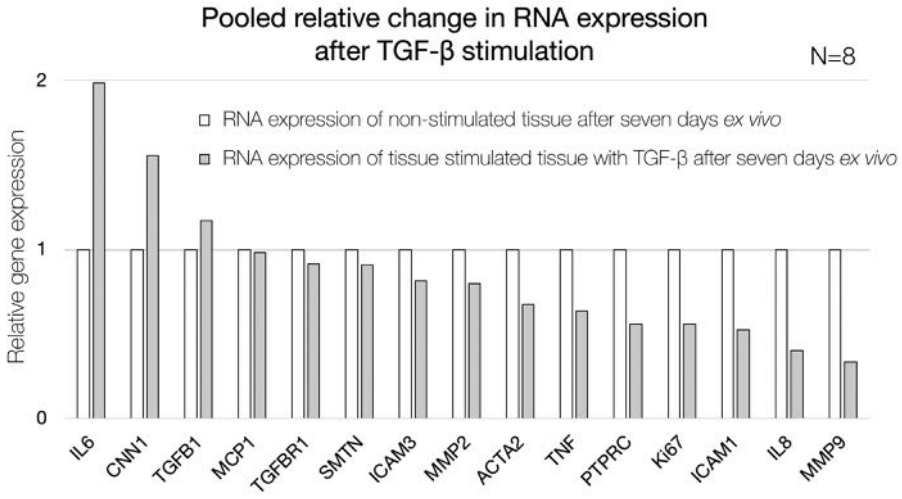

Figure 8.8 Quantification of gene expression of pooled non-stimulated (white) and TGF-β-stimulated (grey) AAA patient tissue sections after seven days *ex vivo*. Relative expression is shown as ratio based on non-stimulated tissue sections. *IL6* indicates interleukin 6; *CNN1*, calponin 1; *TGFB1*, transforming growth factor beta 1; *MCP1*, monocyte chemotactic protein 1; *TFBR1*, transforming growth factor beta receptor 1; *SMTN*, smoothelin; *ICAM3*, intercellular adhesion molecule 3; *MMP*2, matrix metalloproteinase-2; *ACTA2*, alpha smooth muscle actin 2; *TNF*, tumor necrosis factor; *PTPRC*, protein tyrosine phosphatase, receptor type, C; *Ki67*, antigen KI-67; *ICAM1*, intercellular adhesion molecule 1; *IL8 (or CXCL8)*, interleukin 8 and *MMP9*, matrix metalloproteinase-9.

3.3 RNA expression results of stimulated and non-stimulated aortic tissue sections.

Tissue sections of eight AAA patients were subjected to stimulation with TGF-β for 7 days. Control tissue sections of the same patients were cultured without TGF-β stimulation. Pooled RNA analysis of stimulated tissue sections was relatively related to non-stimulated tissue sections. In this feasibility analysis, elevated relative expression of interleukin 6 *(IL6)*, calponin 1 *(CNN1)* and transforming growth factor beta 1 *(TGFB1)* was observed in the pool of TGF-β stimulated tissue sections, while the remainder of the studied genes showed a decrease in expression (figure 8.8).

4. DISCUSSION

The underlying mechanisms of the development, progression, and rupture of AA are still poorly understood. Prior studies on AA were performed in animal models, fixated human tissue, or isolated human cell cultures. An *in vitro* human model to study pathophysiological processes involved in human AA is lacking. For this reason, we

developed a method to obtain vital, ex vivo human vascular tissue. In these cultured aneurysmal and non-aneurysmal vascular specimens, evaluation of viability showed that the larger part of human vascular tissue sections can be kept alive in culture for up to 62 days, while maintaining microstructural organisation of the vascular wall. The live cells were mainly observed in the centre of human tissue. As expected, dead cells were mainly located at the edges of the tissue, which were subjected to cutting trauma. After optimization of the protocol, we attained even higher proportions of surviving tissue.

Interestingly, viability proportion outcomes increased after day 3 compared to day 0. These results are strengthened by not only the significant difference in mean viability of tissue sections between day 0 and day 14, but also between day 5 and day 14. Cells might go through an early phase of apoptosis due to stress factors arising from physical trauma. Initially, these mechanisms might still be reversible,[17,18] with subsequent recovery as of day 3. Another possible explanation for the observed increase of live cells is cell proliferation. This theory is supported by the development and expansion of live cells, observed in the tissues cultured over 60 and 90 days and the growth of new cells at the intimal side.

Another important finding was that we achieved to preserve tissue architecture and infiltrating cells *ex vivo*. In this composition, we found many live smooth muscle cells as the main cell type, but we also observed leucocytes and macrophages involved in the occurrence and aggravation of AA.[19-21.] Based on our composition staining using smoothelin and phalloidin, we provide support for our hypothesis that both tunica media and tunica adventitia are preserved after 14 days. Phalloidin is not specific for fibroblasts. However, phalloidin staining in in spindle shaped cells combined with lack of smoothelin staining in the lower layer of the tissue sections, strongly indicates fibroblasts, which are generally known to be in the tunica adventitia. Quantification results showed an increase in fluorescence per nucleus in both smoothelin and phalloidin. This might implicate, that although over time the viability diminishes, the actual cell size, or expression of cell markers increases over time. However, based on the results of one study patient, caution must be applied, as the findings might not be representative for other patients. Unfortunately, the friable tunica intima is frequently damaged due to vibratome sectioning. Preservation of the AA tissue composition in *ex vivo* tissues facilitates the study of cell behaviour and interaction between different cell types, and provides the opportunity to investigate the effects of pharmacological substances on tissue composition or in organ on a chip models.

Analysis of digested tissue sections showed a high viability of single cells, even after treatment with collagenase. Furthermore, again different cell types could be morphologically distinguished, supporting the purpose of this protocol; creating an *ex vivo* arterial environment, which mimics the *in vivo* interaction of different cell types and extracellular matrix. The ability to digest the tissue sections greatly broadens the possibilities of this protocol. For example, FACS, MACS and traction force microscopy are examples of downstream applications that can be performed to expand the characterisation of cells which have been cultured and potentially stimulated in an *ex vivo* aortic microenvironment. [22-24]

To evaluate the feasibility of live aortic tissue section stimulation and RNA expression analysis, we stimulated aortic vibratome tissue sections with TGF-β, since prior studies have provided paradoxical hypotheses on the role of TGF-β (and thereby stimulation by angiotensin II) in the development and progression of AAA. [25,26] In this pooled stimulated versus non-stimulated analysis, we found elevated RNA expression of interleukin 6 *(IL6)*, calponin 1 *(CNN1)* and transforming growth factor beta 1 *(TGFB1),* in the stimulated tissue sections. Interestingly, TGF-β has previously been reported to elevate expression of interleukin 6 in different types of fibroblasts, which is in line with our results. [27,28] Simultaneously, it has been previously observed, that TGF-β overexpression in animal models decreases MMP2, MMP9 and lymphocytes (PTPRC), consistent with our findings in human tissue sections. [29] However, with a small sample size and pooled patient data, caution must be applied, as the findings might not be representative for all AAA patients. Future studies with the current method are therefore recommended.

The results of this study meet the need for a new *in vitro* model in which the pathophysiological processes involved in human AA can be studied. In our protocol, sectioning is performed using the vibratome, which has been successfully used for the live cutting and *ex vivo* preservation of cardiac mouse tissues and human salivary gland and tumour sections of breast and parathyroid for a maximum of two weeks. [14, 30-33] However, this is the first report of a protocol demonstrating over 60 days *ex vivo* viability in vibratome sectioned aortic tissue.

It can be argued that cells with a short lifespan or cells vulnerable to culturing will not survive for a long period in the *ex vivo* tissue sections. Nevertheless, during the first days of culturing we can study the individual cells, interactions between cells and ECM, behavior of immune cells and remodelling of the tissue as seen in other specialist fields using vibratome sections.[25] Subsequently, we have successfully stimulated the live

tissue sections and the live tissue can serve as a patient specific scaffold on which new cells can be seeded and pharmacological experiments can be performed.

To the best of our knowledge, we are the first to present a method to keep entire aortic tissue sections alive *in vitro*. This method may be applicable also to other human (cardiovascular) tissue. We achieved slicing, preservation, proliferation, and analysis of live aortic tissues for at least 60 days after harvesting. Diverse cell types (including smooth muscle cells and white blood cells) and intracellular characteristics of live tissues were presented. Besides well-known fluorescence imaging, FACS, MACS and traction force microscopy, we are currently investigating the use of these tissue sections in new techniques in which we study elastic properties, aortic wall secretome, and pathways by additional inhibition/stimulation tests. By having established a method for extended *in vitro* preservation of functionally and structurally intact vascular tissue sections, research on the etiopathophysiology of AA and possibly other vascular diseases may have entered a new era.

REFERENCES

1. Dua, A., Kuy, S., Lee, C. J., Upchurch, G. R. & Desai, S. S. Epidemiology of aortic aneurysm repair in the United States from 2000 to 2010. *J. Vasc. Surg.* 59, 1512–1517 (2014).
2. Sidloff, D. *et al.* Aneurysm global epidemiology study public health measures can further reduce abdominal aortic aneurysm mortality. *Circulation* 129, 747–753 (2014).
3. Lozano, R. *et al.* Global and regional mortality from 235 causes of death for 20 age groups in 1990 and 2010: A systematic analysis for the Global Burden of Disease Study 2010. *Lancet* 380, 2095–2128 (2012).
4. Davis, F. M., Rateri, D. L. & Daugherty, A. Mechanisms of aortic aneurysm formation: translating preclinical studies into clinical therapies. *Heart (British Cardiac Society)* 100, 1498–1505 (2014).
5. Hellenthal, F. A. M. V. I., Buurman, W. A., Wodzig, W. K. W. H. & Schurink, G. W. H. Biomarkers of AAA progression. Part 1: Extracellular matrix degeneration. *Nature Reviews Cardiology* 6, 464–474 (2009).
6. Hellenthal, F. A. M. V. I., Buurman, W. A., Wodzig, W. K. W. H. & Schurink, G. W. H. Biomarkers of abdominal aortic aneurysm progression. Part 2: Inflammation. *Nat. Rev. Cardiol.* 6, 543–552 (2009).
7. Cherifi, H. *et al.* Comparative study of abdominal and thoracic aortic aneurysms: their pathogenesis and a gingival fibroblasts-based ex vivo treatment. *Springerplus* 4, (2015).
8. Wang, Q. *et al.* Monocyte Chemoattractant Protein-1 (MCP-1) regulates macrophage cytotoxicity in abdominal aortic aneurysm. *PLoS One* 9, (2014).
9. Airhart, N. *et al.* Smooth muscle cells from abdominal aortic aneurysms are unique and can independently and synergistically degrade insoluble elastin. *J. Vasc. Surg.* 60, 1033–1042.e5 (2014).
10. Xiong, F. *et al.* Inhibition of AAA in a rat model by treatment with ACEI perindopril. *J. Surg. Res.* 189, 166–173 (2014).
11. Liu, Z. *et al.* Murine abdominal aortic aneurysm model by orthotopic allograft transplantation of elastase-treated abdominal aorta. *J. Vasc. Surg.* 62, 1607–1614.e2 (2015).
12. Kloster, B. O., Lund, L. & Lindholt, J. S. Inhibition of early AAA formation by aortic intraluminal pentagalloyl glucose (PGG) infusion in a novel porcine AAA model. *Ann. Med. Surg.* 7, 65–70 (2016).
13. Sasai, Y. Cytosystems dynamics in self-organization of tissue architecture. *Nature* 493, 318–326 (2013).
14. Pillekamp, F. *et al.* Establishment and characterization of a mouse embryonic heart slice preparation. *Cell. Physiol. Biochem.* 16, 127–132 (2005).
15. Ghosh, A., Pechota, L. V. T. A., Upchurch, G. R. & Eliason, J. L. Cross-talk between macrophages, smooth muscle cells, and endothelial cells in response to cigarette smoke: the effects on MMP2 and 9. *Mol. Cell. Biochem.* 410, 75–84 (2015).
16. Vorkapic, E., Lundberg, A. M., Mäyränpää, M. I., Eriksson, P. & Wågsäter, D. TRIF adaptor signaling is important in abdominal aortic aneurysm formation. *Atherosclerosis* 241, 561–568 (2015).
17. Seye, C. I. *et al.* 7-Ketocholesterol induces reversible cytochrome c release in smooth muscle cells in absence of mitochondrial swelling. *Cardiovasc. Res.* 64, 144–153 (2004).
18. Kumar, V., Abbas, A. K. & Aster, J. C. *Robbins Basic Pathology Ninth Edition*. *Elsevier Saunders* (2013).

19. Middleton, R. K. *et al.* The pro-inflammatory and chemotactic cytokine microenvironment of the abdominal aortic aneurysm wall: A protein array study. *J. Vasc. Surg.* 45, 574–580 (2007).

20. Samadzadeh, K. M. *et al.* Monocyte activity is linked with abdominal aortic aneurysm diameter. *J. Surg. Res.* 190, 328–334 (2014).

21. Tsuruda, T. *et al.* Adventitial mast cells contribute to pathogenesis in the progression of abdominal aortic aneurysm. *Circ. Res.* 102, 1368–1377 (2008).

22. Kennedy, E. *et al.* Embryonic rat vascular smooth muscle cells revisited - A model for neonatal, neointimal SMC or differentiated vascular stem cells? *Vasc. Cell* 6, (2014).

23. Levenberg, S., Ferreira, L. S., Chen-Konak, L., Kraehenbuehl, T. P. & Langer, R. Isolation, differentiation and characterization of vascular cells derived from human embryonic stem cells. *Nat. Protoc.* 5, 1115–1126 (2010).

24. Adhikari, N. *et al.* Guidelines for the Isolation and Characterization of Murine Vascular Smooth Muscle Cells. A Report from the International Society of Cardiovascular Translational Research. *J. Cardiovasc. Transl. Res.* 8, 158–163 (2015).

25. Lin, F. & Yang, X. TGF-β signaling in aortic aneurysm: Another round of controversy. *J. Genet. Genomics* 37, 583–591 (2010).

26. Chen, X., Lu, H., Rateri, D. L., Cassis, L. A. & Daugherty, A. Conundrum of angiotensin II and TGF-β interactions in aortic aneurysms. *Current Opinion in Pharmacology* 13, 180–185 (2013).

27. Seong, G. J. *et al.* TGF-β-induced interleukin-6 participates in transdifferentiation of human Tenon's fibroblasts to myofibroblasts. *Mol. Vis.* 15, 2123–2128 (2009).

28. Eickelberg, O. *et al.* Transforming growth factor-β1 induces interleukin-6 expression via activating protein-1 consisting of JunD homodimers in primary human lung fibroblasts. *J. Biol. Chem.* 274, 12933–12938 (1999).

29. Dai, J. *et al.* Overexpression of transforming growth factor-β1 stabilizes already-formed aortic aneurysms: A first approach to induction of functional healing by endovascular gene therapy. *Circulation* 112, 1008–1015 (2005).

30. Riegler, J., Gillich, A., Shen, Q., Gold, J. D. & Wu, J. C. Cardiac tissue slice transplantation as a model to assess tissue-engineered graft thickness, survival, and function. *Circulation* 130, S77–S86 (2014).

31. Su, X. *et al.* Three-dimensional organotypic culture of human salivary glands: the slice culture model. *Oral Dis.* 22, 639–648 (2016).

32. Holliday, D. L. *et al.* The practicalities of using tissue slices as preclinical organotypic breast cancer models. *J. Clin. Pathol.* 66, 253–255 (2013).

33. Koh, J., Hogue, J. A. & Sosa, J. A. A novel ex vivo method for visualizing live-cell calcium response behavior in intact human tumors. *PLoS One* 11, (2016).

CHAPTER 9

GENERAL DISCUSSION AND SUMMARY

9.1 Thesis aim and approach

The aim of the present thesis was to provide more insight into factors that are involved in the development and progression of abdominal aortic aneurysm (AAA). Increased knowledge may facilitate more accurate prediction of the growth rate and risk for rupture of an AAA. As degradation of the abdominal aortic medial layer is a hallmark of this disease, we collected aortic tissue from 80 AAA patients (table 9.1) who underwent either elective or acute aneurysm repair surgery. In these samples we investigated cellular signalling pathways that seemed to have a crucial role in aortic medial layer degradation and eventually in AAA development. We also tested possible prognostic biomarkers in blood of patients and performed a systematic review of the literature on such biomarkers. Finally, also 13 patients with a high risk of AAA development, due to Marfan syndrome, were included.

The above-mentioned pathophysiology leading to aneurysm development is investigated in aortic tissue and blood samples of AAA patients. Therefore, we will first review the characteristics of those patients. Next, the degenerative processes leading to aortic medial layer degradation are described according to the graphical abstract of thesis, presented in figure 9.1 and 9.2. The graphical abstracts are made by adding the main results from our work to the current knowledge of the AAA pathophysiology. Subsequently, we will evaluate the role of prognostic markers for aneurysm growth and rupture in AAA management. The results of the present thesis are critically reviewed before we provide our perspectives on future results. Finally, we present the main conclusions based on our work in the present thesis.

9.2 Patient characteristics

For the present thesis we consecutively collected tissue and blood from all patients treated by open aneurysm surgery in our medical center from March 2010 until May 2014. Samples were treated as described before.[1–3] In table 9.1 patient characteristics are presented for the first time of all patients pooled.

Mean age between patients with a ruptured AAA (rAAA; n=14) and electively treated patients (eAAA; n=66) did not differ, 74 years versus 71, respectively. Although current guidelines recommend elective surgical repair at 5.5 cm for men and 5.0 cm for women, the mean diameter in our eAAA group was 6.5 cm for men and 5.6 cm for women (6.4 for both pooled). In more than 50 percent of the included eAAA the aneurysm was diagnosed as an accidental radiographic finding and had already exceeded the recommended diameter for surgery. Growth rates in our elective group (mean 0.6 cm/year) are higher than described in the literature.[4] This might be explained by the high

percentage of large aneurysms (>5.0 cm) in the group, as the latter expand faster than smaller (3.0-3.9 cm).[4]

Table 9.1 Characteristics of all AAA patients included in the present thesis.

	Rupture	Elective	*p*
N	14	66	-
Age (years)	74	71	0.263
AAA diameter (cm)	6,7	6,4	0.079
AAA growth (cm/year)	NA	0,6	-
Male gender (%)	64	83	0.144
Symptoms			
claudication (%)	8	14	1.000
back pain (%)	31	0	0.001*
stomach pain (%)	38	2	<0.001*
other (%)	23	2	0.015*
AAA location			
supra (%)	15	21	1.000
juxta (%)	46	51	0.768
infra (%)	38	28	0.501
Smoking (%)	38	71	0.051
Hypertension (%)	64	73	0.526
Coronary heart disease (%)	43	57	0.384
Hypercholesterolemia (%)	21	40	0.236
COPD (%)	21	24	1.000
Diabetes mellitus (%)	21	14	0.449
Kidney function (MDRD)	51	65	0.033*
Antihypertensifs (%)	77	84	0.686
Anticoagulans (%)	69	67	1.000
Statines (%)	62	70	0.534

* = $p \leq 0.05$; COPD = chronic obstructive pulmonary disease.

The aneurysm locations (supra-, juxta- and infrarenal) in the rAAA (15, 46 and 38 percent, respectively) did not differ from electively treated AAA (21, 51 and 28 percent, respectively). However, the share of juxtarenal aneurysms (rAAA: 46 precent and eAAA: 51 percent) is in both groups larger than described in the literature (approximately 16 percent).[5] Juxtarenal AAA repair is a more challenging procedure, due to the involvement of renal arteries in the aneurysm. The higher percentage might be explained by the fact that our hospital functions as a referral center for rural hospitals, which could be

seen as a selection bias. Although smoking is an acknowledged risk factor for AAA growth and rupture, our ruptured group had significantly fewer smokers than the elective group. The ruptured AAA clearly differed from non-ruptured in the experience of symptoms like back-pain, stomach-pain and others like pain in the groin or legs. Decreased preoperative kidney function in the rAAA group is probably due to the hypovolemic shock, from which most AAA patients with a rupture suffer.

9.3 Degenerative processes leading to aortic medial layer degradation

In this thesis, we focussed on two major components of the cascade leading to aortic wall deterioration and eventually AAA development. The first is an inflammatory response in the aortic wall and in circulating leukocytes of AAA patients that causes nitrosative and oxidative stress. This results in apoptosis of the surrounding cells and stimulation of further inflammation.[6–8] The second concerns factors involved in degradation of the medial layer of the aortic wall. Components might interact with each other and thus accelerate vessel wall degradation.[9–11]

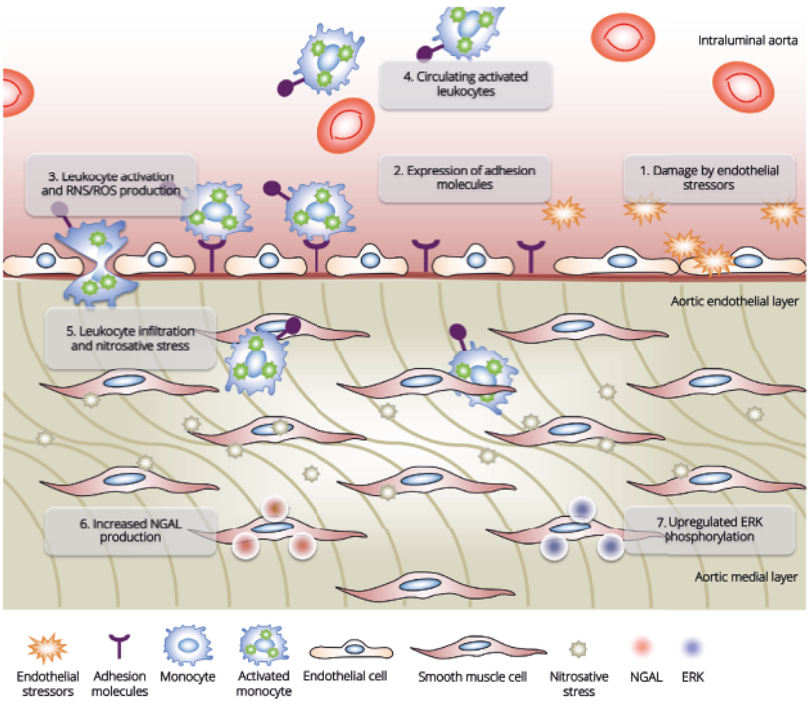

Figure 9.1 Inflammation and production of reactive nitrogen and oxygen species
In this graphical abstract we integrated our results in the pre-existing knowledge of AAA pathophysiology. Mechanical and chemical stressors cause damage to the aortic endothelial layer (1), which in response brings adhesion molecules to expression (2). These adhesion molecules activate circulating leukocytes that upregulate reactive nitrogen and oxygen species (RNS/ ROS) production (3). Activated leukocytes either remain in the blood circulation (4), or infiltrate in the vessel wall and cause nitrosative stress (5). Nitrosative stress activates NGAL production (6) and upregulates ERK phosphorylation (7).

Aortic wall inflammation and reactive species

Histological studies of AAA have demonstrated that aneurysms are associated with a chronic inflammation of the aortic wall.[12,13] The cause of this inflammation remains uncertain. However, it is thought that damage to the endothelial layer by mechanical or chemical stressors, e.g. hypertension or chemicals from cigarette smoke, is possibly involved (figure 9.1 step 1).[14,15] Reactively, endothelial cells present intraluminal adhesion molecules (figure 9.1 step 2).[14,15] The presence of adhesion molecules in AAA patients activates circulating leukocytes (figure 9.1 step 3).[3,16]

In **chapter 3** we investigated the role of circulating leukocytes in oxidative and nitrosative stress production in AAA patients.[3] We measured levels of reactive oxygen and nitrogen species in neutrophils, lymphocytes and monocytes separately, both in-vitro as in-vivo. We demonstrated that circulating neutrophils and monocytes in AAA patients, have a higher production of reactive nitrogen and oxygen species than in controls (figure 9.1 step 4). We hypothesized that circulating leukocytes in AAA patients produce higher amounts of reactive species due to increased amounts of adhesion molecules presented by the damaged endothelial layer in the atherosclerotic AAA.

Adhesion molecules also cause the activated leukocytes to infiltrate into the vessel wall.[3,16] When activated leukocytes accumulate in the aortic wall, increased production of those reactive species cause nitrosative and oxidative stress in the vessel wall (figure 9.1 step 5).[6,17] These are considered to be hallmarks of AAA pathogenesis.[18–20]

In **chapter 4** the expression of Neutrophil Gelatinase-Associated Lipocalin (NGAL, also Lipocalin-2) was examined in the aneurysm wall of ruptured and non-ruptured AAA. We measured its expression in the medial layer as well as the atherosclerotic plaque and determined its correlation with factors of vessel wall degradation, i.e. nitrosative stress, extracellular matrix (ECM) degradation and smooth muscle cell (SMC) apoptosis. We demonstrated that nitrosative stress in the medial layer is associated with increased local production of NGAL.[1] Furthermore, in the atherosclerotic plaque we recognized a typical and recurring pattern of expression. We presented a representative example (chapter 4, figure 4.4): a central core of nitrotyrosine embedded by a diffuse expression of NGAL. In earlier studies, NGAL was suggested to have a protective role against oxidative stress.[21,22] We suggest that in AAA pathogenesis, NGAL expression is reactively upregulated as a result of nitrosative stress to exert its protective effect (figure 9.1 step 6).

In **chapter 5** we focussed on the activation of Extracellular signal-Regulated Kinase (ERK) and its role in AAA development and rupture. ERK is a signalling protein thought to have an important role in regulating inflammatory processes and act as protective factor against damaged and apoptotic cells by stimulating cell proliferation.[23] We measured ERK activation in tissue of ruptured and non-ruptured AAA. We noted that ERK and nitrotyrosine in the medial layer tended to have a positive correlation (Rs=0.43; p=0.06; work in preparation). Our finding that ERK and nitrotyrosine might be correlated is in line with current literature stating that ERK phosphorylation is upregulated by nitrosative stress in the aneurysm wall (figure 9.1, step 7).[24–26]

In conclusion, the inflammatory response of the aortic wall is thought to initiate with damage to the endothelial layer. Activated leukocytes then infiltrate into the vessel wall, causing increased production of reactive species as well as other inflammatory factors. In turn, the inflammatory response activates factors of medial layer degradation, which will be discussed in the following paragraph.

Factors involved in aortic medial layer degradation

he increased production of NGAL and phosphorylation of ERK stimulates pro-proteolytic factors. In chapter 4 we demonstrated that NGAL was positively correlated with matrix metalloproteinase-9 (MMP-9) expression in the medial layer (figure 9.2, step 1). MMP-9 is an endopeptidase involved in connective tissue turnover.[27] In AAA development, more specific, it is responsible for ECM degradation.[11,28] This causes SMC migration and loss of medial layer strength, which eventually leads to aortic dilation. NGAL promotes a pro-proteolytic effect by binding to MMP-9 and thus protecting it from degradation.[9] It seems that NGAL has contradictive effects in AAA pathogenesis as we mentioned earlier that NGAL performs a protective effect against nitrosative stress. In unpublished work we found an inverse correlation between NGAL and the medial layer thickness (Rs=-0.71; p<0.01). Overall, we suggest that NGAL has a detrimental role on the aortic medial layer and stimulates AAA progression.

In chapter 5 we demonstrated that ERK activation is higher in tissue of non-ruptured AAA than in ruptured AAA and controls.[2] ERK is an intracellular signalling protein with many downstream effects, of which a pro-proteolytic effect by upregulating MMP-2 expression (figure 9.2, step 2).[23,29] In the aortic wall MMP-2 is not only responsible for vessel wall degeneration but also with ECM synthesis and repair.[30] Despite the suggested upregulation of MMP-2 by ERK, we found no correlation between the two in AAA tissue.[2] This lacking correlation can be explained by the above-mentioned divergent role that MMP-2 performs. We did find a positive correlation between ERK

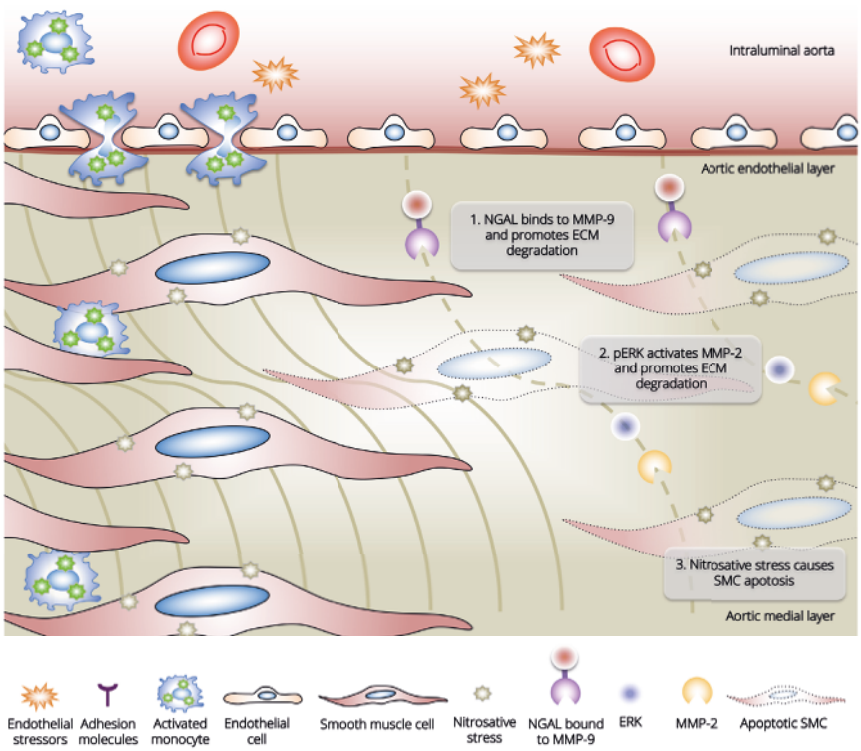

Figure 9.2 Factors involved in aortic medial layer degradation
In this graphical abstract we integrated our results in the pre-existing knowledge of AAA pathophysiology. This figure corresponds to figure 9.1 and can be seen as downstream steps in the cascade. Infiltrating leukocytes cause local production and release of RNS and eventually increased nitrosative stress in the medial layer. This local inflammation results in several deteriorating factors in the medial layer: (1) increased NGAL that promotes ECM degradation by binding MMP-9 and thus protecting it from autodegradation; (2) increased ERK phosphorylation that activates MMP-2 and thus stimulates ECM degradation; (3) nitrosative stress causes smooth muscle cell apoptosis and migration. These factors together result in a decrease of the medial layer thickness, loss of medial layer strength and eventually in aortic dilation.

activation and medial layer thickness of AAA (Rs 0.48; p=0.014).[2] Therefore initially, in chapter 5, we suggested that in response to local endothelial damage ERK had a protective effect by stimulating proliferation and thus vessel wall repair.[2]

In **chapter 6** we performed a research update on the role of ERK in AAA development.[31] Based on new insights from current literature we concluded that the main outcome of ERK phosphorylation is a detrimental effect by activation of MMP-2 rather than a protective effect, as we earlier concluded in chapter 5 (figure 9.2, step 2).[2,31]

As discussed earlier in this thesis, apoptosis is an important degenerative process in the development of AAA.[1,3,32] In chapter 4 we demonstrated significant more apoptosis

in the atherosclerotic plaque of eAAA as compared to rAAA and healthy aorta (p=0.02; chapter 4, figure 4.3F).[1] Additionally, we measured a significant correlation between apoptosis and nitrosative stress (Rs 0.33; p<0.05). These results are in line with earlier literature hypothesizing that free radicals, i.e. reactive nitrogen and oxygen species, are responsible for SMC apoptosis (figure 9.2, step 3).[6,33]

Table 9.2 Baseline patient characteristics of patients with dominant negative and haploïnsufficient FBN-1 gene mutations and the ratio of Betaglycan positive cells per subgroup.

	Dominant Negative	**Haploïnsufficient**	***p***
N	4	9	-
Male / Female	1 / 3	6 / 3	0.043*
Age (years)	45 (33 - 56)	27 (9 - 64)	0.235
Betaglycan positive cells (ratio of total)	0.47 (0.14 - 0.80)	0.33 (0.11 - 0.80)	0.015*

Hereditary connective tissue disorder leading to AAA development

In **chapter 7** we investigated the role of TGF-ß receptor 3 (TGFBR3, also Betaglycan) in the TGF-ß signalling pathway in fibroblasts of two Marfan patient subgroups (table 9.2). Subgroups were patients with a dominant negative (DN) versus a haploinsufficient (HI) Fibrillin-1 (FBN1) mutation. DN mutations lead to a malfolded or malfunctioning fibrillin-1 protein and thus a disturbed ECM.[34,35] HI mutations are caused by the deletion of one copy of the whole gene, degradation of the mutant protein, or nonsense-mediated decay by degradation of fibrillin-1 mRNA.[35–37] The latter mutation will cause a reduced level of fibrillin-1 protein, and thus compromised functionality.[34,35] TGF-β is an upstream activator of ERK and the cause of dysfunctional connective tissue in Marfans syndrome.[38,39] Several receptors are involved in the pathological activation of downstream intracellular TGF-ß pathways. We demonstrated an increased activation of TGF-ß and its downstream signalling pathways in patients with DN mutations as compared to HI mutations and to controls.[40] Also, Betaglycan expressions are increased in the DN group and correlate positively with TGFB1 expressions in groups pooled.[40] These data suggest that Betaglycan expression is involved in the upregulation of TGF-ß signalling in Marfan patients with a DN FBN1 gene mutation. Increased TGF-ß upregulation results in dysfunctional connective tissue and eventually in aneurysm development, mainly in the thoracic and abdominal aorta.[34,41,42] We acknowledge that this is just a limited step in the multifactorial process leading to aneurysm development. However, these results emphasize important differences in the effect of a DN versus HI mutation of the FBN1 gene in Marfan patients. A recent study showed that Marfan patients with HI FBN1 mutations had higher therapeutic benefit from

Losartan treatment compared to patients with DN FBN1 mutations which indicates a distinct pathological mechanism.[43] Thus, the different types of FBN1 mutations must be approached in a different manner in the search for therapeutic options.

Table 9.3 Markers for AAA expansion with suggested threshold values and concomitant follow up intervals.

Marker	Threshold	Expansion (mm/ year)	Suggested FU (months)
AAA diameter (mm)			
Low threshold	30 - 39	1.3 - 3.0	24
High threshold	40 - 54	2.9 - 4.9	< 50 = 6; ≥ 50 = 3
C. pneumoniae (IgA titre)			
Low threshold	< 64	3.2	12
High threshold	≥ 64	5.4	3
relative ILT volume (% of total)			
Low threshold	< 32	0	none
High threshold	≥ 32	3	12
S-elastin peptides (mg/L)			
Low threshold	< 330	1.1	36
High threshold	≥ 330	3.4	12
^{18}F-FDG uptake (SUVmax)			
Low threshold	> 2.0	0.9	36
High threshold	1.0 - 2.0	2.1	24

FU = follow up; AAA = abdominal aortic aneurysm; C. pneumonia = chlamydophila pneumonia; IgA = Immunoglobulin A; ILT = intraluminal thrombus; S-elastin peptides = serum elastin peptides; ^{18}F-FDG = fluorodeoxyglucose; SUV = standardized uptake volumes.

9.4 Prognostic markers for aneurysm growth and rupture

In **chapter 2** we presented a systematic review describing studies on predictive markers for AAA growth and rupture. Circulating biomarkers, biomechanical properties as well as genetic variations were investigated as potential prognostic markers. Several promising circulating markers and aneurysm properties were demonstrated to have prognostic value for aneurysm growth and rupture (table 9.3 and 9.4, respectively). However, only little is known about genetic markers for AAA progression. To date, there is no role for genetic markers as prognostic tool in AAA management.

In the current guidelines of AAA management no circulating or biomechanical markers are implemented, except for AAA diameter and growth speed.[44,45] This thesis identified several circulating and biomechanical markers with potential value for the prognosis of AAA expansion and rupture. We suggested the following circulating markers and

biomechanical properties to be considered as potential markers for AAA growth: 1) AAA diameter; 2) chlamydophila pneumoniae in case of seropositivity; 3) ILT size; 4) S-elastin peptides; and 5) inverse fluorodeoxyglucose uptake (table 9.3). Markers with the best prognostic value for AAA rupture are: 1) AAA diameter; 2) NGAL; 3) Peak wall stress; 4) Plasminogen activator inhibitor 1; and 5) S-elastin peptides (table 9.4). In the following paragraph we will speculate on possible threshold values for AAA follow-up and aneurysm repair surgery for the above-mentioned prognostic markers.

Table 9.4 Markers for AAA rupture with suggested threshold values and concomitant the period within surgical repair is advised.

Marker	Threshold	Annual rupture risk (%)	Surgery advised within (months)
AAA diameter (mm)			
Low threshold	40 - 49	0.5 - 5	none
High threshold	50 - 59	3 - 15	< 3
NGAL (mg/L)			
Low threshold	20 - 39	unknown	< 3
High threshold	> 40	unknown	< 1
Peak wall stress (N/cm2)			
Low threshold	30 - 49	unknown	3 - 6
High threshold	> 50	unknown	< 1
PAI-1 (IU/mL)			
Low threshold	< 15	unknown	none
High threshold	≥ 15	unknown	< 3
S-elastin peptides (mg/L)			
Low threshold	330 - 349	unknown	none
High threshold	> 350	unknown	< 3

AAA = abdominal aortic aneurysm; NGAL = neutrophil gelatinase-associated lipocalin; PAI = plasminogen activator inhibitor; S-elastin peptides = serum elastin peptides.

In table 9.3 we present possible threshold values for the use of these markers in the prediction of AAA expansion. The thresholds are based on averages from the several studies included in chapter 2. These values may be considered a draft for future studies. For all markers we defined a low and a high range. For each range we calculated the average expansion (in mm/year) and suggested a period within which the patient should be followed by ultrasound or CT-scan. Using AAA diameter as a marker we suggest follow up after 24, 6 and 3 months for the following measurements: 30 - 39 mm, 40 - 49 mm and ≥ 50 mm, respectively. This is according to the current guidelines of the European and American societies of vascular surgery.[44,45] Chlamydophila pneumoniae IgA titre < 64 or ≥ 64 should be followed after 12 and 3 months, respectively. When

the ILT volume is ≥ 32% of the total aneurysm volume, we suggest a follow up after 12 months. In case of an AAA with a relative ILT volume < 32% no follow up is necessary, except when other markers give reason to do so. Using S-elastin peptides as marker, we suggest follow up after 36 and 12 months when the blood levels are < 330 and ≥ 330 in mg/L, respectively; we suggest that AAA with 18F-FDG uptake > 2.0 or 1.0 – 2.0 SUV_{max} should be followed after 36 and 24 months, respectively.

In table 9.4 we present possible threshold values for the use of markers in the prediction of AAA rupture and a suggestion within which time surgical AAA treatment should be performed. As for table 9.3, these values are based on averages from the included studies in chapter 2. We suggest that AAA with a diameter exceeding 50 mm in women and 55 mm in men should be surgically repaired, while AAA smaller than 50 mm can be followed. This suggestion is in line with the current guidelines of the European and America societies of vascular surgery.[44,45] NGAL blood concentrations of 20 – 39 or ≥ 40 mg/L should indicate aneurysm repair within 3 months and 1 month, respectively. When PWS values are measured between 30 and 49 or ≥ 50 N/cm^2 we suggest surgery within 3 – 6 and within 1 month, respectively. Plasminogen levels in AAA patients lower than 15 IU/ml need no surgery yet, but when levels are higher than 15 IU/ml aneurysm repair within 3 months should be considered. As presented in table 9.4, levels of S-elastin peptides ranging 330 – 349 can be followed, however when exceeding these values we suggest that surgical repair should be performed within 3 months.

In conclusion, the present guidelines for AAA management provide a limited role for prognostic markers to determine the timing of follow up or aneurysm repair surgery. Based on the current literature we selected potential markers for AAA growth or rupture and suggested concomitant threshold values. Before these prognostics markers can be implemented in AAA management, threshold values should first be validated.

9.5 Critical review of present results

In chapter 2 we executed a systematic review of the literature on prognostic markers for AAA growth and rupture. The studies we included in our review provided rather heterogenic data for the markers of interest. Also, statistical tests often differed between studies. For example, chlamydophila pneumoniae was investigated in four studies.[46–49] In three studies differences in means were measured between groups and while one study the correlation between the blood titer and AAA expansion rate. The three studies, which measured a difference in means, all used variable cutoff values for the groups. These differences made the data unsuitable for extracting reliable threshold

values for clinical implementation. Prospective biomarker studies are necessary, in which threshold values for follow-up and surgical intervention are determined.

In chapter 3 we investigated the production of reactive nitrogen and oxygen species (RNS and ROS) by circulating leukocytes in AAA patients versus controls.[3] We retrospectively calculated whether aneurysm growth was associated with production of those species. We found no correlation between production of RNS and ROS in circulating leukocytes with the expansion rate of AAA. As it was not designed as a biomarker study we had no set points in time to measure aneurysm expansion versus production of RNS and ROS in circulating leukocytes. Therefore, we could not draw firm conclusions on the potential of RNS and ROS as marker for AAA expansion. However, we found too little association between the two values to motivate further prospective biomarker research for RNS and ROS.

In chapter 4 we demonstrated that NGAL is increased in blood plasma of ruptured AAA as compared to non-ruptured AAA. These results might indicate that NGAL is associated with a forthcoming rupture. However, our data do not clarify whether NGAL was increased before the rupture or as a result of the rupture. Patients were included in the rAAA group after the aneurysm was ruptured. Therefore, we know little about the NGAL blood values before the rupture had occurred. We would rather have followed these patients in the period before the AAA rupture with frequent NGAL measurements. Again, the work was not designed as a biomarker study and thus we had no set measurement points in time to determine NGAL values in the period before rupture occurred. However, we found highly significant differences in NGAL blood concentrations between rAAA versus eAAA that we therefore suggest further biomarker research for NGAL as a marker for rupture.

In chapter 5 we investigated ERK activation in the vessel wall of ruptured and non-ruptured AAA. An important methodological limitation is the fact that we could only take biopsies from the ventral wall of the aneurysm. As we know, inflammation and degradation of the aorta are heterogeneously spread throughout the aneurysm wall. Therefore the biopsy location is potentially very important as the ERK activation at one sight might possibly differ greatly from another in the same aneurysm. This limitation also accounts for the samples used in chapter 4. A clinical relevant improvement for future studies would be to adjust the protocol and perform biopsies at multiple sites in the aneurysm wall.

In chapter 7 the role of TGFBR3 expression was determined in Marfan patients. We had limited access to the clinical characteristics of the patients. Therefore we were also limited in correlating the specific mutations to the clinical consequences. If we would have had full access it might have given us the opportunity to relate more clinical features to either the DN or the HI mutations. This would help to provide an earlier diagnosis and more specific treatment of these high-risk AAA.

9.6 Perspectives for future research

A new model for the observation of cell interactions in the aneurysm wall

Prior studies on aortic aneurysm were performed in animal models, fixated human tissue, or isolated human cell cultures. An in vitro human model to study pathophysiological processes involved in human aortas is lacking. In **chapter 8** we investigated a novel technique to keep full thickness aneurysm wall tissue alive for several weeks. This new model will enable real-life research of signalling pathways in living aneurysm tissue. We developed a method to obtain vital, ex vivo human vascular tissue. In these cultured aneurysmal and non-aneurysmal vascular specimens, evaluation of viability showed that the larger part of human vascular tissue sections can be kept alive in culture for up to 62 days, while maintaining microstructural organization of the vessel wall.

Preservation of the aortic tissue composition in ex-vivo specimens facilitates the study of cell behavior and interaction between different cell types, and provides the opportunity to investigate the effects of pharmacological substances on tissue composition. The ability to digest the tissue sections greatly broadens the possibilities of this protocol. We are currently investigating the use of these tissue sections in new techniques in which we study elastic properties, aortic wall secretome, and pathways by additional inhibition and stimulation tests. By having established a method for extended in-vitro preservation of functionally and structurally intact vascular tissue sections, research on the pathophysiology of aortic aneurysms and also other vascular diseases may have entered a new era.

Identification of new circulating markers

The use of a multi-laser nanosope in combination with the above-mentioned model to keep aortic tissue alive for several weeks enables the possibility to study subcellular and even molecular three-dimensional details in living cells. This will further elucidate the numerous signalling pathways in the aortic wall and makes it possible to identify new markers involved in aortic degeneration and AAA development.

Validation of markers for AAA growth and rupture

Based on the present thesis, we suggest that a combination of markers for AAA growth will predict the aneurysm growth and risk of rupture more accurately than just its diameter. At this moment, however, there is too little clinical experience with the potential markers to give definitive threshold values. A clinical trial could prospectively investigate the accuracy of the markers of interest, before markers can be implemented in guidelines for AAA management.

9.7 Conclusions

In the current AAA management there is a limited role for prognostic markers. Timing of AAA follow up or of surgical aneurysm repair is based on its diameter, growth speed or the presence of symptoms. In this thesis we presented multiple circulating and biomechanical markers with high potential as a prognostic marker. We demonstrated five markers for future aneurysm growth and five markers for a forthcoming rupture. Based on the current literature we suggested for each marker the threshold values for follow up or for the timing within which aneurysm repair should be considered. These threshold values can be seen as a draft for future prospective marker studies to validate these markers and make them suitable for clinical implementation.

Increased production of reactive nitrogen and oxygen species, also reactive species, causes nitrosative and oxidative stress (RNS and ROS) in the aortic wall. RNS and ROS result in medial layer degradation, which is seen as a hallmark of AAA development. We demonstrated that circulating neutrophils and monocytes in AAA patients have a higher production of these reactive species than controls. Our data suggest that monocytes and neutrophils contribute to RNS and ROS in the vessel wall of AAA.

NGAL is an acute phase protein that is suggested as a marker for cardiovascular diseases such as heart failure, acute myocardial infarction and carotid atherosclerosis. We demonstrated that its expression was increased in the atherosclerotic plaque and medial layer of AAA tissue as compared to non-dilated aortas. Also, its expression in the aneurysm wall was positively correlated with factors of vessel wall degradation, i.e. nitrosative stress, ECM decline and apoptosis. Additionally, we measured increased levels of NGAL in the blood of ruptured AAA patients compared to electively treated AAA patients and controls. The data from this thesis suggests that NGAL plays a role in AAA development and might be of interest as a marker for AAA rupture.

ERK is an intracellular signalling protein with a broad spectrum of downstream effects involved in the turnover of aortic wall components, i.e. ECM and SMC proliferation

or apoptosis. Initially, we suggested that ERK might have a protective role in the development of AAA. This conclusion was based on the association between increased ERK activation with the presence of non-ruptured AAA and an inverse correlation of ERK activation with medial layer thickness. However, according to the results of recently published studies, it seems that ERK activation is in fact associated with MMP-2 expression and might rather have a detrimental role in AAA development.

TGFBR3 expression is involved in the upregulation of TGF-ß signalling in Marfan patients. In patients with a mutation leading to malfolded Fibrillin-1 proteins the effect is greater than in patients with a mutation leading to insufficient production. These findings suggest basic differences in the pathophysiology of these two types of Fibrillin-1 gene mutations and thus might require a different approach in the diagnosis and treatment of the disease.

Investigation of AAA samples is currently limited to the use of fixated tissue or isolated cell cultures. We established a method for extended in vitro preservation of functionally and structurally intact full thickness aortic sections. Research on AAA pathophysiology, and more specific on cellular signalling in the aortic wall, may have entered a new era.

REFERENCES

1. Groeneveld, M. E. *et al.* The potential role of Neutrophil Gelatinase-Associated Lipocalin (NGAL) in the development of abdominal aortic aneurysms. *Ann. Vasc. Surg.* (2019).
2. Groeneveld, M. E. *et al.* Activation of extracellular signal-related kinase in abdominal aortic aneurysm. *Eur. J. Clin. Invest.* 46, (2016).
3. Groeneveld, M. E. *et al.* Peroxynitrite Footprint in Circulating Neutrophils of Abdominal Aortic Aneurysm Patients Is Lower in Statin than in Non-statin Users. *Eur. J. Vasc. Endovasc. Surg.* (2017). doi:10.1016/j.ejvs.2017.06.003
4. Vega de Ceniga, M. *et al.* Growth Rate and Associated Factors in Small Abdominal Aortic Aneurysms. *Eur J Vasc Endovasc Surg* 231–236 (2006). doi:10.1016/j.ejvs.2005.10.007
5. Taylor, S. M., Mills, J. L. & Fujitani, R. M. The Juxtarenal Abdominal Aoric Aneurysm. *Arch. Surg.* 129, 734–737 (1994).
6. McCormick, M. L., Gavrila, D. & Weintraub, N. L. Role of oxidative stress in the pathogenesis of abdominal aortic aneurysms. *Arteriosclerosis, Thrombosis, and Vascular Biology* 27, 461–469 (2007).
7. Ahmed, R., Ghoorah, K. & Kunadian, V. Abdominal Aortic Aneurysms and Risk Factors for Adverse Events. *Cardiol. Rev.* 24, 88–93 (2016).
8. Thompson, R. W., Geraghty, P. J. & Lee, J. K. Abdominal aortic aneurysms: Basic mechanisms and clinical implications. *Curr. Probl. Surg.* 39, 110–230 (2002).
9. Folkesson, M. *et al.* Presence of NGAL/MMP-9 complexes in human abdominal aortic aneurysms. *Thromb. Haemost.* 98, 427–433 (2007).
10. Petersen, E., Wågberg, F. & Ängquist, K. A. Proteolysis of the abdominal aortic aneurysm wall and the association with rupture. *Eur. J. Vasc. Endovasc. Surg.* 23, 153–157 (2002).
11. Palombo, D. *et al.* Matrix metalloproteinases. Their role in degenerative chronic diseases of abdominal aorta. *J. Cardiovasc. Surg. (Torino).* 40, 257–260 (1999).
12. Freestone, T. *et al.* Inflammation and Matrix Metalloproteinases in the Enlarging Abdominal Aortic Aneurysm. *Arterioscler. Thromb. Vasc. Biol.* 15, 1145–1151 (1995).
13. Golledge, J., Muller, J., Daugherty, A. & Norman, P. Abdominal aortic aneurysm: Pathogenesis and implications for management. *Arterioscler. Thromb. Vasc. Biol.* 26, 2605–2613 (2006).
14. Guo, D.-C., Papke, C. L., He, R. & Milewicz, D. M. Pathogenesis of thoracic and abdominal aortic aneurysms. *Ann NY Acad Sci* 1085, 339–352 (2006).
15. McCarron, J. G., Lee, M. D. & Wilson, C. The Endothelium Solves Problems That Endothelial Cells Do Not Know Exist. *Trends Pharmacol. Sci.* 38, 322–338 (2017).
16. Kar, S. & Kavdia, M. Local oxidative and nitrosative stress increases in the microcirculation during leukocytes-endothelial cell interactions. *PLoS One* 7, (2012).
17. Martin-Ventura, J. L. *et al.* Erythrocytes, leukocytes and platelets as a source of oxidative stress in chronic vascular diseases: Detoxifying mechanisms and potential therapeutic options. *Thromb. Haemost.* 108, 435–442 (2012).

18. Ramos-Mozo, P. *et al.* Proteomic analysis of polymorphonuclear neutrophils identifies catalase as a novel biomarker of abdominal aortic aneurysm: Potential implication of oxidative stress in abdominal aortic aneurysm progression. *Arterioscler. Thromb. Vasc. Biol.* 31, 3011–3019 (2011).

19. Boddy, A. M. *et al.* Basic research studies to understand aneurysm disease. *Drug News Perspect.* 21, 142–148 (2008).

20. Kuivaniemi, H. *et al.* Update on abdominal aortic aneurysm research: from clinical to genetic studies. *Scientifica (Cairo).* 2014, 564734

21. Roudkenar, M. H. *et al.* Neutrophil Gelatinase-associated Lipocalin Acts as a Protective Factor against H2O2 Toxicity. *Arch. Med. Res.* 39, 560–566 (2008).

22. Bahmani, P. *et al.* Neutrophil gelatinase-associated lipocalin induces the expression of heme oxygenase-1 and superoxide dismutase 1, 2. *Cell Stress Chaperones* 15, 395–403 (2010).

23. Lu, Z. & Xu, S. ERK1/2 MAP kinases in cell survival and apoptosis. *IUBMB Life* 58, 621–631 (2006).

24. Chan, L. *et al.* IL-8 promotes inflammatory mediators and stimulates activation of p38 MAPK / ERK-NF-κB pathway and reduction of JNK in HNSCC. *Oncotarget* [Epub ahea, (2017).

25. Rui, W., Guan, L., Zhang, F., Zhang, W. & Ding, W. PM2.5-induced oxidative stress increases adhesion molecules expression in human endothelial cells through the ERK/AKT/NF-κB-dependent pathway. *J. Appl. Toxicol.* 36, 48–59 (2016).

26. Wang, X. *et al.* ROS-activated p38MAPK/ERK-Akt cascade plays a central role in palmitic acid-stimulated hepatocyte proliferation. *Free Radic. Biol. Med.* 51, 539–551 (2011).

27. Galis, Z. S. & Khatri, J. J. Matrix metalloproteinases in vascular remodeling and atherogenesis: the good, the bad, and the ugly. *Circ. Res.* 90, 251–262 (2002).

28. Matthew Longo, G. *et al.* Matrix metalloproteinases 2 and 9 work in concert to produce aortic aneurysms. *J. Clin. Invest.* 110, 625–632 (2002).

29. Cho, A., Graves, J. & Reidy, M. A. Mitogen-activated protein kinases mediate matrix metalloproteinase-9 expression in vascular smooth muscle cells. *Arterioscler. Thromb. Vasc. Biol.* 20, 2527–32 (2000).

30. Shen, M. *et al.* Divergent roles of matrix metalloproteinase 2 in pathogenesis of thoracic aortic aneurysm. *Arterioscler. Thromb. Vasc. Biol.* 35, 888–898 (2015).

31. Groeneveld, M. E. & Yeung, K. K. Research update for articles published in EJCI in 2016. *Eur. J. Clin. Invest.* (2018). doi:10.1111/eci.13016

32. López-Candales, A. *et al.* Decreased Vascular Smooth Muscle Cell Density in Medial Degeneration of Human Abdominal Aortic Aneurysms. *Am. J. Pathol.* 150, 993–1007 (1997).

33. Dimmeler, S. & Zeiher, A. M. Reactive oxygen species and vascular cell apoptosis in response to angiotensin II and pro-atherosclerotic factors. *Regul. Pept.* 90, 19–25 (2000).

34. Faivre, L. *et al.* Effect of Mutation Type and Location on Clinical Outcome in 1,013 Probands with Marfan Syndrome or Related Phenotypes and FBN1 Mutations: An International Study. *Am. J. Hum. Genet.* 81, 454–466 (2007).

35. Hilhorst-Hofstee, Y. *et al.* The clinical spectrum of complete FBN1 allele deletions. *Eur. J. Hum. Genet.* 19, 247–52 (2011).

36. Schrijver, I., Liu, W., Brenn, T., Furthmayr, H. & Francke, U. Cysteine substitutions in epidermal growth factor-like domains of fibrillin-1: distinct effects on biochemical and clinical phenotypes. *Am. J. Hum. Genet.* 65, 1007–20 (1999).

37. Schrijver, I. *et al.* Premature Termination Mutations in FBN1: Distinct Effects on Differential Allelic Expression and on Protein and Clinical Phenotypes. *Am. J. Hum. Genet.* 71, 223–237 (2002).

38. Gillis, E., Van Laer, L. & Loeys, B. L. Genetics of thoracic aortic aneurysm: At the crossroad of transforming growth factor-β signaling and vascular smooth muscle cell contractility. *Circ. Res.* 113, 327–340 (2013).

39. Ten Dijke, P. & Arthur, H. M. Extracellular control of TGFβ signalling in vascular development and disease. *Nat. Rev. Mol. Cell Biol.* 8, 857–869 (2007).

40. Groeneveld, M. E. *et al.* Betaglycan (TGFBR3) up-regulation correlates with increased TGF-β signaling in Marfan patient fibroblasts in vitro. *Cardiovasc. Pathol.* 32, 44–49 (2018).

41. Franken, R. *et al.* Beneficial Outcome of Losartan Therapy Depends on Type of FBN1 Mutation in Marfan Syndrome. *Circ. Cardiovasc. Genet.* 8, 383–388 (2015).

42. Habashi, J. P. *et al.* Losartan, an AT1 antagonist, prevents aortic aneurysm in a mouse model of Marfan syndrome. *Science (80-.).* 312, 117–21 (2006).

43. Franken, R. *et al.* Relationship between fibrillin-1 genotype and severity of cardiovascular involvement in Marfan syndrome. *Heart* Published Online First: [3rd May 2017] (2017). doi:10.1136/heartjnl-2016-310631

44. Moll, F. L. *et al.* Management of abdominal aortic aneurysms clinical practice guidelines of the European society for vascular surgery. *Eur. J. Vasc. Endovasc. Surg.* 41, (2011).

45. Chaikof, E. L. *et al.* SVS practice guidelines for the care of patients with an abdominal aortic aneurysm: Executive summary. *J. Vasc. Surg.* 50, 880–896 (2009).

46. Falkensammer, B. *et al.* Lack of microbial DNA in tissue specimens of patients with abdominal aortic aneurysms and positive Chlamydiales serology. *Eur. J. Clin. Microbiol. Infect. Dis.* 26, 141–145 (2007).

47. Lindholt, J. S., Fasting, H., Henneberg, E. W. & Østergaard, L. A review of Chlamydia pneumoniae and atherosclerosis. *Eur. J. Vasc. Endovasc. Surg.* 17, 283–289 (1999).

48. Lindholt, J. S., Ashton, H. A. & Scott, R. A. P. Indicators of infection with Chlamydia pneumoniae are associated with expansion of abdominal aortic aneurysms. *J. Vasc. Surg.* 34, 212–215 (2001).

49. Lindholt, J. S., Jørgensen, B., Shi, G. P. & Henneberg, E. W. Relationships between activators and inhibitors of plasminogen, and the progression of small abdominal aortic aneurysms. *Eur. J. Vasc. Endovasc. Surg.* 25, 546–551 (2003).

APPENDICES

Dutch summary
List of publications
Acknowledgements

NEDERLANDSE SAMENVATTING

Een aneurysma wordt gedefinieerd als een pathologische verwijding van een arterie. Een voorkeurslocatie van een aneurysma is in de abdominale aorta. Doorgaans is een abdominaal aorta aneurysma (AAA) asymptomatisch tot het moment dat er een ruptuur van de wand optreedt of aanstaande is. Een ruptuur zorgt voor een levensbedreigende bloeding. Er zijn vooralsnog geen medicamenteuze opties om de groei van een aneurysma tegen te gaan. Derhalve is een chirurgische behandeling van het AAA de enige mogelijkheid om een ruptuur te voorkomen. Een aneurysma hersteloperatie is niet vrij van perioperatieve morbiditeit en zelfs mortaliteit. Derhalve moeten patiënten nauwkeurig worden geselecteerd om in aanmerking komen voor een dergelijke behandeling. Het blijft echter uitdagend om accuraat aan te geven welk AAA zal ruptureren en welke niet.

Het doel van dit promotieonderzoek is: i) het ontrafelen van enkele pathofysiologische processen die leiden tot een ruptuur; en ii) onderzoeken of er markers zijn die de groei of een aanstaande ruptuur van een AAA nauwkeuriger kunnen voorspellen dan de huidige indicatoren.

In **deel 1** van dit proefschrift wordt een overzicht gepresenteerd van de reeds bekende maar ook potentiële nieuwe markers voor aneurysma groei en ruptuur. Een literatuuroverzicht wordt beschreven in **hoofdstuk 2** waarbij we studies hebben geïncludeerd die potentiële markers voor AAA groei en/ of ruptuur hebben onderzocht. We hebben een onderverdeling gemaakt in mechanische, circulerende en genetische markers. Met name in de eerste twee categorieën hebben we meerdere veelbelovende markers geïdentificeerd. Deze zijn nog niet direct klinisch toepasbaar, maar lijken de moeite waard om verder te onderzoeken. Genetische afwijkingen daarentegen blijken vooralsnog lastig in te zetten als marker voor AAA groei of ruptuur.

In **hoofdstuk 3** hebben we de productie van vrije zuurstofradicalen gemeten in circulerende leukocyten van zowel AAA patiënten als van gezonde controles. We hebben daarbij separaat de productie gemeten in neutrofielen, lymfocyten en monocyten. Het blijkt dat neutrofielen en monocyten de hoogste productie hebben en ook significant verschillen van de controle groep. We concluderen dan ook dat de mate van vrije zuurstofradicalen productie door neutrofielen en monocyten een rol speelt in de ontwikkeling van een aneurysma. Er blijkt echter geen relatie te bestaan tussen de hoeveelheid vrije zuurstofradicalen en de groeisnelheid van AAA.

In **hoofdstuk 4** is de rol van een acute fase eiwit, genaamd *neutrophil gelatinase-associated lipocalin* (NGAL), onderzocht in de ontwikkeling en ruptuur van AAA. Bloedmonsters en aneurysmaweefsels van zowel geruptureerde als niet-geruptureerde AAA patiënten werden verzameld, evenals bloedmonsters en aortaweefsel van gezonde controles. Deze zijn allen onderzocht op de hoeveelheid en lokalisatie van NGAL. In aneurysmaweefsels wordt een grotere hoeveelheid NGAL gemeten dan in gezond aortaweefsel. Het bloed van geruptureerde patiënten heeft een hogere concentratie NGAL dan bloed van niet-geruptureerde patiënten en controles. Daarnaast we hebben positieve correlaties aangetoond tussen NGAL en factoren van vaatwand degeneratie zoals bindweefsel afbraak, geprogrammeerde celdood en productie van vrije zuurstofradicalen. We concluderen dan ook in hoofdstuk 4 dat NGAL een rol speelt in de ontwikkeling van AAA en mogelijk als marker voor aneurysma ruptuur zou kunnen fungeren.

In **deel 2** van dit proefschrift worden intercellulaire signaleringsroutes onderzocht die mogelijk de groei en ruptuur van AAA beïnvloeden. Hoofdstuk 5 en 6 richten zich op een extracellulair signaaleiwit dat *extracellular signal-regulated kinase* (ERK) wordt genoemd. In **hoofdstuk 5** wordt de activering van ERK gemeten in aneurysmaweefsel van zowel geruptureerde als niet-geruptureerde AAA. Ook is de mate van bindweefsel afbraak en de wanddikte van de aneurysmata onderzocht. ERK wordt in hogere mate geactiveerd in niet-geruptureerde AAA in vergelijking tot geruptureerde AAA en gezonde aorta's. Er bestaat een lineair verband tussen ERK activering en de wanddikte van het aneurysma. We concludeerden initieel in hoofdstuk 5 dat ERK lijkt te beschermen tegen AAA ruptuur. Echter, in **hoofdstuk 6** moeten die conclusie bijstellen nadat we een kort overzicht hebben gemaakt van de meest recente literatuur. De activering van ERK in de aneurysmawand lijkt eerder vaatwand degeneratie te stimuleren dan te beschermen tegen ruptuur.

In **hoofdstuk 7** wordt een signaleringsroute uitgelicht die een belangrijke rol speelt in de ontwikkeling van AAA in patiënten met een genetische predispositie voor het krijgen van aneurysmata. Een bekend voorbeeld van een dergelijke afwijking is een mutatie in het Fibrilline-1 gen, wat leidt tot de ziekte van Marfan. Deze patiënten hebben een grote kans op het krijgen van AAA op relatief jonge leeftijd. Een groeifactor die centraal staat in het ontwikkelen van de Marfan symptomen is *transforming growth factor beta* (TGF-ß). In celkweken met levende fibroblasten van zowel Marfan patiënten als gezonde controles is de rol van TGF-ß receptor-3 onderzocht. We concluderen dat TGF-ß receptor-3 verantwoordelijk is voor de verhoogde activering van TGF-ß in een subgroep van Marfan patiënten. Deze conclusie benadrukt dat er binnen het Marfan spectrum

nog belangrijke verschillen zijn in de pathofysiologie. De resultaten benadrukken de noodzaak van het een gerichte specifieke behandeling voor de subgroepen binnen de totale groep van Marfan patiënten.

In **deel 3** wordt de ontwikkeling van een nieuw model beschreven om in-vitro onderzoek te doen naar cel interactie in de aorta- en aneurysmawand. In **hoofdstuk 8** snijden we met behulp van een zogenaamde Vibratome coupes van nog levende biopten waarin alledrie de lagen van de aortawand zijn opgenomen. In onze studie hebben we voor het eerst aangetoond dat de cellen in deze coupes tot wel 62 dagen in leven kunnen blijven. Tot nu toe is het onderzoek naar signaleringsroutes voor interactie tussen cellen grotendeels beperkt geweest tot gefixeerd dan wel diep bevroren materiaal of celkweken van afzonderlijke cellen uit de aortawand. Deze nieuwe techniek maakt het mogelijk om onderzoek te doen naar cel interactie in een veel realistischer model.

Concluderend, blijkt het tot de dag van vandaag uitdagend om AAA groei en een eventuele ruptuur te voorspellen. Een accurate prognose helpt de besluitvorming omtrent een aneurysma hersteloperatie. In dit proefschrift is een overzicht gegeven van reeds geïdentificeerde markers voor aneurysmagroei en –ruptuur die nog niet in de dagelijkse praktijk worden toegepast. Tevens zijn er mogelijke nieuwe markers onderzocht middels weefsel- en bloedonderzoek. Vervolgens is de interactie onderzocht tussen cellen die bijdraagt aan de ontwikkeling en ruptuur van aneurysmata. Tot slot presenteren we een nieuwe en meer realistischer methode om signaleringsroutes voor cel interactie te bestuderen. De resultaten van dit proefschrift hebben het begrip van de AAA pathofysiologie vergroot en brengen het accuraat voorspellen van aneurysmagroei en -ruptuur een stap dichterbij.

LIST OF PUBLICATIONS

The potential role of Neutrophil Gelatinase-Associated Lipocalin (NGAL) in the development of abdominal aortic aneurysms.
Groeneveld ME, Musters RJP, Tangelder GJ, Struik J, Niessen HW, Coveliers HM, Blankensteijn JD, Hoksbergen AW, Nederhoed JH, De Bruin JL, Wisselink W, Yeung KK
Ann Vasc Surg. 2019 May;57:210-219.

Update on Activation of Extracellular signal-Regulated Kinase in abdominal aortic aneurysm.
Groeneveld ME, Yeung KK
Eur J Clin Invest. 2018 Oct;48(10):e13016.

Systematic Review of Circulating, Biomechanical, and Genetic Markers for the Prediction of Abdominal Aortic Aneurysm Growth and Rupture.
Groeneveld ME, Meekel JP, Rubinstein SM, Merkestein LR, Tangelder GJ, Wisselink W, Truijers M, Yeung KK.
J Am Heart Assoc. 2018 Jun 30;7(13).

An in vitro method to keep human aortic tissue sections functionally and structurally intact.
Meekel JP, **Groeneveld ME**, Bogunovic N, Keekstra N, Musters RJP, Zandieh-Doulabi B, Pals G, Micha D, Niessen HWM, Wiersema AM, Kievit JK, Hoksbergen AWJ, Wisselink W, Blankensteijn JD, Yeung KK.
Sci Rep. 2018 May 25;8(1):8094.

Betaglycan (TGFBR3) up-regulation correlates with increased TGF-β signaling in Marfan patient fibroblasts in vitro.
Groeneveld ME, Bogunovic N, Musters RJP, Tangelder GJ, Pals G, Wisselink W, Micha D, Yeung KK.
Cardiovasc Pathol. 2018 Jan - Feb;32:44-49.

Peroxynitrite footprint in circulating neutrophils of abdominal aortic aneurysm patients is lower in statin than in non-statin users.
Groeneveld ME, Van der Reijden JJ, Tangelder GJ, Westin LC, Renwarin L, Musters RJ, Wisselink W, Yeung KK
Eur J Vasc Endovasc Surg. 2017 Sep;54(3):331-339.

Organ protection during aortic cross-clamping.
Yeung KK, **Groeneveld ME**, Lu JJN, Van Diemen P, Jongkind V, Wisselink W
Best Practice & Research Clinical Anaesthesiology (2016) 1-11.

Activation of extracellular signal-related kinase in abdominal aortic aneurysm.
Groeneveld ME, Van Burink MV, Begieneman MP, Niessen HW, Eringa EC, Yeung KK
Eur J Clin Invest. 2016 May;46(5):440-7.

DANKWOORD

Zeer geachte **professor Wisselink**, beste Willem, voor u is alleen het beste goed genoeg en dat heb ik vaak mogen ondervinden. We gingen door tot het bittere eind en dus totdat iedere punt perfect op de i stond. Zonder u hadden we deze kwaliteit niet gehaald. Ik kijk uit naar de tijd dat u me met dezelfde discipline de vaatchirurgische knepen van ons mooie vak zal leren.

Zeer geachte **professor Tangelder**, uw gave om data te doorgronden en de essentiële punten eruit te pikken is ongeëvenaard. Die kwaliteit heeft ervoor gezorgd dat we alles uit onze onderzoeken hebben gehaald wat erin zat en geen experiment onbesproken is gebleven! De avonden bij u thuis in Oegstgeest met een kopje thee van Sandra zal ik nooit vergeten.

Beste **Kakkhee**, je plukte me als student uit de collegebanken en hebt me net zo lang gedrild totdat ik de noodzakelijke discipline had om in een biomedisch laboratorium te werken. Onder andere middels jouw legendarische en speciaal voor mij opgestelde "10 geboden". Vele wegen leiden naar Rome, maar door jouw weg te volgen ben ik precies daar terecht gekomen waar ik nu wilde zijn. Mijn dank daarvoor is niet in deze paar regels te beschrijven.

Beste **René**, zonder jouw onuitputtelijk positieve energie en enthousiasme was dit boek er nooit gekomen. We hebben hele dagen in de Doka foto's bekeken van mijn celkweken en andere kleuringen en je kreeg er nooit genoeg van. Je input is van wezenlijk belang geweest voor onze mooie resultaten.

Thank you, dear members of the reviewing committee, for your time and effort spent for this manuscript: **prof. dr. J.D. Blankensteijn**, **prof. dr. J.A.M. Zeebregts**, **prof. dr. D.A. Legemate**, **prof. dr. G.W.H. Schurink**, **dr. D. Nio**, **dr. E.C. Eringa.** I am looking forward to the dissertation. A special thank you to **prof. dr. R.L. Dalman,** it is a great honour to have you in our committee and that you are willing to travel all the way to Amsterdam.

Beste (voormalig) vaatchirurgen van het VUmc: **Willem, Jan, Arjan, Hillian, Kakkhee, Hans, Maarten, Vincent, Ernst, Jorg**. Bijzonder dat jullie zo vaak tijdens het acute herstel van een geruptureerd aneurysma aan wetenschapsstudent Menno dachten. Zonder jullie aandacht voor onze weefselbank hadden wij geen onderzoek. En misschien

wel veel belangrijker, dank voor alle geweldige avonden tijdens congressen en andere feesten, *You Guys Rock*!
Collega, vriend en paranimf **dr. Harm P. Ebben**, dat onze wegen elkaar ergens in ons leven zouden kruisen was *written in the stars*. Er is niemand in mijn omgeving met wie ik zo veel interesses en eigenschappen deel, onze loopbaan is nagenoeg identiek en, zo blijkt, waren onze voorouders ook al bevriend sinds de jaren '80 van de vorige eeuw. We hebben sinds onze eerste stappen in het onderzoek samen opgetrokken en ik kan niet wachten om te ontdekken wat onze carrières binnen de chirurgie ons nog meer gaan brengen! Ik ben er trots op dat je naast me staat tijdens mijn verdediging.

Dr. C. Zwiers, lieve Carolien, je begon als het schattige schoonzusje met een niet te snoeren grote mond. Ondertussen ben je mijn wijze zus, collega AIOS, zeil- en snowboardmaatje, en ben je mij vooruit gestreefd in onze promotietrajecten! Onze bijzondere vriendschap koester ik. Het is een eer dat je me als paranimf bijstaat!

Onderzoekers van de vaatchirurgie: **Kakkhee, Jorn, Ted, Natalija, Harm, Wouter, Stefan, Orkun, Sabrina, Jacqueline**. De beer is los! Na jaren van zaaien is het nu tijd om te oogsten. Harm heeft het startschot gegeven, er zullen nu veel promoties volgen. Wat een geweldige tijd heb ik met jullie gehad! Kakkhee je mag trots zijn op de club die je hebt opgezet.

Beste **Laura van Wieringen** en **Ron de Hoon**, jullie hadden altijd wel honderd andere zaken aan je hoofd en toch maakten jullie tijd om ons te helpen door het logistieke oerwoud van de VU. Jullie maken het leven van de Heelkunde collega's een heel stuk aangenamer, veel dank daarvoor!

Beste **professor Bonjer**, uw opzwepende speeches in de bus op weg naar de Chirurgencup hebben een onuitwisbare indruk op mij gemaakt, alsof we op weg waren naar de Olympische finale hockey! Dit bleek tekenend te zijn voor uw visie op onze afdeling Heelkunde.

Beste **chirurgen van het Spaarne Gasthuis**, in het bijzonder opleider Rijna, ik ben er trots op te kunnen zeggen dat ik in dit gasthuis en door jullie wordt opgeleid tot chirurg. Het is een bijzondere prestatie om binnen een afdeling van deze omvang zo een goede sfeer en samenwerking te creëren.

Beste arts-assistenten van het Spaarne Gasthuis, we werken ons allemaal een slag in de rondte in onze eeuwige strijd tegen de onuitstaanbare piepers, de consulten

van de interne, de vragen over infuusstanden en verzoeken voor orders in Epic. Aan het einde van de dag winnen we altijd weer van bovenstaande plaaggeesten door jullie ongekende collegialiteit en teamgevoel!

Weledelzeergeleerde heer Scherder, beste Erik, op het moment dat ik de eindstreep even uit het vizier verloren was schudde jij me wakker en gaf me een schop op een plek waar ik het nodig had. Korte tijd later lag mijn manuscript bij de leescommissie. Je energie en enthousiasme is cruciaal geweest voor het afronden van dit proefschrift.

Lieve schoonfamilie: **Marijke, Grady, Katinka, Martijn, Yasmaine, Carolien en Rogier**, dank dat jullie mij hebben opgenomen in jullie familie. Je familie heb je niet voor het kiezen maar ik had jullie stuk voor stuk gekozen als ik het voor zeggen had gehad!

Lieve familie, **Pap, Mam, Eelke, Laura, Michel en Hessel**. Vaak zijn we strategisch verspreid over de hele wereld, maar op de momenten dat we elkaar nodig hebben staan we er allemaa lvoor elkaar. Dank voor jullie onvoorwaardelijke steun en vertrouwen.

Beste lezers, hier de belangrijkste *take home message:* ik ben gezegend met een hele lieve, knappe en bijzonder attente vrouw en dat is wel mijn meisje Maaike. Zij zorgt ervoor dat alles in mijn leven mooier, kleurvoller en dierbaarder wordt. Lieve **Maaike**, dank je wel dat je mijn leven zo verrijkt en niet in de minste plaats door ons twee waanzinnig goed gelukte dochters, **Félin** en **Annamae**, te schenken. Je vergeleek ons leven ooit met de cadans van onze hardloopsessies; zoals ik het zie rennen we nu de *Two Oceans*, met alleen maar schitterende uitzichten om ons heen en een oneindige mooie weg voor ons uit waarover we samen de horizon tegemoet gaan.

Menno Evert Groeneveld was born May 27th 1985 in Singapore. He followed his primary education in Kloof (South Africa), Joppe and Leeuwarden. His secondary education was at the Christelijk Gymnasium in Leeuwarden. In his first university year he studied Law, after which he switched to Medical Studies at the VU University Medical Center in Amsterdam. As a medical student he started his scientific career as a research-student and would later follow a MD-PhD program at the Department of Vascular Surgery in collaboration with the Department of Physiology. Currently, he is general surgical resident in the greater VU University Medical Center region and will commence his vascular surgical residency in 2020. As an entrepreneur he advises several medical clinics and hospitals in correct and optimal medical billing.

Amsterdam UMC
Universitair Medische Centra

Menno E. Groeneveld

Cellular signalling in abdominal aortic aneurysms

Cellular signalling in abdominal aortic aneurysms

Towards better prediction of aneurysm progression and rupture

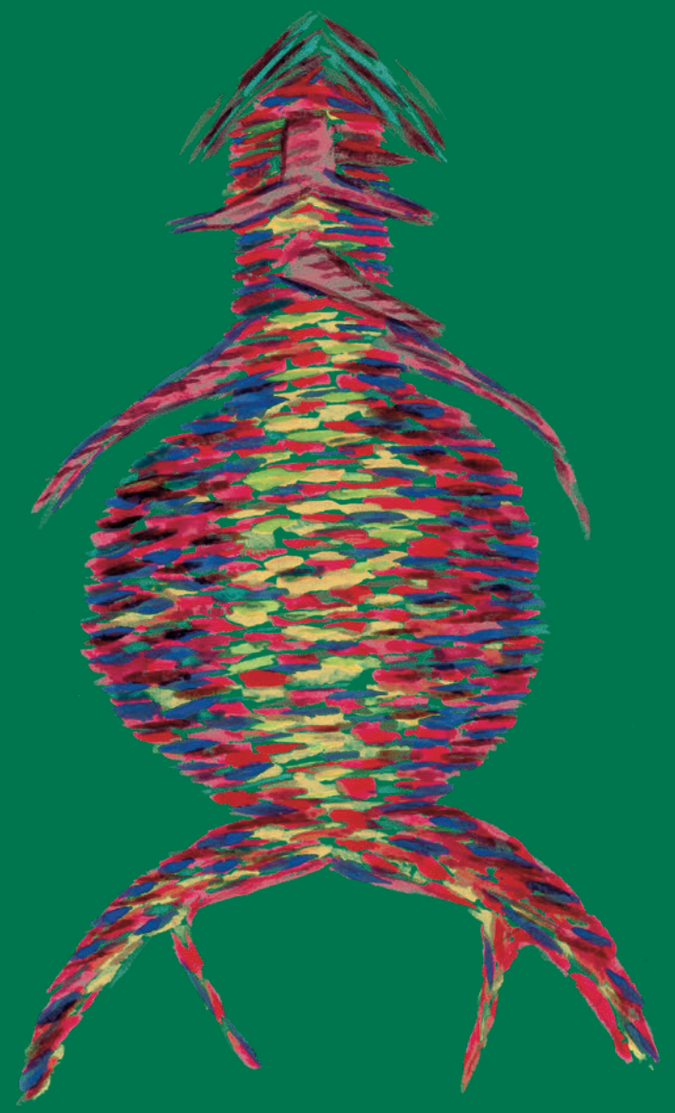

Menno E. Groeneveld